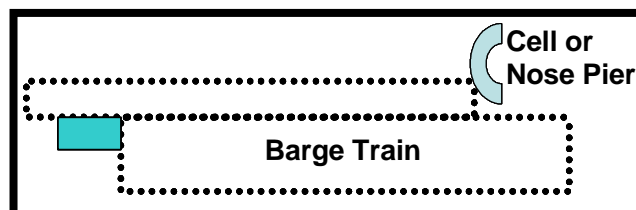Information Technology Laboratory

US Army Corps of Engineers®
Engineer Research and
Development Center

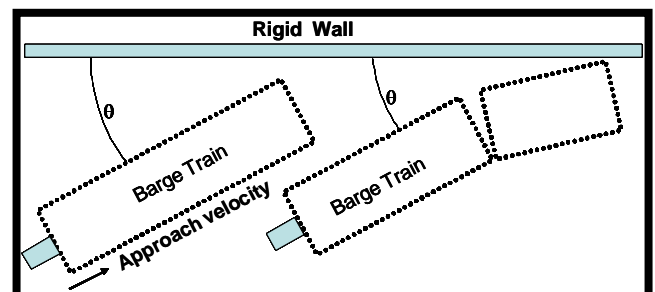*Navigation Systems Research Program*

A Numerical Method for Computing Barge Impact Forces Based on Ultimate Strength of the Lashings between Barges
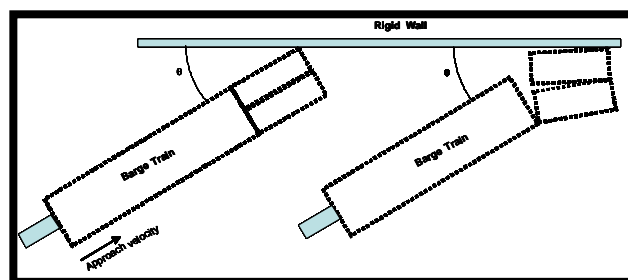
José Ramón Arroyo, Robert M. Ebeling   August 2004

Longitudinal Failure

Transverse Failure

Corner Failure

A Numerical Method for Computing Barge Impact Forces Based on Ultimate Strength of the Lashings between Barges

José Ramón Arroyo

*General Engineering Department
University of Puerto Rico
P.O. Box 9044
Mayagüez, PR 00681*

Robert M. Ebeling

*Information Technology Laboratory
U.S. Army Engineer Research and Development Center
3909 Halls Ferry Road
Vicksburg, MS 39180-6199*

Final report

ABSTRACT:

In 1993 Headquarters, U.S. Army Corps of Engineers, issued the first formal Corps-wide analysis procedure providing guidance for analyzing the effects of barge impact loading on navigation structures. According to the ETL 1110-2-338 engineering procedure, the magnitude of the impact forces generated by a particular collision event is dependent on the mass including hydrodynamic added mass of the barge train, the approach velocity, the approach angle, the barge train moment of inertia, *damage sustained by the barge structure*, and friction between the barge and the wall. Two significant concerns have been raised since the release of the ETL 1110-2-338 procedure: (1) A key aspect of the ETL 1110-2-338 engineering formulation is computation of collision energy dissipated in nonrecoverable, plastic hull deformation of (i.e., damage to) the corner of the barge where impact with the wall occurs. However, the majority of the impacts made by barge trains transiting Corps locks do not result in damage to the barge structure nor damage to the walls. (2) In addition, several engineers who have used the ETL 1110-2-338 engineering procedure have questioned the accuracy of the computed results.

In 2003, the U.S. Army Engineer Research and Development Center issued the report ERDC/ITL TR-03-3, "Analysis of Impact Loads from Full-Scale, Low-Velocity, Controlled Barge Impact Experiments, December 1998," by Arroyo, Ebeling, and Barker. This report addresses the interpretation of 8 of the 44 December 1998 full-scale, low-velocity, controlled-impact, barge train impact experiments conducted at the decommissioned Gallipolis Lock at Robert C. Byrd Lock and Dam, Gallipolis Ferry, WV. According to ERDC/ITL TR-03-3, an easy-to-use empirical correlation is derived that reports the maximum impact force (normal to the wall) as a function of the linear momentum normal to the wall (immediately prior to impact), using the results from the impact forces measured during these full-scale impact experiments. This new empirical correlation will be used for impacts that do not involve damage during impact to either the corner barge of a barge train or to the wall. An alternate empirical correlation is given for the maximum impact force (normal to the wall) as a function of the kinetic energy normal to the wall (immediately prior to impact).

However, ERDC/ITL TR-03-3 did not present the limit value of the force normal to the wall based on the empirical correlations. The present report presents the analysis of a barge train impacting a rigid wall. The limit value of the force normal to the wall is based on the yield of the lashing. That is, predefined failure planes are analyzed and based on the yield of the lashing, a maximum force normal to the wall is calculated. The three failure mechanisms studied are longitudinal, transverse, and corner. Finally, the maximum force normal to the struck wall is calculated from the equations of motion and the yielding of the lashing.

Contents

List of Tables

Conversion Factors, Non-SI to SI Units of Measure

To convert non-SI units of measure used in this report to SI units, multiply by the following factors.

Multiply	By	To Obtain
feet	0.3048	meters
inches	25.4	millimeters
kips	4,448.222	newtons
kips per square inch	6.894757	megapascals
kips per square foot	47.8803	kilopascals
kip-seconds	4.448222	kilonewtons-seconds
kip-seconds squared per foot	14.5939	kilonewton-seconds squared per meter
miles per hour	1.609344	kilometers per hour
pounds (mass)	0.4535924	kilograms
pounds (force) per square inch	0.006894757	megapascals
square inches	645.16	square millimeters
tons (short, 2,000 lb)	907.1847	kilograms

Preface

The research described in this report was authorized by Headquarters, U.S. Army Corps of Engineers (HQUSACE), as part of the Navigation Systems Research Program. This study was conducted under Work Unit (WU) 33143, "Design of Innovative Lock Walls for Barge Impact." Dr. Robert M. Ebeling of the U.S. Army Engineer Research and Development Center (ERDC) Information Technology Laboratory (ITL), Vicksburg, MS, is the Principal Investigator of this work unit. Mr. Robert C. Patev, currently with the U.S. Army Engineer District (USAED), New England, was the original Principal Investigator of WU 33143.

Dr. Sandra Knight, Coastal and Hydraulics Laboratory (CHL), Vicksburg, MS, ERDC, was the Technical Director for Navigation. The Navigation Business Line Leader was Mr. Barry Holliday, HQUSACE. Mr. James E. Clausner, Coastal Engineering Branch, CHL, was Navigation Systems Program Manager.

This research was conducted and the report prepared by Dr. José Ramón Arroyo, General Engineering Department, University of Puerto Rico at Mayagüez; and Dr. Robert M. Ebeling, Computer-Aided Engineering Division (CAED), ITL. The authors of this report would like to acknowledge the contribution of Dr. Drianfel E. Vázquez Torres, professor of the University of Puerto Rico at Ponce, for the development of the graphic user interface (GUI) for **Limit_LASHING**. The assistance during the development of this research of Mr. Carlos Rivera, graduate student of the Civil Engineering Department, University of Puerto Rico at Mayagüez, is also acknowledged. Dr. Ebeling was the author of the scope of work for the research effort discussed in this report. The research was monitored by Dr. Ebeling, under the supervision of Dr. Charles R. Welch, Chief of Engineering and Informatics Systems Division, ITL; Dr. David R. Richards, Director, Computational Sciences and Engineering, ITL; and Dr. Jeffery P. Holland, Director, ITL.

The creation of the Limit_LASHING user's manual presented in Appendix E was made possible by the support provided by ERDC, Vicksburg, MS, who sponsored the development of this computer program under the research project *Research into a Numerical Method for Computing Barge Impact Forces Based on Limit States for the Lashings Between Barge*.

The support provided by the University of Puerto Rico at Mayagüez to the researcher and graduate students who worked on the development of this product is also acknowledged.

At the time of publication of this report, Dr. James R. Houston was Director of ERDC, and COL James R. Rowan, EN, was Commander and Executive Director.

1 Introduction

1.1 Background

One of the most frequent loads applied to the locks of the inland waterway system is the impact made by a barge train as it aligns itself to transit the lock. Consequently, this load case represents one of the primary design loads considered by the U.S. Army Corps of Engineers for lock approach walls, guide walls, and guard walls. The primary focus of engineers performing these impact computations has been on the lock approaches where the worst-case loads are likely to occur.

In 1993, the Headquarters, U.S. Army Corps of Engineers, issued the first formal Corps-wide analysis procedure in the form of Engineer Technical Letter (ETL) 1110-2-338[1] providing guidance for analyzing the effects of barge impact loading on navigation structures. This ETL gives the basic equations of an engineering procedure for the collision of a barge train with a rigid structure. According to the ETL 1110-2-338 engineering procedure, the magnitude of the impact forces generated by a particular collision event is dependent on the mass including hydrodynamic added mass of the barge train, the approach velocity, the approach angle, the barge train moment of inertia, damage sustained by the barge structure, and friction between the barge and the wall. A major distinction between this procedure and the traditional Navy method for determining berthing forces is the estimation of collision energy dissipated in deformation of the barge structure and transferred to the rotation of the barge train. The analytical method uses the structural interaction mechanism of Minorsky (1959), which provides an empirical relationship between the nonrecoverable hull deformation and the energy absorbed in a collision. The relationship between kinetic energy lost in a collision and the volume of in-plane (barge) material damaged is used to determine impact force as a relationship to instantaneous contact area of damaged structure.

Minorsky used the conservation laws of momentum and energy and the principles of rigid-body mechanics to estimate the kinetic energy lost during a

---

[1] Headquarters, U.S. Army Corps of Engineers. 1993 (Apr). "Barge Impact Analysis," ETL 1110-2-338, Washington, DC. Headquarters, USACE, rescinded this Engineer Technical Letter in 2001.

collision between two vessels. He then calculated a resistance factor that is essentially the volume of material damaged in the bow of the striking ship and in the side of the struck ship. Minorsky reasoned that the principal resistance to collision penetration is provided by deep structure that suffers in-plane damage. For the case of a barge striking a fixed wall, the main deck, the bottom plate, the head log, and the transverse frames would offer resistance to damage. Minorsky selected and analyzed 26 actual ship collisions and correlated the energy absorbed in the collision with the Minorsky resistance factor. Using the equivalency between energy absorbed and the work performed in deforming the structure, a constant described as the force per unit of damaged surface area was defined (=13.7 ksi[1]). The Minorsky structural interaction mechanism is a constant pressure process operating with a pressure of 13.7 ksi acting over the instantaneous face area of the damaged element. This allows for the definition of an equivalent, *linear* spring constant representing the crushing of the barge structure in the ETL 1110-2-338 analytical formulation. It is important to note that the entire structural interaction mechanism is modeled as a linear spring in the direction of collision corresponding to the energy absorption in the *crushed* barge structure. The formulation becomes one of an initial value problem for barge train collision with a rigid wall, representing a lock wall in this case, and leads to the solution given in ETL 1110-2-338.

Two significant concerns have been raised since the ETL 1110-2-338 procedure had been released:

a. A key aspect of the ETL 1110-2-338 engineering formulation is computation of collision energy dissipated in nonrecoverable, plastic hull deformation of (i.e., damage to) the corner of the barge where impact with the wall occurs. However, the majority of the impacts made by barge trains transiting Corps locks do not result in damage to the barge structure or damage to the walls.

b. In addition, several engineers who have used the ETL 1110-2-338 engineering procedure have questioned the accuracy of the computed results.

To investigate these issues as well as to provide a basis for the development of an improved numerical impact model, a fully instrumented, full-scale impact experiment was devised to directly measure the impact forces (Patev et al. 2003). A easy-to-use empirical correlation was derived by Arroyo, Ebeling, and Barker (2003) that reports the maximum impact force (normal to the wall) as a function of the linear momentum normal to the wall (immediately prior to impact), using the results from the impact forces measured during these low-velocity, controlled, full-scale impact experiments. Arroyo, Ebeling, and Barker (2003) envision that this new empirical correlation will be used for impacts that do not involve damage during impact to either the corner barge of a barge train or to the wall. An alternate empirical correlation was given for the maximum impact force

---

[1] A table of factors for converting non-SI units of measure to SI units is found on page v.

(normal to the wall) as a function of the kinetic energy normal to the wall (immediately prior to impact) in Arroyo, Ebeling, and Barker (2003).

1.1.1 Full-scale, low-velocity controlled barge impact experiments

In December 1998, full-scale, low-velocity, controlled barge impact experiments were conducted at the decommissioned Gallipolis Lock at Robert C. Byrd Lock and Dam, Gallipolis Ferry, WV (Patev et al. 2003). The primary goal of these experiments was to measure the actual impact forces normal to the wall using a load-measuring device. The focus of these experiments was to obtain and measure the baseline response of an inland waterway barge, quantify a multiple-degree-of-freedom system during the impact, and investigate the use of energy-absorbing fenders. The full-scale experiment used a 15-barge commercial barge train with the configuration shown in Figure 1-1. Each barge was a jumbo open hopper rake design (35 by 195 ft) and was ballasted with anthracite coal to a draft of 9 ft. The total weight of the flotilla was 30,012 short tons. The total mass was 1,865.59 k-sec^2/ft, which was equal to the total weight divided by the gravitational constant, g. A total of 44 impact experiments were successfully conducted against the unaltered guide wall and a prototype fendering system. The angle of impacts ranged from approximately 5 to 25 deg, with velocities of 0.5 to 4 fps. Of these 44 experiments, a total of 12 bumper experiments were conducted at the lock, Experiments 28 through 31 and Experiments 37 through 44. The approach angle and velocity for the 12 most credible bumper experiments are summarized in Table 1-1. Impact velocity for these experiments ranged from 0.88 to 2.87 fps, with approach angles ranging from 8.8 to 21.1 deg.
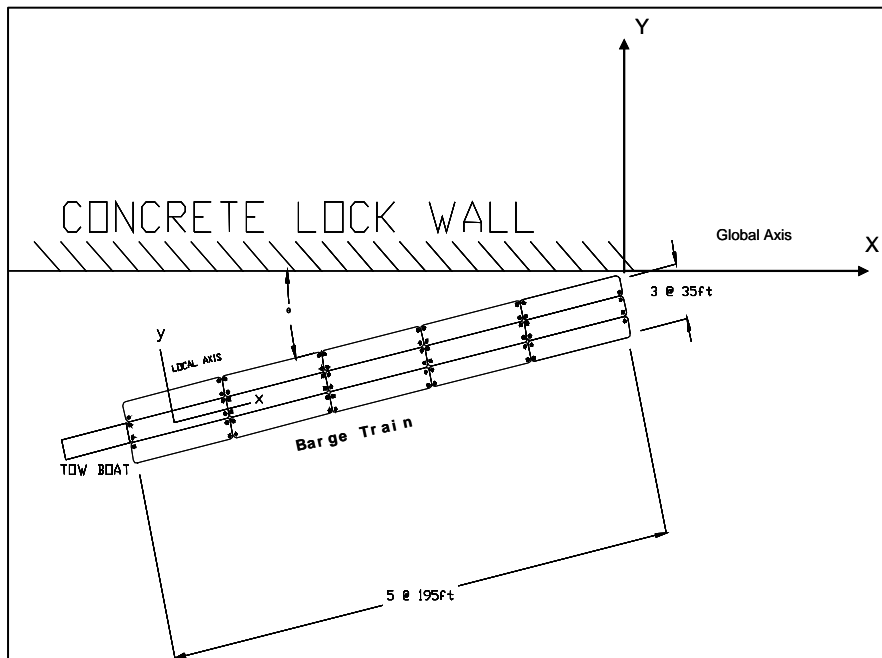
Figure 1-1.   Barge train-wall system

Table 1-1
Impact Velocity/Angle Data for Bumper Experiment

Experiment Number	Impact Angle, deg	Velocity		Velocity Normal to the Wall	
		fps	mph	fps	mph
28	9.7	2.41	1.64	0.41	0.28
29	12.7	2.2	1.5	0.48	0.33
30	12.2	2.35	1.60	0.50	0.34
31	10.6	1.61	1.10	0.30	0.20
37	10.3	1.92	1.33	0.35	0.24
38	11.9	1.83	1.25	0.38	0.26
39	14.1	1.61	1.10	0.39	0.27
40	17.5	1.91	1.30	0.57	0.39
41	8.8	2.86	1.95	0.44	0.30
42	17.5	1.83	1.25	0.55	0.38
43	21.1	0.88	0.60	0.32	0.22
44	20.90	1.22	0.83	0.44	0.30

The load bumper (or more specifically, the arc load beam) used to record the impact force time-histories during the experiments was constructed of mild steel with an outer radius of 72.6 in., outer arc length of 43.6 in., cross section measuring 9 in. in width by 5 in. in height, and separation between the 6-in.-diam load pins of 35.5 in. The interpretation of the instrumentation data recorded by Patev et al. (2003) is discussed in Arroyo, Ebeling, and Barker (2003). The following summarizes key aspects of the Arroyo/Ebeling/Barker interpretation. Once the time of impact was identified, the impact angle (the angle formed by the port side of the corner barge with the lock wall) was determined from the corrected Global Positioning System (GPS) data. This angle was critical to the bumper geometry and resulting force system. Velocity (actually speed) was simply calculated from the displacement of the front corner GPS unit per unit time (1 sec). The initial orientation of the bumper relative to the longitudinal axis of the barges was adopted to be 54 deg. Initially, the recorded forces at the pins were assumed to be in the radial direction. The precise orientation of the bumper on the barge was critical to this effort. The as-built orientation of the bumper was then determined from a combination of design drawings and documentary photos. The survey data were intended for this purpose; however, the uncertainty caused by the barges shifting and the tow drifting against its moorings between sightings compromised the accuracy of these measurements sufficiently to make them unusable for this purpose. Subsequently, it was established from the design drawings and documentary photos that the recorded forces were not aligned in the radial direction of the arc load beam. Taking into account this observed discrepancy, a new recorded forces orientation was established. This second configuration was analyzed considering the magnitude of the angles associated with the support reactions orientation. The results of this analysis indicated that an impossible geometrical arrangement was produced by this second set of assumptions. A final geometrical configuration was then established based on (a) the range of probable angles for the force orientations relative to the radial

direction, (b) the location of the bumper related to the longitudinal axis of the barges, and (c) the appropriate coefficient of friction between concrete (for the unarmored wall face) and steel arc load beam. It was demonstrated in Arroyo, Ebeling, and Barker (2003) that this final configuration produces reasonable results based on the values of the coefficient of friction between the wall and the steel bumper found in technical literature, and using the fact that the bumper must be in compression during the impact process. Based on a careful assessment of the results from this bumper study, only eight of the initial eleven bumper impact experiments were used in the empirical correlation developed by Arroyo, Ebeling, and Barker (2003) to estimate the maximum impact force normal to the wall.

1.1.2 Empirical correlations

The concept of mass arises in two of Newton's laws. In the second law, inertial mass is considered to be a measure of the resistance of a particle to acceleration. In Newton's fourth law, gravitational mass is defined as the property of the particle that influences its gravitational attraction. Newton further assumed that these two concepts of mass were equivalent. The mathematical form of Newton's second law states that a resultant external force F applied to a body is equal to the mass of the body m multiplied by the absolute acceleration a the body experiences. Also, it can be expressed in terms of the absolute velocity of the body by introducing the first derivative with respect to time of the velocity, which is the acceleration. One useful tool that can be derived from Newton's second law, $F = ma$, is obtained by integrating both sides of the equation with respect to time. This integration can be done only if the forces acting on the particle are known functions of time. The external forces acting on the particle change the linear momentum. The mathematical form of the resulting expression after the process of integration states that the impulse during a period of time due to the applied impulsive force is equal to the difference in linear momentum during the same interval of time. This relationship establishes the *Principle of Impulse and Linear Momentum*. The units of both impulse and momentum are force and time, and therefore, impulse and momentum are expressed in Newtons-second, or kips-second. The impulsive force is a function of time and, in general, varies during its period of application. A large force that acts over a short period of time is called an *impulsive force* and occurs during phenomena such as the impact of a bat with a ball, collisions of cars, or a barge impacting a lock wall. If the average impulse force is zero, the linear momentum does not change during that interval of time.

The linear momentum is defined as the mass of the particle multiplied by the velocity of the particle. It is a vector quantity oriented in the same direction as the velocity of the particle (tangent to the trajectory). The velocity of a barge train is usually specified in the local barge axis: longitudinal = local x-axis and transverse = local y-axis. In this case two velocities are specified, that is, V_x and

V_y.[1] To obtain the velocity normal to the wall, an axis transformation equation is needed:

$$\begin{Bmatrix} V_{par} \\ V_{norm} \end{Bmatrix} = [C]^{-1} \begin{Bmatrix} V_x \\ V_y \end{Bmatrix} \qquad (1\text{-}1)$$

where

$$[C]^{-1} = \begin{bmatrix} cos\,\theta & -sin\,\theta \\ sin\,\theta & cos\,\theta \end{bmatrix},$$

and V_{par} and V_{norm} are the velocity parallel (global X-axis) and normal (global Y-axis) to the wall, respectively. Equation 1-1 can be easily obtained from Figure 1-2.
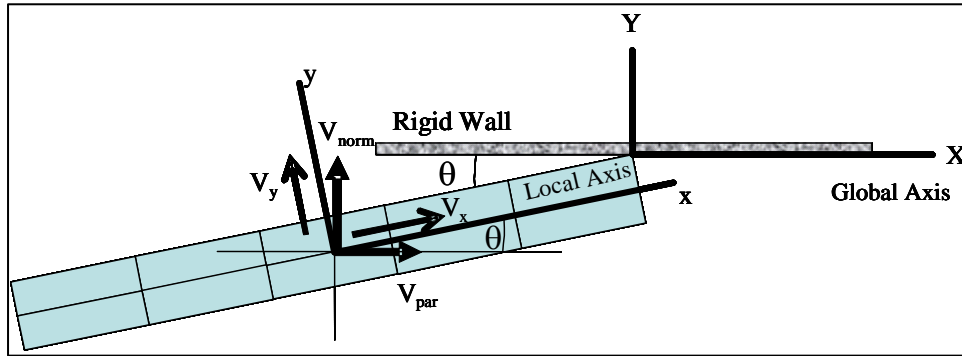
Figure 1-2.   Velocity vector transformation from local to global axis

The empirical correlation between the maximum force normal to the wall and the linear momentum normal to the wall immediately prior to impact, developed by Arroyo, Ebeling, and Barker (2003), was based on statistical procedures and the values of maximum impact force obtained from the acceptable bumper configuration. Using values for the maximum normal force $(F_W)_{max}$ and the linear momentum normal to the wall mV_{norm}, a best-fit straight line was calculated using data from eight of the full-scale impact experiments. This approach relates the maximum F_W obtained from the energy method directly to the linear momentum. It is important to note that only one data point of the entire F_W time-history for each of the eight experiments was used to develop this empirical correlation. The least squares regression procedure was used to develop the best-fit straight line through the eight data points (for the eight impact experiments) for the empirical correlation (see Appendix D in Arroyo, Ebeling, and Barker 2003). The line was assumed to start at the origin (i.e., no intercept term was used for the linear equation). The resulting best-fit straight line, average minus one standard error

---

[1] For convenience symbols are listed and defined in the Notation (Appendix F).

(SE), and average plus one standard error lines were developed as shown in Figure 1-3. The resulting best-fit equation for this set of eight data values is $(F_W)_{max} = 0.435 m V_{norm}$, with units of the resulting force in kips, mass (including the mass of the loaded barges and towboat but excluding hydrodynamic added mass) in kip-sec^2/ft, and approach angle in degrees. That is, a coefficient times the linear momentum normal to the wall determines the maximum force normal to the wall. The greater the magnitude for the linear momentum, the larger will be the maximum value for the impact force normal to the wall. This relationship was based on low-velocity, shallow-impact (up to 21.1 deg) experiments that, by definition, do not account for factors that manifest themselves at higher velocities. Additionally, no damage occurred to the flotilla of barges and no lashings broke during these eight impact experiments. This empirical correlation was derived using data obtained from a 3 by 5 barge train that had a velocity normal to the wall up to and not exceeding 0.57 fps (0.39 mph) with no damage occurring during impact events, for impact angles up to 21.1 deg, and for a barge flotilla with a linear momentum normal to the wall between 649.84 and 1,025.48 kip-sec.

Figure 1-3. Empirical correlation using the linear momentum normal to the wall concept (Figure 6.3 in Arroyo, Ebeling, and Barker 2003)

The maximum normal force $(F_W)_{max}$ by the empirical correlation is equal to the reaction force provided by the lock wall on the barge train during the impact. Note that the masses used to develop the correlation of linear momentum normal to the wall with values of $(F_W)_{max}$ use the mass of the barge train and do *not* include the computation of any hydrodynamic added masses. (However, hydrodynamic effects on the barge train are accounted for in the measured impact forces.) A single lumped mass was used to characterize the barge train in this simplified correlation.

An additional empirical correlation between the maximum force normal to the wall and the kinetic energy of the barge train normal to the wall was presented in Arroyo, Ebeling, and Barker (2003). The kinetic energy is defined as $T = \frac{1}{2}(mv^2)$, where *m* is the mass of the object (not including hydrodynamic

added mass) in units of kip-sec^2/ft and v is the speed of the object in units of ft/sec. The kinetic energy has the same units as work, e.g., ft-lb. Using the values of maximum normal force $(F_W)_{max}$ from eight of the impact experiments and the kinetic energy of the system normal to the wall immediately prior to impact, a best-fit straight line was calculated. A least squares regression procedure was used to develop the best-fit straight line through the eight data points (for the eight impact experiments). The line was assumed to start at the origin (i.e., no intercept term was used for the linear equation). The resulting best-fit straight line, average minus one standard error, and average plus one standard error lines are shown in Figure 1-4. It can be observed that the greater the magnitude for the kinetic energy, the larger will be the maximum value for the impact force normal to the wall. This correlation is also based on low-velocity, shallow-impact (up to 21.1 deg) experiments that, by definition, do not account for factors that manifest themselves at higher velocities. Additionally, no damage occurred to the flotilla of barges and no lashings broke during these eight impact experiments. This second empirical correlation was derived using data for a 3 by 5 barge train that had a velocity normal to the wall up to and not exceeding 0.57 fps (0.39 mph) with no damage occurring during impact events, for impact angles up to 21.1 deg, and for a barge flotilla with a kinetic energy normal to the wall between 83.95 and 282.17 kip-ft.
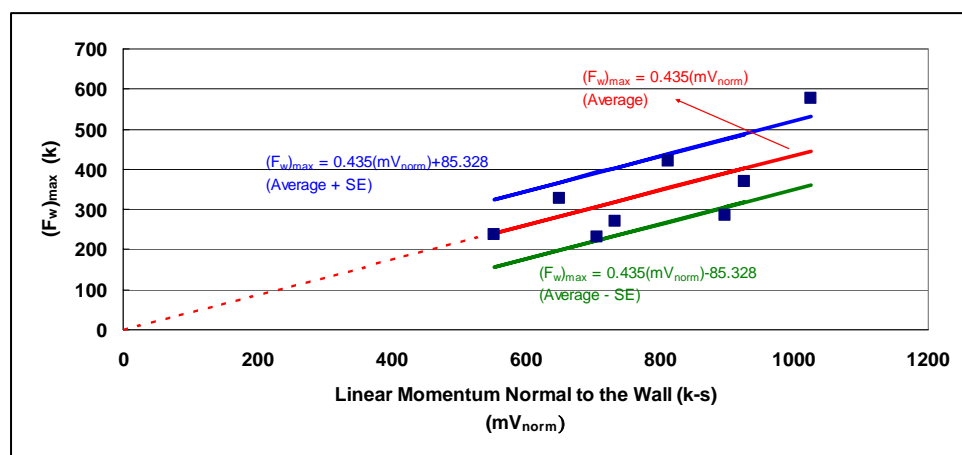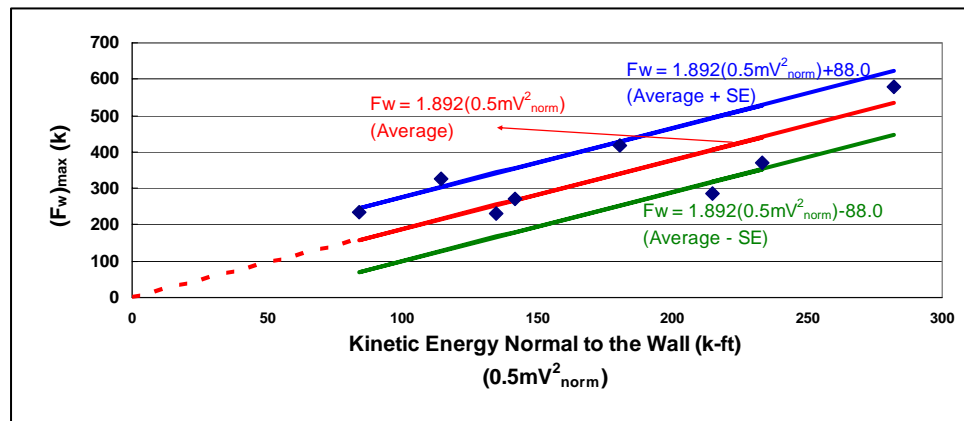

Figure 1-4.   Empirical correlation using the kinetic energy normal to the wall concept (Figure 6.4 in Arroyo, Ebeling, and Barker 2003)

It is important to mention that the velocity normal to the wall now designated as V_{norm} in Figure 1-2 was originally designated as $V* \sin \theta$ in Arroyo, Ebeling, and Barker (2003). That is, $V* \sin \theta$ is equivalent to the term $V_x* \sin \theta$ with V_y equal to zero. In the same way, the kinetic energy T normal to the wall in Arroyo, Ebeling, and Barker (2003) was expressed as $(0.5mv^2)$ where v is the velocity normal to the wall and now is expressed as $(0.5mV^2_{norm})$. Of these two empirical correlations (Figures 1-3 and 1-4) from Arroyo, Ebeling, and Barker (2003) the authors are recommending Figure 1-3 at the time of this publication.

1.2 Failure Mechanisms – Longitudinal, Transverse, and Corner

The empirical correlations given in Figures 1-3 and 1-4 are based on data from eight low-velocity, controlled barge impact experiments in which there was *no damage* to the barge and *no failure* of the lashing(s). Thus these two linear empirical correlations are valid only below a limit state in which either crushing of the corner of the impacted barge or ultimate strength of the lashing(s) occurs. Either limit state would introduce an asymptote to Figures 1-3 and 1-4 empirical correlations. The Figure 1-5 idealization demonstrates the point that the empirical correlations must have a limiting force value that occurs, for example, when the lashings yield and the barge train breaks apart into individual barges.
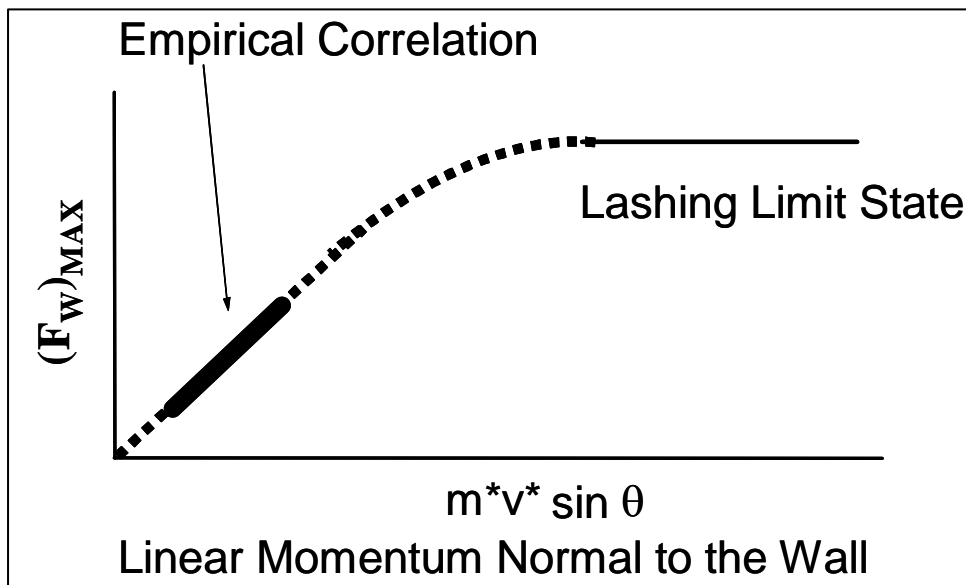
Figure 1-5.   The empirical correlation and the lashing limit state

During the impact of a barge train against the wall, forces are transferred from the point of contact to the barges that form the barge train. These forces are transferred by the contact between the barges and the lashings that join the barges. The lashings are prestressed in an attempt to prevent any initial angular motion between the barges before the internal stress begins to increase within the lashings. At the instant of impact, a failure plane can be defined such that all lashings break along this plane; thus the forces acting on the wall are reduced compared with those of an intact barge train impact. Three principal lashing failure mechanisms were identified. These potential failure planes are designated by the authors of this report as the (a) longitudinal, (b) transverse, and (c) corner failure mechanisms. During the course of research to be discussed in this report, each of these three failures mechanism was studied in detail. In each case a single type of failure plane was required to occur in such a way that the force normal to the wall was computed. Each of these idealized failure planes defines two

systems of barges. That is, two systems of barges are obtained by analyzing each of the barge systems created, one on each side of the potential failure plane. The limit state can be reached as soon as the lashing achieves its ultimate (tensile) stress and possibly even brakes across a predefined plane that is designated as a potential failure plane.

1.2.1 Longitudinal failure mechanism

Figures 1-6 and 1-7 show the longitudinal failure mechanism. The two barge systems are defined as System 1, the row of barges in direct contact with the wall; and System 2, a second barge system that tries to continue motion as shown in Figure 1-6. The relative motion between the two barge systems is the source of the strain in the lashing, increasing the internal force until the lashings reach ultimate strength.
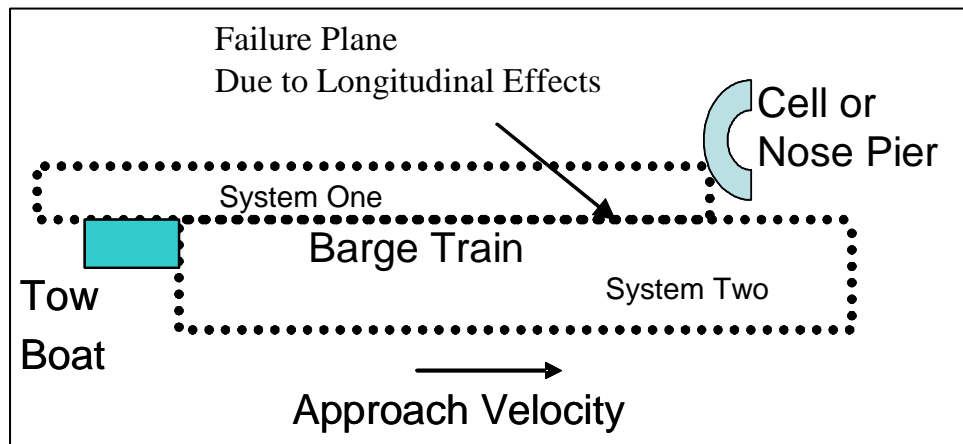
Figure 1-6.   Longitudinal failure mechanism for a head-on impact (θ = 90 deg)

In this longitudinal failure mechanism the following general assumptions are made:

a. One group of barges in the system, System 1, stops immediately after impact occurs with a "rigid" wall.
b. The second barge group, System 2, continues the forward motion, thereby increasing the internal force of the lashings along the designated potential failure plane (i.e., the plane along which relative motion occurs).
c. Each of the two systems is assumed to be a rigid body.
d. The lashings are modeled as having elastoplastic behavior that breaks when an ultimate (tensile) strain value is achieved within the lashing.
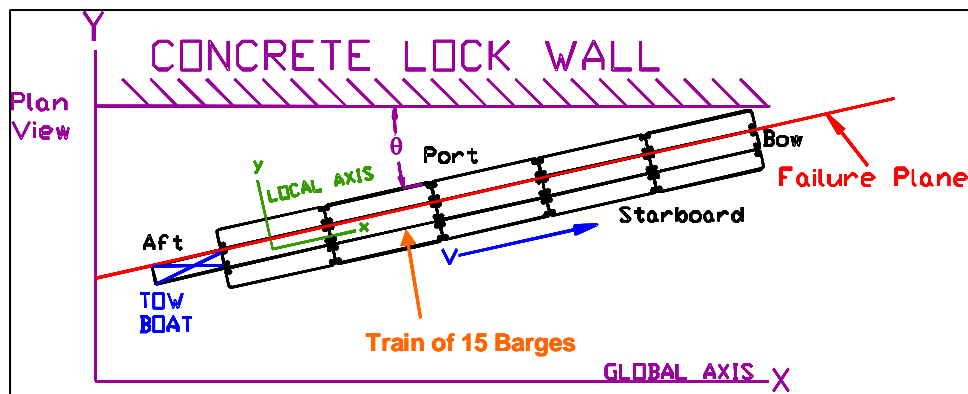
Figure 1-7. Longitudinal failure mechanism: Lashing yields along a longitudinal failure plane between barges

1.2.2 Transverse failure mechanism

The transverse failure mechanism results from achieving the ultimate tensile stress within the lashings that join the first column of barges to the rest of the system as idealized in Figure 1-8. The first line of transverse lashings from the bow to the aft of the barge train is the line that defines this potential failure mechanism. Generally speaking, it is a failure plane that is perpendicular to the longitudinal failure mechanism. For this failure mechanism, two barge systems define this potential failure plane. System 1 is defined by the first column of barges, the barges in direct contact to the wall. System 2 is defined by the remaining barges. It is hypothesized that immediately after the impact the first column of barges begins to rotate with a pivot on the starboard side at the first connection behind the bow, as can be observed in Figure 1-8. It is envisioned that a barge train with a shallow approach angle (e.g., a "glancing" blow) will be susceptible to this potential failure mechanism. The lashing in the first connection from the bow to the aft on the port side is the lashing with the higher deformation (i.e., elongation). The other internal lashings along this potential failure plane will have lower elongation than the elongation in the lashing(s) on the port side (closest to the wall). As the barge train continues the motion toward the wall, the lashings across this idealized failure plane continue to elongate up to their ultimate tensile value due to the rotation of System 1.

In this transverse failure mechanism the following general assumptions are made:

a. The barges of System 1 have zero acceleration normal to the wall immediately after impact occurs with the "rigid" wall.
b. System 2 continues the forward motion, and System 1 continues the rotation, increasing the internal force of the lashing(s) across the failure plane.
c. Each of the two barge systems is assumed to be a rigid body.

d. The lashings are modeled as having elastoplastic behavior that causes them to break when an ultimate (tensile) strain value is achieved within the lashing.
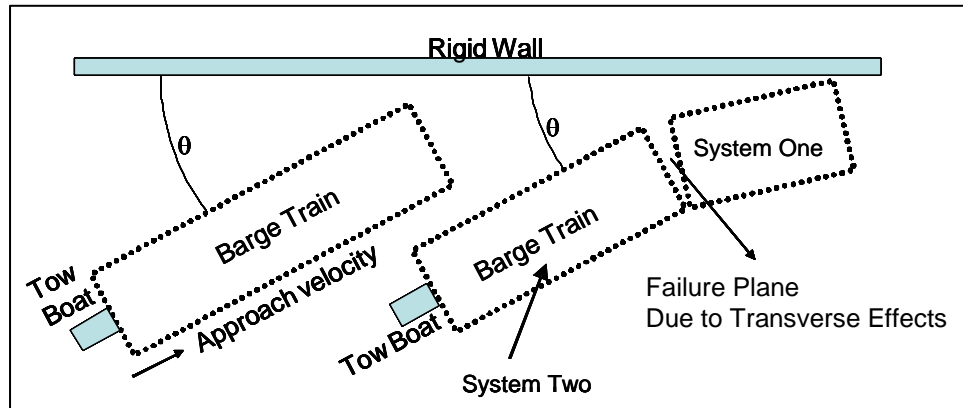
Figure 1-8.   Transverse failure mechanism

There are two possible tendencies of rotation in the transverse failure mechanism. If the line of action of the resultant force at the point of contact lies to the front of the center of mass of System 1, then the pivot point will be at the starboard side of the barge train as shown in Figure 1-9. On the other hand, if the line of action of the resultant force at the point of contact of the barge train and the rigid wall lies behind the center of mass, then the pivot point will be at the port side of the barge train as shown in Figure 1-10. These two possibilities will be presented in Chapter 3, and the parameters required for the occurrence of both conditions will be shown.

1.2.3. Corner failure mechanism

The third failure mechanism studied in this research is designated the corner failure mechanism. It is a special case of the transverse failure mechanism because it includes all but one of the general assumptions made for the transverse failure mechanism. The third assumption (that each of the two barge systems is assumed to behave as rigid bodies) is not adopted in this failure mechanism. In this mechanism, a relative rotation of the impacted barge (corner barge) in System 1 is allowed. As shown in Figure 1-11, System 1 allows for a relative rotation of the corner barge. This condition can be reached if the lashings that join the barges of System 1 to the rest of the barge train are considered to elongate during the process of impact.
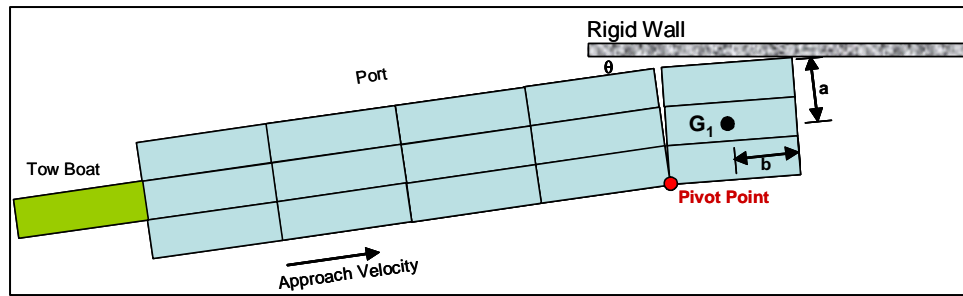
Figure 1-9.   Pivot point at the starboard side of the barge train
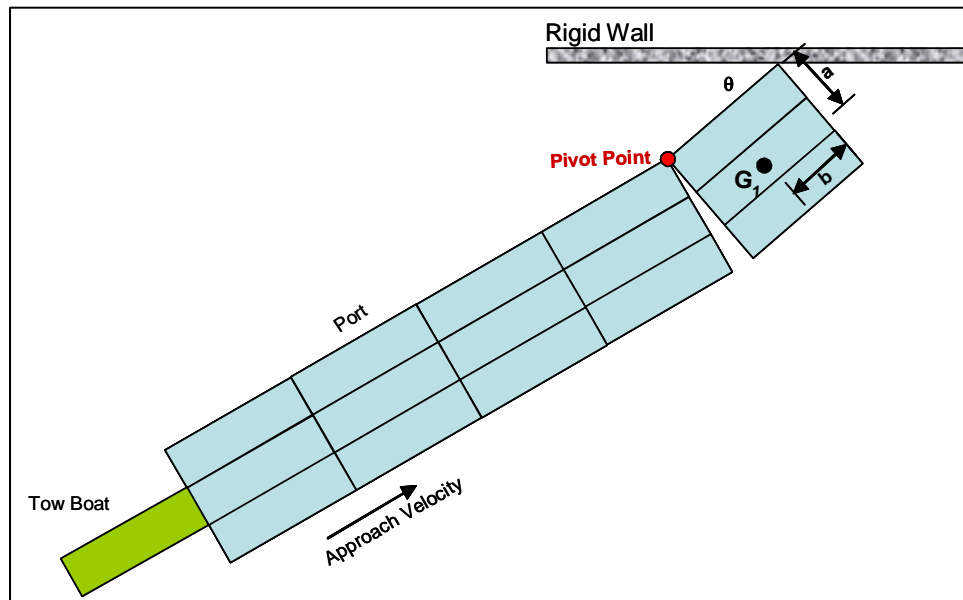
Figure 1-10. Pivot point at the port side of the barge train
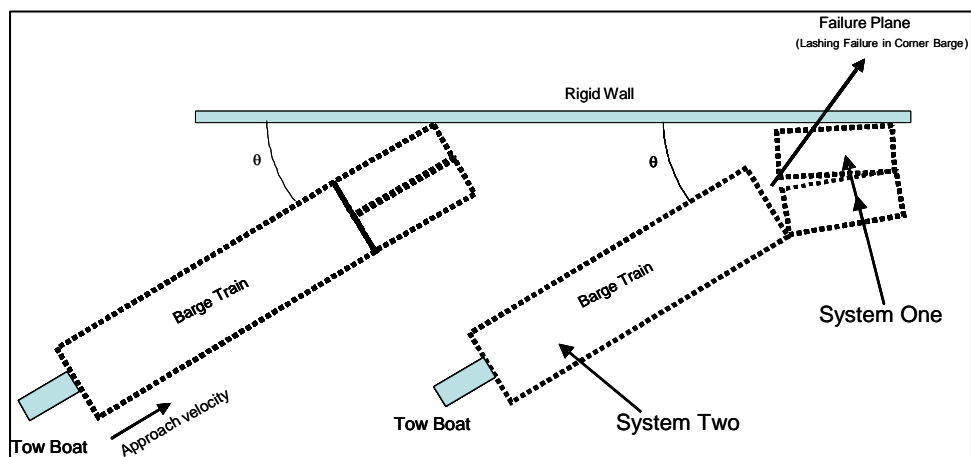
Figure 1-11. Corner failure mechanism

In this case, as was the case for the other two idealized potential failure mechanisms, the potential failure plane defines two barge systems. System 1 is defined by the barges in direct contact with the wall, and System 2 consists of the remaining barges. Basically, it is the same behavior as the transverse failure mechanism but with the addition of the relative rotation of the corner barge in System 1. The relative rotation occurring in System 1 is easily addressed. To produce this relative rotation, one has to provide some elongation in the lashing that joins the corner barge to the other barges in System 1. As soon as these lashings achieve their ultimate (tensile) strain value and break, the corner barge alone rotates toward the wall as idealized in Figure 1-11. In general, for shallow approach angles with lashing configurations typical of those given in Appendix A, the authors of this report found in a limited number of studies that the corner failure mechanism prevailed over the other two failure mechanisms. This behavior is possible due to the nonrigid connections assumptions in System 1 of the corner failure mechanism.

In this corner failure mechanism the following general assumptions are made:

a. The barges of System 1 have zero acceleration normal to the wall immediately after impact occurs.
b. System 2 continues its forward motion, and System 1 continues the rotation, increasing the internal force within the lashings across the failure plane.
c. The connections of barges in System 1 are flexible, allowing the relative rotation as shown in Figure 1-11.
d. The lashings are modeled as having elastoplastic behavior causing them to break when an ultimate (tensile) strain value is achieved within the lashings, as shown in Figure 1-12.

The analysis of these idealized failure mechanisms is dependent on many factors that will be explained in the subsequent chapters. However, the most important variables are the lashing properties and lashing configurations. Lashing configurations are the arrangements of the lashing between barges from bit to bit. Also, the number of turns of the lashings around the bits impact computed results for all three idealized limit states. A detailed example of lashing configuration is discussed in Appendix A, and the calculation of bit locations on a barge is presented in Appendix C.
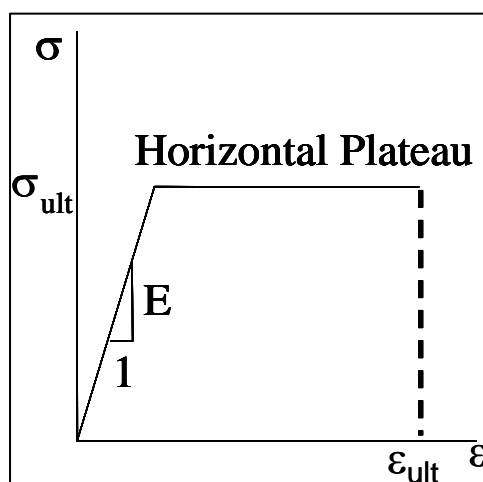
Figure 1-12. Elastoplastic constitutive relationship used for the lashings

1.2.4 Progressive yielding of lashings

Lastly, the limit state, which is defined as an event that occurs when lashings yield, can be used to define a value of $(F_W)_{max}$ due to the impact process. This maximum normal force to the wall can be calculated assuming the lashings provide the maximum strength to the connections between barges. The progressive process that defines the failure of the system for the transverse failure mechanism is idealized in Figure 1-13. This figure presents the state of the lashings as the process of impact develops. As impact begins, the internal stress within the lashing increases, but this increase occurs within the elastic zone (Figure 1-13a). Later, as the rotation of the front barges (i.e., System 1) increases, the lashing at the port side of the transverse failure plane is in a state of ultimate stress but the internal lashings are in an elastic state (Figure 1-13b). Finally, the rotation continues increasing until all lashings across the failure plane achieve ultimate stress and their ultimate (tensile) strain value, producing a transverse failure of the lashings across the transverse failure plane of the barge system (discussed in Chapter 3). This sketch idealizes the progressive development of the transverse failure mechanism process assuming an elastoplastic behavior of the lashings and their ultimate rupture. A similar process will apply to the longitudinal and corner failure mechanisms. In the longitudinal failure mechanism process, the ultimate strength is reached as the relative motion between System 1 and System 2 increases, as discussed in Chapter 2. The corner failure mechanism exhibits the same general behavior depicted in Figure 1-13 but includes a relative rotation between the corner barge and the remaining barges of System 1, resulting in a failure of the lashing that joins the corner barge to the rest of the barge train, as discussed in Chapter 4.

The analysis is conducted by applying Newton's second law (equations of motion applied to Systems 1 and 2), and the unknown internal and external forces are computed. The equations of motion as stated by Newton's second law were developed for each of the three failure mechanisms. The resulting three limit state models follow this approach where the angular acceleration, translational (linear) acceleration, and external and internal forces are variables to be assessed in the computations. These formulations are discussed in detail in Chapters 2 through 4.
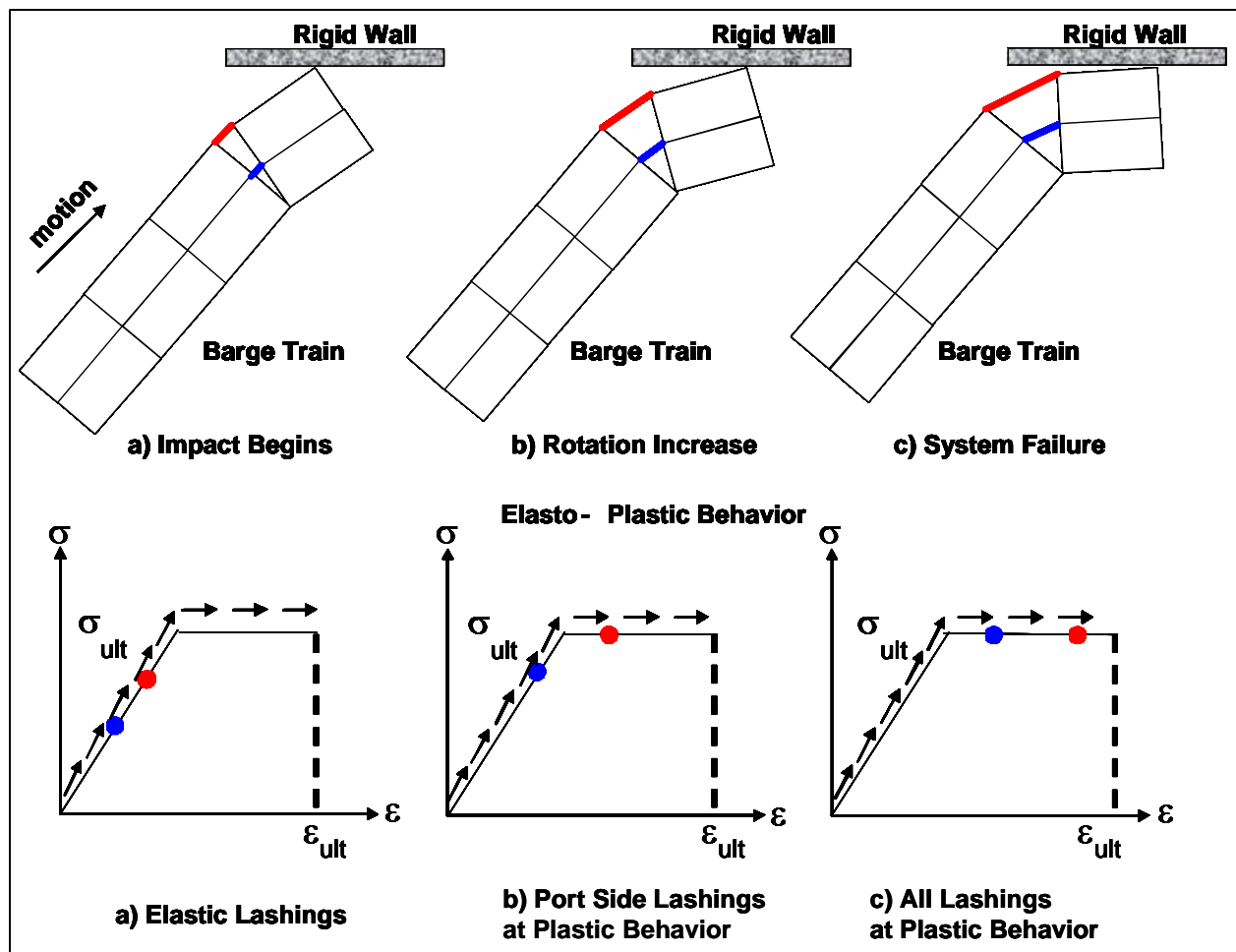
Figure 1-13. Example of a progressive barge train failure for the transverse failure mechanism

2 Longitudinal Failure Mechanism

2.1 Longitudinal Failure Mechanism

A barge train system consists of a group of barges joined together with steel cables, which are referred to as lashings. These lashings define a system of potentially weak zones at each barge-to-barge contact. The motion of each barge relative to the others has direct bearing on how the barge train system distributes the impact forces among the barges during the impact process. As has been observed during barge train impact events, an almost direct impact of a barge train system on an end cell or nose pier can produce a failure of lashings in the longitudinal axis of the barge system. This failure extends from the bow to the aft of the barge train system. This is comparable to a shear failure mechanism in which the barge train separates into two columns of barges with one system of barges moving relative to the other system of barges. An example of this idealized failure mechanism is shown in Figure 2-1 for a barge train of 15 barges that impacts a concrete lock wall at an approach angle θ. This potential failure mechanism, designated as the longitudinal failure mechanism, is based on the relative motion of a two-system barge train with each system of barges developing on each side of a longitudinal failure plane.
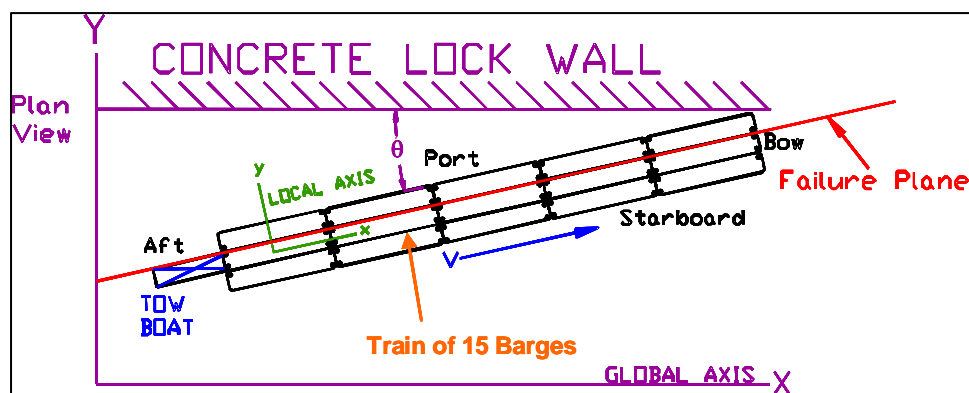
Figure 2-1.   Longitudinal failure mechanism: Lashing fails along a longitudinal failure plane between barges
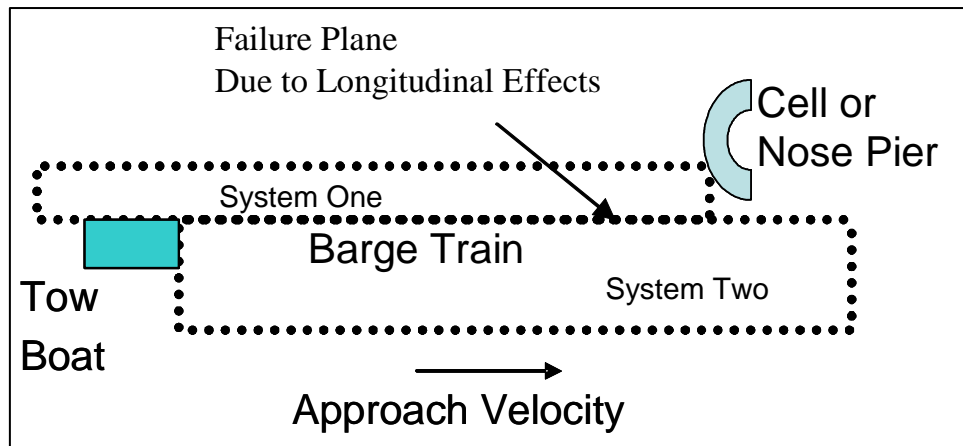
Figure 2-2. Longitudinal failure mechanism for a head-on impact (θ = 90 deg) (repeated from earlier text for convenience of the reader)

Figure 2-2 idealizes a barge train impacting an end cell or nose pier and the development of a failure plane along the longitudinal axis of the system. Based on this figure, two systems of barges can be identified. The system that is in direct contact with the wall is called System 1, and the remaining barges form System 2. If the impact is with the corner barge of the barge train, then the row of lashings between the first and second row of barges along the longitudinal axis will deform more than the other lashings in the barge train. In this idealized failure mechanism both systems of barges are assumed to be rigid and no transverse relative motion is allowed.

In this simplified model, each of the barge systems is idealized as a rigid body and the wall is assumed rigid. When barge System 1 impacts the *rigid* wall head-on (as depicted in Figure 2-2), it is subject to a boundary condition of no further forward movement. Barge System 2 would tend to continue its forward motion as if it were not subject to "constraints." Note that System 2 is not subject to the same severe constraint that System 1 is (i.e., forward movement being prevented by the presence of a rigid wall). Instead, System 2 is subject to a constraint that is imposed by its lashings connection to System 1. It is reasoned that barge System 2 rigid body will have to decelerate only because it is "lashed" to barge System 1 with a finite number of cables (i.e., lashings), each with a finite tensile strength. Note that in the extreme, should the lashings between Systems 2 and 1 be of zero or only a nominal tensile strength, System 2 would continue its forward motion without decelerating. It is further reasoned that when System 1 stops its forward motion upon impact with a rigid wall, it will decelerate at a more rapid rate than will System 2, as shown in Figure 2-3. Consequently, it is envisioned for this simplified model that the deceleration of barge System 2 will be at a far different and lower deceleration rate than occurs for System 1. The magnitude of the deceleration for System 2 is a function of the number and orientation of the lashings as well as their size, ultimate capacity, and condition (e.g., new, used but in good condition, used and in poor condition, etc.).
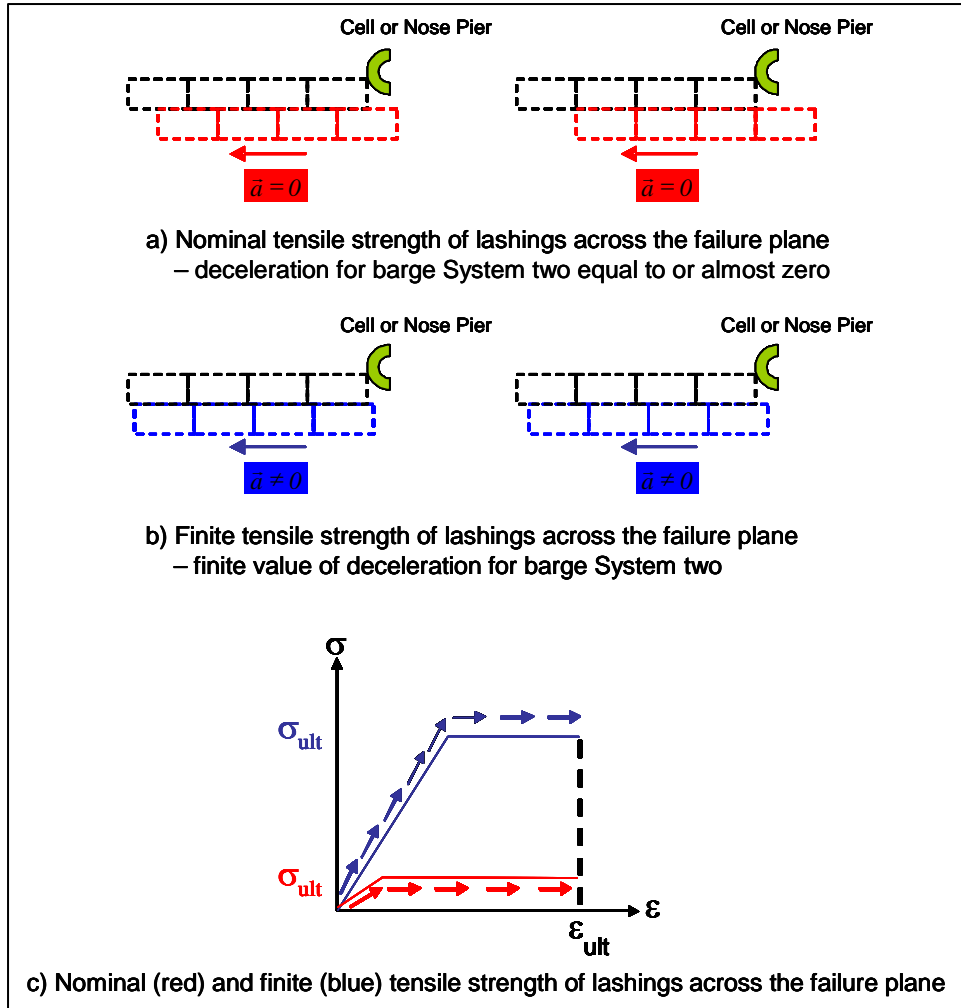
Figure 2-3.   Nominal and finite tensile strength of lashing

In this model, the longitudinal failure mechanism allows the relative displacement between barges in the local (barge) *x*-direction (see Figure 2-1). In this way, all the lashings along the longitudinal failure plane will break by means of the relative displacement between barges of System 1 and System 2, as shown in Figure 2-2. The relative displacement can be obtained by assuming different linear accelerations in the global Y-direction for Systems 1 and 2. A zero linear global acceleration in the Y-direction of System 1 is assumed in this simplified model because the impact with a *rigid* wall occurs with this system in the global Y-direction. System 2 motion continues and the lashings that connect System 1 to System 2 will try to stop or decelerate System 2. Thus, the deceleration of System 2 is nonzero. As will be shown in Equation 2-1, the summation of forces in the global Y-direction of System 1 is set equal to zero, consistent with this assumption. However, as will be seen in Equation 2-3, the global Y-linear deceleration of System 2 is nonzero.

To study this failure mechanism, the equations of motion based on Newton's second law are used. First, a free-body diagram is defined as shown in Figure 2-4. In this diagram appear all the known and unknown forces in the system. The

unknown external forces are F_W and S_W, and the internal unknown forces are the resultant barge-to-barge normal F_{NC} and the internal moment M. In this model the internal shear is related to the normal force by means of the steel-steel kinetic coefficient of friction μ_K; $S_{NC} = \mu_K F_{NC}$. The known forces are the internal force in each lashing as the motion takes place. These forces are labeled as f_{Ni} and f_{Si}
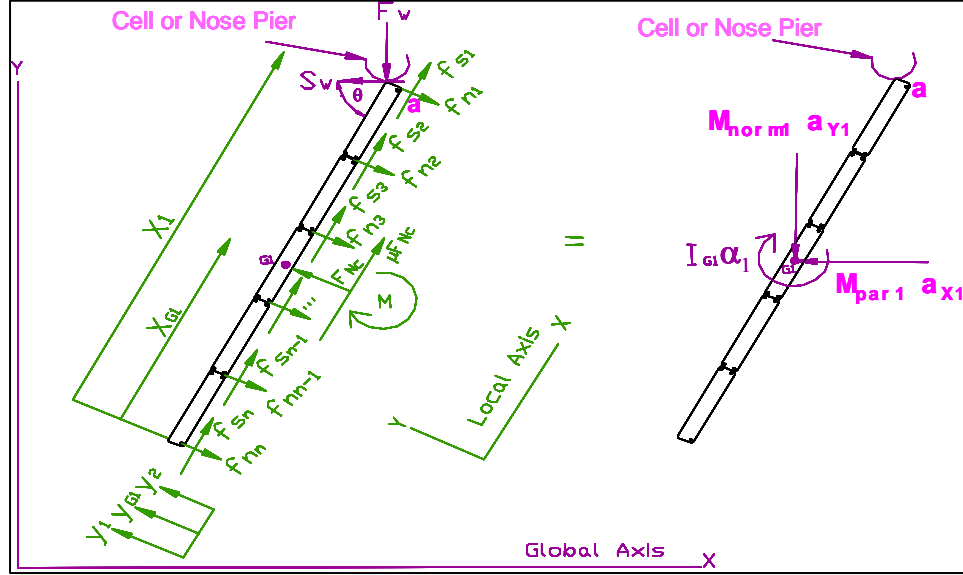
Figure 2-4. Longitudinal failure mechanism: Free body diagram and kinetic diagram of System 1 oriented at approach angle θ

The free-body diagram should be equal to the kinetic diagram as stated by Newton's second law. Figure 2-4 also depicts the linear accelerations and angular accelerations of System 1. In this case the linear accelerations are oriented in the global X- and Y-axes. From Figure 2-4 the three equations of motion can be written with the summation of moments about point *a:* the intersection of the bow and the longitudinal failure plane. For System 1, which is in contact with the wall, the equations of motion are

$$\oplus \to \sum F_X = ma_X \therefore -S_W + Rs_X + Rn_X - F_{NC}\sin\theta + \mu_K F_{NC}\cos\theta = -M_{par1}a_{X1} \qquad (2\text{-}1)$$

$$\oplus \uparrow \sum F_Y = ma_Y \therefore -F_W + Rs_Y - Rn_Y + F_{NC}\cos\theta - \mu_K F_{NC}\sin\theta = -M_{norm1}a_{Y1} = 0; \qquad (2\text{-}2)$$
$$M_{norm1}a_{Y1} = 0$$

$$\oplus \sum M_a = (\sum M_{EQUIVALENT})_a \therefore M - M_{Rfn} + F_{NC}(x_1 - x_{G1}) - (F_W\sin\theta + S_W\cos\theta)(y_1 - y_2) = \qquad (2\text{-}3)$$
$$I_{\theta1}\alpha_1 - (M_{par1}a_{X1}\cos\theta)(y_{G1} - y_2) + (M_{par1}a_{X1}\sin\theta)(x_1 - x_{G1})$$

where

S_W = shear force between corner barge and the wall

Rs_X = global X-axis component of the resultant force parallel to the failure plane obtained from the lashing forces

Rn_X = global X-axis component of the resultant force perpendicular to the failure plane obtained from the lashing forces

F_{NC} = resultant normal force at the failure plane due to contact of barges (normal pressure between barges sides at the failure plane)

μ_K = steel-to-steel kinetic coefficient of friction between the barges

θ = approach angle

M_{par1} = mass of System 1 parallel to the wall (including hydrodynamic added mass)

a_{X1} = global X-axis linear acceleration of System 1

F_W = force normal to the wall at point of impact

Rs_Y = global Y-axis component of the resultant force parallel to the failure plane obtained from the lashing forces

Rn_Y = global Y-axis component of the resultant force perpendicular to the failure plane obtained from the lashing forces

M_{norm1} = mass of System 1 normal to the wall (including hydrodynamic added mass)

a_{Y1} = global Y-axis linear acceleration of System 1 equal to zero

M = internal moment at failure plane (it is due to eccentricity of the resultant normal force related to the center of mass)

M_{Rfn} = resultant moment due to the lashing forces normal to the failure plane

x_1 = length of barge train

x_{G1}, y_{G1} = local axis coordinates of the mass center of gravity measured from the corner between the aft and the starboard sides

y_1 = distance measured along the local y-axis that locates the port side from the corner between the aft and starboard sides

y_2 = distance measured along the local y-axis that locates the failure plane from the corner between the aft and the starboard sides

$I_{\theta 1}$ = mass moment of inertia of System 1 (including hydrodynamic added mass)

α_1 = angular acceleration of System 1

Four parameters that affect the force normal to the wall are the global *X*- and *Y*-axis components of the forces parallel (Rs_x and Rs_y) and perpendicular (Rn_x and Rn_y) to the failure plane obtained from the internal force in the lashings. These forces are obtained in the following form. Due to the elongation of the lashing during the deformation process, an internal force appears in the lashings. The angle of each segment of the lashings with the longitudinal local axis is calculated using the local coordinates of the start (x_s, y_s) and end (x_e, y_e) bits that connect each segment of each lashing. Then, the components of these forces in local coordinates are easily transformed to forces in the global coordinates system by means of the transformation matrix that contains the sine and cosine functions. As shown in Figure 2-5, these forces can be easily obtained by the use of trigonometric functions. For example, $Rn_x = F_L * sin\ \delta$, and

$Rn_Y = Rn * cos\ \theta$, where R_n is the internal force at each segment (from bit to bit) of each lashing at failure plane; F_L is the internal force at each segment (from bit to bit) of each lashing; and δ is the angle of each segment (from bit to bit) for each lashing, measured from the local positive x-axis.
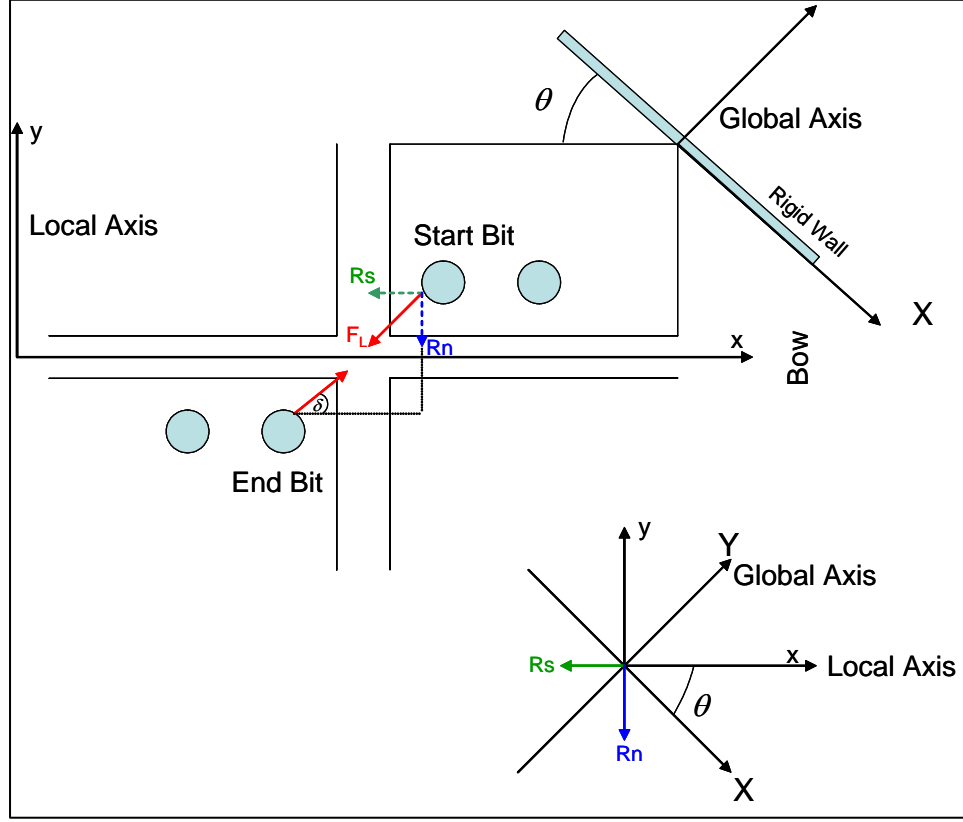
Figure 2-5.   Global components of lashing force

Hydrodynamics effects are included in barge System 1 using the ETL 1110-2-338 approach:

$$M_{x1} = (1 + \eta_x) * m_1 \tag{2-4}$$

$$M_{y1} = (1 + \eta_y) * m_1 \tag{2-5}$$

$$I_{\theta 1} = (1 + \eta_\theta) * I_{G1} \tag{2-6}$$

$$I_{G1} = \frac{1}{12} * m_1 * \left(L_1^2 + B_1^2\right) \tag{2-7}$$

$$M_{norm1} = \frac{M_{x1} * M_{y1}}{M_{x1} cos^2\ \theta + M_{y1} sin^2\ \theta} \tag{2-8}$$

$$M_{par1} = \frac{M_{x1} * M_{y1}}{M_{x1} sin^2\ \theta + M_{y1} cos^2\ \theta} \tag{2-9}$$

with the hydrodynamic added mass coefficients defined in the local barge coordinate system, according to ETL 1110-2-338, as

$$\eta_x = 0.05$$
$$\eta_y = 0.4$$
$$\eta_\theta = 0.4$$

and where

M_{x1} = mass plus hydrodynamic added mass of barge System 1 in the barge longitudinal direction

m_1 = mass of System 1 (excluding hydrodynamic added mass)

M_{y1} = mass plus hydrodynamic added mass of barge System 1 in the barge transverse direction

I_{G1} = second mass moment of inertia for barge System 1

L_1 = length of barge System 1

B_1 = width of barge System 1

The angular acceleration for System 1, α_1, is assumed equal to the angular acceleration for System 2, α_2, for this simplified longitudinal failure mechanism: $\alpha_1 = \alpha_2 = \alpha$.

The authors of this report recommend that hydrodynamic effects be considered in the simplified limit state analyses. Therefore, Equations 2-1 through 2-3 will include hydrodynamic added mass terms via Equations 2-4 through 2-9.

Applying the same procedure to System 2, which contains the rest of the barge train, gives three additional equations of motion. As always, its free-body diagram must be equal to the kinetic diagram as stated by Newton's second law. For this system, the free-body diagram is given in Figure 2-6. In this diagram appear all the unknown and known forces in the system. Note that for System 2 there are no *external* unknown forces. The internal unknown forces are the normal F_{NC} due to the barge-to-barge contact along the longitudinal failure plane between barge Systems 1 and 2 and the internal moment M. In this system the internal shear between barge Systems 1 and 2 is related to the normal by means of the coefficient of friction μ_K; $S_{NC} = \mu_K F_{NC}$. The known forces are the internal force in each lashing as the motion takes place. The forces are labeled as f_{Ni}, and f_{Si}. Figure 2-7 presents the linear accelerations and angular accelerations of the system. In this case the linear accelerations are oriented in the global X- and Y-axes.

The three equations of motion of System 2 are

$$\oplus \rightarrow \sum F_X = ma_X \therefore -Rs_X - Rn_X + F_{NC} \sin\theta - \mu_K F_{NC} \cos\theta = -M_{par2} a_{X2} \qquad (2\text{-}10)$$

$$\oplus \uparrow \sum F_Y = ma_Y \therefore -Rs_Y + Rn_Y - F_{NC} \cos\theta - \mu_K F_{NC} \sin\theta = -M_{norm2} a_{Y2} \qquad (2\text{-}11)$$

Figure 2-6. Longitudinal failure mechanism free-body diagram of System 2.
Note: $F_{SC} = \mu_K F_{NC}$

Figure 2-7. Longitudinal failure mechanism kinetic diagram of System 2

$$\oplus \curvearrowright \sum M_a = (\sum M_{EQUIVALENT})_a \therefore -M + M_{Rfn} - F_{NC}(x_{G2} - x_2) =$$
$$I_{\theta 2}\alpha + (M_{par2}a_{X2}\cos\theta + M_{norm2}a_{Y2}\sin\theta)(y_2 - y_{G2}) +$$
$$(M_{par2}a_{X2}\sin\theta - M_{norm2}a_{Y2}\cos\theta)(x_2 - x_{G2})$$

(2-12)

where

M_{par2} = mass of System 2 parallel to the wall (including hydrodynamic added mass)
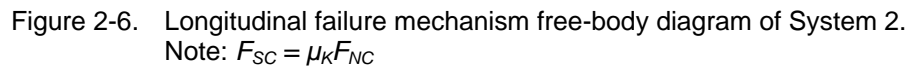
M_{norm2} = mass of System 2 normal to the wall (including hydrodynamic added mass)

$I_{\theta2}$ = mass moment of inertia of System 2 (including hydrodynamic added mass)

M_{par2}, M_{norm2} and $I_{\theta2}$ are computed for barge System 2 using Equations 2-4 through 2-9 modified for System 2 geometry and masses. The mass of barge System 2, excluding hydrodynamic added mass, is designated m_2. Barge System 2 decelerates at a different rate from barge System 1 during impact. The displacement of System 2 relative to the displacement of System 1 during an impact event allows this simplified model to crudely capture this behavior. The lashings transmit the effects of the System 2 inertial forces to System 1 and onto the wall. However, for this simplified model, the number of equations limits the number of variables to be considered in the solution process. Consequently, a crude assumption that System 2 was still decelerating in the global Y-axis after the deceleration of barge System 1 had concluded was made in order to match the number of variables with the number of equations. Recall that one of the primary features of this simplified model is to account for the forces in the lashings and to consider how these forces reflect the inertia of the two barge system bodies and their relative displacement. With consideration of all of these factors, the decision was made to assume the global Y acceleration of barge System 1 equal to zero in the calculations. Equations 2-1 through 2-3 and 2-10 through 2-12 provide six equations but seven unknowns for both systems: F_W, S_W, M, F_{NC}, $a_{X1} = a_{X2}$, a_{Y2}, and α. Observe that the global X linear accelerations of both systems are assumed equal for this simplified longitudinal failure mechanism. Therefore, another equation is required. A relationship between the shear and normal force between the impact corner barge and wall is introduced.

$$S_W - \mu_K^* F_W = 0 \tag{2-13}$$

where μ_K^* is the steel (barge)-to-steel (armor) kinetic coefficient of friction between barge train and wall.

Solving Equations 2-1 through 2-3 and 2-10 through 2-13 gives the resulting F_W expression:

$$F_W = \frac{M_{par}\left[(Rs_X + Rn_X)(\cos\theta + \mu_K \sin\theta) + \mu_K(Rn_Y - Rs_Y)\cos\theta + (Rs_Y - Rn_Y)\sin\theta\right]}{(M_{par1}\sin\theta + M_{par2}\sin\theta - \mu_K M_{par1}\cos\theta - \mu_K M_{par2}\cos\theta + \mu_K \mu_K^* M_{par2}\sin\theta + \mu_K^* M_{par2}\cos\theta)} \tag{2-14}$$

where M_{par} is the total mass of barge train ($M_{par1} + M_{par2}$), including hydrodynamic added mass

Notice here that the hydrodynamic added mass affects the F_W expression. If the denominator of Equation 2-14 equals zero, then

$$M_{par1}\sin\theta + M_{par2}\sin\theta - \mu_K M_{par1}\cos\theta - \mu_K M_{par2}\cos\theta + \mu_K \mu_K^* M_{par2}\sin\theta + \mu_K^* M_{par2}\cos\theta = 0$$

Solving for the coefficient of friction between the wall and the corner barge and for the critical value of the approach angle gives the following expressions:

$$\mu_K^* = \frac{M_{par}(\mu_K \cos\theta - \sin\theta)}{M_{par2}(\mu_K \sin\theta + \cos\theta)}$$

(2-15)

and

$$\theta_{CR} = \tan^{-1}(\frac{M_{par}\mu_K - M_{par2}\mu_K^*}{M_{par} + M_{par2}\mu_K\mu_K^*})$$

(2-16)

Equations 2-14 through 2-16 were obtained from the solution provided by Maple™ Worksheet (Appendix B). Derivation of Equation 2-14 is presented in Appendix D. There are combinations of variables for which Equation 2-14 is either indeterminate (e.g., the case of a value of zero in the denominator) or negative. Either of these cases provides unrealistic values for F_W. Equation 2-16 defines the asymptote for Equation 2-14 via the approach angle designated θ_{CR}. Approach angles equal to or less than θ_{CR} produce infinite values or negative values, respectively, for F_W for the longitudinal failure mechanism. For approach angles less than θ_{CR}, other failure mechanisms are more likely to occur. These alternative failure mechanisms will be discussed in subsequent chapters.

In summary, the following assumptions are made for the longitudinal failure mechanism:

a. The linear acceleration in the global Y-direction in barge System 1 is assumed to be zero. This means that in the global Y-direction the barge stops instantly at the moment of impact. This condition ensures the relative motion between the two barge systems.

b. The linear acceleration in the global X-direction for barge System 1 is assumed to be equal to the global X linear acceleration for barge System 2.

c. The angular acceleration for barge System 1 is assumed to be equal to the angular acceleration for barge System 2.

d. The kinetic coefficient of friction between barges must be defined. A review of the technical literature, discussed in Chapter 5, indicates a value between 0.2 and 0.5.

e. The kinetic coefficient of friction between the corner barge and the struck wall must be defined. A review of the technical literature, discussed in Chapter 5, indicates a value between 0.2 and 0.5.

f. The lashings are assumed to behave in an elastic-plastic manner, breaking when an ultimate (tensile) strain value is achieved within the lashing. Should the lashings reach the ultimate stress, they could not carry additional force with additional deformations. Achieving the ultimate tensile strain results in rupturing of the lashing.

g. This failure mechanism is valid for high approach angles; research indicates values greater than 70 degrees. Lower approach angles are likely to produce a failure path other than in the longitudinal direction.

h. Hydrodynamic effects are considered by means of an increase in the barge train mass in the local x- and y-axes and rotational directions. This hydrodynamic effect influences the kinetic variables (e.g., linear accelerations and angular acceleration).

i. Barge System 1, which is in contact with the struck wall, abruptly/instantaneously stops motion while barge System 2 continues motion. The lashings across the longitudinal failure plane provide resistance to the motion of barge System 2.

Two special cases for the longitudinal failure mechanism exist when a direct impact occurs (i.e., with an approach angle of 90 degrees). For a 90-degree impact, a central impact or an oblique impact can occur. In the subsequent sections these two special cases will be discussed in detail.

2.1.1 Impact at 90 degrees with eccentricity (oblique impact)

An oblique impact occurs when the outside corner barge of a barge train impacts an end cell or nose pier at 90 degrees. This situation can also occur when a barge train impacts a bridge pier. Loading eccentricity is present because the center of mass of the barge train is not aligned with the line of action of the impact reaction force normal to the end cell or nose pier. A second idealization made in this simplified model is that no shear force develops at the contact point between barge and rigid wall during the impact because it is a direct impact (i.e., head-on). Figure 2-8 provides a general description of this case. Note the impact force normal to the wall F_W and the acceleration of the system depicted in this figure. The global X accelerations for Systems 1 and 2 are assumed zero. The eccentricity between center of gravity and the point of impact is distance Δy and is expressed in the local coordinates of the barge train.

In this simplified model, the longitudinal failure mechanism in a direct impact with eccentricity allows the relative displacement between barges in the local (barge) x-direction (Figure 2-2). In this way, all the lashings along the longitudinal failure plane will break by means of the relative displacement between barges of Systems 1 and 2, as shown in Figure 2-8. The relative displacement can be obtained by assuming different linear accelerations in the global Y-direction for System 1 and for System 2. A zero linear global acceleration is assumed in the global Y-direction of System 1 for this simplified model because impact occurs with a *rigid* wall. System 2 motion continues and the lashings that connect System 1 to System 2 will try to stop (or decelerate) System 2. Thus, the deceleration of System 2 is nonzero. In the equation of motion for System 1 (Equations 2-17 through 2-19), the summation of forces in the global Y-direction is set equal to zero according to this assumption.

$$\oplus \rightarrow \sum F_X = ma_X \therefore -F_{NC} + f_{N1} + f_{N2} + f_{N3} + f_{N4} + f_{N5} + f_{N6} = 0 \qquad (2\text{-}17)$$

a. Free-body diagram   b. Kinetic diagram
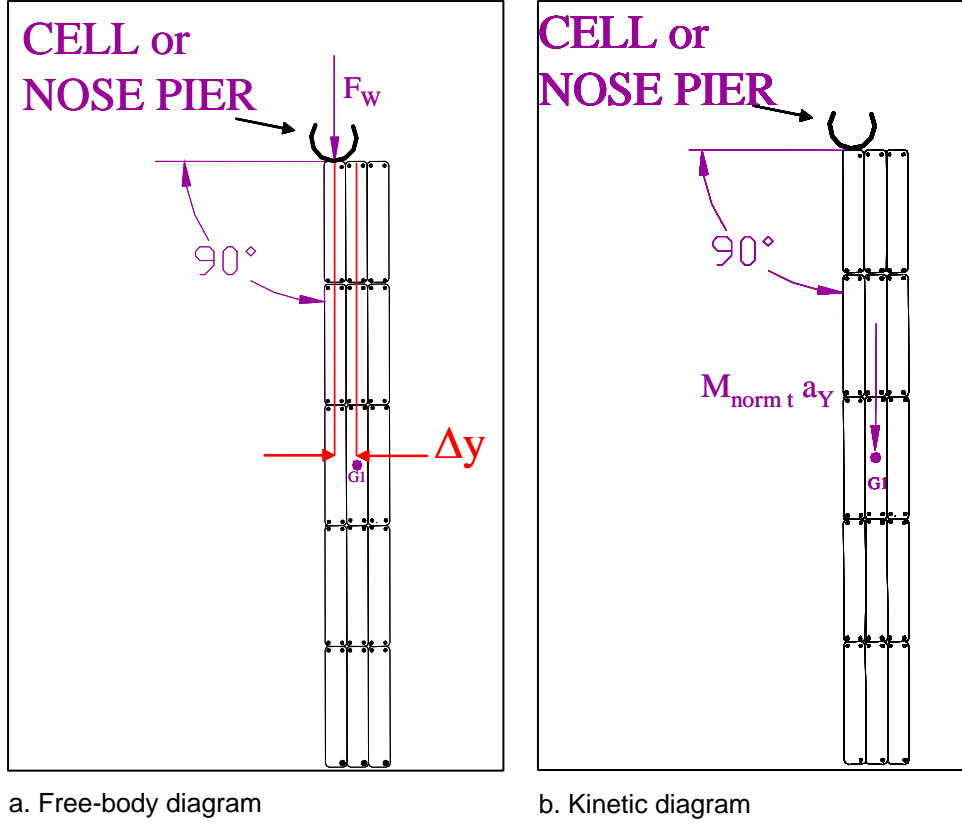
Figure 2-8.   Scheme of barge train with an eccentric direct impact

$$\oplus \uparrow \sum F_Y = ma_Y \therefore -F_W - \mu_K F_{NC} + R_{fs} = 0 \quad ; \quad M_{norm1}a_{Y1} = 0 \tag{2-18}$$

$$\oplus \circlearrowleft \sum M_{G1} = I_G \alpha \therefore -F_W(y_1 - y_{G1}) - R_{fs}(y_{G1} - y_2) + f_{N1}(x_1 - x_{G1}) +$$
$$f_{N2}(x_2 - x_{G1}) + f_{N3}(x_3 - x_{G1}) - f_{N4}(x_{G1} - x_4) + f_{N5}(x_{G1} - x_5) +$$
$$M - f_{N6}X_{G1} = I_{\theta 1}\alpha \tag{2-19}$$

where

F_W = force normal to the wall at point of impact

f_{Ni} = normal component of the lashing force at the failure plane

R_{fs} = resultant of the tangential component of the lashing force at the failure plane

$I_{\theta l}$ = second moment of inertia of System 1 (including hydrodynamic added mass moment of inertia)

α = angular acceleration for System 1 and System 2 (assumed equivalent)

However, in the equation of motion for System 2 (Equations 2-20 through 2-22) the global Y linear deceleration of System 2 is nonzero.

$$\oplus \to \sum F_X = ma_X \quad \therefore -f_{N1} - f_{N2} - f_{N3} - f_{N4} - f_{N5} - f_{N6} + F_{NC} = 0 \quad (2\text{-}20)$$

$$\oplus \uparrow \sum F_Y = ma_Y \quad \therefore \mu_K F_{NC} - f_{S2} - f_{S3} - f_{S4} - f_{S5} = -M_{norm2} a_{Y2} \quad (2\text{-}21)$$

$$\oplus \circlearrowright \sum M_G = I_G \alpha \quad \therefore -f_{N1}(x_1 - x_{G2}) - f_{N2}(x_2 - x_{G2}) - f_{N3}(x_3 - x_{G2}) +$$
$$f_{N4}(x_{G2} - x_4) + f_{N5}(x_{G2} - x_5) - f_{N6}(x_{G2}) - \mu_k F_{NC}(y_2 - y_{G2}) - \quad (2\text{-}22)$$
$$(f_{S2} + f_{S3} + f_{S4} + f_{S5})(y_2 - y_{G2}) - M = I_{\theta2}\alpha$$

where M_{norm2} is the mass of System 2 normal to the wall (including hydrodynamic added mass).

This failure mechanism is described by the equations of motion based on Newton's second law. First, a free-body diagram is defined as shown in Figure 2-9. All of the unknown and known forces in the system appear in this diagram. The unknown external impact forces are F_W and S_W, and the internal unknown forces are the resultant barge-to-barge normal, F_{NC}, and the internal moment M. In this model the internal shear is related to the normal force by means of the steel-steel kinetic coefficient of friction μ_K; $S_{NC} = \mu_K F_{NC}$. The known forces are the internal force in each lashing as the motion takes place. The forces are labeled as f_{Ni} and f_{Si}.

a. Free-body diagram   b. Kinetic diagram
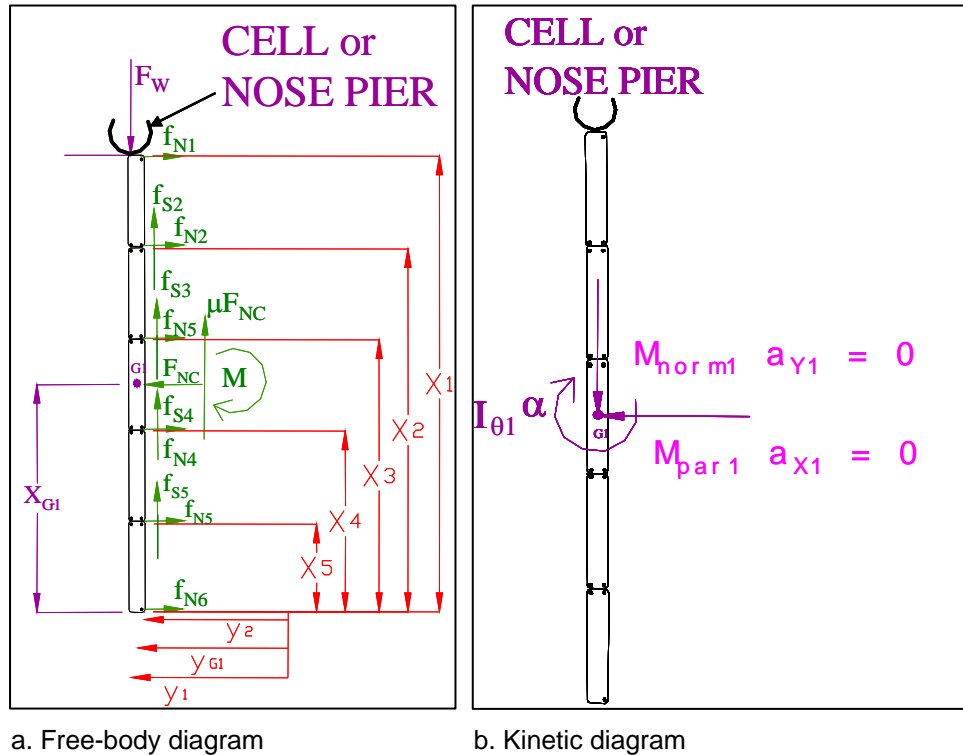
Figure 2-9. Force and kinetic diagram of System 1 for a direct impact with eccentricity

The free-body diagram equals the kinetic diagram as stated by Newton's second law. Figure 2-9 also presents the linear accelerations and angular accelerations of System 1. In this case the linear accelerations are oriented in the global x- and y-axes. From Figure 2-9 the three equations of motion can be written. For System 1, which is in contact with the wall, the equations of motion are Equations 2-17 through 2-19.

Recall that the angular acceleration for System 1 is assumed equal to the angular acceleration for System 2 for the longitudinal failure mechanism (see Section 2.1).

Because the linear accelerations in the global x- and y-axes for barge System 1 are zero, the only hydrodynamic term included in this special case of the longitudinal failure mechanism (using the ETL 1110-2-338 approach) is

$$I_{\theta 1} = (1 + \eta_\theta) * I_{G1} \quad ; \quad I_{G1} = \frac{1}{12} * m_1 * \left(L_1^{\,2} + B_1^{\,2}\right) \qquad (2\text{-}23)$$

where the hydrodynamic added mass coefficient defined in the local barge coordinate system, according to ETL 1110-2-338, as $\eta_\theta = 0.4$, and where I_{G1} is the second mass moment of inertia of System 1.

The authors of this report recommend that hydrodynamic effects be considered in the simplified limit state analyses. Therefore, Equations 2-17 to 2-19 will include hydrodynamic added mass terms via Equation 2-23.

Applying the same procedure to System 2, i.e., the rest of the barge train, three more equations of motion are obtained. As always, the free-body diagram is equal to the kinetic diagram as stated by Newton's second law. For this system, the free-body diagram must be defined as shown in Figure 2-10a. In this diagram appear all the unknown and known forces in the barge train system. Note that for System 2 there are no *external* unknown forces. The internal unknown forces are the normal, F_{NC}, due to the barge-to-barge contact along the longitudinal failure plane between barge Systems 1 and 2 and the internal moment M. In this system the internal shear between barge Systems 1 and 2 is related to the normal by means of the coefficient of friction μ_K; $S_{NC} = \mu_K F_{NC}$. The known forces are the internal force in each lashing as the motion takes place. The forces are labeled as f_{Ni}, and f_{Si}. Figure 2-10b presents the linear accelerations and angular accelerations of the system. In this case the linear accelerations are oriented in the global X- and Y-axes.

Equations 2-20 through 2-22 are the three equations of motion for System 2, which are based on Figure 2-10. There are five unknown variables in Equations 2-17 through 2-22: F_W, F_{NC}, M, a_{Y2}, and α. Among the six equations, Equations 2-17 and 2-20 are the same. Thus there are five independent equations and five unknowns. Solving these five equations gives the following expression for the force normal to the wall:

$$F_W = \mu_K R_n + R_s \qquad (2\text{-}24)$$

where

R_n = resultant normal force in the lashing at the failure plane

R_s = resultant longitudinal force in the lashing at the failure plane

a. Free-body diagram
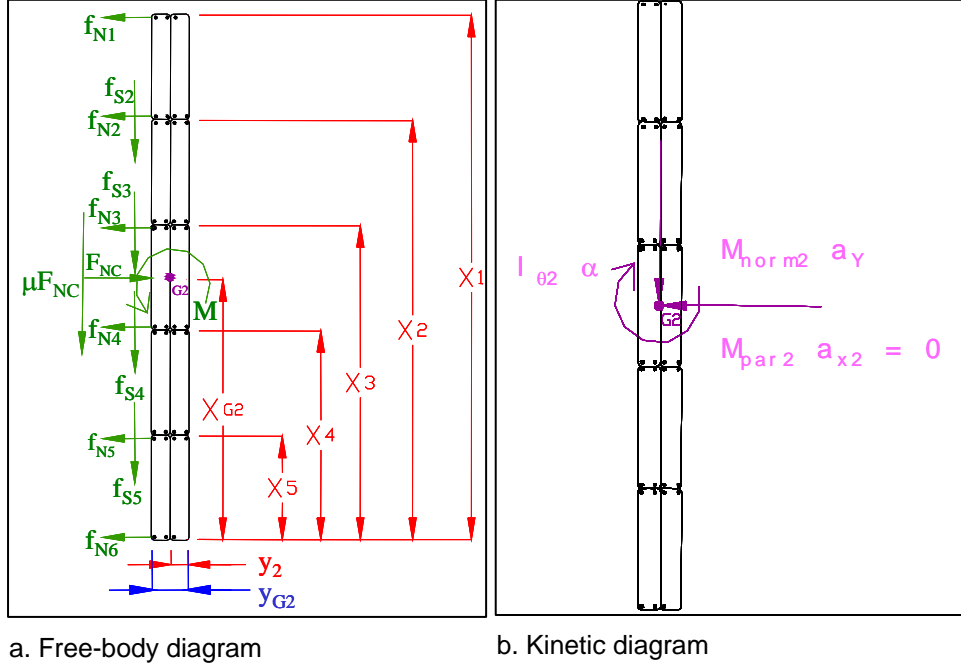
b. Kinetic diagram

Figure 2-10. Force and kinetic diagram of System 2 for a direct impact with eccentricity

Four parameters that affect the force normal to the wall are the global X- and Y-axis components of the forces parallel (Rs_x, Rs_y) and perpendicular (Rn_x and Rn_y) to the failure plane obtained from the internal force in the lashings. These forces are obtained in the following form. Due to the elongation of the lashing during the deformation process, an internal force appears in the lashings. The angle that defines each segment of the lashings with the longitudinal local axis is calculated using the local coordinates of the start (x_s, y_s) and end (x_e, y_e) bits that connect each segment of each lashing. Then, the components of these forces expressed in local coordinates are easily transformed to forces in the global coordinates system by means of the transformation matrix that contains the sine and cosine functions. As shown in Figure 2-5, these forces can be easily obtained by the use of trigonometric functions. For example, $Rn_x = F_L * \sin \delta$, and $Rn_Y = Rn * \cos \theta$.

In summary, the following assumptions are made for the longitudinal failure mechanism with eccentricity:

a. The linear acceleration in the global Y-direction in barge System 1 is assumed to be zero. This means that in the Y-direction the barge stops instantly at the moment of impact. This condition ensures the relative motion between the two barge systems.

b. The linear accelerations in the global X-direction for barge Systems 1 and 2 are assumed to be zero.

c. The angular acceleration for barge System 1 is assumed to be equal to the angular acceleration for barge System 2.

d. The kinetic coefficient of friction between barges must be defined. A review of the technical literature, discussed in Chapter 5, indicates a value between 0.2 and 0.5.

e. The kinetic coefficient of friction between the corner barge and the struck wall must be defined. A review of the technical literature, discussed in Chapter 5, indicates a value between 0.2 and 0.5.

f. The lashings are assumed to behave in an elastic-plastic manner and break when an ultimate (tensile) strain value is achieved within the lashing. Should the lashings reach the ultimate stress, no additional force can be carried by the lashing with additional deformations. Achieving the ultimate tensile strain results in rupturing of the lashing.

g. This failure mechanism is valid for an approach angle equal to 90 degrees and in the case of the line of action of the impact normal force eccentric to the center of mass of the complete barge train.

h. The hydrodynamic effect can be considered by means of an increase in mass in the local x- and y-axes and rotational directions.

i. Barge System 1, which is in contact with the struck wall, abruptly/instantaneously stops the motion while barge System 2 continues the motion. The lashings across the longitudinal failure plane provide resistance to the motion of System 2.

2.1.2 Impact at 90 degrees without eccentricity

Central impact occurs when a barge train impacts a cell or nose pier at 90 degrees and the line of action of the impact normal force is in alignment with the center of mass of the entire barge train system. This case can occur when a barge train impacts a bridge pier, a nose pier, or end cells. Loading eccentricity is absent because the center of mass of the barge train is aligned with the line of action of the impact force normal to the cell or nose pier. (It is assumed that the mass distribution among the barges is uniform.) Because it is a direct impact, no shear force between the corner barge and the wall is assumed to develop during the impact. This case has also two failure planes because the central barge system stops its motion at impact while the two side systems continue their motion until the lashings fail. Figure 2-11 provides a general description of this case. A force normal to the wall F_W and linear acceleration for the system exist. This failure mechanism obeys the equations of motion, which are based on Newton's second law. First, a free-body diagram of System 1 is defined as shown in Figure 2-12. In this diagram appear the center column of barges for the entire barge train system and all the unknown and known forces in this system. The unknown external force is F_W, and the internal unknown forces are the resultant barge-to-barge normal F_{NC} and the internal moment M at each side of the center barges. In this model the internal shear is related to the normal force by means of the

steel-steel coefficient of friction μ_K; $S_{NC} = \mu_K F_{NC}$. The known forces are the internal force in each lashing as the motion takes place. The forces are labeled as f_{Ni} and f_{Si}.

a. Free-body diagram   b. Kinetic diagram
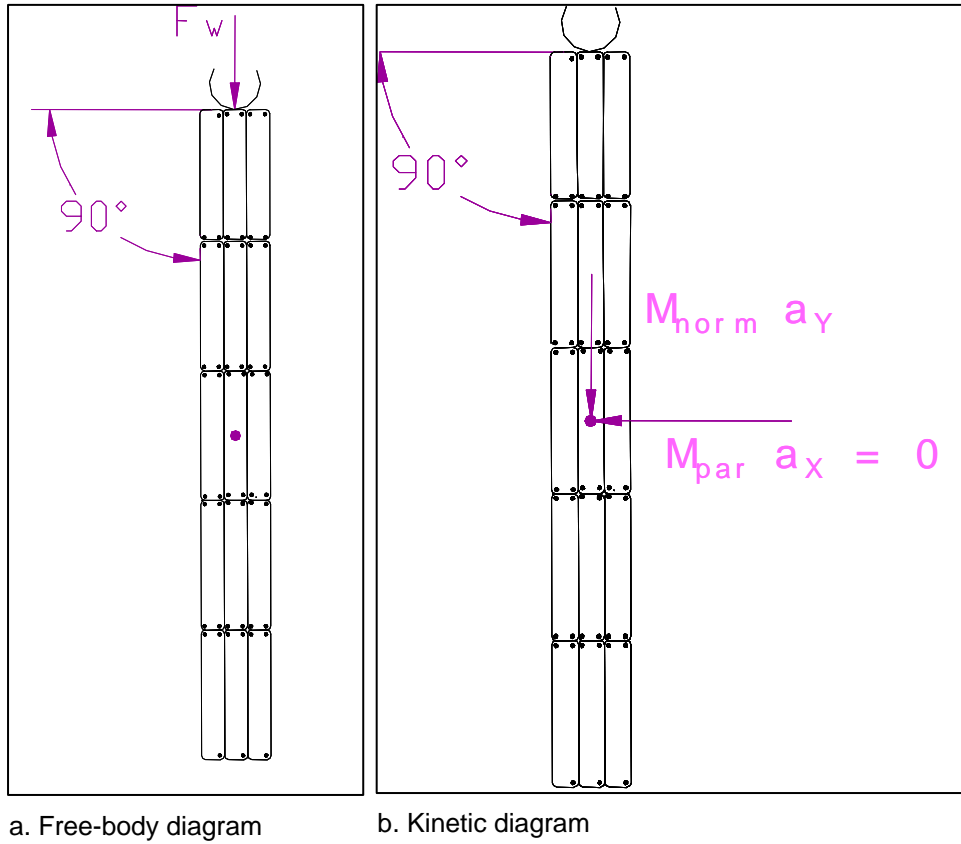
Figure 2-11. Scheme of barge train with a direct impact without eccentricity

In this model, the longitudinal failure mechanism in a direct impact without eccentricity allows the relative displacement between barges in the local (barge) x-direction, which for θ < 90 degrees corresponds to the global Y-axis. In this way, all the lashings along the failure planes will break by means of the relative displacements between the barges of System 1 and those of Systems 2 and 3. System 1 is defined by the column of center barges that impact the rigid wall, and Systems 2 and 3 are defined by the side column of barges. The relative displacement between barge systems is obtained by assuming independent linear accelerations in the global Y-direction for System 1, System 2, and System 3. In this simplified impact model, zero linear global acceleration in the Y-direction of System 1 is assumed because impact with a rigid wall occurs for this particular system. Systems 2 and 3 continue their motion and the lashings that connect System 1 to System 2 and System 1 to System 3 will try to stop or decelerate Systems 2 and 3. Thus, deceleration of Systems 2 and 3 is nonzero. In Equation 2-26, to be introduced later, the summation of forces in the global Y-direction is equal to zero for System 1. However, in the equations of motion for Systems 2 and 3 (Equations 2-14 and 2-15, respectively), the global Y-axis linear deceleration of Systems 2 and 3 is nonzero. The global X-axis accelerations for Systems 1 and 2 are assumed zero.

The free-body diagram equals the kinetic diagram as stated by Newton's second law. Figure 2-12 also presents the linear accelerations and angular accelerations of System 1, the central barge system. In this case the linear accelerations are oriented in the global X- and Y-axes. From Figure 2-12, the three equations of motion can be written for System 1 in contact with the wall as

$$\oplus \rightarrow \sum F_X = ma_X \therefore R_{nR} - R_{nL} + F_{NCL} - F_{NCR} = 0 \tag{2-25}$$

$$\oplus \uparrow \sum F_Y = ma_Y \therefore -F_W + R_{sR} + R_{sL} + \mu_K F_{NCR} + \mu_K F_{NCL} = 0 \quad ; \quad M_{norm1} a_{Y1} = 0 \tag{2-26}$$

$$\oplus \circlearrowright \sum M_G = I_G \alpha \therefore M_{2R} - M_{1L} + M_R = 0 \tag{2-27}$$

where

R_{nR} = right-side resultant of the normal component of the lashing force at the failure plane

R_{nL} = left-side resultant of the normal component of the lashing force at the failure plane

F_{NCL} = left-side resultant normal force at the failure plane due to contact of barges (normal pressure between barge sides at the failure plane)

F_{NCR} = right-side resultant normal force at the failure plane due to contact of barges (normal pressure between barge sides at the failure plane)

R_{sR} = right-side resultant of the tangential component of the lashing force at the failure plane

R_{sL} = left-side resultant of the tangential component of the lashing force at the failure plane

M_{2R} = internal moment at right failure plane (it is due to eccentricity of the resultant normal force related to the center of mass)

M_{1L} = internal moment at left failure plane (it is due to eccentricity of the resultant normal force related to the center of mass)

M = resultant moment from the lashing forces

M_R = resultant moment produced by the internal forces in the lashings with respect to the mass center of gravity

Applying the same procedure to System 2, the left column of barges, gives three more equations of motion. The free-body diagram equals the kinetic diagram as stated by Newton's second law. For this system, the free-body diagram is defined as shown in Figure 2-13a. Note that no external unknown forces exist in this diagram. The internal unknown forces are the resultant barge-to-barge normal force F_{NC} and the internal moment M. In this system the internal shear is related to the normal force by means of the steel-steel kinetic coefficient of friction μ_K; $S_{NC} = \mu_K F_{NC}$. The known forces are the internal force in each lashing as motion takes place. The forces are labeled as f_{Ni} and f_{Si}. Figure 2-13b presents the linear accelerations and angular accelerations for System 2. In this case the linear accelerations are oriented in the global X- and Y-axes. Note that

the linear acceleration in the global X-direction and the angular acceleration are assumed zero for barge System 2.

a. Free-body diagram   b. Kinetic diagram
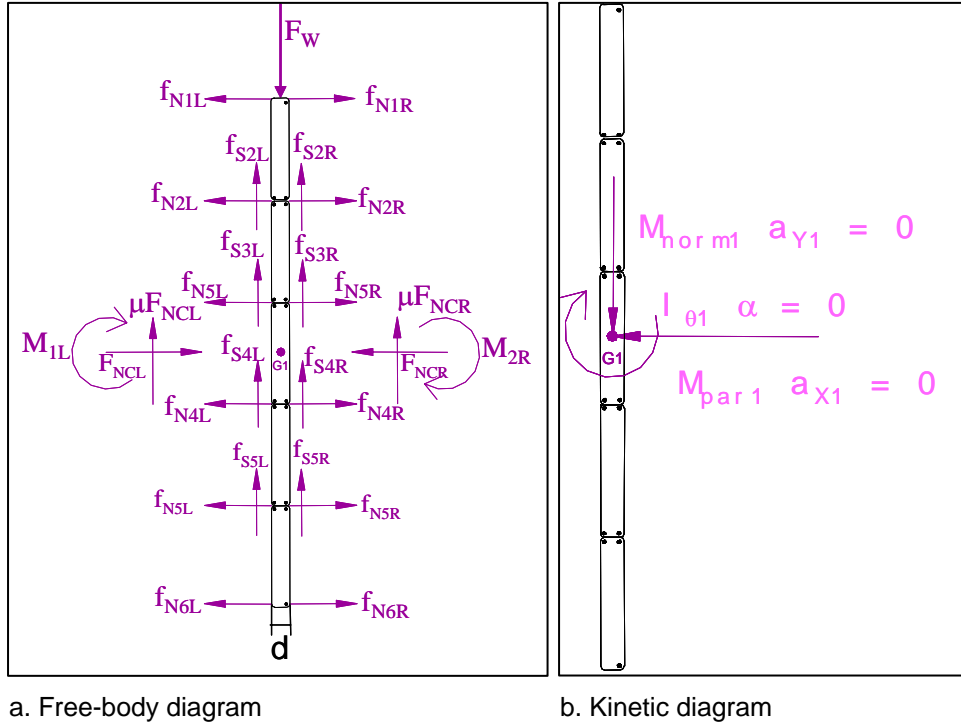
Figure 2-12. Force and kinetic diagram of System 1 for a direct impact without eccentricity

The three equations of motion of System 2 are as follows:

$$\oplus \rightarrow \sum F_X = ma_X \therefore -F_{NCL} + f_{N1L} + f_{N2L} + f_{N3L} + f_{N4L} + f_{N5L} + f_{N6L} = -F_{NCL} + R_{nL} = 0 \qquad (2\text{-}28)$$

$$\oplus \uparrow \sum F_Y = ma_Y \therefore -\mu_K F_{NCR} - R_{sL} = -M_{norm2} a_{Y2} \qquad (2\text{-}29)$$

$$\oplus \circlearrowright \sum M_G = I_G \alpha \therefore \mu_K F_{NCL} \frac{a}{2} + \frac{a}{2}(R_{sL}) + M_{1L} = 0 \qquad (2\text{-}30)$$

Hydrodynamics effects are included in barge System 2 using the ETL 1110-2-338 approach as expressed in Equations 2-4 to 2-9. The authors of this report recommend that hydrodynamic effects be considered in the simplified limit state analyses. Therefore, Equations 2-25 to 2-30 will include hydrodynamic added mass terms via Equations 2-4 and 2-5.
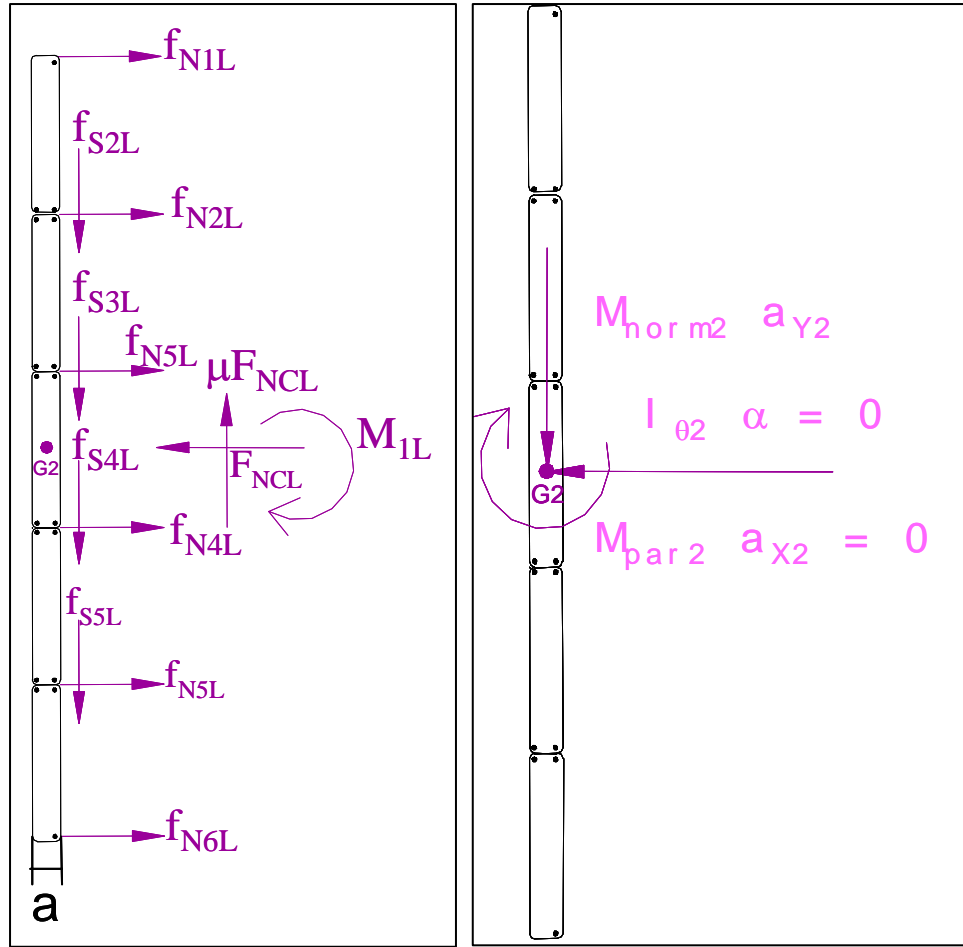
a. Left free-body diagram

b. Left kinetic diagram

Figure 2-13. Force and kinetic diagram of System 2 for a direct impact without eccentricity

Applying the same procedure to barge System 3, the right column of barges, gives three more equations of motion. The free-body diagram is equal to the kinetic diagram as stated by Newton's second law. For this system, the free-body diagram is defined as shown in Figure 2-14a. In this diagram appear all the unknown and known forces. Note that for System 3 there are no external unknown forces. The internal unknown forces are the normal F_{NC} due to the barge-to-barge contact along the longitudinal failure plane and the internal moment M. In this system the internal shear between barge Systems 1 and 3 is related to the normal force by means of the coefficient of friction μ_K; $S_{NC} = \mu_K F_{NC}$. The known forces are the internal force in each lashing as the motion takes place. The forces are labeled f_{Ni} and f_{Si}. Figure 2-14b presents the linear accelerations and angular accelerations of the system. In this case the linear accelerations are oriented in the global X- and Y-axes. Note that the linear acceleration in the global X-direction and the angular acceleration are assumed zero for barge System 3.
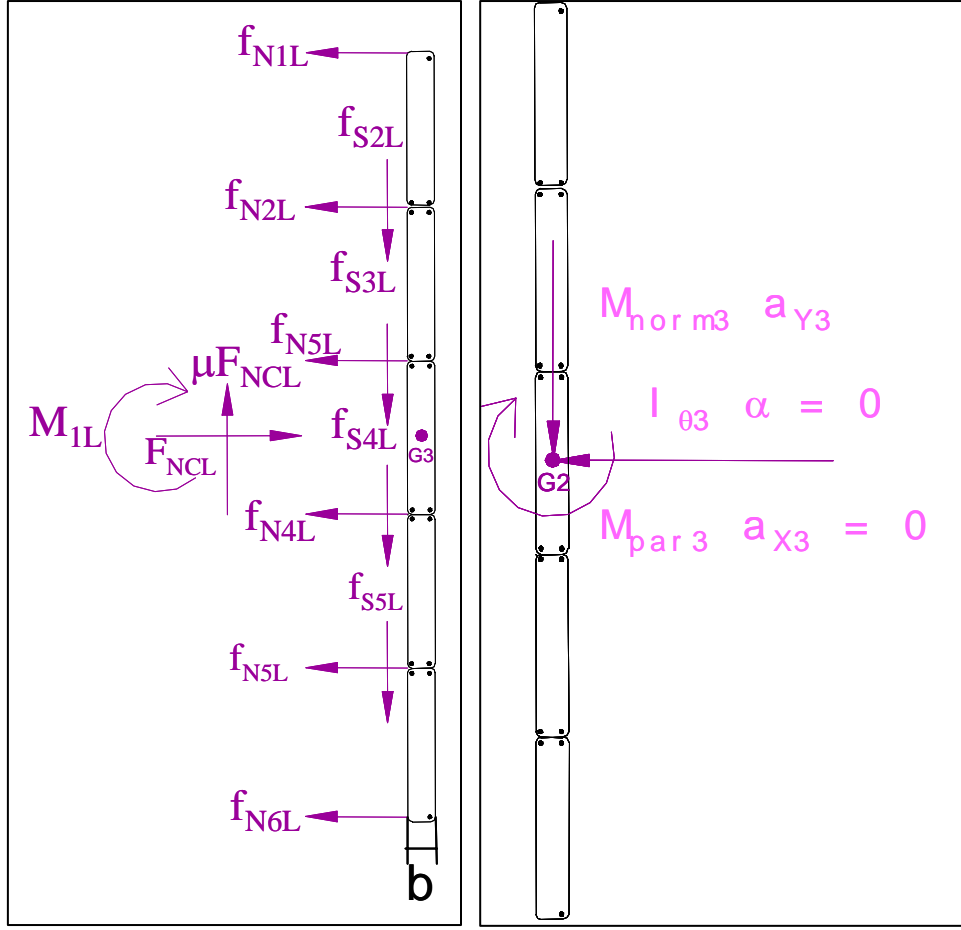
a. Left free-body diagram   b. Left kinetic diagram

Figure 2-14. Forces and kinetic diagram of System 3 for a direct impact without eccentricity

The three equations of motion of barge System 3 are as follows:

$$\oplus \rightarrow \sum F_X = ma_X \therefore -F_{NCR} - f_{N1R} - f_{N2R} - f_{N3R} -$$
$$f_{N4R} - f_{N5R} - f_{N6R} = F_{NCR} - R_{nR} = 0 \tag{2-31}$$

$$\oplus \uparrow \sum F_Y = ma_Y \therefore -\mu_K F_{NCR} - R_{sR} = -M_{norm3}a_{Y3} \tag{2-32}$$

$$\oplus \circlearrowright \sum M_G = I_G \alpha \therefore -M_{2R} - (\mu_K F_{NCR} + f_{S2R} + f_{S3R} + f_{S4R} + f_{S5R})\frac{b}{2} = 0 \tag{2-33}$$

where *a, b* are the widths of the barge train (left and right of the center row of barges, respectively).

This system of equations has seven unknowns:

F_W = force normal to the wall

F_{NCR} = internal normal force between Systems 1 and 3

F_{NCL} = internal normal force between Systems 1 and 2

M_{IL} = internal moment between Systems 1 and 2

M_{IR} = internal moment between Systems 1 and 3

a_{Y2} = linear acceleration in the global Y-direction for System 2

a_{Y3} = linear acceleration in the global Y-direction for System 3

Nine equations describe the three barge systems. However, two equations of motion in the global X-direction, 2-28 and 2-31, produce the following expressions:

$$F_{NCR} = f_{N1R} + f_{N2R} + f_{N3R} + f_{N4R} + f_{N5R} + f_{N6R} = R_{nR} \qquad (2\text{-}34)$$

$$F_{NCL} = f_{N1L} + f_{N2L} + f_{N3L} + f_{N4L} + f_{N5L} + f_{N6L} = R_{nL} \qquad (2\text{-}35)$$

In addition, from the moment equation from Equations 2-27, 2-30, and 2-33, the following internal moment equations are obtained:

$$M_{2R} = \left[\mu_K R_{nR} + R_{sR}\right]\frac{b}{2} \qquad (2\text{-}36)$$

$$M_{1R} = \left[\mu_K R_{nL} + R_{sL}\right]\frac{a}{2} \qquad (2\text{-}37)$$

$$M_R = M_{1L} - M_{2R} \qquad (2\text{-}38)$$

Using the equations of motion in the Y-direction from Equations 2-29 and 2-32 gives the following equations:

$$a_{Y2} = \frac{\mu_K R_{nL} + R_{sL}}{M_{norm2}} \qquad (2\text{-}39)$$

$$a_{Y3} = \frac{\mu_K R_{nR} + R_{sR}}{M_{norm3}} \qquad (2\text{-}40)$$

Finally, the expression for the force normal to the wall is given by

$$F_W = R_{sR} + R_{sL} + \mu_K R_{nR} + \mu_K R_{nL} \qquad (2\text{-}41)$$

where

a_{Y2} = linear absolute acceleration of System 2 in the global Y-direction

a_{Y3} = linear absolute acceleration of System 3 in the global Y-direction

The parameters that affect the force normal to the wall are the global X- and Y-components of the forces parallel (Rs_X, Rs_Y) and perpendicular (Rn_X, Rn_Y) to the failure plane obtained from the internal force in the lashings. These forces are obtained in the following form. Due to the elongation of the lashing during the deformation process, an internal force appears in the lashings. The angle that defines each segment of the lashings with the longitudinal local axis is calculated using the local coordinates of the start (x_s, y_s) and end (x_e, y_e) bits that connect each segment of each lashing. Then, from the components of these forces in local coordinates, the forces in the global coordinates system are easily determined by means of the transformation matrix that contains the sine and cosine functions. As shown in Figure 2-5, these forces can be easily obtained by the use of trigonometric functions. For example, $Rn_x = F_L * \sin \delta$, and $Rn_Y = Rn * \cos \theta$. In this case these forces are computed in both sides of the central barge system. This introduced the use of the subscripts denoting left and right.

In summary, the following assumptions are made for the longitudinal failure mechanism without eccentricity:

    a.   The linear acceleration in the global Y-direction in barge System 1 is assumed to be zero. This means that in the Y-direction the barge stops instantly at the moment of impact. This condition ensures the relative motion between the three barge systems.

    b.   The linear acceleration in the global X-direction and the angular acceleration in barge System 1 are assumed to be zero.

    c.   The linear acceleration in the global X-direction and the angular acceleration are assumed zero for barge System 2.

    d.   The linear acceleration in the global X-direction and the angular acceleration are assumed zero for barge System 3.

    e.   The kinetic coefficient of friction between barges must be defined. A review of the technical literature, as discussed in Chapter 5, indicates a value between 0.2 and 0.5.

    f.   The kinetic coefficient of friction between the corner barge and the struck wall must be defined. A review of the technical literature, as discussed in Chapter 5, indicates a value between 0.2 and 0.5.

    g.   The lashings are assumed to behave in an elastic-plastic manner and break when an ultimate (tensile) strain value is achieved within the lashing. Should the lashings reach the ultimate stress, no additional force can be carried by the lashing with additional deformations. Achieving the ultimate tensile strain results in rupturing of the lashing.

    h.   This failure mechanism is valid for an approach angle equal to 90 degrees and the line of action of the impact normal force passing through the center of mass of the entire barge train.

    i.   The hydrodynamic effects are considered by means of an increase in the barge train mass in the local x- and y-axes and rotational directions.

    j.   System 1, which is in contact with the struck wall, abruptly/ instantaneously stops the motion while barge Systems 2 and 3 continue

their motion. The lashings across the longitudinal failure planes provide resistance to the motions of Systems 2 and 3.

k. Two longitudinal failure planes develop in this special case.

l. Each of the three systems tests three different linear accelerations. System 1 has zero acceleration, and Systems 2 and 3 have accelerations a_{Y2}, and a_{Y3}, respectively.

2.2 Numerical Solution Procedure

Formulations presented in the previous sections are used to calculate the force normal to the wall assuming a longitudinal failure mechanism during impact. In this simplified impact model, the value computed for the resultant F_W is dependent on the magnitude of the lashing forces. The relative motion between the barges of System 1 and System 2 is produced by a different linear acceleration in the local x-axis for the two systems. This can be achieved by means of an elongation of the lashing in the forward direction as shown in Figure 2-15. Thus an analytical approach is developed to assess these lashing forces based on the relative displacement of the two (or three) barge systems. This incremental relative displacement translates into incremental changes in the lashing forces across the longitudinal failure plane between barge systems. The sequential process to calculate F_W by Limit_LASHING is the following:

a. The initial length of the lashing is calculated using the initial internal force in the lashing. (Lashings usually have a tensile force that is introduced when the barges are initially assembled into a barge train.) If the initial force is known, then the initial elongation produced by the initial force can be calculated using the expression $F = (AE/L_0)\Delta$ where A = cross-sectional area of the lashing, E = Young's modulus of elasticity, L_0 = initial length of the lashing before initial load is applied, and Δ = the elongation of the lashing. This equation comes from the stress-strain relationship and the stress and strain definitions. If $\Delta = L_f - L_0$, then $L_0 = A*E*L_f / (F + A*E)$; where L_f is the elongated length.

b. Using the initial length of the lashing, an increment of length is added to the lashing, which then elongates in the longitudinal failure plane. Note that some of the lashings might reduce their internal load should they be oriented opposite to the direction of the relative motion. For example, it is observed in Figure 2-15a that the green lashings are oriented in a direction such that an increment of relative displacement (between Systems 1 and 2) according to the simplified longitudinal failure mechanism reduces their internal lashing force.

c. A continuous increment of the relative displacement between the barge systems (and along the longitudinal failure plane) produces an incremental stretch in the red and blue lashings in Figure 2-15a.
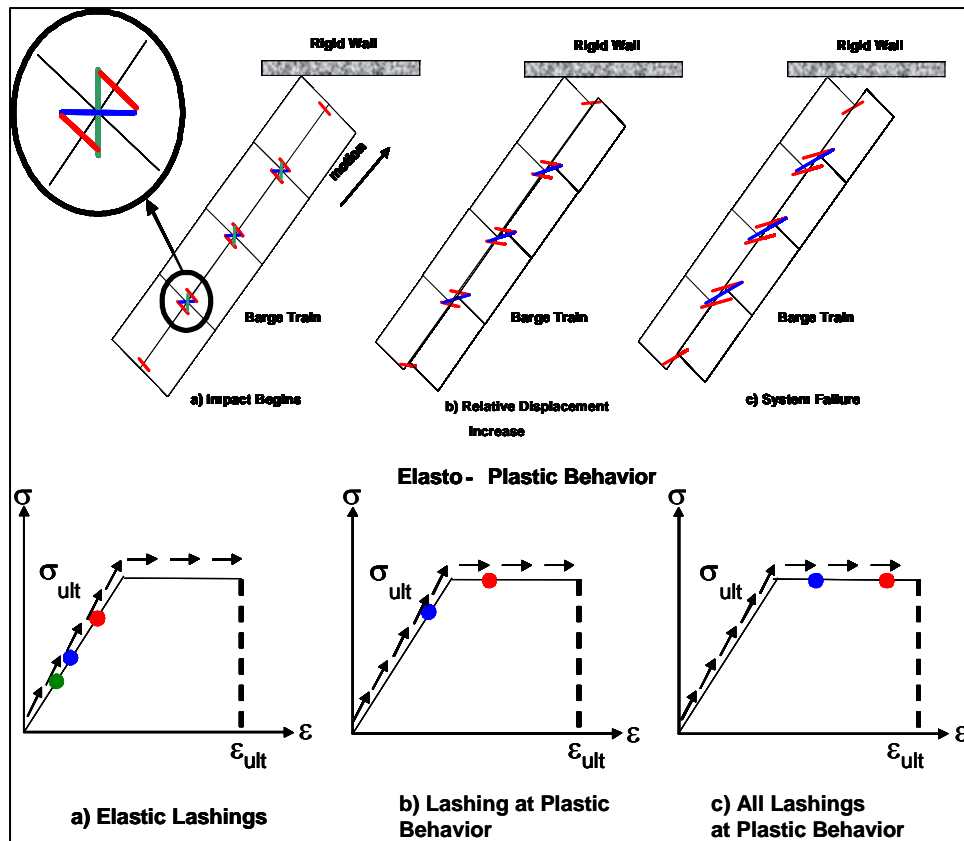
Figure 2-15. Progressive longitudinal failure of lashings across a longitudinal failure plane within the barge train where σ = normal stress; ε = normal strain; σ_{ult} = ultimate normal stress; and ε_{ult} = ultimate normal strain

d. As the incremental displacements increase, the green lashings ultimately reach a value of zero internal force. This lashing is then deleted from the analysis because it is unstretched.

e. As shown in the Figure 2-15b idealization, as the relative motion between barge systems increases, the lashing (red) can reach the horizontal plateau of the elastoplastic stress-strain model.

f. With sufficient relative deformation between the barge systems, all lashings can yield, as idealized in Figure 2-15c and ultimately break when the strains ε equal ε_{ult}.

g. In the incremental solution process an incremental relative displacement between barge systems is assumed. The incremental relative displacement value used in each computational step is set equal to 0.001 ft. Parametric studies have shown this to be a small value considering that the calculations are made numerous times; e.g., 1,000 calculations will result in 1 ft of elongation. With this magnitude of elongation, lashings will reach their ultimate value.

h. Different lashing geometry configurations among the bits result in different lengths of lashings between bits across the idealized longitudinal failure plane. Thus, for each of the lashings a different length of deformation will result at each incremental computation step. The deformation of each lashing also depends on the initial load (tension) applied to the lashing (during initial formation of the barge train) and the position of the bits on the barges.

i. The location of the bits defines the initial length of the lashings. This difference in the length of the lashing can result in different normal strain within each lashing. This is the reason that there are different stress-strain levels in the lashings even for the same relative displacement across the longitudinal failure plane between System 1 and System 2.

j. Each of the lashings is likely to reach its ultimate stress value at different instants during the relative motion process (between Systems 1 and 2), as specified in the previous subparagraph. As soon as the lashing reaches the ultimate stress, the lashing cannot accrue additional stress (or tensile force) in the incremental analysis. This is due to the elastoplastic behavior of the lashing adopted in this failure mechanism. The lashing can accrue additional strain based upon the additional stretching from the continued relative displacement between the two barge systems.

k. Should a lashing accrue a strain equal to the user-specified ultimate strain, the lashing is assumed to rupture and is removed from the connection system across the longitudinal failure plane.

l. These resultant lashing forces are then used as input data to the expressions for F_W previously presented.

It is important to mention that the lashing failures occur in a sequence; it is not assumed that all lashings reach their ultimate stress at once. Actual impact response among the barges and the lashings during impact is quite complex: the difference in bit locations and lashing configurations between bits as well as the different initial (tension) forces set in the lashings provide the system with an uneven distribution of forces at the lashing connections. In addition, as soon as the corner barge impacts the *rigid* wall, the impact wave generated internal to the barge train reaches all points throughout the barge train at different instants of time, producing different stresses and strains among the lashings. To model this behavior in this *simplified model*, relative motion between barge systems is assumed. This relative motion produces different relative decelerations in the local x-axis of the barge train for the two components in the model of the barge systems. These different decelerations for System 1 and System 2 are responsible for the stress and strain that develop in the lashings across the failure plane. In the computations, the relative displacement across the longitudinal failure plane is constant for each incremental step. However, this condition does not imply that this relative displacement occurs at equal time-steps. Remember that the deceleration may not be constant. So if it is not a constant, the time at which the increment of the relative displacement occurs is not constant. In other words, the time to produce a relative displacement increment from 0.0 to 0.001 is different from the time needed to produce a relative displacement increment from 0.01 to

0.011, because the deceleration at each relative displacement increment is different. The incremental computational procedure was implemented in a new PC-based computer program named Limit_LASHING. Its user's guide is given in Appendix E.

2.3 Additional Information Regarding the Longitudinal Failure Mechanism

In this simplified model, each of the barge systems is idealized as a rigid body and the wall is assumed rigid. When barge System 1 impacts the *rigid* wall head-on, it is subject to a boundary condition of no further forward movement. The tendency for barge System 2 would be to continue its forward motion if it were not subject to "constraints." Note that System 2 is not subject to the same severe constraint that System 1 is (i.e., forward movement being prevented by the presence of a rigid wall). Instead, System 2 is subject to a constraint that is imposed by its lashings connection to System 1. It is reasoned that barge System 2 rigid body will have to decelerate only because it is lashed to barge System 1 with a finite number of cables (i.e., lashings), each with a finite tensile strength. Note that in the extreme, should the lashings between Systems 2 and 1 be of zero or only a nominal tensile strength, System 2 would continue its forward motion without decelerating. It is further reasoned that when System 1 stops its forward movement upon impact with a rigid wall, barge System 1 will decelerate at a more rapid rate than will System 2, as shown in Figure 2-3. Consequently, it is envisioned for this simplified model that the deceleration of barge System 2 will be at a far different and lower (magnitude) deceleration rate than for System 1. The magnitude of the deceleration for System 2 is a function of the number and orientation of the lashings as well as their size, ultimate capacity, and condition (e.g., new, used but in good condition, used and in poor condition, etc.). It is important to recognize that the time of maximum normal force against the rigid wall produced by System 1 may not coincide with the time of maximum normal force during deceleration of System 2. The maximum impact force of System 2 depends on the number and orientation of the lashings as well as their size, ultimate capacity, and condition (e.g., new, used but in good condition, used and in poor condition, etc.). That is, immediately after impact of System 1, the force normal to the wall increases and the lashings that keep System 1 and System 2 together do not develop their internal stress until System 2 begins to move relative to System 1. When System 2 begins to move and the lashings reach their ultimate strength, System 1 is at rest in the global Y-direction. This procedure produces different maximum values of the force normal to the wall.

At this time and awaiting the results of additional research, the authors of this report suggest that it be assumed that these maximum force values for Systems 1 and 2 are coincident. This may be a conservative assumption. Limit_LASHING is used to account for the deceleration of System 2 and its contribution to maximum F_W. However the assumption of deceleration equal to zero in the global Y-axis for System 1 implies that the inertia of System 1 does not contribute to maximum F_W in the Limit_LASHING computations of maximum F_W. Pending additional research results, the authors further suggest that the empirical correlation be used to account for, in an approximate sense, the

System 1 inertia effects during impact and that this contribution to the maximum F_W value be added to the maximum F_W value of System 2, computed using Limit_LASHING.

Finally, the percentage of total mass participating in System 1 and System 2 will be different depending upon the number of barges in the train. For example, in the 15-barge train system used in the full-scale experiments in 1998 (Patev et al. 2003), the total mass of the barge train was 1,865.59 kip*sec^2/ft; System 1 (5 barges) had a mass of 621.8633 kip*sec^2/ft, and System 2 (10 barges) had a mass of 1,243.7266 kip*sec^2/ft. Therefore, System 1 had 33 percent of the total mass, and System 2 had 66 percent of the total mass of the barge train.

2.4 Numerical Examples

In this section two numerical examples are presented. The barge train used for these examples consisted of 15 barges with a total mass of 1,865.59 kips*sec^2/ft. This is the same configuration used in the 1998 full-scale experiments. The kinetic coefficient of friction was set equal to 0.2 between barges, and set equal to 0.2 between the corner barge and the rigid wall. The first computation was made using an approach angle of 10 degrees, and for the second example, 80 degrees was used. The lashing configurations are shown in Appendix A. The lashing ultimate loads were set equal to 90 and 120 kips for the 1- and 1.25-in. diameter, respectively. The modulus of elasticity was 29,000 ksi and the ultimate strain (at rupture of the lashing) was set equal to 0.05. The hydrodynamic added mass coefficients were 0.05, 0.4, and 0.4 for the local x- and y-axes, and rotation, respectively.

It is important to note that for shallow impact angles (i.e., glancing blows), a large magnitude of the force normal to the wall is computed for the assumed longitudinal failure mechanism. This indicates that for shallow approach angles, another failure mechanism will dominate. (These other failure mechanisms will be discussed in subsequent chapters.) However, for high approach angles, the longitudinal failure mechanism will produce a positive value of force normal to the wall, and these other failure mechanisms will predict negative force values. A negative force is impossible because the barge train pushes on the wall and does not pull the wall. The resulting maximum values of the force normal to the wall were computed using Limit_LASHING to be the following: for an approach angle of 10 degrees, $F_W = 21,197.42$ kips; and for an approach angle of 80 degrees, $F_W = 2,388.58$ kips, as shown in Figures 2-16 and 2-17.
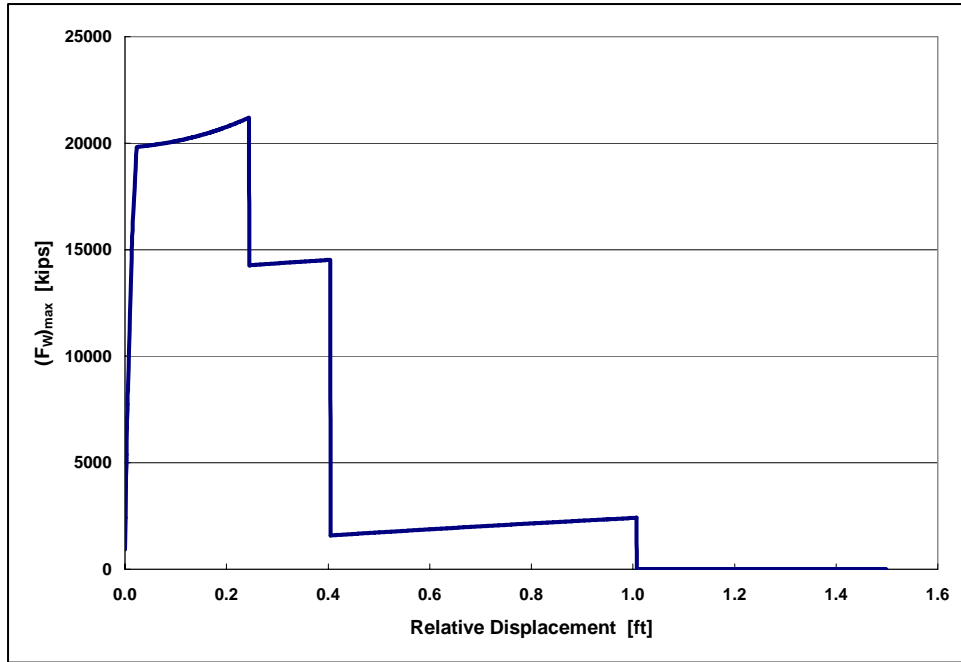
Figure 2-16. F_W versus relative displacement for $\theta = 10^0$, $\mu^*_k = 0.2$, $\mu_k = 0.2$, $m_T = 1,865.59$ kip*sec^2/ft, $m_2 = 621.863$ kip*sec^2/ft, $m_1 = m_T - m_2$ where m_T is the total mass of the barge train without hydrodynamic added mass
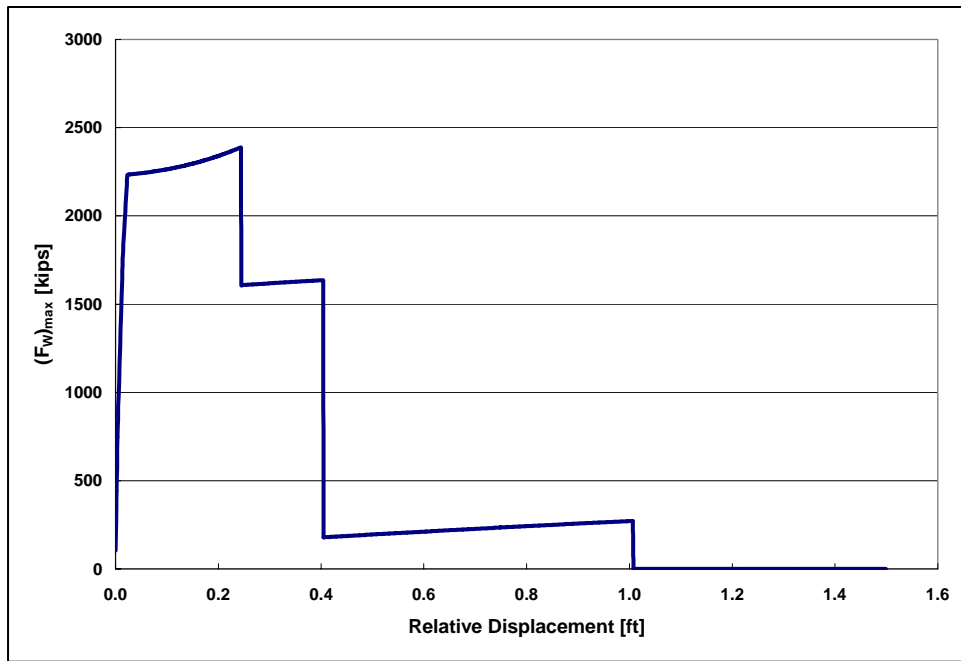
Figure 2-17. F_W versus relative displacement for $\theta = 80^0$, $\mu^*_k = 0.2$, $\mu_k = 0.2$, $m_T = 1,865.59$ kip*sec^2/ft, $m_2 = 621.863$ kip*sec^2/ft, $m_1 = m_T - m_2$

3 Transverse Failure Mechanism

3.1 Introduction

A barge train system consists of a group of nearly rigid barges joined together with steel cables, which are referred to as lashings. These lashings define a barge train system where the weak zones are assumed to occur at each barge-to-barge contact. The motion of each barge relative to the other is how the system distributes the impact forces among the barges during the impact process. As has been observed during barge train impacts events at shallow approach angles (i.e., "glancing" blows) as shown in Figure 3-1, the impact event can produce a failure of the lashings in an "opening wedge" fashion along a transverse plane between barges. The lashings develop tensile strains across the wedge-opening transverse plane as this opening develops. The barges rotate a small amount in such a way that the force normal to the wall is transferred to the connections between the barges. This transverse failure mechanism occurs in the local barge y-axis along the first transverse line of lashing connections behind the row of barges that form the bow to the barge train. This type of failure has a significant contribution from the rotation of the first column of three barges that form the bow.

Figure 3-2 depicts the barge train impacting a rigid wall and the development of a failure plane along the transverse axis of the barge train system. Two systems of barges are identified in this figure. The system that is in direct contact with the wall is referred to as System 1, and the remaining barges form System 2. System 1 rotates with a pivot assumed at the first connection from the bow on the starboard side. All the lashings across this potential failure plane elongate, resulting in an increase in the internal lashing forces. The lashings on the port side of this transverse plane are the most stressed and will be the first to fail. The idealized failure mechanism assumes that the internal connections rupture in sequence toward the pivot point as System 1 continues the rotation. In this failure mechanism both systems of barges are assumed to be rigid and no longitudinal relative motion is assumed. It is recognized by the authors that this is an idealization; however, this simple model attempts to capture a failure mechanism whereby most of the energy comes from the rotational degree(s) of freedom.
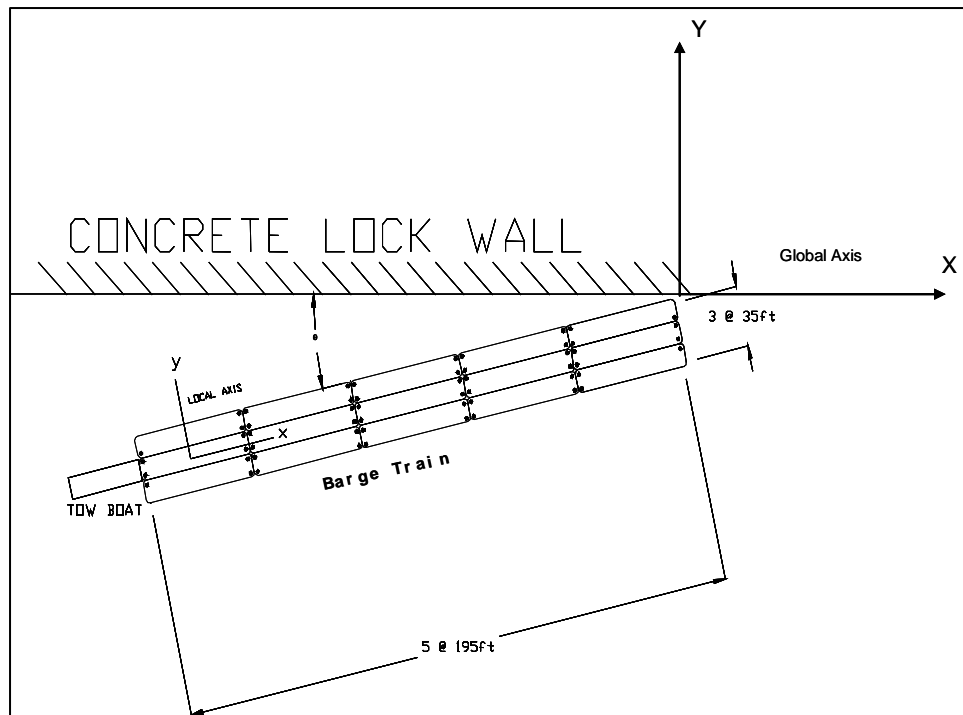
Figure 3-1. An idealized shallow approach angle for a barge train-wall system (repeated from earlier text for the convenience of the reader)
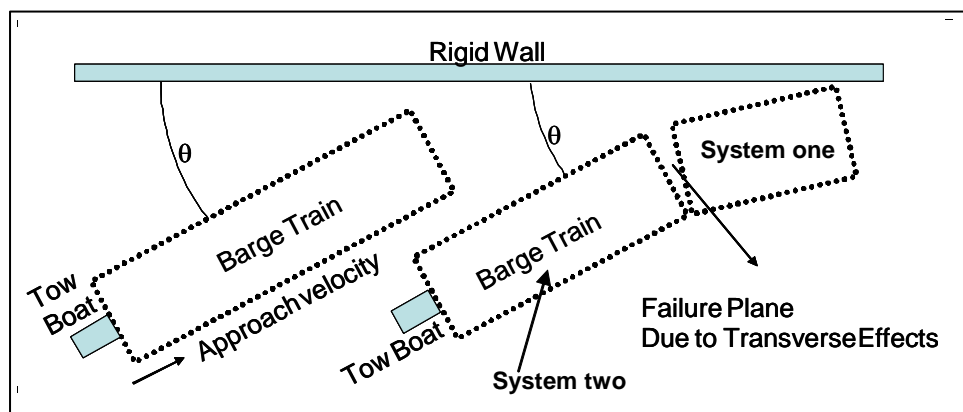
Figure 3-2. Transverse failure mechanism (repeated from earlier text for convenience of the reader)

This transverse failure mechanism model allows for the rotation of the first column of barges (Figure 3-2). In this way, all the lashings along the transverse failure plane break caused by the rotation between barges of System 1 and System 2, as shown in Figure 3-2. In this model, different linear accelerations (in actuality, decelerations) in the global Y-direction for System 1 and System 2 were assumed. It is reasoned that when System 1 stops its forward global Y-axis motion with its impact with a rigid wall, barge System 1 will decelerate at a more rapid rate than will System 2. Consequently, it is envisioned for this simplified model that the deceleration of System 2 will be at a far different and lower deceleration rate than System 1. A zero linear global acceleration in the

Y-direction of System 1 is assumed in this simplified model because the impact with a *rigid* wall occurs with this system in the global Y-direction. System 2 motions continue and the lashings that connect System 1 to System 2 will try to rotate System 2 toward the wall. Thus, the deceleration of System 2 in the global Y-direction is nonzero. As will be shown in Equation 3-2, the summation of forces in the global Y-direction of System 1 is equal to zero according to this assumption. However, as will be seen in Equation 3-11, the global Y-axis linear deceleration of System 2 is nonzero.

The transverse failure mechanism does not allow for the relative displacement between barges that form System 1 nor in System 2 in the local x-direction. In this manner, all lashings located in the Figure 3-3 shaded zone break by means of the transverse mechanism with no contribution made by the longitudinal relative displacement between barges. This failure mechanism is described by the equations of motion based on Newton's second law. First, a free-body diagram is defined as shown in Figure 3-4. All unknown and known forces for System 1 appear in this diagram. The unknown external forces are F_W and S_W, and the internal unknown forces are the normal F_{NC} and the internal moment M. In this model the internal shear is related to the normal force by means of the kinetic coefficient of friction μ_K; $S_{NC} = \mu_K F_{NC}$. The known forces are the internal force in each lashing as the rotation takes place. These forces are labeled as f_{Ni} and f_{Si}.

Figure 3-3.   No relative displacement allowed in the local x-axis among the three barges of System 1

The free-body diagram is equal to the kinetic diagram as stated by Newton's second law. Figure 3-5 presents the linear accelerations and angular accelerations for System 1. In this case the linear accelerations are oriented in the global X- and Y-axes.

Figure 3-4.   Transverse failure mechanism, free-body diagram of System 1
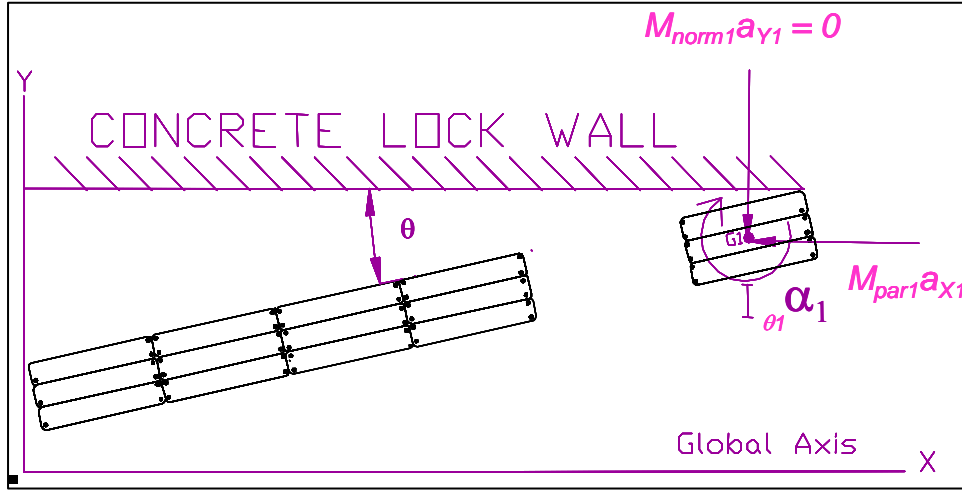
Figure 3-5.   Transverse failure mechanism, kinetic diagram of System 1

For barge System 1, which is in contact with the wall, the equations of motion are

$$\oplus \rightarrow \sum F_X = ma_X \ \therefore \ -S_W - Rn_X + Rs_X + F_{NC}\cos\theta - \mu_K F_{NC}\sin\theta = -M_{par1}a_{X1} \quad (3\text{-}1)$$

$$\oplus\uparrow \sum F_Y = ma_Y \ \therefore \ -F_W - Rs_Y - Rn_Y + F_{NC}\sin\theta + \mu_K F_{NC}\cos\theta = -M_{norm1}a_{Y1} = 0 \ ; M_{norm1}a_{Y1} = 0 \quad (3\text{-}2)$$

$$\oplus \circlearrowright \sum M_o = (\sum M_{EQUIVALENT})_o \ \therefore \ M + M_{Rfn} - M_{Rfs} - F_{NC}(y_1 - y_{G1}) + \mu_K F_{NC} a =$$

$$I_{\theta1}\alpha_1 + (M_{par1}a_X\cos\theta + M_{norm1}a_Y\sin\theta)(y_1 - y_{G1}) + (M_{par1}a_X\sin\theta - M_{norm1}a_Y\cos\theta)\frac{a}{2} \quad (3\text{-}3)$$

where moment is taken about the point o, which is the point of contact between the barge train and the wall, and M_{Rfs} is the resultant moment about the mass center of gravity due to the f_{Si} forces.

Four parameters that affect the force normal to the wall are the global X- and Y-components of the forces parallel (Rs_X, Rs_Y) and perpendicular (Rn_X, Rn_Y) to the failure plane obtained from the internal force in the lashings. These forces are obtained in the following manner. Due to the elongation of the lashing during the

deformation process, an internal force appears in the lashings. The angle that defines each segment of the lashings with the longitudinal local axis is calculated using the local coordinates of the start (x_s, y_s) and end (x_e, y_e) bits that connect each segment of each lashing. Then, the components of these forces in local coordinates are easily transformed to forces in the global coordinate system by means of the transformation matrix that contains the sine and cosine functions. As shown in Figure 3-6, these forces can be easily obtained by the use of trigonometric functions. For example, $Rn_X = F_L * \sin \delta,$ and $Rn_Y = Rn_Y * \cos \theta.$
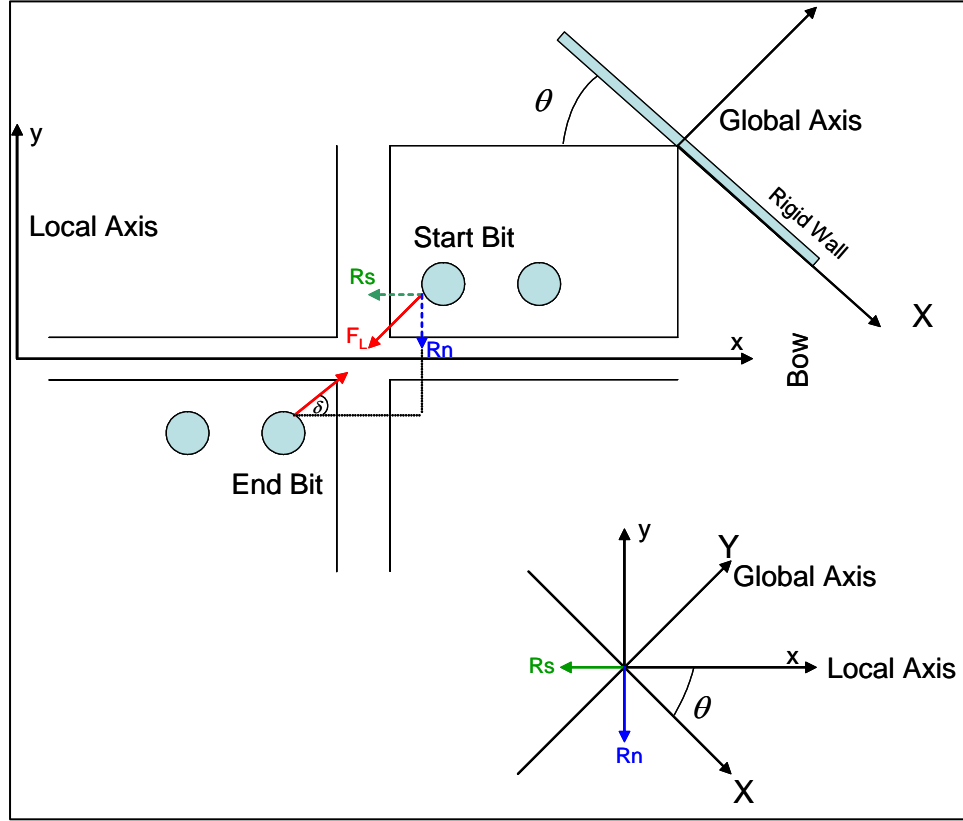
Figure 3-6.   Global components of lashing force

Hydrodynamics effects are included in barge System 1 using the ETL 1110-2-338 approach:

$$M_{x1} = (1 + \eta_x) * m_1 \tag{3-4}$$

$$M_{y1} = (1 + \eta_y) * m_1 \tag{3-5}$$

$$I_{\theta 1} = (1 + \eta_\theta) * I_{G1} \tag{3-6}$$

$$I_{G1} = \frac{1}{12} * m_1 * \left(L_1^2 + B_1^2\right) \tag{3-7}$$

$$M_{norm1} = \frac{M_{x1} * M_{y1}}{M_{x1} \cos^2 \theta + M_{y1} \sin^2 \theta} \qquad (3\text{-}8)$$

$$M_{par1} = \frac{M_{x1} * M_{y1}}{M_{x1} \sin^2 \theta + M_{y1} \cos^2 \theta} \qquad (3\text{-}9)$$

with the hydrodynamic added mass coefficients defined in the local barge coordinate system, according to ETL 1110-2-338, as

$$\eta_x = 0.05$$
$$\eta_y = 0.4$$
$$\eta_\theta = 0.4$$

The angular acceleration for System 1, α_1, is assumed equal to the angular acceleration for System 2, α_2, for this simplified transverse failure mechanism; $\alpha_1 = \alpha_2 = \alpha$.

The authors of this report recommend that hydrodynamic effects be considered in the simplified limit state analyses. Therefore, Equations 3-1 through 3-3 will include hydrodynamic added mass terms via Equations 3-4 through 3-9.

Applying the same procedure to System 2, which contains the rest of the barge train, gives three additional equations of motion. As always, its free-body diagram must be equal to the kinetic diagram as stated by Newton's second law. For this system, the free-body diagram is given in Figure 3-7. In this diagram appear all the unknown and known forces in the system. Note that for System 2 there are no *external* unknown forces. The internal unknown force is the normal, F_{NC}, due to the barge-to-barge contact along the longitudinal failure plane between barge Systems 1 and 2, and the internal moment M. In this system the internal shear between barge Systems 1 and 2 is related to the normal by means of the kinetic coefficient of friction μ_K; $S_{NC} = \mu_K F_{NC}$. The known forces are the internal force in each lashing as the rotation takes place. The f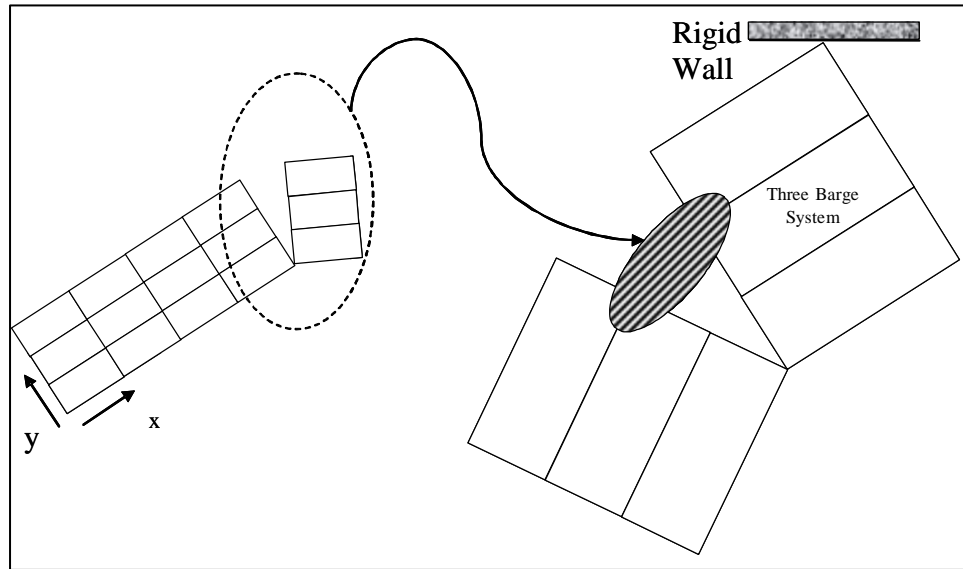orces are labeled as f_{Ni}, and f_{Si}. Figure 3-8 presents the linear accelerations and angular accelerations of the system. In this case the linear accelerations are oriented in the global X- and Y-axes.
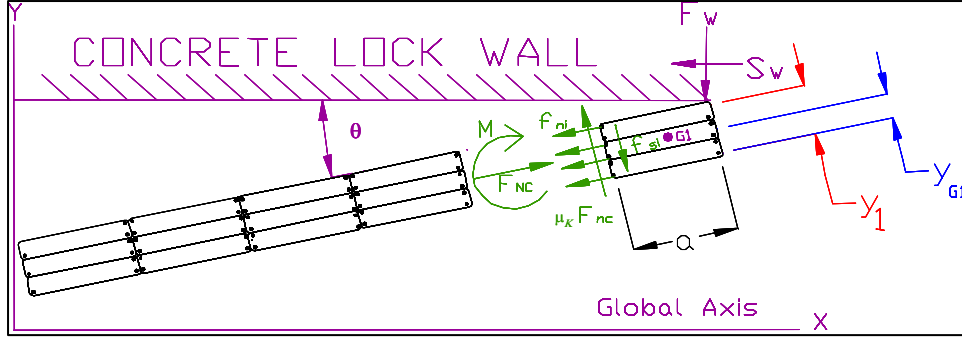
The three equations of motion of barge System 2 based on Figures 3-7 and 3-8 are

$$\oplus \rightarrow \sum F_X = ma_X \ \therefore -Rs_X + Rn_X - F_{NC} \sin\theta + \mu_K F_{NC} \cos\theta = -M_{par2} a_{X2} \ (3\text{-}10)$$

$$\oplus \uparrow \sum F_Y = ma_Y \ \therefore Rs_Y + Rn_Y - F_{NC} \sin\theta - \mu_K F_{NC} \cos\theta = -M_{norm2} a_{Y2} \qquad (3\text{-}11)$$

$$\oplus \circlearrowright \sum M_{G2} = (\sum M_{EQUIVALENT})_{G2} \ \therefore -M + M_{Rfn} - M_{Rfs} + \mu_K F_{NC}(c - x_{G2}) = I_{\theta2}\alpha_2 \quad (3\text{-}12)$$

where

$c =$ location of the failure plane along the local x-axis measured from the aft

$x_{G2} =$ location of the center of mass of barge System 2 along the local x-axis measured from the aft
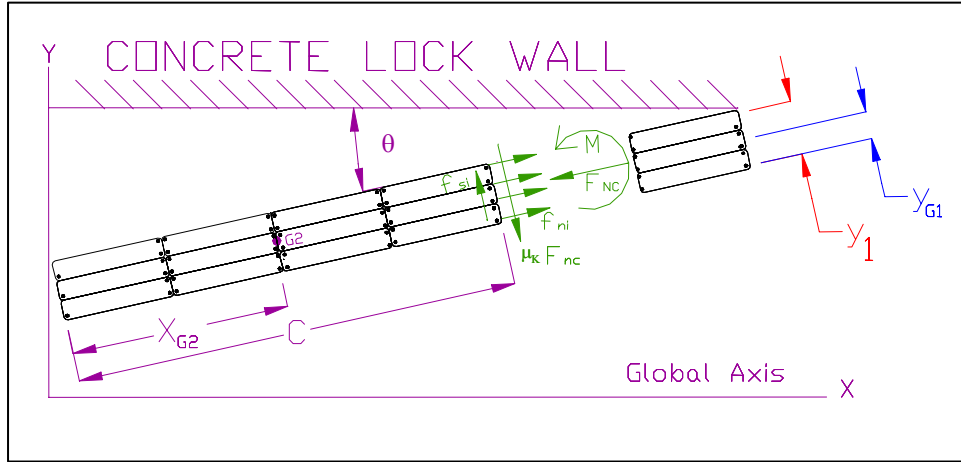
Figure 3-7. Transverse failure mechanism, free-body diagram of System 2
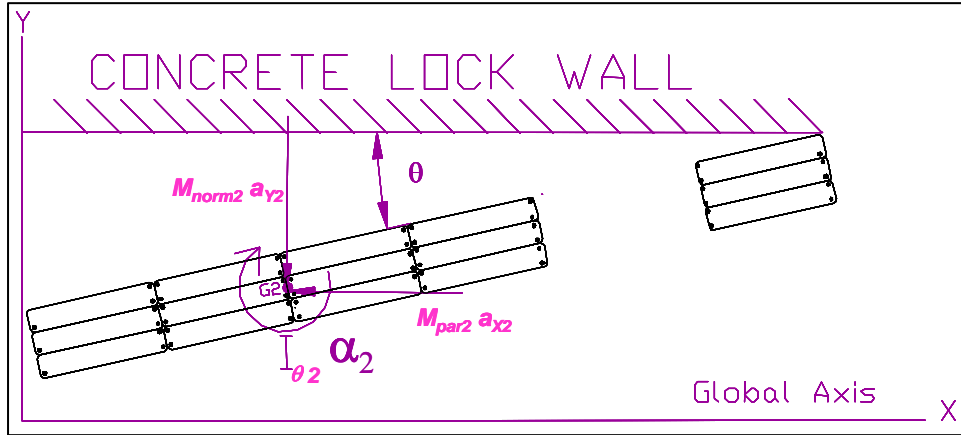
Figure 3-8. Transverse failure mechanism, kinetic diagram of System 2

M_{par2}, M_{norm2}, and $I_{\theta 2}$ are computed for barge System 2 using Equations 3-4 through 3-9 modified for System 2 geometry and masses. The mass of barge System 2, excluding hydrodynamic added mass, is designated m_2. Recall barge System 2 is assumed to decelerate at a different rate from barge System 1 during impact. The rotation of System 2 relative to the rotation of System 1 during an impact event allows this simplified model to crudely capture this behavior. The lashings transmit the effects of the System 2 inertial forces to System 1 and onto the wall. However, for this simplified model, the number of equations limits the number of variables to be considered in the solution process. Consequently, a crude assumption that System 2 was still decelerating in the global Y-axis after the deceleration of barge System 1 had concluded was made to match the number of variables with the number of equations. Recall that one of the primary features

of this simplified model is to account for the forces in the lashings and to consider how these forces reflect the inertia of the two barge system bodies and their rotation. With consideration of all of these factors the decision was made to assume that the global Y-axis acceleration of barge System 1 is zero in the calculations. The six equations (3-1 through 3-3 and 3-10 through 3-12) have seven unknowns: F_W, S_W, M, F_{NC}, $a_{X1} = a_{X2}$, a_{Y2}, and α for both systems. The global X-axis linear accelerations of both systems are assumed equal for this simplified transverse failure mechanism. Therefore, another equation is required. A relationship between the shear and normal force between corner barge and wall is introduced:

$$S_W - \mu_K^* F_W = 0 \tag{3-13}$$

Solving Equations 3-1 through 3-3 and 3-10 through 3-12 gives the resulting F_W expression:

$$F_W = \frac{M_{par}\left[(Rn_X - Rs_X)\sin\theta + \mu_K(Rn_X - Rs_X)\cos\theta + \mu_K(Rs_Y + Rn_Y)\sin\theta - (Rn_Y + Rs_Y)\cos\theta\right]}{(M_{par1}\cos\theta + M_{par2}\cos\theta - \mu_K M_{par1}\sin\theta - \mu_K M_{par2}\sin\theta - \mu_K \mu_K^* M_{par2}\cos\theta - \mu_K^* M_{par2}\sin\theta)} \tag{3-14}$$

Notice here that the hydrodynamic added mass affects the F_W expression. If the denominator of Equation 3-14 is zero, then

$$M_{par1}\cos\theta + M_{par2}\cos\theta - \mu_K M_{par1}\sin\theta - \mu_K M_{par2}\sin\theta$$

$$- \mu_K \mu_K^* M_{par2}\cos\theta - \mu_K^* M_{par2}\sin\theta = 0$$

Solving for the critical value of the approach angle produces the following expression:

$$\theta_{CR} = \tan^{-1}\left(\frac{M_{par} - \mu_K \mu_K^* M_{par2}}{\mu_K M_{par} + \mu_K^* M_{par2}}\right) \tag{3-15}$$

Equations 3-14 and 3-15 were obtained from the solution provided by Maple's Worksheet. Derivation of Equation 3-14 is presented in Appendix D. There are combinations of variables for which Equation 3-14 is either indeterminate (e.g., the case of a value of zero in the denominator) or negative. Either of these cases provides unrealistic values for F_W. Equation 3-15 defines the asymptote for Equation 3-14 via the approach angle designated θ_{CR}. Approach angles equal to or greater than θ_{CR} produce infinite values or negative values for F_W for the transverse failure mechanism, respectively. For approach angles greater than θ_{CR}, other failure mechanisms are more likely to occur. An alternative failure mechanism was discussed in Chapter 2. A negative value of F_W means that the barge train pulls the rigid wall instead of pushing the wall during the impact process. Mathematically speaking, all models produce a number, but in an engineering sense, these numbers must be rational in terms of the process involved. In Chapter 6 numerical examples will be presented. When this simplified, idealized model produces a negative value for F_W, a zero value will be

assigned indicating that the impact model will not predict physically real values for F_W based on the input data provided.

In summary, the following assumptions are made for the transverse failure mechanism:

a. The linear acceleration in the global Y-direction in barge System 1 is assumed to be zero. This means that in the global Y-direction the barge stops instantly at the moment of impact. This condition ensures the motion normal to the wall is stopped, but motion parallel to the wall is not restricted.

b. The linear acceleration in the global X-direction for barge System 1 is assumed to be equal to the global X-axis linear acceleration for barge System 2.

c. The angular acceleration for barge System 1 is assumed to be equal to the angular acceleration for barge System 2.

d. The kinetic coefficient of friction between barges must be defined. A review of the technical literature, discussed in Chapter 5, indicates a value between 0.2 and 0.5.

e. The kinetic coefficient of friction between the corner barge and the struck wall must be defined. A review of the technical literature, discussed in Chapter 5, indicates a value between 0.2 and 0.5.

f. The lashings are assumed to behave in an elastic-plastic manner and break when an ultimate (tensile) strain value is achieved within the lashing. Should the lashings reach the yield stress, no additional force can be carried by the lashing with additional deformations. Achieving the ultimate tensile strain results in rupturing of the lashing.

g. This failure mechanism is valid for low approach angles; research indicates values lower than 30 degrees. Greater approach angles are likely to produce a failure path other than in the transverse direction with a pivot on the starboard side.

h. Hydrodynamic effects are considered by means of an increase in the barge train mass in the local x- and y-axes and rotational directions. This hydrodynamic effect influences the kinetic variables (e.g., linear accelerations and angular acceleration).

i. System 1, which is in contact with the struck wall, abruptly/ instantaneously stops motion while barge System 2 continues motion. The lashings across the transverse failure plane pull System 2 towards the wall.

3.2 Transverse Failure Mechanism: Two Possible Pivot Locations

There are two possible tendencies of rotation in the transverse failure mechanism. If the line of action of the resultant force at the point of contact lies to the front of the center of mass of System 1, then the pivot point will be at the

starboard side of the barge train as shown in Figure 3-9. On the other hand, if the line of action of the resultant force at the point of contact of the barge train and the rigid wall lie behind the center of mass, then the pivot point will be at the port side of the barge train as shown in Figure 3-10. Equation 3-14 applies in both cases. The following variables can be identified in Equation 3-14:

- The approach angle.

- The mass of System 1 and System 2 including the hydrodynamic effects.

- The kinetic coefficient of friction between barges.

- The kinetic coefficient of friction between the wall and the barge train.

- The internal force of the lashings along the assumed failure plane.

The location of the center of mass of System 1 does not affect Equation 3-14. The location of the center of mass of System 1 does not affect the normal force at the point of barge-to-wall contact. However, it can be possible to have the pivot point dependent on the magnitude of the coefficient of friction developed at the wall during impact. The angle β between the resultant force at the wall with respect to the global X-axis is calculated as

$$\beta = \tan^{-1}\left(\frac{F_W}{S_W}\right) = \tan^{-1}\left(\frac{1}{\mu_K^*}\right)$$

On the other hand, the angle that defines the line from the point of contact to the center of mass from the rigid wall can be calculated as

$$\gamma = \theta + \alpha \quad ; \quad \alpha = tan^{-1}\left(\frac{a}{b}\right)$$

If γ is less than β, then the pivot point will occur on the starboard side of the barge train, as shown in Figure 3-9. If γ is greater than β, then the pivot point will occur on the port side of the barge train, as shown in Figure 3-10. In summary, two possible pivot points exist in the transverse failure mechanism depending on the kinetic coefficient of friction between the barge train and the wall.

For example, determine the approach angle that is needed for each of the pivot point possibilities for the 15-barge train used in the experiments in 1998 (Patev et al. 2003). The main variable for this calculation is the kinetic coefficient of friction between the barge train and the armored rigid wall. It is an unknown value, but it can be approximated by using a lower value of 0.2 and an upper value of 0.5, as will be presented in Chapter 5. The dimensions a and b to the center of mass of System 1 are the following: $a = 52.5$ ft and $b = 97.5$ ft. Each of the limiting values of the kinetic coefficient of friction, 0.20 and 0.50, is determined to be $\beta = 78.7$ degrees and 63.4 degrees, respectively. This is the orientation of the resultant force at the wall with respect to the global X-axis. Equating the expression of β and γ produces a value for the approach angle: $\theta = 50.4$ degrees and $\theta = 35.1$ degrees for $\mu_K^* = 0.2$ and 0.5, respectively (Figure 3-11).
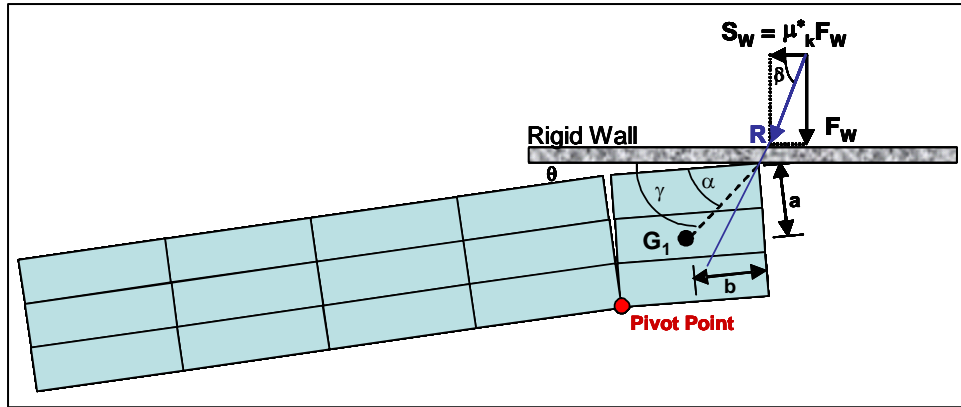
Figure 3-9.   Pivot point at starboard side of the barge train
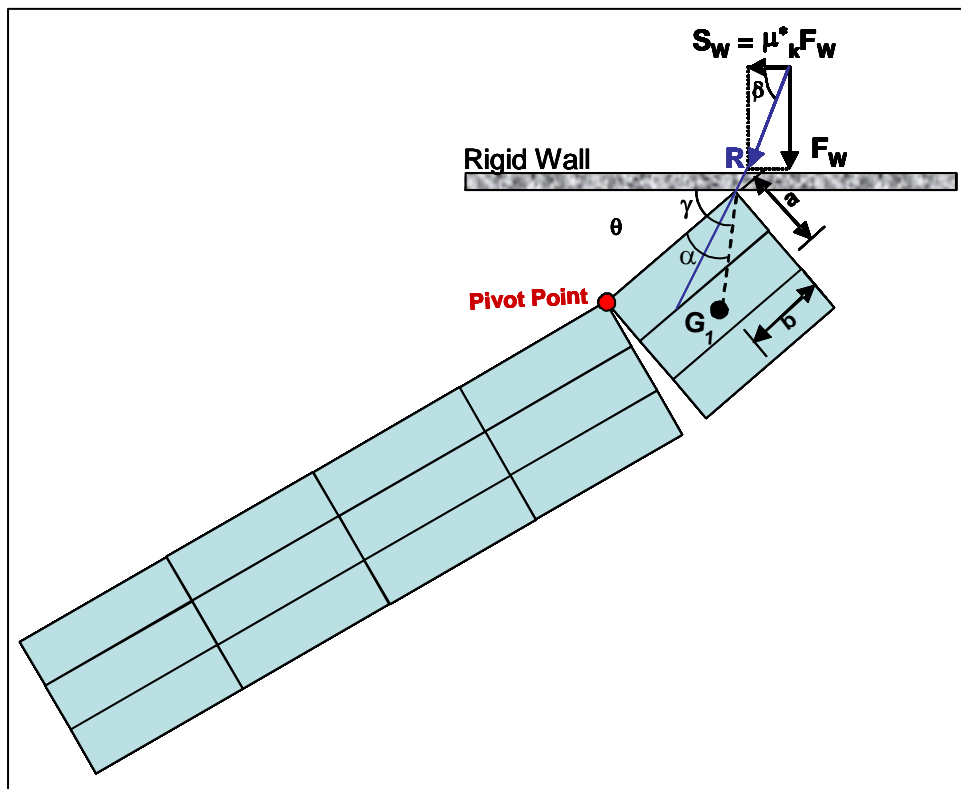
Figure 3-10. Pivot point at port side of the barge train

If the approach angle is equal to 50.4 degrees, then the center of mass of System 1 would be along the line of action of the resultant force at the point of contact between the barge train and the wall. For an approach angle lower than 50.4 degrees, the pivot point will be at the starboard side; and if the approach angle is greater than 50.4 degrees, the pivot point will be at the port side. This condition is reached if the kinetic coefficient of friction is 0.2.

However, for a kinetic coefficient of friction equal to 0.50, the resulting approach angle is equal to 35.1 degrees and the center of mass of System 1 would be along the line of action of the resultant force at the point of contact between the barge train and the wall. For an approach angle lower than 35.1 degrees, the

pivot point will be at the starboard side, and if the approach angle is greater than 35.1 degrees the pivot point will be at the port side. In the same way, the following expressions can be obtained if β and γ are equal:

$$\mu_K^* < \cot[\theta + \alpha] \qquad \text{pivot point at starboard side} \qquad (3\text{-}16)$$

$$\mu_K^* > \cot[\theta + \alpha] \qquad \text{pivot point at port side} \qquad (3\text{-}17)$$
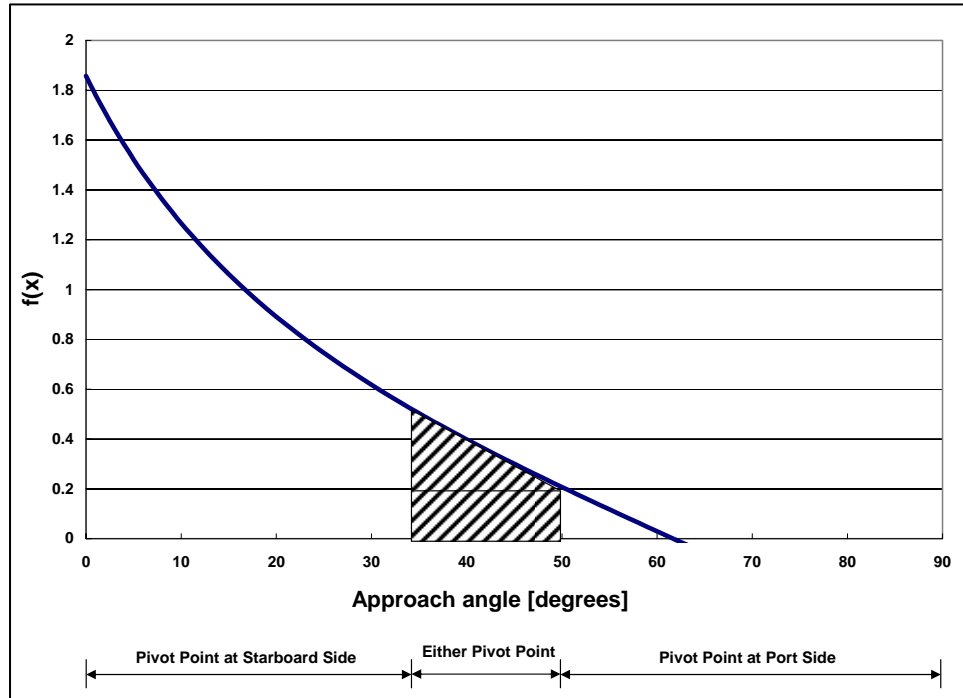
Figure 3-11. Pivot point location for the 15-barge system with $a/b = 52.5/97.5 = 0.538$

The inequalities presented in Equations 3-16 and 3-17 indicate the range where each location of the pivot point will occur. For example, if the 15-barge system is used and the approach angle is 10 degrees, only one of the expressions presented in Equations 3-16 and 3-17 will be valid. In this case, *cot [θ+α] =* 1.266, which is greater than the reasonable kinetic coefficient of friction between steel-to-steel as presented in Chapter 5 (between 0.2 and 0.5). For this reason, if the approach angle is 10 degrees, the transverse failure mechanism is likely to occur with a pivot point at the starboard side of the barge train, as demonstrated by Equation 3-16.

However, if the 15-barge system is used and the approach angle is 70 degrees, the valid expression is Equation 3-17, that is, *cot [θ+α] = -0.1458,* which is lower than the reasonable kinetic coefficient of friction between steel-to-steel as presented in Chapter 5 (between 0.2 and 0.5). For this reason, if the approach angle is 70 degrees, the transverse failure mechanism could occur with a pivot point on the port side of the barge train.

If the approach angle is between 35 and 50 degrees, both locations of the pivot point (i.e., port and starboard) are valid. Between this range, for example, 40 degrees, the right side of Equations 3-16 and 3-17 produces cot $[\theta + \alpha] = 0.398$, which is inside the acceptable range for the steel-to-steel kinetic coefficient of friction (between 0.2 and 0.5).

It is important to mention the difference between the approach angle calculated with the previous equations and the critical approach angle calculated with Equation 3-15. The value of the approach angle obtained with Equation 3-15 is the limiting value for which Equation 3-14 produces positive results.

3.3 Additional Information Regarding the Transverse Failure Mechanism

In this simplified model, each of the two barge systems is idealized as a rigid body and the wall is assumed rigid. When barge System 1 impacts the *rigid* wall, it is subject to a boundary condition of no further forward motion. Barge System 2 would tend to continue its translational motion if it were not subject to "constraints." Note that System 2 is not subject to the same severe constraint that System 1 is (i.e., forward motion being prevented by the presence of a rigid wall). Instead, System 2 is subject to a constraint imposed by its lashings connections to System 1. It is reasoned that the barge System 2 rigid body will have to decelerate only because it is lashed to barge System 1 with a finite number of cables (i.e., lashings), each with a finite tensile strength. Note that in the extreme, should the lashings between System 2 and System 1 be of zero or only a nominal tensile strength, System 2 would continue its forward motion without angular deceleration. It is further reasoned that when System 1 stops its forward motion upon impact with a rigid wall, barge System 1 will decelerate at a more rapid rate than will System 2. Consequently, it is envisioned for this simplified model that the deceleration of barge System 2 will be at a far different and lower deceleration rate from System 1. The magnitude of the deceleration for System 2 is a function of the number and orientation of the lashings as well as their size, ultimate capacity, and condition (e.g., new, used but in good condition, used and in poor condition, etc.). It is important to note that the time of maximum normal force against the rigid wall produced by System 1 may not coincide with the time of maximum normal force during deceleration of System 2. The maximum impact force of System 2 depends on the number and orientation of the lashings as well as their size, ultimate capacity, and condition (e.g., new, used but in good condition, used and in poor condition, etc.). That is, immediately after impact of System 1, the force normal to the wall increases and the lashings that keep System 1 and System 2 together do not develop the strength until System 1 begins to rotate relative to System 2. When System 1 begins to rotate and the lashings reach their ultimate strength, System 2 is at rest in the global Y-direction. This mechanism produces different maximum values for the force normal to the wall.

At this time and awaiting the results of additional research, the authors of this report suggest that it be assumed that these maximum force values for Systems 1 and 2 are coincident. This may be a conservative assumption. Limit_LASHING

is used to account for the deceleration of System 2 and its contribution to maximum F_W. However the assumption of deceleration equal to zero in the global Y-axis for System 1 implies that the inertia of System 1 does not contribute to maximum F_W in the Limit_LASHING computations of maximum F_W. Pending additional research results, the authors further suggest that the empirical correlation be used to account for, in an approximate sense, the System 1 inertia effects during impact and that this contribution to the maximum F_W value be added to the maximum F_W value of System 2, computed using Limit_LASHING.

Finally, the percentage of total mass participating in System 1 and System 2 will be different depending upon the number of barges in the train. For example, in the 15-barge train system used in the full-scale experiments in 1998, the total mass of the barge train was 1,865.59 kip*sec^2/ft; System 1 (3 barges) had a mass of 373.118 kip*sec^2/ft, and System 2 (12 barges) had a mass of 1492.472 kip*sec^2/ft. System 1 had 20 percent of the total mass, and System 2 had 80 percent of the total mass of the barge train.

3.4 Numerical Solution Procedure

The formulation presented in this chapter is used to calculate the force normal to the wall assuming a transverse failure mechanism during impact. The value computed for the resultant F_W is dependent on the magnitude of the lashing forces. The rotation of System 1 relative to System 2 produces tensile strain in the lashings across the transverse failure plane. This can be achieved by means of an elongation of the lashing when the barges of System 1 rotate as shown in Figure 3-12. Thus an analytical approach is developed to assess these lashing forces based on the rotation of the two (or three) barges in System 1. This incremental rotation translates into incremental changes in the lashing forces across the transverse failure plane between barge systems. The sequential process to calculate the FW by Limit_LASHING is the following:

a. The initial length of the lashing is calculated using the initial internal force in the lashing. (Lashings usually have a tensile force that is introduced when the barges are initially assembled into a barge train.) If the initial force is known, then the initial elongation produced by the initial force can be calculated using the following expression: $F = AE/L_o)\Delta$. This equation comes from the stress-strain relationship and the stress and strain definitions. If $\Delta = L_f - L_0$, then $L_0 = A*E*L_f / (F+A*E)$.

b. Using the calculated initial length of the lashing, an assumed increment of length is added to the lashing due to the progressive rotation of System 1. Note that all the lashings increase in internal load as rotation of System 1 increases.

c. A continuous increment of the rotation of System 1 leads to the lashing at the port side (and across the transverse failure mechanism) to reach the ultimate load first.
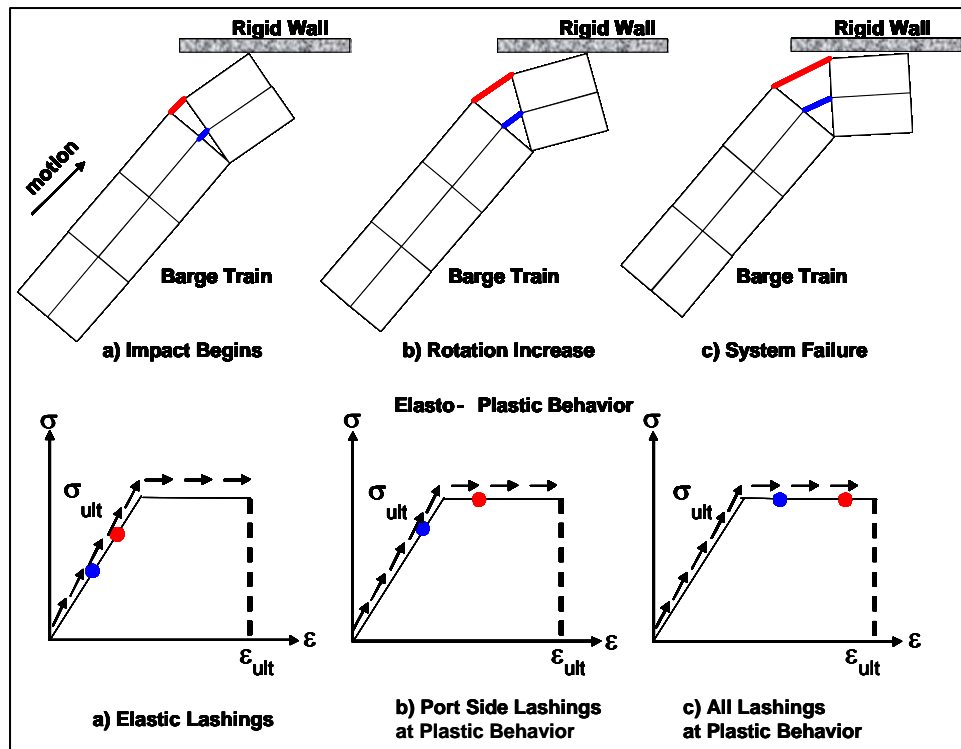
Figure 3-12. Progressive transverse failure of lashings across a transverse failure plane within the barge train (repeated from earlier text for the convenience of the reader)

d. As the incremental rotation increases, the inner lashing configurations will eventually reach their ultimate load. The ultimate condition is reached in sequence from the port side to starboard side.

e. As shown in the Figure 3-12b idealization, as the rotation of System 1 increases, the lashing indicated in red can reach the horizontal plateau of the elastoplastic stress-strain model.

f. With sufficient rotation of System 1, the strains within each of the lashings reach their ultimate (tensile) values and all lashings yield, as idealized in Figure 3-12c, and ultimately break when the strains ε equal ε_{ult}.

g. In the incremental solution process an incremental rotation of System 1 is assumed. The incremental rotation value used in each computational step is set equal to 0.001 ft/(width in feet) of the barge train system. For example, for a 105-ft-width system, the rotation step is equal to $0.001/105 = 0.000009523809524$ radian. Parametric studies have shown this to be a small value considering that the calculations are made numerous times; e.g., 1000 calculations will result in 1 ft of elongation at the port side. With this magnitude of elongation, lashings will reach their ultimate value.

h. The location of the bits defines the initial length of the lashings. This difference in the lengths of the lashings can result in different tensile strain within each lashing. This is the reason there are different

stress-strain levels within the lashings even for the same relative displacement across the failure plane between System 1 and System 2.

i. Each of the lashings is likely to reach its ultimate tensile stress value at different instances during the relative motion process (between Systems 1 and 2), as specified in the previous subparagraph. As soon as the lashing reaches the ultimate stress, the lashing cannot accrue additional stress (or tensile force) in the incremental analysis. This is due to the elastoplastic behavior of the lashing adopted in this failure mechanism. The lashing can accrue additional strain based upon the additional stretching from the continued relative displacement between the two barge systems.

j. Should a lashing accrue a strain equal to the user-specified ultimate strain, the lashing is assumed to rupture and is removed from the connection system across the failure plane.

k. These resultant lashing forces are then used as input data to the expressions for F_W previously presented.

It is important to mention that the lashing failures occur in a sequence; it is not assumed that all lashings reach their ultimate stress at once. Actual impact response among the barges and the lashings during impact is quite complex: the difference in bit locations and lashing configurations between bits as well as the different initial tension forces set in the lashings provide the system with an uneven distribution of forces at the lashing connections. In addition, as soon as the corner barge impacts the *rigid* wall, the impact wave generated internal to the barge train reaches all points throughout the barge train at different instants of time, producing different stresses and strains among the lashings. To model this behavior in this *simplified model*, relative motion between barge systems and the rotation of System 1 are assumed. This rotation produces different kinematics for the two systems in the local x-axis of the barge train. This difference in kinematics for the two systems is responsible for the stress and strain that develop in the lashings across the failure plane. In this simplified model, the rotation of System 1 is constant for each incremental step. However, this condition does not mean that this rotation occurs at an equal time-step. Remember that the deceleration may not be constant. So if it is not a constant, the time at which the increment of the rotation occurs is not constant. In other words, the time to produce a rotation increment from $1*10^{-6}$ to $1*10^{-5}$ radian is different from the time needed to produce a rotation increment from $1*10^{-4}$ to $1*10^{-3}$ radian, because the kinematics variables for each rotational increment are different. The incremental computational procedure was implemented in a new PC-based computer program named Limit_LASHING. Its user's guide is given in Appendix E.

3.5 Numerical Examples

In this section two numerical examples are presented. The barge train used for these examples consists of 15 barges with a total mass of 1,865.59 kip*sec^2/ft. This is the same configuration used during the 1998 full-scale experiments (Patev et al. 2003). The kinetic coefficient of friction is set equal to 0.2 between barges

and between the corner barge and the rigid wall. The first computation was made using an approach angle of 10 degrees, and for the second example, 20 degrees. The lashing configurations used are shown in Appendix A. The ultimate load of the lashings was 90 and 120 kips for the 1- and 1.25-in. diameter, respectively. The modulus of elasticity was 29,000 ksi and the ultimate strain was set equal to 0.05. The hydrodynamic added mass coefficients were 0.05, 0.4, and 0.4 for the local x- and y-axes and rotation, respectively.

It is important to note that the transverse failure mechanisms are more likely to occur for shallow approach angles. However, at higher approach angles, this failure mechanism can predict negative values of the force normal to the wall. This indicates that for high approach angles (> 70 degrees), another failure mechanism such as the one discussed in Chapter 2 will dominate. The resulting maximum values of the force normal to the wall were the following: for an approach angle of 10 degrees, 690.3431 kips, and for an approach angle of 20 degrees, 781.879 kips. In the analysis performed by the PC-based computer program Limit_LASHING, a negative F_W is set equal to zero because it is physically impossible for the barge train to pull on the rigid wall instead of push the rigid wall.

Figures 3-13 and 3-14 show two positions where local, secondary peaks appear before the zero F_W is reached. This pattern occurs because at this point all the lashings are at yield condition, and the lashing in the diagonal (scissors layout) produces opposite components in the global Y-direction, resulting in a reduction of the force normal to the wall. That is, it is not a peak, it is a lower point that occurred due to the opposite components that the scissors scheme produces. After one of the diagonals reaches ultimate strain, only one of the scissors legs is actively increasing the force normal to the wall. Referring to Figure 3-15, point *d* moves more than point *c* due to the same rotation about the pivot point. The force in lashing *db* applied to System 1 produces a component in the global Y-axis in the same direction of F_W. However, the force in lashing *ca* applied to System 1 produces a component in the global Y-axis in the opposite direction of F_W. These opposite directions in the lashings *db* and *ca* produce a reduction in F_W. As lashing *db* reaches the ultimate strain first (because it experiences higher displacement than *ca* about the pivot point), only the lashing *ca* contributes to F_W, the global Y-component of which is opposite the F_W direction. With no reduction of force because *db* does not exist (failed), the force normal to the wall increases again producing the peak in Figures 3-13 and 3-14.
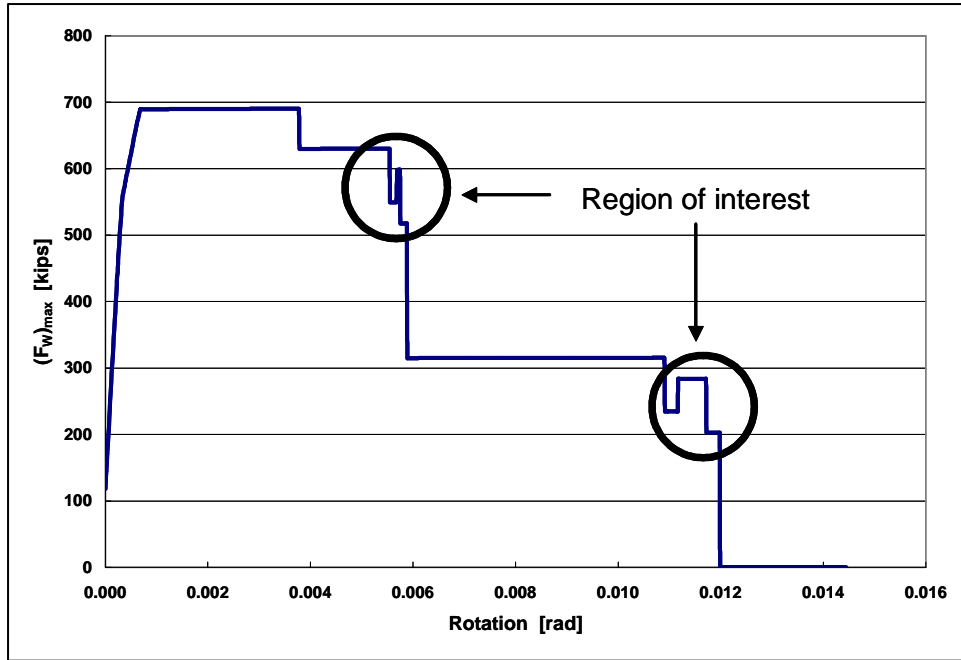
Figure 3-13. F_W versus rotation for $\theta = 10^0$, $\mu^*_k = 0.2$, $\mu_k = 0.2$, $m_T = 1,865.59$ kip*sec²/ft, $m_2 = 1,492.472$ kip*sec²/ft, $m_1 = m_T - m_2$
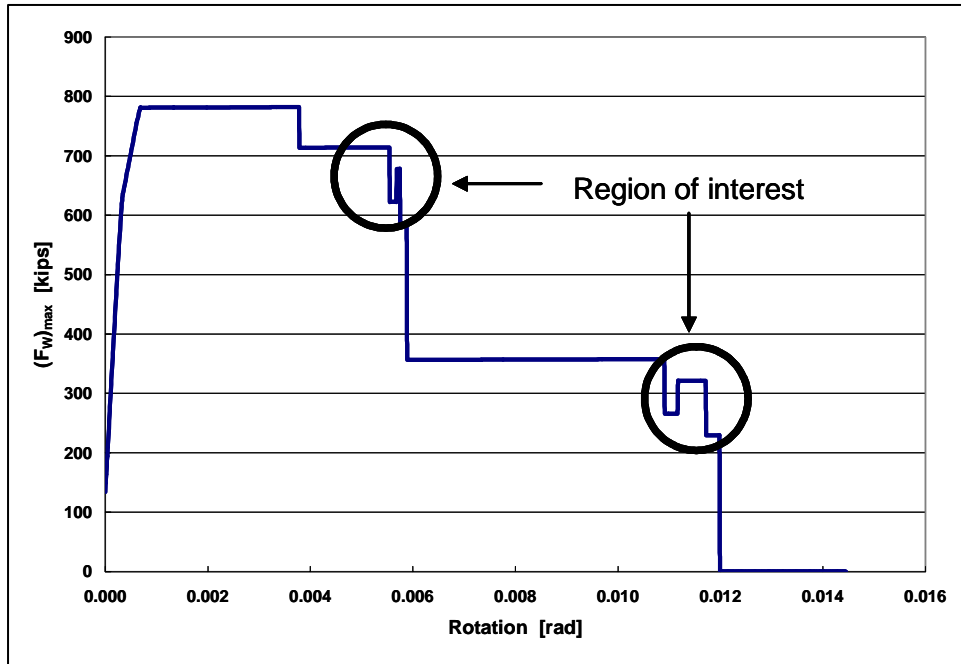
Figure 3-14. F_W versus rotation for $\theta = 20^0$, $\mu^*_k = 0.2$, $\mu_k = 0.2$, $m_T = 1,865.59$ kip*sec²/ft, $m_2 = 1,492.472$ kip*sec²/ft, $m_1 = m_T - m_2$
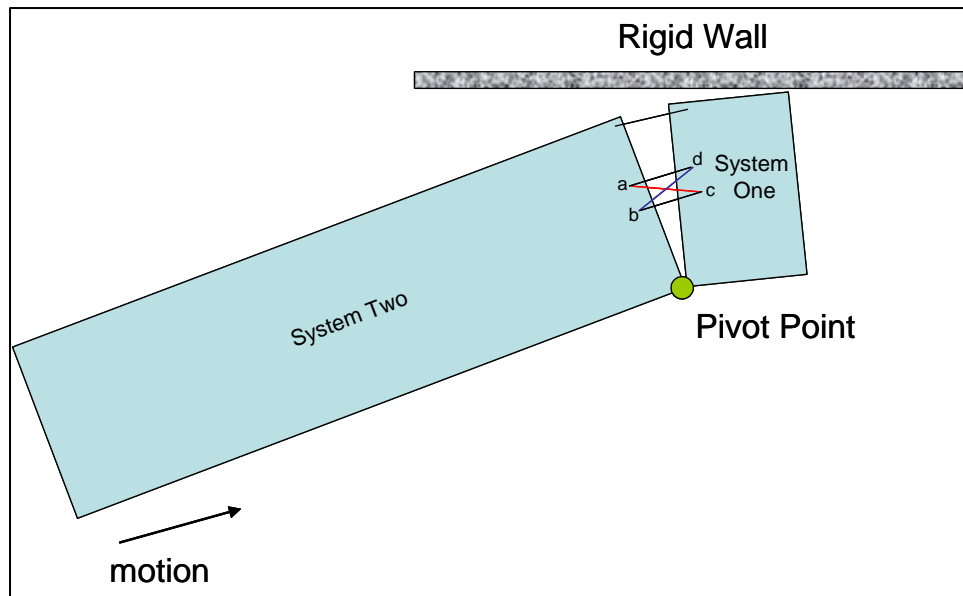
Figure 3-15. Contribution of the scissor scheme to the peak in the transverse failure mechanism

4   Corner Failure Mechanism

4.1 Background

A barge train system consists of a group of nearly rigid barges joined with steel cables, which are referred to as lashings. These lashings define a barge train system where the weak zones are assumed to occur at each barge-to-barge contact. The motion, including rotation, of each barge relative to the others is how the system distributes the impact forces among the barges during the impact process. As has been observed during barge train impacts at shallow approach angles (i.e., glancing blows), the impact event can produce a failure of the lashings in an "opening wedge" fashion along a transverse plane between barges. (The lashings develop tensile strains across the wedge-opening transverse plane as this opening develops.) The barges move and rotate a small amount in such a way that the force normal to the wall is transferred to the connections between the barges. This potential failure mechanism was presented in Chapter 3 and designated as the transverse failure mechanism. However, the actual failure process may not be as simple as the simple transverse wedge opening fashion. A local rotation of the corner barge (barge one) is likely to occur, as depicted in Figure 4-1. A second pivot point is generated after the first pivot point develops in the starboard side of the barge train. This second pivot point is located at the corner barge on the bow opposite the impact point.
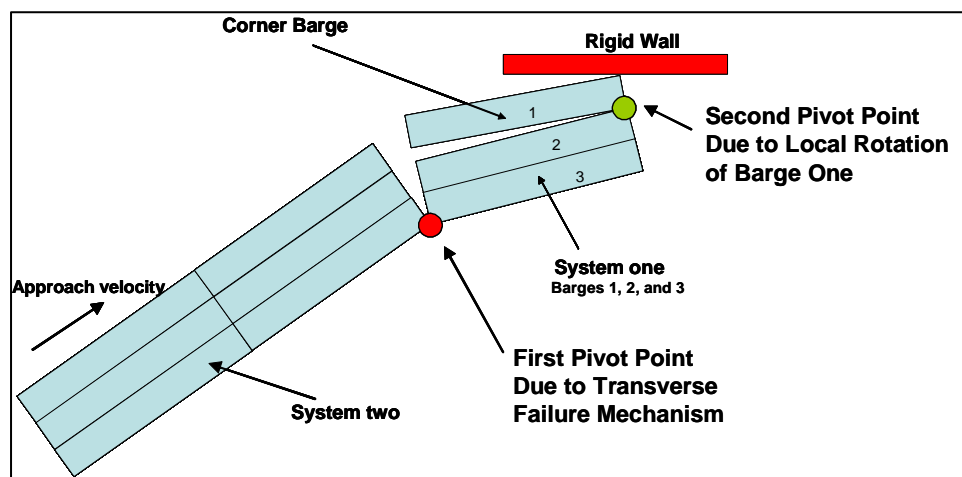
Figure 4-1. Scheme for the corner failure mechanism

This failure mechanism is believed to be a more realistic model than the transverse failure mechanism with a starboard pivot point alone. In the transverse failure mechanism presented in Chapter 3, the three-barge system in contact with the wall was considered as a single rigid body; no local rotation was allowed (Figure 4-2). In this potential failure mechanism, designated the corner failure mechanism, local rotation of the corner barge is allowed, as shown in Figure 4-3. Thus, the lashings in the shaded zone will break by means of the transverse shearing mechanisms and the local rotation of Barge 1 as depicted in Figure 4-3.
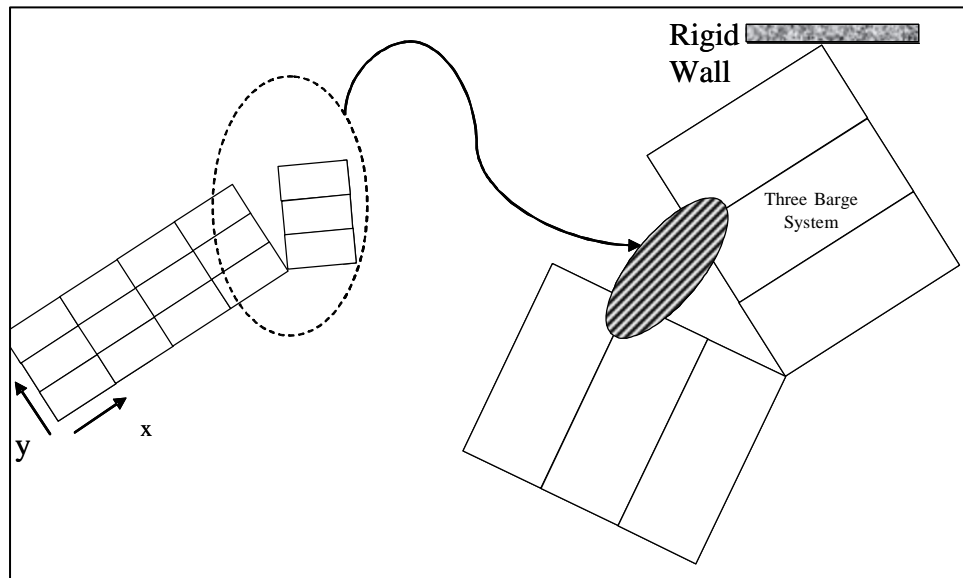
Figure 4-2. No local rotation of corner barge allowed in the transverse failure mechanism
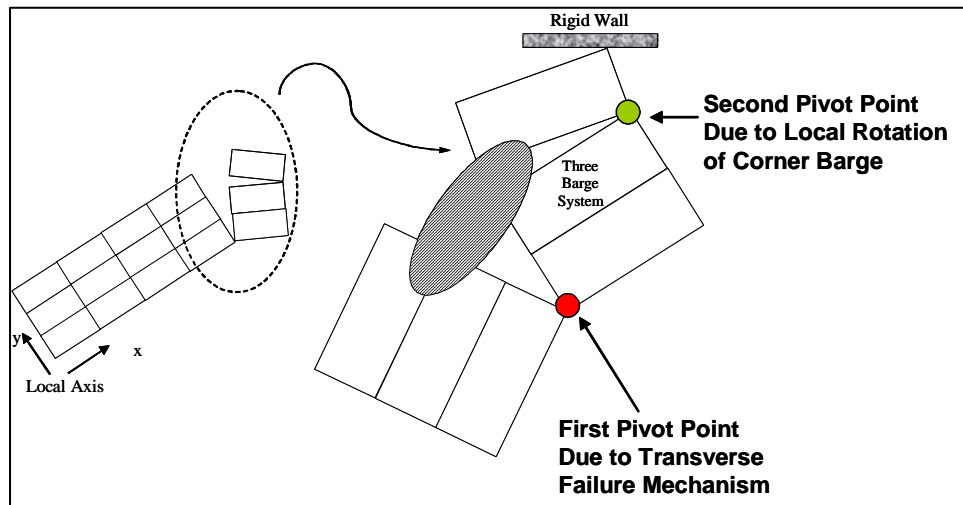
Figure 4-3. Local rotation of corner barge allowed, two pivot points develop, corner failure mechanism

In this new model, typical lashing configurations must be included in addition to the lashing configurations used in the transverse failure mechanism. Appendix A provides typical lashing layouts that were used during the 1998

full-scale experiments (Patev et al. 2003; Arroyo, Ebeling, and Barker 2003). From these typical lashing configurations, three layouts must exist at ultimate load condition for the corner failure mechanism to occur (Figure 4-4). The lashings that go across the "*L*" failure plane are the lashings that have to fail to produce the rotation toward the wall of the corner barge alone. The corner barge, defined as the one that is in contact with the wall during the impact (upper right barge in Figures 4-3 and 4-4), has to lose contact with the rest of the system for the corner failure mechanism to occur.

a. Top configuration
sequence: 7-6-7

b. Bottom configuration
sequence: 4-6-2-8

c. Middle configuration
sequence: 8-3-6-8-3
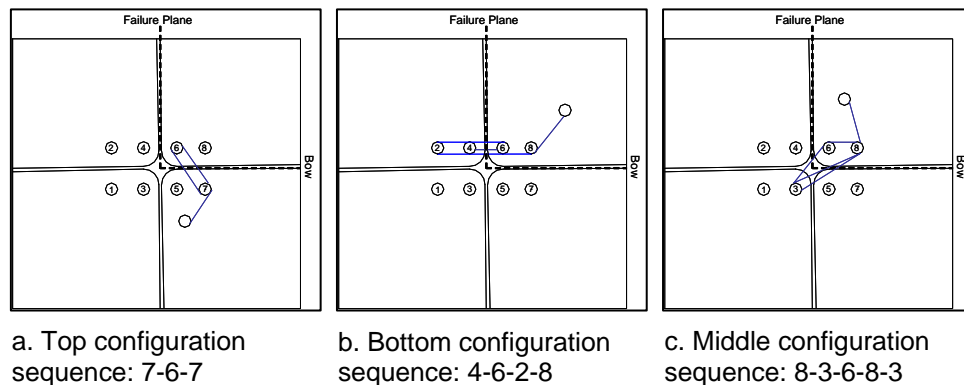
Figure 4-4. Effective lashing configurations in the corner failure mechanism

If these Figure 4-4 lashings break, then the contact between the corner barge and the rest of the barge train system will be lost. This simplified failure mechanism produces a rotation of only the corner barge toward the wall because the lashings fail and the connection with all other barges is lost. ***Note that the only difference between this failure mechanism and the transverse failure mechanism is that the lashing layout presented in Figure 4-4a must be included in this analysis.*** The transverse failure mechanism must break the lashing configurations shown in Figure 4-4b and 4-4c.

The lashings involved with the corner failure mechanism must also include the lashings along the transverse planes between the three front barges (i.e., a local, transverse failure mechanism, plus the lashings that restrain the relative rotation of System 1 relative to System 2). The incremental analysis stops after the lashing configurations presented in Figure 4-4 and the lashing at the port side reach ultimate strain.

For this simplified failure mechanism, the lashings in System 1 (see Figure 4-1) located at the bow (i.e., the lashings at the bow that join the corners of Barge 1 to Barge 2) are not included in the calculation of the lashing forces because if Barge 1 tries to rotate, then the rotation will be around the connection at the bow. If the corner failure mechanism occurs, the corner barge (Barge 1) is assumed to rotate with a "pivot" point at the bow, at the connection of Barges 1 and 2. In this manner the corner barge rotates toward the wall as soon as all lashings joining it to the rest of the barge train fail. In this process the lashings that join the barges of System 1 at the bow are not included.

In this model, different linear accelerations (in actuality, decelerations) in the global Y-direction for System 1 and System 2 were assumed. It is reasoned that

when System 1 stops its forward movement in the global Y-axis upon its impact with a rigid wall, barge System 1 will decelerate at a more rapid rate than will System 2. Consequently, it is envisioned for this simplified model that the deceleration of System 2 will be at a far different and lower deceleration rate from System 1. A zero linear global acceleration in the Y-direction of System 1 is assumed in this simplified model because the impact with a *rigid* wall occurs with this system in the global Y-direction. System 2 motions continue and the lashings that connect System 1 to System 2 will try to rotate System 2 toward the wall. Thus, the deceleration of System 2 in the global Y-direction is nonzero. As will be shown in Equation 4-1, the summation of forces in the global Y-direction of System 1 is equal to zero according to this assumption. However, as will be seen in Equation 4-3, the linear deceleration of System 2 in the global Y-axis is nonzero.

This failure mechanism is described by the equations of motion using Newton's second law. First, a free-body diagram is defined as shown in Figure 4-5. All unknown and known forces for the system are shown in this diagram. The unknown external forces are F_W and S_W, and the internal unknown forces are the normal F_{NC} and the internal moment M. In this model the internal shear is related to the normal force by means of the kinetic coefficient of friction μ_K; $S_{NC} = \mu_K F_{NC}$. The known forces are the internal force in each lashing as motion takes place. These forces are labeled as f_{Ni} and f_{Si}. It is important to note that the contribution of the force in the lashing due to the local rotation of Barge 1 is considered in forces f_{Ni} and f_{Si}.

Figure 4-5. Corner failure mechanism, free-body diagram of System 1

The free-body diagram is equal to the kinetic diagram as required by Newton's second law. Figure 4-6 (kinetic diagram) shows the linear accelerations and angular accelerations for System 1, the front three-barge system. In this case the linear accelerations are oriented in the global X- and Y-axes.

Figure 4-6. Corner failure mechanism, kinetic diagram

The three equations of motion are written for Figures 4-5 and 4-6. For barge System 1, the equations of motion are as follows:

$$\oplus \rightarrow \sum F_X = ma_X \therefore -S_W - Rn_X + Rs_X + F_{NC} \cos\theta$$
$$- \mu_K F_{NC} \sin\theta = -M_{par1}a_{X1} \tag{4-1}$$

$$\oplus \uparrow \sum F_Y = ma_Y \therefore -F_W - Rn_Y - Rn_Y + F_{NC}\sin\theta + \mu_K F_{NC}\cos\theta$$
$$= -M_{norm1}a_{Y1} = 0 \quad ; \quad M_{norm1}a_{Y1} = 0 \tag{4-2}$$

$$\oplus \circlearrowright \sum M_o = (\sum M_{EQUIVALENT})_o \therefore M + M_{Rfn} - M_{Rfs} - F_{NC}(y_1 - y_{G1}) + \mu_K F_{NC}a$$
$$= I_{\theta 1}\alpha_1 + (M_{par1}a_X \cos\theta + M_{norm1}a_Y \sin\theta)(y_1 - y_{G1}) \tag{4-3}$$
$$+ (M_{par1}a_X \sin\theta - M_{norm1}a_Y \cos\theta)\frac{a}{2}$$

where moment is taken about the point o, which is the point of contact between the barge train and the wall.

Four parameters that affect the force normal to the wall are the global X- and Y-components of the forces parallel (Rs_X, Rs_Y) and perpendicular (Rn_X, Rn_Y) to the failure plane obtained from the internal force in the lashings. These forces are obtained in the following manner. Due to the elongation of the lashing during the deformation process, an internal force appears in the lashings. The angle that defines each segment of the lashings with the longitudinal local axis is calculated using the local coordinates of the start (x_s, y_s) and end (x_e, y_e) bits that connect each segment of each lashing. Then, the components of these forces in local coordinates are easily transformed to forces in the global coordinates system by means of the transformation matrix that contains the sine and cosine functions. As shown in Figure 4-7, these forces can be easily obtained by the use of trigonometric functions. For example, $Rn_x = F_L * \sin\delta$, and $Rn_Y = Rn * \cos\theta$.
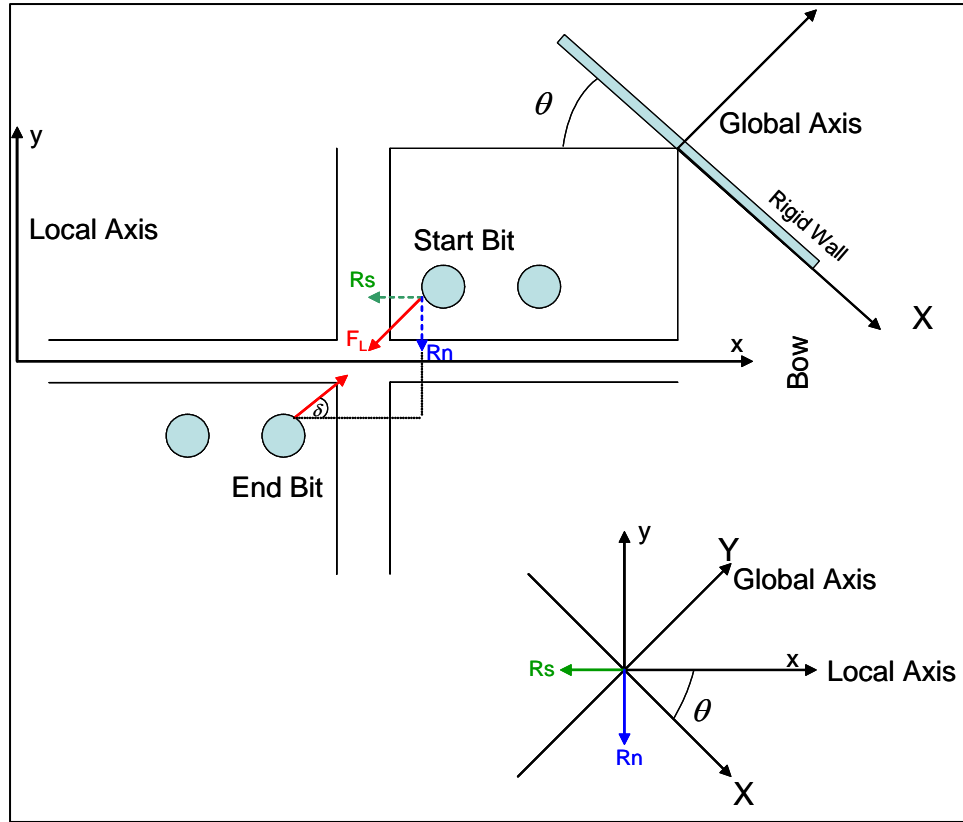
Figure 4-7. Global components of lashing force (repeated from earlier text for convenience of the reader)

Hydrodynamics effects are included in barge System 1 using the ETL 1110-2-338 approach:

$$M_{x1} = (1 + \eta_x) * m_1 \qquad (4\text{-}4)$$

$$M_{y1} = (1 + \eta_y) * m_1 \qquad (4\text{-}5)$$

$$I_{\theta1} = (1 + \eta_\theta) * I_{G1} \qquad (4\text{-}6)$$

$$I_{G1} = \frac{1}{12} * m_1 * \left(L_1^{\,2} + B_1^{\,2} \right) \qquad (4\text{-}7)$$

$$M_{norm1} = \frac{M_{x1} * M_{y1}}{M_{x1} \cos^2 \theta + M_{y1} \sin^2 \theta} \qquad (4\text{-}8)$$

$$M_{par1} = \frac{M_{x1} * M_{y1}}{M_{x1} \sin^2 \theta + M_{y1} \cos^2 \theta} \qquad (4\text{-}9)$$

Chapter 4   Corner Failure Mechanism

with the hydrodynamic added mass coefficients defined in the local barge coordinate system, according to ETL 1110-2-338, as

$$\eta_x = 0.05$$
$$\eta_y = 0.4$$
$$\eta_\theta = 0.4$$

The angular acceleration for System 1, α_1, is assumed equal to the angular acceleration for System 2, α_2, for this simplified transverse failure mechanism: $\alpha_1 = \alpha_2 = \alpha$.

The authors of this report recommend that hydrodynamic effects be considered in the simplified limit state analyses. Therefore, Equations 4-1 through 4-3 will include hydrodynamic added mass terms via Equations 4-4 through 4-9.

Applying this same procedure to barge System 2, which contains the rest of the barges of the barge train, three more equations of motion are obtained. As always, its free-body diagram should be equal to the kinetic diagram as stated by Newton's second law. For this system, the free-body diagram is given in Figure 4-8. In this diagram appear all the unknown and known forces in the system. Note that System 2 has no external unknown forces. The internal unknown forces are the normal F_{NC} and the internal moment M. In this system the internal shear is related to the normal by means of the kinetic coefficient of friction μ_K; $S_{NC} = \mu_K F_{NC}$. The known forces are the internal force in each lashing as the rotation takes place. These forces are labeled as f_{Ni} and f_{Si}. Again, it is important to note that the contribution of the force in the lashing due to the local rotation of barge one is considered in forces f_{Ni} 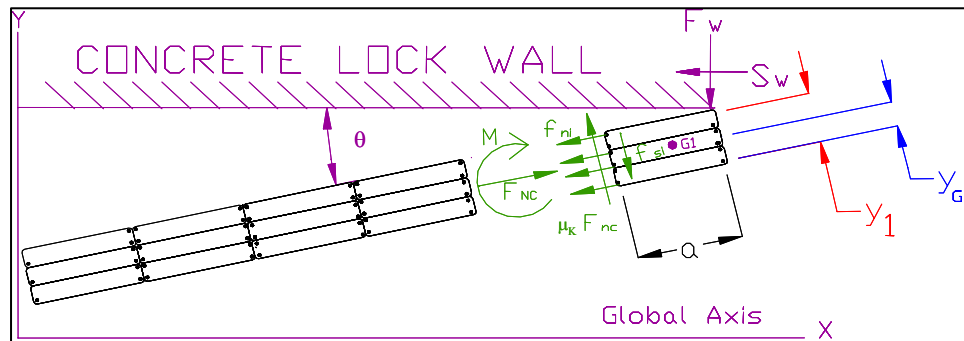and f_{Si}. Figure 4-9 presents the linear accelerations and angular accelerations of System 2. In this case the linear accelerations are oriented in the global X- and Y-axes.
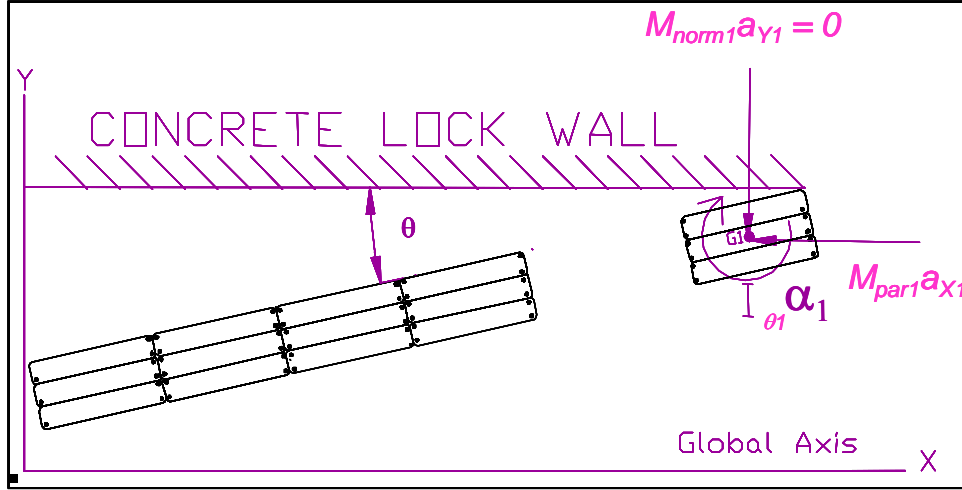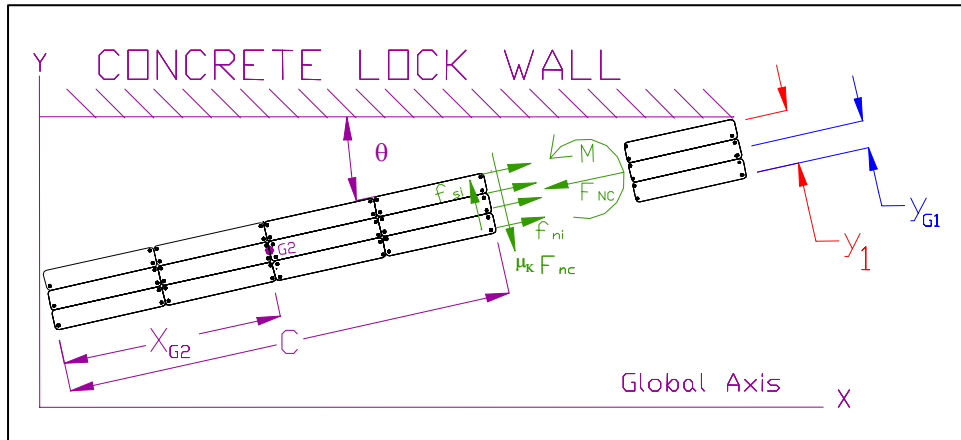

Figure 4-8. Corner failure mechanism, free-body diagram of System 2
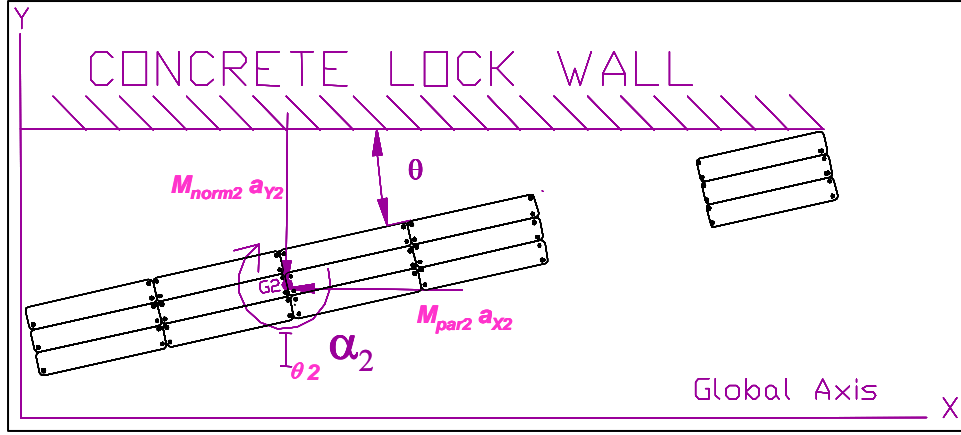
Figure 4-9. Corner failure mechanism, kinetic diagram of System 2

The three equations of motion for System 2 (the barge system that is not in direct contact with the wall) are as follows:

$$\oplus \rightarrow \sum F_X = ma_X \therefore -Rs_X + Rn_X - F_{NC}\sin\theta + \mu_K F_{NC}\cos\theta = -M_{par2}a_{X2} \quad (4\text{-}10)$$

$$\oplus \uparrow \sum F_Y = ma_Y \therefore Rs_Y + Rn_Y - F_{NC}\sin\theta - \mu_K F_{NC}\cos\theta = -M_{norm2}a_{Y2} \quad (4\text{-}11)$$

$$\oplus \!\!\! \curvearrowright \sum M_{G2} = (\sum M_{EQUIVALENT})_{G2} \therefore -M + M_{Rfn} - M_{Rfs} + \mu_K F_{NC}(c - x_{G2}) = I_{\theta2}\alpha_2 \quad (4\text{-}12)$$

M_{par2}, M_{norm2}, and $I_{\theta2}$ are computed for barge System 2 using Equations 4-4 through 4-9 modified for System 2 geometry and masses. The mass of barge System 2, excluding hydrodynamic added mass, is designated m_2. Barge System 2 decelerates at a different rate from barge System 1 during impact. The rotation of System 2 relative to the rotation of System 1 during an impact allows this simplified model to crudely capture this behavior. The lashings transmit the effects of the System 2 inertial forces to System 1 and onto the wall. However, for this simplified model, the number of equations limits the number of variables to be considered in the solution process. Consequently, a crude assumption that System 2 was still decelerating in the global Y-axis after the deceleration of barge System 1 had concluded was made to match the number of variables with the number of equations. Recall that one of the primary features of this simplified model is to account for the forces in the lashings and to consider how these forces reflect the inertia of the two barge system bodies and their rotation. With consideration of all of these factors the decision was made to assume the acceleration of the global Y-axis of barge System 1 is zero in the calculations. The six equations 4-1 to 4-3 and 4-10 to 4-12 have seven unknowns: F_W, S_W, M, F_{NC}, $a_{X1} = a_{X2}$, a_{Y2}, and α for both systems. The linear accelerations of the global X-axis of both systems are assumed equal for this simplified failure mechanism. Therefore, another equation is required. A relationship between the shear and normal force between corner barge and wall is introduced.

$$S_W - \mu_K^* F_W = 0 \quad (4\text{-}13)$$

Solving Equations 4-1 through 4-3 and 4-10 through 4-13 results in the following F_W expression:

$$F_W = \frac{M_{par}\left[(Rn_X - Rs_X)\sin\theta + \mu_K(Rn_X - Rs_X)\cos\theta + \mu_K(Rs_Y + Rn_Y)\sin\theta - (Rn_Y + Rs_Y)\cos\theta\right]}{(M_{par1}\cos\theta + M_{par2}\cos\theta - \mu_K M_{par1}\sin\theta - \mu_K M_{par2}\sin\theta - \mu_K \mu_K^* M_{par2}\cos\theta - \mu_K^* M_{par2}\sin\theta)} \quad (4\text{-}14)$$

Note that the hydrodynamic added mass affects the F_W expression. If the denominator of Equation 4-14 equals zero, then

$$M_{par1}\cos\theta + M_{par2}\cos\theta - \mu_K M_{par1}\sin\theta - \mu_K M_{par2}\sin\theta$$

$$- \mu_K \mu_K^* M_{par2}\cos\theta - \mu_K^* M_{par2}\sin\theta = 0$$

Solving for the critical value of the approach angle gives the following expression:

$$\theta_{CR} = \tan^{-1}\left(\frac{M_{par} - \mu_K \mu_K^* M_{par2}}{\mu_K M_{par} + \mu_K^* M_{par2}}\right) \qquad 4\text{-}15$$

Equations 4-14 and 4-15 were obtained from the solution provided by Maple's Worksheet. Derivation of Equation 4-14 is presented in Appendix D. There are combinations of variables for which Equation 4-14 is either indeterminate (e.g., the case of a value of zero in the denominator) or negative. Either of these cases provides unrealistic values for F_W. Equation 4-15 defines the asymptote for Equation 4-14 via the approach angle designated θ_{CR}. Approach angles equal to or greater than θ_{CR} produce infinite values or negative values for F_W for the transverse failure mechanism, respectively. For approach angles greater than θ_{CR}, other failure mechanisms are more likely to occur. These alternatives failure mechanisms were discussed in Chapter 2. A negative value of F_W means that the barge train pulls the rigid wall instead of pushing it during the impact process. Mathematically speaking, all models produce a number, but in engineering, these numbers must be understood in terms of the process involved. In Chapter 6 some numerical examples will be presented. When this model produces a negative value, a zero value will be assigned in these examples indicating that the impact model will not predict physically real values of F_W based on the input data provided.

Note that the expression for F_W is the same as that for the transverse failure mechanism (Equation 3-14). *The difference between the transverse failure mechanism and the corner failure mechanism is that in the former case the lashings that prevent the local rotation of the corner barge toward the wall are also included. In this case, the resultant lashing forces (e.g., Rn, Rs) are different because the lashings considered in both potential failure mechanisms are different.*

In summary, the following assumptions are made for the corner failure mechanism:

a. The linear acceleration in the global Y-direction in barge System 1 is assumed to be zero. This means that in the Y-direction the barge stops instantly at the moment of impact. This condition ensures the motion normal to the wall is stopped, but motion parallel to the wall is not restricted.

b. The linear acceleration in the global X-direction for barge System 1 is assumed to be equal to the linear acceleration in the global X-axis for barge System 2.

c. The angular acceleration for barge System 1 is assumed to be equal to the angular acceleration for barge System 2.

d. The kinetic coefficient of friction between barges must be defined. A review of the technical literature, discussed in Chapter 5, indicates a value between 0.2 and 0.5.

e. The kinetic coefficient of friction between the corner barge and the struck wall must be defined. A review of the technical literature, discussed in Chapter 5, indicates a value between 0.2 and 0.5.

f. The lashings are assumed to behave in an elastic-plastic manner and break when an ultimate (tensile) strain value is achieved within the lashing. Should the lashings reach the ultimate stress, no additional force can be carried by the lashing with additional deformations. Achieving the ultimate tensile strain results in rupturing of the lashing.

g. This failure mechanism is valid for low approach angles; research indicates values lower than 30 degrees. Greater approach angles are likely to produce a failure path other than in the transverse direction with a pivot on the starboard side.

h. Hydrodynamic effects are considered by means of an increase in the barge train mass in the local x- and y-axes and rotational directions. This hydrodynamic effect influences the kinetic variables (e.g., linear accelerations and angular acceleration).

i. Barge System 1, which is in contact with the struck wall, abruptly/ instantaneously stops motion while barge System 2 continues motion. The lashings across the transverse failure plane pull System 2 toward the wall.

j. Barge one, which is in contact with the struck wall, rotates around a pivot located in the connection between Barge 1 and Barge 2 of barge System 1 at the bow.

k. If the lashings that join the corner barge to the rest of the barge train, with the exception of the bow connection, fail, then the corner failure mechanism is likely to occur.

4.2 Additional Information Regarding the Corner Failure Mechanism

In this simplified model, each of the two barge systems is idealized as rigid bodies and the wall is assumed rigid. When barge System 1 impacts the *rigid* wall, it is subject to a boundary condition of no further forward movement. Barge System 2 would tend to continue its translational motion if it were not subject to "constraints." Note that System 2 is not subject to the same severe constraint that System 1 is (i.e., forward motion being prevented by the presence of a rigid wall). Instead, System 2 is subject to a "constraint" that is imposed by its lashings connections to System 1. It is reasoned that the barge System 2 rigid body will have to decelerate only because it is "lashed" to barge System 1 with a finite number of cables (i.e., lashings), each with a finite tensile strength. Note that in the extreme, should the lashings between System 2 and System 1 be of zero or only a nominal tensile strength, System 2 would continue its forward motion without angular deceleration. It is further reasoned that when System 1 stops its forward motion upon impact with a rigid wall, it will decelerate at a more rapid rate than will System 2. Consequently, it is envisioned for this simplified model that the deceleration of barge System 2 will be at a far different and lower deceleration rate from System 1. The magnitude of the deceleration for System 2 is a function of the number and orientation of the lashings as well as their size, ultimate capacity, and condition (e.g., new, used but in good condition, used and in poor condition, etc.). It is important to note that the time of maximum normal force against the rigid wall produced by System 1 may not coincide with the time of maximum normal force during deceleration of System 2. The maximum impact force of System 2 depends on the number and orientation of the lashings as well as their size, ultimate capacity, and condition (e.g., new, used but in good condition, used and in poor condition, etc.). That is, immediately after impact of System 1, the force normal to the wall increases and the lashings that keep Systems 1 and 2 together do not develop the strength until System 1 begins to rotate relative to System 2, and the corner barge presents a local rotation. When System 1 begins to rotate and the corner barge locally rotates, the lashings reach their ultimate strength, and System 1 is at rest in the global Y-direction. This produces different maximum values for the force normal to the wall.

At this time and awaiting the results of additional research, the authors of this report suggest that it be assumed that these maximum force values for Systems 1 and 2 are coincident. This may be a conservative assumption. Limit_LASHING is used to account for the deceleration of System 2 and its contribution to maximum F_W. However, the assumption of deceleration equal to zero in the global Y-axis for System 1 implies that the inertia of System 1 does not contribute to maximum F_W in the Limit_LASHING computations of maximum F_W. Pending additional research results at this time, the authors further suggest that the empirical correlation be used to account for, in an approximate sense, the effects of System 1 inertia during impact and that this contribution to the maximum F_W value be added to the maximum F_W value of System 2, computed using Limit_LASHING.

Finally, the percentage of total mass participating in System 1 and System 2 will be different depending upon the number of barges in the train. For example,

in the 15-barge train system used in the full-scale experiments in 1998 (Patev et al. 2003), the total mass of the barge train was 1,865.59 kips*sec^2/ft, System 1 (3 barges) had a mass of 373.118 kips*sec^2/ft, and System 2 (12 barges) had a mass of 1,492.472 kips*sec^2/ft. System 1 has 20 percent of the total mass, and System 2 has 80 percent of the total mass of the barge train.

4.3 Numerical Solution Procedure

The formulation presented in this chapter is used to calculate the force normal to the wall assuming a corner failure mechanism during impact. The value computed for the resultant F_W is dependent on the magnitude of the lashing forces. The rotation of the barges of System 1 relative to the barges in System 2 and the relative displacement between barges of System 1 produce tensile strains in the lashings across the failure plane. This can be achieved by means of an elongation of the lashing when the barges of System 1 rotate and move as shown in Figure 4-10. Thus an analytical approach is developed to assess these lashing forces based on the rotation and motion of the two (or three) barges in System 1. This incremental rotation and motion translate into incremental changes in the lashing forces across the transverse failure plane between barge systems. The sequential process to calculate the F_W by Limit_LASHING is the following:

a. The initial length of the lashing is calculated using the initial internal force in the lashing. (Lashings usually have a tensile force that is introduced when the barges are initially assembled into a barge train.) If the initial force is known, then the initial elongation produced by the initial force can be calculated using the following expression: $F = (AE/L_0)\Delta$. This equation comes from the stress-strain relationship and the stress and strain definitions. If $\Delta = L_f - L_0$, then $L_0 = A*E*L_f / (F+A*E)$.

b. Using the calculated initial length of the lashing, an assumed increment of length is added to the lashing due to the progressive rotation of System 1. Note that all the lashings across the transverse failure plane increase the internal load as the rotation of System 1 increases.

c. A continuous increment of the rotation of System 1 leads to the lashing at the port side (and across the transverse failure mechanism) to reach the ultimate load first.

d. As the incremental rotations increase, the inner lashing configurations reach their ultimate load. The ultimate condition is reached in sequence from the port side to starboard side.

e. As shown in the Figure 4-10b idealization, as the rotation and motion of System 1 increase, the lashing indicated in red can reach the horizontal plateau of the elastoplastic stress-strain model.

f. With sufficient rotation of System 1, the strains within each of the lashings reach their ultimate (tensile) values and all lashings yield, as idealized in Figure 4-10c and ultimately break when the strains ε equal ε_{ult}.
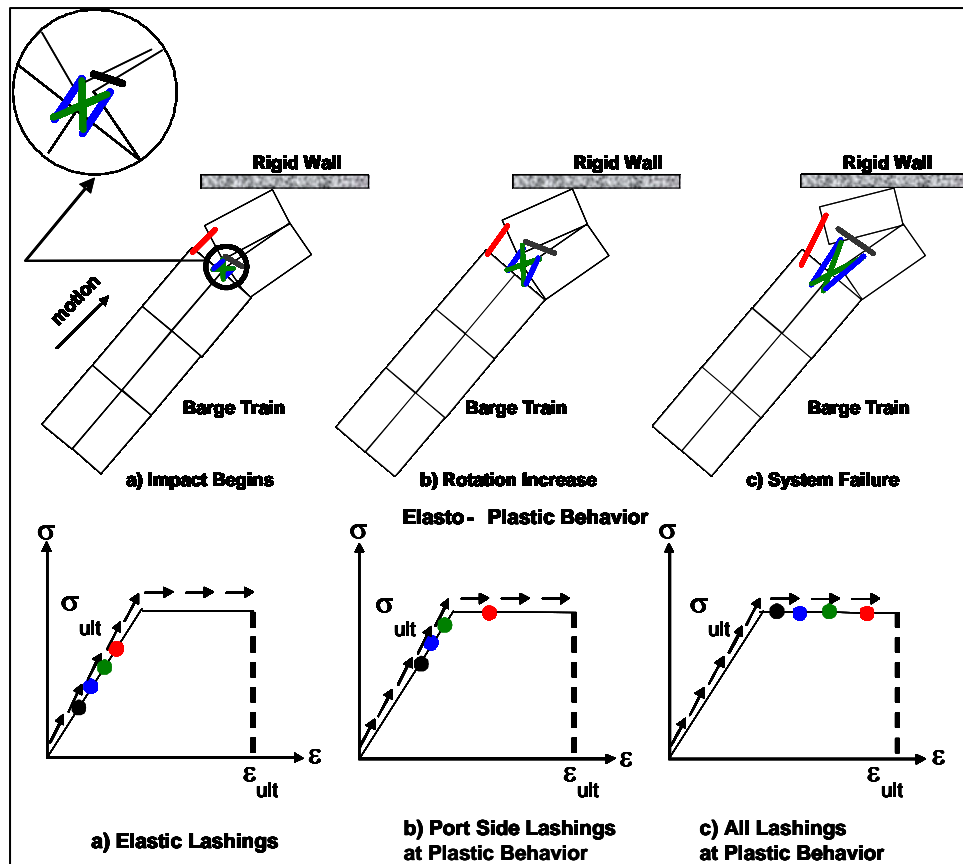
Figure 4-10. Progressive corner failure of lashings across a failure plane within
the barge train

g. In the incremental solution process an incremental rotation of System 1 is
assumed. The incremental rotation value used in each computational step
is set equal to 0.001 ft/width in feet of the barge train system. For
example, for a 105-ft-width system, the rotation step is equal to
0.001/105 = 0.000009523809524 radian. Parametric studies have shown
this to be a small value considering that the calculations are made
numerous times; e.g., 1000 calculations will result in 1 ft of elongation at
the port side. With this magnitude of elongation, lashings will reach their
ultimate load.

h. The local relative rotation of the corner barge with a second pivot point
at the bow is assumed to have the same rotation step as the rotation of
System 1. For example, a rotation step of 0.000009523809524 radian
multiplied by the length of the corner barge (local x-direction) will
provide the displacement of the lashings that join the corner barge to the
rest of the barge train.

i. Different lashing geometry configurations among the bits result in
different lengths of lashings between bits across the idealized failure
plane. Thus, for each of the lashings a different length of deformation
will result at each incremental computation step. The deformation of
each lashing also depends on the initial tensile load applied to the lashing

(during initial formation of the barge train) and the position of the bits on the barges.

j. All lashings may develop different deformation for each incremental step. The deformation in each lashing depends on the initial (tensile) load applied to the lashing to keep barges together and the location of the bits in the barges.

k. The location of the bits defines the initial length of the lashings. This difference in the length of the lashings can result in different normal strain within each of the lashings. This is the reason there are different stress-strain levels within the lashings even for the same relative displacement across the failure plane between System 1 and System 2.

l. Each of the lashings is likely to reach its ultimate (tensile) stress value at different instances during the relative rotation process (between Systems 1 and 2), as specified in the previous subparagraph. As soon as the lashing reaches the ultimate stress, it cannot accrue additional stress (or tensile force) in the incremental analysis because of the elastoplastic behavior of the lashing adopted in this failure mechanism. The lashing can accrue additional strain based upon the additional stretching from the continued relative rotation between the two barge systems.

m. Should a lashing accrue a strain equal to the user-specified ultimate strain, the lashing is assumed to rupture and is removed from the connection system across the failure plane.

n. These resultant lashing forces are then used as input data to the expressions for F_W previously presented.

It is important to mention that the lashing failures occur in a sequence; it is not assumed that all lashings reach their ultimate stress at once. Actual impact response among the barges and the lashings during impact is quite complex: the difference in bit locations and lashing configurations between bits as well as the different initial (tension) forces set in the lashings provide the system with an uneven distribution of forces at the lashing connections. In addition, as soon as the corner barge impacts the *rigid* wall, the impact wave generated inside the barge train reaches all points throughout the barge train at different instants of time, producing different stresses and strains among the lashings. To model this behavior in this *simplified model*, rotation between barge systems and the local rotation between the corner barge and the rest of the barges of System 1 are assumed. This rotation produces different kinematic results of the systems in the local x-axis of the barge train. These results of the kinematic variables of both systems are responsible for the stress and strain in the lashings along the failure planes. In this model, the rotations of System 1 and the corner barge are constant for each incremental step. However, this condition does not mean that this rotation occurs at equal time-steps. Remember that the deceleration may not be constant. So if it is not a constant, the time at which the increment of the rotation and motion occurs is not constant. For example, the time to produce a rotation increment from $1*10^{-6}$ to $1*10^{-5}$ radian is different from the time needed to produce a rotation increment from $1*10^{-4}$ to $1*10^{-3}$ radian, because the kinematic variables for each rotational increment are different. The incremental

computational procedure was implemented in a new PC-based computer program named Limit_LASHING. Its user's guide is given in Appendix E.

4.4 Numerical Examples

In this section two numerical examples are presented. The barge train used for these examples consisted of 15 barges with a total mass of 1,865.59 kip*sec^2/ft. This is the same configuration used in the 1998 full-scale experiments. The kinetic coefficient of friction is set equal to 0.2 between barges, and set equal to 0.2 between the corner barge and the rigid wall. The first computation was made using an approach angle of 10 degrees, and for the second example, 20 degrees was used. The lashing configurations are presented in Appendix A. The lashing ultimate load was 90 and 120 kips for the 1- and 1.25-in. diameters, respectively. The modulus of elasticity was 29,000 ksi, and the ultimate strain was set equal to 0.05. The hydrodynamic added mass coefficients were 0.05, 0.4, and 0.4 for the local x- and y-axes and rotation, respectively.

It is important to note that the corner failure mechanism is more likely to occur at shallow approach angles. However, at higher approach angles this failure mechanism can predict negative values of the force normal to the wall. This indicates that for high approach angles ($>$ 70 degrees), another failure mechanism such as the one discussed in Chapter 2 will dominate. The resulting maximum values of the force normal to the wall were the following: for an approach angle of 10 degrees F_W equal to 360.83 kips was obtained, and for 20 degrees F_W equal to 408.68 kips was obtained. In the analysis performed by the PC-based computer program Limit_LASHING, a negative F_W is transformed to a zero value, because it is physically impossible for the barge train to pull instead of push the rigid wall. This model predicts values of F_W lower than the estimated transverse failure mechanism results in Chapter 3. As shown in Figures 4-11 and 4-12, the local, secondary peaks that appeared in the transverse failure mechanism (Figures 3-13 and 3-14) disappeared in the corner failure mechanism. They disappeared because the lashings that join the corner barge to the rest of the system break before the scissor scheme lashings break (refer to Section 3.5 in Chapter 3).
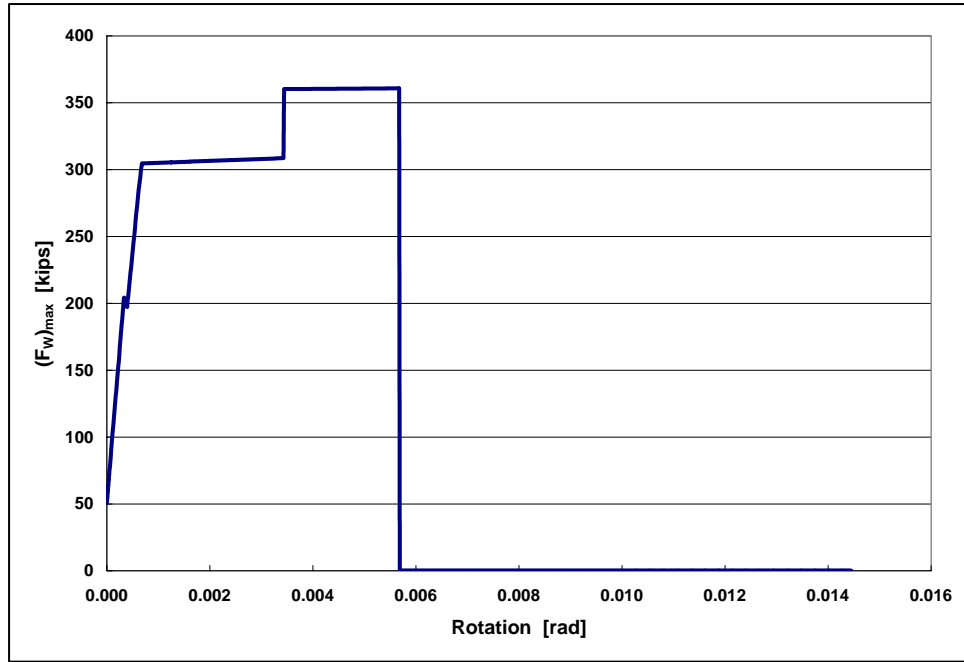
Figure 4-11. F_W versus rotation for $\theta = 10^\circ$, $\mu^*_k = 0.2$, $\mu_k = 0.2$, $m_T = 1{,}865.59$ kips-sec^2/ft, $m_2 = 1{,}492.472$ kips-sec^2/ft, $m_1 = m_T - m_2$
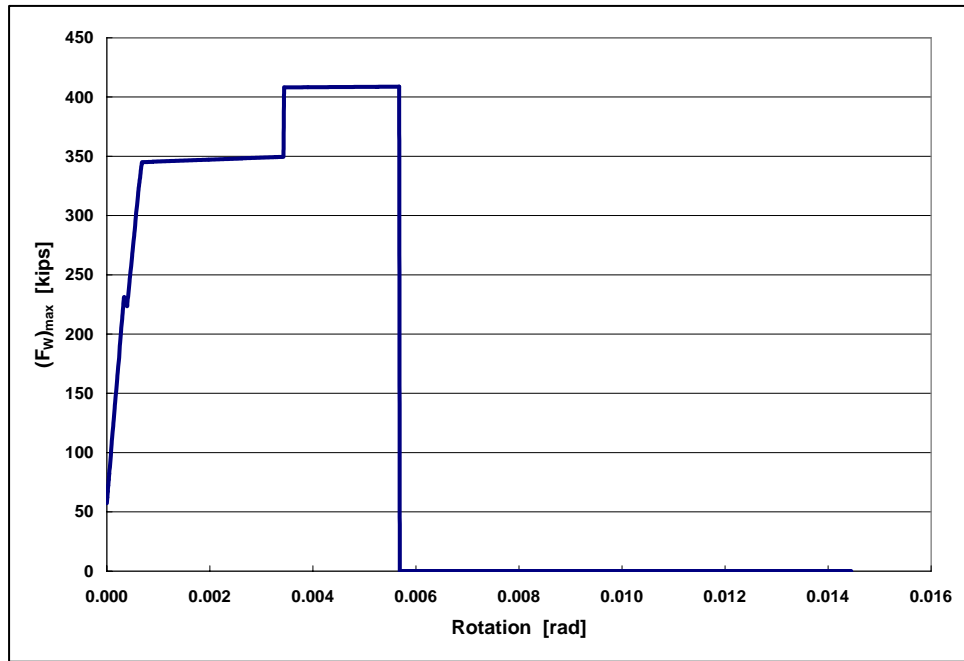
Figure 4-12. F_W versus rotation for $\theta = 20^\circ$, $\mu^*_k = 0.2$, $\mu_k = 0.2$, $m_T = 1{,}865.59$ kips-sec^2/ft, $m_2 = 1{,}492.472$ kips-sec^2/ft, $m_1 = m_T - m_2$

5 Steel-Steel Coefficient of Friction

5.1 Theory

Friction may be defined as a force of resistance acting on a body that prevents or retards slipping of the body relative to a second body or surface with which it is in contact. This force always acts tangent to the surface at points of contact with other bodies and is directed so as to oppose the possible or existing motion of the body relative to these points. In general, two types of friction can occur between surfaces. Fluid friction exists when the contacting surfaces are separated by a film of fluid. The second type of friction is the dry friction, often called Coulomb friction. Specifically, dry friction occurs between the contacting surfaces of bodies in the absence of a lubricating fluid. The following are some characteristics of dry friction:

a. The frictional force acts tangent to the contacting surfaces in a direction opposed to the relative motion or tendency for motion along the contact surface.

b. The maximum static frictional force F_s that can be developed is independent of the area of contact, provided the normal pressure is not very low or great enough to severely deform or crush the contacting surfaces of the bodies.

c. The maximum static frictional force is generally greater than the kinetic frictional force F_k for any two surfaces in contact.

d. When slipping at the surface of contact is about to occur, the maximum static frictional force is proportional to the normal force, such that $F_s = \mu_s N$ where μ_s is the static coefficient of friction and N is the normal force.

e. When slipping at the surface of contact is occurring, the kinetic frictional force is proportional to the normal force, such that $F_k = \mu_k N$ where μ_k is the kinetic coefficient of friction.

The coefficient of friction is a ratio of the shear force to the normal force. This coefficient varies between the materials and with the condition of the surface. There exist two types of coefficient of friction, the static and the kinetic. The static coefficient is the ratio of the tangential force to the normal force that is needed to disrupt the state of rest for the body, while the kinetic coefficient is the

ratio of tangential force to the normal force that is needed to produce the motion of a body. The kinetic coefficient of friction is applicable to this problem because sliding movement occurs between a single barge or a train of barges as they impact approach walls during locking; the magnitude of normal force changes during the motion of the barges during the course of the impact. A literature review was conducted and focused on values for the steel-to-steel coefficient of friction. Barges are made of steel, and the concrete approach walls have steel armor embedded within the wall surface.

5.2 Literature Review

Table 5-1 summaries the kinetic steel-to-steel coefficient of friction from eight publications. This table shows the steel-to-steel coefficient of friction is between 0.20 and 0.50. Higher values will represent the static coefficient of friction for steel-steel surfaces. Key details regarding the experiments leading to these data are summarized in this section.

Table 5.1
Summary of Steel-Steel Kinetic Coefficients of Friction

Reference	Load	Velocity	μ_x	Observation
Marshall B. Peterson and Robert L. Johnson. (1952). "Friction and Surface Damage of Several Corrosion-Resistant Materials," NACA Research Memorandum E51L20, National Advisory Committee for Aeronautics, Washington, DC.	900 to 4200 grams 300 to 1557 grams	N/A	0.79 Initial = 0.65 With time = 0.79	The increase of coefficient of friction may be the result of the breakdown of surface, cold worker metal and welding. To measure the coefficient of friction, use a machine that works at 15 rpm.
John M. Bailey and Douglas Godfrey. (1954). "Coefficient of Friction and Damage to Contact Area During the Early Stage of Fretting," Technical Note 3144, National Advisory Committee for Aeronautics, Washington, DC.	150 grams	N/A	Initial = 0.6 With time = 0.7	To measure the coefficient of friction use load applied with frequency of 5 cycles per minute with amplitude of 0.006 in. The coefficient of friction increases if the number of cycles increases.
Edmond E. Bisson, Robert L. Johnson, Max A. Swikert, and Douglas Godfrey. (1955). "Friction, Wear, and Surface Damage of Metal as Affected by Solid Surface Films," Report 1254, National Advisory Committee for Aeronautics, Washington, DC.	269 grams, 126,000 psi 519 grams, 155,000 psi 1,017 grams, 194,000 psi	0 to 2,400 ft/sec 2,400 to 5,600 ft/sec	0.54 Down linearity at to 0.25	The different values of pressure produce similar values of coefficient of friction. The most significant variable is the velocity. At more velocity there is less coefficient of friction.
P. J. Pantermuehl and A. J. Smalley. (1997). "Friction Tests Typical Chock Materials and Cast Iron," Technical Report TR 97-3, Mechanical and Fluid Engineering Division, Southwest Research Institute, San Antonio, TX.	N/A	N/A	0.16	Table 3-7B summarized coefficient of friction data for steel, cast iron, aluminum.
Peter J. Blau. (1992). "Appendix: Static and Kinetic Friction Coefficient for Selected Material," Friction, Lubrication, and Wear Technology, ASM Handbook, Vol 18, Metal and Ceramics Division, Oak Ridge Laboratory, Materials Park, OH.	N/A	N/A	0.62	Table 1 Friction coefficient data for metals sliding on metals.
Headquarters, U.S. Army Corps of Engineers. (1993). "Barge Impact Analysis," Engineer Technical Letter 1110-2-338, Washington, DC.	N/A	N/A	0.176	Data obtained by the example of the report.
General Magnaplate Corporation, Linden, NJ. *http://www.magnaplate.com*.	N/A	N/A	0.23	General Magnaplate friction data guide.
Bharat Bhushan and B. K. Gupta. (1991). *Handbook of Tribology.* McGraw-Hill, New York, p 2.11.	N/A	N/A	0.42	Table 2.1 Coefficient of Friction for Various Material Combinations. Chapter 2 Friction, Wear and Lubrication.

Marshall B. Peterson and Robert L. Johnson. (1952). "Friction and Surface Damage of Several Corrosion-Resistant Materials," NACA Research Memorandum E51L20, National Advisory Committee for Aeronautics, Washington, DC. An experiment was conducted at room temperature and at an extremely slow speed sliding. The friction experiments were performed with an apparatus whose principal part is a rider part, which holds the ball specimen and a plate with which the ball is in contact. Three ball specimens were securely clamped in position on the rider holder, which corresponds to vertices of a equilateral triangle. A deadweight load was applied at the center of the triangle normal to the plate. The specimen plate was clamped to the base of the apparatus, and a load was applied to the rider. Motion between the plate and rider was produced by applying a force through a dynamometer ring on which force-indicating strain gauges were mounted. The dynamometer ring was connected to the rider assembly by fine music wire. The frictional force was continuously recorded on a photoelectric recording potentiometer. A 1-rpm motor rotating at a fine pitch (64 threads/in.) screw resulted in a contact displacement rate of 0.0156 in. per minute.

The specimens for this experiment were prepared in the following manner:

1. Ground to a surface finish of 10 to 15 rms.
2. Abraded lightly under acetone with 4/0 emery cloth.
3. Scrubbed with levigated alumina and water.
4. Washed with water to remove adhering alumina.
5. Rinsed with triple distilled water.
6. Rinsed with 90 percent alcohol.
7. Flushed with consecutive rinsing(s) of freshly distilled acetone and vapor in soxhlet extractor.
8. Dried in a chamber containing the friction apparatus.

The following procedure was used in the experiments. According to Amonton's Law the coefficient of friction of dry metals should be independent of load. For this reason, measurements were made for each combination of metals with a range in loadings. From 300 to 4,200 grams were applied to determine an average value of coefficient of friction. The frictional force was measured initially for a load of 300 grams without removing the slider from the plate. Additional weight was added to the slider and the frictional force corresponding to this greater load was measured. The load was reduced to 300 grams and the frictional force was measured again. The procedure was continued until the highest load had been applied. The rider and the plate were kept in contact during the entire test in order to avoid misalignment and contamination by air. Loads greater than 300 grams were applied during the experiment, followed by a test using a 300-gram load. The 300-gram-load experiments gave reproducible results, indicating that the damage resulting from one load test did not affect the results from the succeeding tests. For a few of the material combinations, two values of friction force were obtained: the force to initiate sliding and the first steady value of kinetic frictional force.

If the ball and plate were allowed to experience relative motion for a sustained period of time, the frictional force would increase considerably because of the accumulation of wear debris in front of the slider. This effect was also observed by Bowden and Tabor with other materials. This accumulation of debris would result in an increase in the friction coefficient of approximately 0.25 by choosing the first stable value of frictional force. However, these data were found to be reproducible to within ± 0.05. During the alternate light-load runs the ball specimen passed over the debris accumulation from the preceding run; this also happened intermittently throughout the run with heavier loads. As a result, wear debris accumulated only to a limited extent before being passed over. Consequently, the effect on friction throughout the experiment was limited and not cumulative.

Summary: Four tests established the average coefficient of friction to be 0.79 for steel on steel over the load range of 900 to 4,200 grams. When a continuous run was made with alternate loading of 300 and 1,557 grams, the initial friction coefficient was approximately 0.65, and after continued sliding the friction coefficient increased to approximately 0.79. This increase in friction coefficient may be the result of the breakdown of surface layer.

John M. Bailey and Douglas Godfrey. (1954). "Coefficient of Friction and Damage to Contact Area During the Early Stage of Fretting," Technical Note 3144, National Advisory Committee for Aeronautics, Washington, DC. The apparatus used for this experiment was a flat specimen slider (able to move back and forth) in contact with a convex specimen under a load of approximately 150 grams with amplitude of 0.006 in. and a frequency of 5 cycles per minute. The relative humidity of the air surrounding the specimen during the testing was held to less than 10 percent. The humidity was measured with a hygrometer calibrated against a dewpoint potentiometer. Friction force was measured by a strain gauge attached to a dynamometer ring and recorded by a photoelectric potentiometer. Normal load was measured for each run by determining the upward force required to separate the specimen. The accuracy of measurement of coefficient of friction was estimated to be ± 5 percent.

The specimens were prepared in the following manner:

1. Washed in uncontained naptha.
2. Rinsed at least 10 times with benzene in a soxhlet extractor.
3. Rinsed at least 10 times with ethyl alcohol in a soxhlet extractor.
4. Dried using an air blower.
5. Cleaned anodically in a solution composed of 2 percent NaOH and 10 percent Na_2CO_3 at a temperature of 80 and 90 ℃ with current density of about 0.3 ampere per square inch.
6. Quickly rinsed in water.
7. Rinsed with alcohol and dried with air blower.

All specimens, with the exception of glass, were abraded on 2/0 emery paper to give a uniform surface finish of 10-20 microinches (root mean square). Consistent and thorough cleaning of specimens to remove the last trace of grease

was important for reproducibility. Freedom from grease was indicated by high initial values for the coefficient of friction. The testing process is as follows:

1. The cleaned specimens were mounted in the specimen holder of the apparatus and the load applied by adding weight.

2. The cover of the Lucite box was put in place and air started flowing through the enclosure.

3. When the relative humidity of the escaping air had dropped to 10 percent, the reciprocating action was started. For metal-metal combination the surfaces were separated and examined microscopically after runs lasting 1/2, 1, 5, 10, 20, 100, 200, 300, and 400 cycles.

For this series of experiments, in all steel-against-steel tests, fretting started with a value of 0.60 to 0.70.

Edmond E. Bisson, Robert L. Johnson, Max A. Swikert, and Douglas Godfrey. (1955). "Friction, Wear, and Surface Damage of Metal as Affected by Solid Surface Films," Report 1254, National Advisory Committee for Aeronautics, Washington, DC. The testing apparatus used in this experiment was composed of different components. However, the significance of the apparatus to this research project was the part used for the kinetic coefficient calculation. These principal parts involve specimens of an elastically restrained spherical rider and a 13-in.-diameter rotating disk. The rider is loaded by weight applied along its vertical axis. Friction force(s) between the rider and disk is measured by four strain gauges mounted on a beryllium-copper dynamometer ring. The coefficient of friction is computed by dividing the measured friction force by the applied normal force. In most cases, the specimens were a sphere and a flat surface to enable calculation of both initial contact area and initial contact stress by the Hertz equation. The friction data presented by Bisson et al. are typical of the data obtained in many of their tests. The limit of experimental error in the friction values presented was not uniform among all experiments because of the difficulties in maintaining absolute control of film thickness. However, the maximum experiment error in friction coefficient based on reproducibility was ±0.03. In most cases, it was considerably less than 0.03. For comparison, a load of 269 grams was used in obtaining most of the data presented. This load produces an initial Hertz surface stress of 126,000 psi. This experiment resulted in a surface operating with a friction coefficient of 0.54. As sliding velocity increased (up to about 1,600 ft per minute), the friction coefficient was relatively constant with a value of 0.54.

P. J. Pantermuehl and A. J. Smalley. (1997). "Friction Tests Typical Chock Materials and Cast Iron," Technical Report TR 97-3, Mechanical and Fluid Engineering Division, Southwest Research Institute, San Antonio, TX. Friction tests were performed at Southwest Research Institute on a modified test apparatus originally used to measure friction between rock surfaces. The test apparatus is ideal because of its horizontal and vertical load capabilities of 60,000 lb. The vertical load was applied in the apparatus with three hydraulic cylinders, and the center cylinder pushed and pulled a sliding center structure. This paper used cool rolled steel for one of the materials that was tested. The average of test results was 0.16 in a dry surface and for sliding.

Peter J. Blau. (1992). "Appendix: Static and Kinetic Friction Coefficient for Selected Material," Friction, Lubrication, and Wear Technology, ASM Handbook, Vol 18, Metal and Ceramics Division, Oak Ridge Laboratory, Materials Park, OH. In Table 1 of this reference a value of 0.62 for the kinetic coefficient of friction for steel, mild on steel, mild, is reported. That table also gives the values for many other combinations of materials.

Headquarters, U.S. Army Corps of Engineers. (1993). "Barge Impact Analysis," Engineer Technical Letter 1110-2-338, Washington, DC. This Engineer Technical Letter determines the impact force during barge crushing. It was rescinded in 2001. It lists an angle of friction of 10 degrees (equivalent to a coefficient of friction of 0.176). No reference to test data was cited in this source.

General Magnaplate Corporation, Linden, NJ.
http://www.magnaplate.com. A Friction Data Guide was created by Magnaplate. It reports a value for the kinetic coefficient of friction of 0.23 for steel to steel. That information is cited as a reference in the *ASM Handbook*.

Bharat Bhushan and B. K. Gupta. (1991). *Handbook of Tribology.* **McGraw-Hill, New York, p 2.11.** Table 2.1 lists values for the kinetic coefficients of friction for various materials and gives a value for hard steel on hard steel of 0.42.

6   Numerical Examples

This chapter presents a description of the input data, examples of barge train models, and the results computed using the formulation developed in this research. The first example is the model used as an example in ETL 1110-2-338. The model is presented in Figure 6-1, where the 8-barge train has dimensions of 84 ft wide by 650 ft long, and the total mass of the system is 1,299 kips-sec^2/ft. Hydrodynamic added masses were included in the Limit_LASHING computations. The hydrodynamic added mass coefficients assigned to the analyses are $\eta_x = 0.05$, $\eta_y = 0.4$, and $\eta_\theta = 0.4$. The analyses were done using different combinations of input variables. As shown in Table 6-1, different values for each one of the input variables were adopted. For example, the barge train model was analyzed using the three failure mechanisms with the approach angle equal to 10, 20, 80, and 90 degrees. Each case studied is obtained by assigning one value to each variable per calculation.
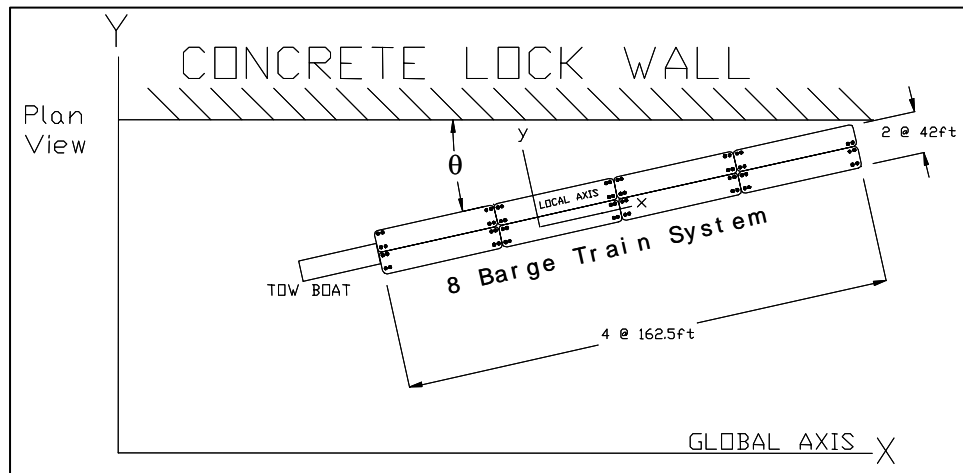
Figure 6-1. Eight-barge train configuration

The second example consists of the barge train used in the full-scale, low-velocity, controlled-impact barge experiments conducted in December 1998 at the decommissioned Gallipolis Lock at Robert C. Byrd Lock and Dam, Gallipolis Ferry, WV. The size of this system, presented in Figure 6-2, is 105 ft wide by 975 ft long with a total mass of 1,825 kips-sec^2/ft. Hydrodynamic added masses were included in the Limit_LASHING computations. The hydrodynamic added mass coefficients assigned to the analyses are $\eta_x = 0.05$, $\eta_y = 0.4$, and $\eta_\theta = 0.4$.

Table 6-1
Input Data Used for the 8-Barge Train System

Input Variable	Approach Angle, deg			
	10	20	80	90
Longitudinal				
μ_{wall}	0.2	0.3	0.4	
μ_{barge}	0.2	0.4		
m_t	1299	1299	1299	1299
m_1	649.5	649.5	649.5	649.5
m_2	649.5	649.5	649.5	649.5
Transverse				
μ_{wall}	0.2	0.3	0.4	
μ_{barge}	0.2	0.4		
m_t	1299	1299	1299	1299
m_1	324.75	324.75	324.75	324.75
m_2	974.25	974.25	974.25	974.25
Corner				
μ_{wall}	0.2	0.3	0.4	
μ_{barge}	0.2	0.4		
m_t	1299	1299	1299	1299
m_1	324.75	324.75	324.75	324.75
m_2	974.25	974.25	974.25	974.25
Note: Mass given in kips-sec^2/ft.				
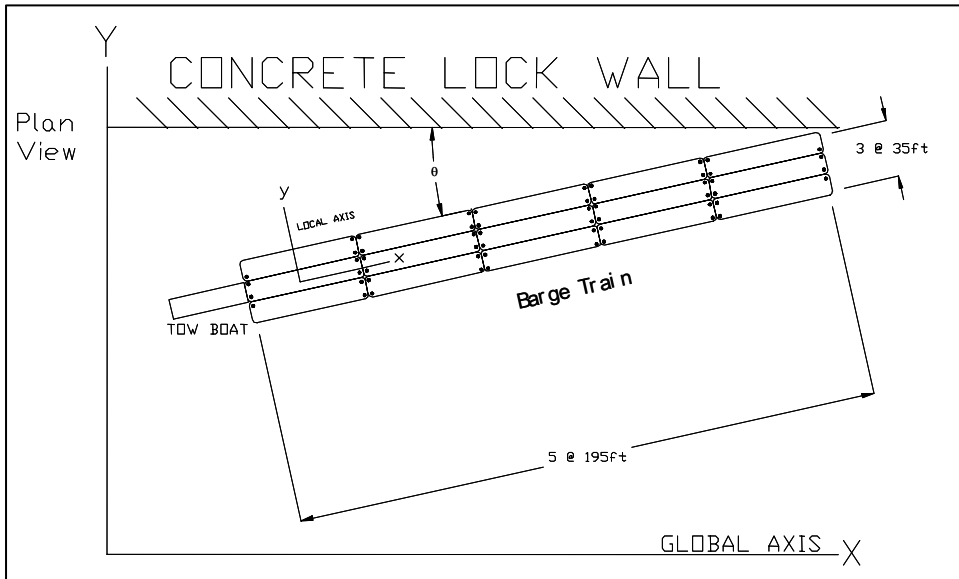
Figure 6-2. Barge train configuration of 1998 experiment

Table 6-2
Input Data Used for the 15-Barge Train System

Input Variable	Approach Angle, deg				
	10	20	80	90	90woe
Longitudinal					
μ_{wall}	0.2	0.3	0.4		
μ_{barge}	0.2	0.4			
m_t	1825	1825	1825	1825	1825
m_1	608.333	608.333	608.333	608.333	608.333
m_2	1216.667	1216.667	1216.667	1216.667	1216.667
Transversal					
μ_{wall}	0.2	0.3	0.4		
μ_{barge}	0.2	0.4			
m_t	1825	1825	1825	1825	1825
m_1	365	365	365	365	365
m_2	1460	1460	1460	1460	1460
Corner					
μ_{wall}	0.2	0.3	0.4		
μ_{barge}	0.2	0.4			
m_t	1825	1825	1825	1825	1825
m_1	365	365	365	365	365
m_2	1460	1460	1460	1460	1460
Note: Mass given in kips-sec^2/ft.					

The analyses were conducted using different combinations of input variables. As shown in Table 6-2, different values for each one of the input variables were adopted. For example, the barge train model was analyzed for the three failure mechanisms with the approach angle equal to 10, 20, 80, and 90 degrees. Each case studied is obtained by assigning one value to each variable per calculation. In addition, there is an impact case in which direct impact can occur but without eccentricity, as discussed in Section 2.3. The input data for this case is presented in the last column of Table 6-2 (90woe).

The lashing configurations and lashing properties definitions are other important factors in the solution process. In both numerical examples, the lashing configuration, the bits location, and lashing properties were assumed to be the same. The lashing configuration at the edges of the barge train is presented in Figure 6-3. The internal connections have three levels of lashings, presented in Figures 6-4 to 6-6. The generic connectivity of the lashings is also defined in these figures. Appendix A presents more information about the connectivity and the incidence of lashings. It is important to mention that the Limit_LASHING computer program needs the connectivity specified from System 1 to System 2, even in the case of multiple wraps using the same lashing. Systems 1 and 2 were defined in previous chapters for each of the three idealized failure mechanisms.

These lashings are made of steel, and in this formulation an elastoplastic relationship was used to describe their mechanical behavior. This constitutive relationship allows the lashing to carry load from zero up to the yield stress of the lashing. At this instant, the lashing cannot carry more load but allows for

increased deformation. The load that produces the yield stress is the ultimate load divided by the cross-sectional area of the lashing. The slope of the stress-strain initial line is Young's modulus of elasticity *E,* which is around 29,000 ksi. Typical lashing properties are presented in Table 6-3. The lashing diameters are 1.0 or 1.25 in. and the ultimate load is 90 or 120 kips, respectively. Using these data the yield stress of a lashing with 1-in. diameter and ultimate load of 90 kips produces a yield stress of 114.591559 ksi or 16,501.18 ksf.
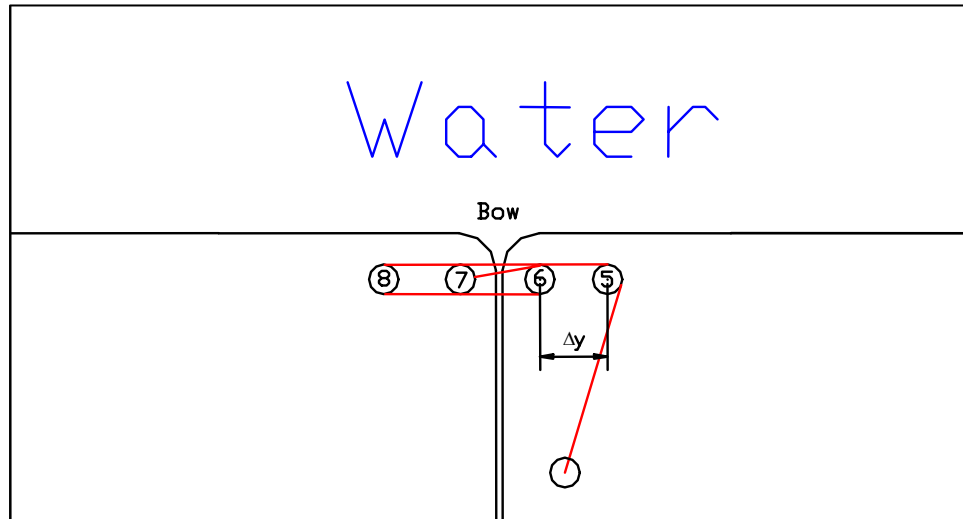
Figure 6-3. Configuration 1 located at bow, port, aft, and starboard sides: generic sequence – 7,6,8,5
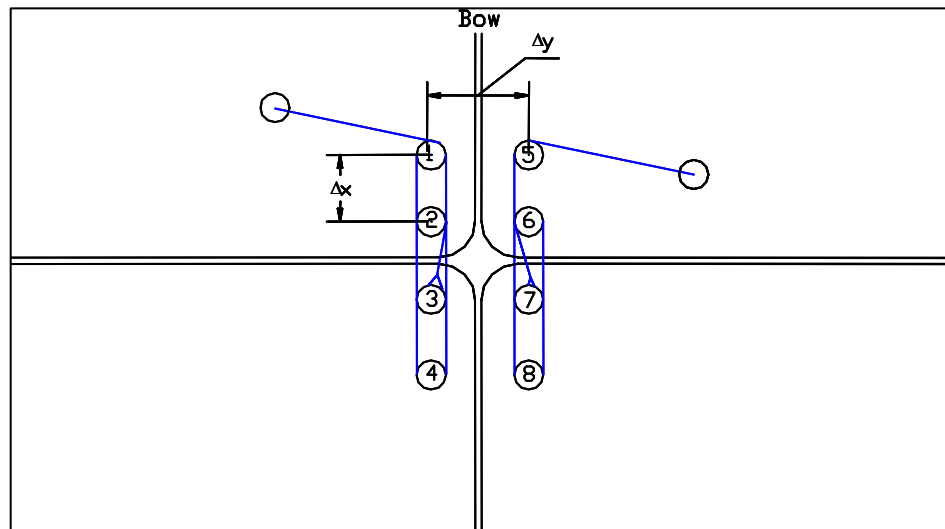
Figure 6-4. Configuration 2 located at the bottom layer in the inside connection: generic sequence – 7, 6, 8, 5 and 3, 2, 4, 1
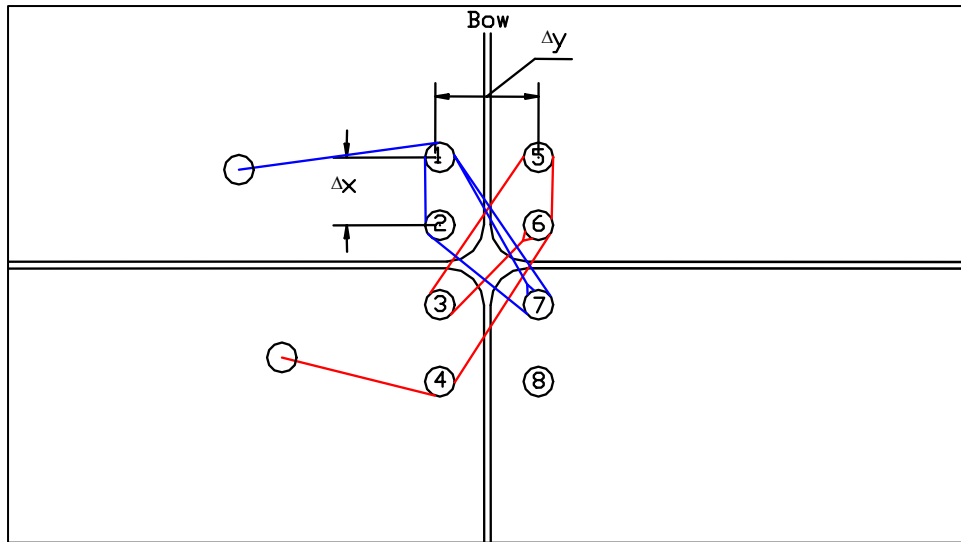
Figure 6-5. Configuration 3 located at the middle layer in the inside connection: generic sequence – 6, 3, 5, 6, 4 and 7, 1, 2, 7, 1
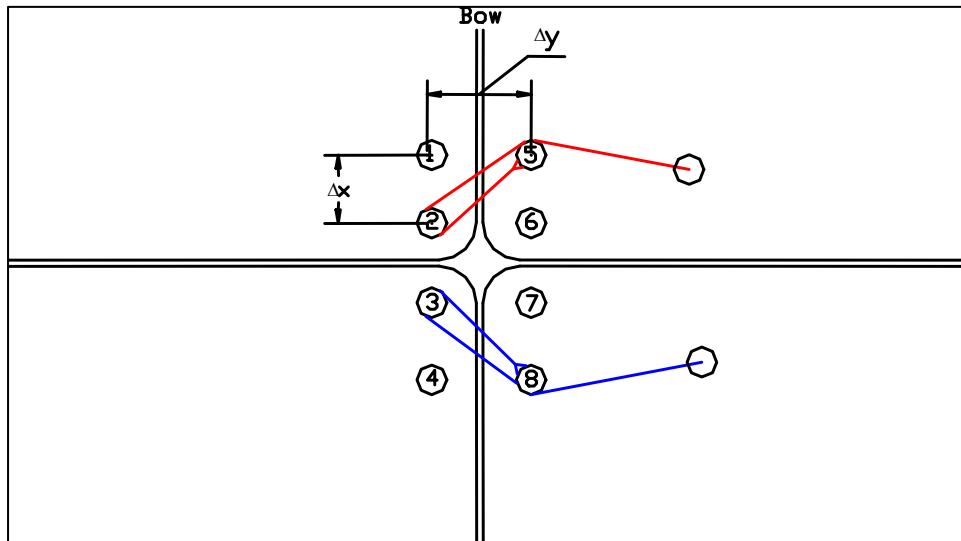
Figure 6-6. Configuration 4 located at the top layer in the inside connection: generic sequence – 5, 2, 5 and 8, 3, 8

Table 6-3 Typical Lashing Properties				
Lashing Type	Diameter, in.	Modulus of Elasticity, ksi	Cross-sectional Area, in.^{2}	Ultimate Load, kips
1	1	29,000	0.7854	90
2	1.25	29,000	1.2272	120

Another important variable that needs to be defined prior to analysis is the location of the bits. This parameter is important because the position of the bits will define the length and normal strain within the lashings. With these data and

the constitutive equations, the internal stress and internal forces in the lashing are calculated. Typical values for bit locations are presented in Appendix C.

The results for all the examples studied are presented in Tables 6-4 to 6-6. Use these tables as follows:

  a. Select the failure mechanism.
  b. Select the barge train (8 or 15 barges).
  c. Select the option of total mass, total m_1 and m_2, or half of the mass for System 2, Total m_1 and half m_2.
  d. Select the approach angle.
  e. Select the kinetic coefficient of friction at the wall-to-barge and barge-to-barge contacts.
  f. Read the tabulated F_W value.

For example,

  a. Select the failure mechanism: corner from Table 6-6.
  b. Select the barge system: 15 from the right side of Table 6-6.
  c. Select the approach angle: 10 degrees.
  d. Select the kinematic coefficient of friction: barge-to-wall = 0.2; barge-to-barge = 0.2.
  e. $F_W = 251$ kips.

From these tables the following can be observed:

  a. The longitudinal failure mechanism produces very high values of F_W for shallow approach angles. The corner failure mechanism produces the lower value of F_W for shallow approach angles. Results indicate that for a shallow angle it is impossible for the longitudinal failure mechanism to occur because to reach the F_W predicted by this case, the F_W value of the corner failure mechanism has already been achieved.

  b. On the other hand, for a high approach angle, the corner and transverse failure mechanisms produce negative values of F_W, which is impossible, because the barge train pushes the wall and does not pull the wall. A negative F_W indicates that the barge train is pulling the rigid wall.

  c. A zero F_W appearing in these tables indicates that a negative value was produced. This means that the failure mechanism that presents a zero F_W will not occur.

  d. Compare the corner failure mechanism results with the empirical correlation using the linear momentum of the barge train before impact: From Table 1-1, Experiment 37 had an approach angle of 10.3 degrees, and a velocity before impact of 1.96 fps. The total mass of the 15-barge system was 1,825 kips-sec^2/ft. With these data and using the empirical correlation, a maximum force normal to the wall equal to 278 kips is calculated.

  e. From Table 6-6, the corner failure mechanism, estimate the force normal to the wall to be between 251 kips and 864 kips (depending on the coefficients of friction), if the lashings that join the corner barge to the rest of the system yields.

f. During the experiments listed in Table 1-1, no breaking of lashings was observed. This indicates that the coefficient of friction between the wall and the corner barge was between 0.2 and 0.4. Also, it is important to note that the impacts during the experiments involved a concrete rigid wall without any protection (i.e., no armor). This means that the coefficient of friction between the wall and the corner barge is greater than the coefficient of friction between steel-to-steel.

g. Figure 6-7 presents a typical elastoplastic stress-strain curve for a 1-in.-diameter lashing with an ultimate load of 90 kips. The yield stress is calculated as

$$\sigma_{yield} = \frac{90\ kips}{\frac{\pi}{4}(1)^2} * 144 = 16,501.18\ ksf$$

Table 6-4
Maximum F_W (in kips) for the Longitudinal Failure Mechanism

Approach Angle	$(F_W)_{max}$ for 8 Barges, kips			$(F_W)_{max}$ for 15 Barges, kips		
	$\mu_{wall}=0.2$	$\mu_{wall}=0.3$	$\mu_{wall}=0.4$	$\mu_{wall}=0.2$	$\mu_{wall}=0.3$	$\mu_{wall}=0.4$
Total m_1 and m_2 $\mu_{barges}=0.2$						
10	16658	10107	7254	15435	9626	6994
20	5139	4291	3683	6026	4887	4110
80	1327	1303	1279	1739	1697	1657
90 No Ecc.	0	0	0	3477	3477	3477
90 Ecc.	1310	1310	1310	1738	1738	1738
Total m_1 and m_2 $\mu_{barges}=0.4$						
10	0	0	0	0	0	32404
20	20212	11687	8220	17982	10870	7789
80	1534	1491	1450	1990	1917	1849
90 No Ecc.	0	0	0	3944	3944	3944
90 Ecc.	1492	1492	1492	1972	1972	1972
Total m_1 and half m_2 $\mu_{barges}=0.2$						
10	29336	16658	11632	22105	13411	9626
20	5920	5139	4541	6820	5694	4887
80	1344	1327	1311	1761	1729	1697
90 No Ecc.	0	0	0	3477	3477	3477
90 Ecc.	1310	1310	1310	1738	1738	1738
Total m_1 and half m_2 $\mu_{barges}=0.4$						
10	0	0	0	0	0	0
20	39344	20212	13599	26726	15454	10870
80	1565	1534	1505	2029	1971	1917
90 No Ecc.	0	0	0	3944	3944	3944
90 Ecc.	1492	1492	1492	1972	1972	1972

Table 6-5
Maximum F_W (in kips) for the Transverse Failure Mechanism

Approach Angle	$(F_W)_{max}$ for 8 Barges, kips			$(F_W)_{max}$ for 15 Barges, kips		
	μ_{wall}=0.2	μ_{wall}=0.3	μ_{wall}=0.4	μ_{wall}=0.2	μ_{wall}=0.3	μ_{wall}=0.4
Total m_1 and m_2 μ_{barges}=0.2						
10	291	300	310	470	486	504
20	328	346	365	533	563	597
80	0	0	0	0	0	0
90 No Ecc.	0	0	0	0	0	0
90 Ecc.	0	0	0	0	0	0
Total m_1 and m_2 μ_{barges}=0.4						
10	633	667	705	1024	1084	1151
20	755	319	894	1227	1339	1473
80	0	0	0	0	0	0
90 No Ecc.	0	0	0	0	0	0
90 Ecc.	0	0	0	0	0	0
Total m_1 and half m_2 μ_{barges}=0.2						
10	287	294	302	465	478	492
20	322	335	349	523	547	574
80	0	0	0	0	0	0
90 No Ecc.	0	0	0	0	0	0
90 Ecc.	0	0	0	0	0	0
Total m_1 and half m_2 μ_{barges}=0.4						
10	620	646	674	1005	1053	1105
20	733	575	833	1194	1281	1381
80	0	0	0	0	0	0
90 No Ecc.	0	0	0	0	0	0
90 Ecc.	0	0	0	0	0	0

Table 6-6
Maximum F_W (in kips) for the Corner Failure Mechanism

Approach Angle	$(F_W)_{max}$ for 8 Barges, kips			$(F_W)_{max}$ for 15 Barges, kips		
	$\mu_{wall}=0.2$	$\mu_{wall}=0.3$	$\mu_{wall}=0.4$	$\mu_{wall}=0.2$	$\mu_{wall}=0.3$	$\mu_{wall}=0.4$
Total m_1 and m_2 $\mu_{barges}=0.2$						
10	280	289	299	251	260	269
20	316	333	352	285	301	319
80	0	0	0	0	0	0
90 No Ecc.	0	0	0	0	0	0
90 Ecc.	0	0	0	0	0	0
Total m_1 and m_2 $\mu_{barges}=0.4$						
10	467	492	520	600	635	675
20	557	604	660	719	785	864
80	0	0	0	0	0	0
90 No Ecc.	0	0	0	0	0	0
90 Ecc.	0	0	0	0	0	0
Total m_1 and half m_2 $\mu_{barges}=0.2$						
10	277	284	291	249	617	263
20	310	323	337	280	293	307
80	0	0	0	0	0	0
90 No Ecc.	0	0	0	0	0	0
90 Ecc.	0	0	0	0	0	0
Total m_1 and half m_2 $\mu_{barges}=0.4$						
10	457	476	497	590	617	648
20	457	575	614	700	751	810
80	0	0	0	0	0	0
90 No Ecc.	0	0	0	0	0	0
90 Ecc.	0	0	0	0	0	0

Figure 6-7. Elastoplastic behavior of a 1-in.-diameter lashing

7 Conclusions and Recommendations

In this research, the complex, dynamic problem of a barge train-rigid wall system was analyzed using the equations of motion to determine the maximum force applied to the rigid wall by a barge train during an impact event. Three failure mechanisms were studied: longitudinal, transverse, and corner failure. The longitudinal failure mechanism is a failure that can occur at high approach angles, for example, greater than 70 degrees. It is based on the relative motion of one set of barges to another set of barges. All the lashings in the first line of connections and parallel to the port side will fail first. Two special cases of this failure mechanism were also studied: a direct impact to a cell or nose pier with and without eccentricity. In the case of no eccentricity, two failure planes were identified. The second failure mechanism was the transverse failure mechanism, which consists of a flexure-type failure. In this case, the first line of lashings parallel to the bow breaks due to the rotation of the barges at the bow of the system. In this model no relative motion between the front barges was assumed. This failure mechanism can occur for shallow approach angles, for example, less than 30 degrees. For higher approach angles, another failure plane will be adopted by the system. In this failure mechanism exist two possible locations for the pivot point. An expression was derived to determine where the pivot point will occur, in the port side or in the starboard side. This location will depend on the coefficient of friction between the barge system and the armored wall, and also on the location of the center of mass of System 1. A third failure mechanism was the corner failure mechanism. This model is similar to the transverse failure mechanism. The difference is that the rotation toward the wall is allowed only for the corner impacting barge of System 1. This effect can be introduced into the formulation of the transverse failure mechanism by including the lashing forces that join the corner barge to the rest of the barge train. In other words, the transverse failure mechanism assumes the front barges as a single rigid body, and the corner failure mechanism assumes that the corner barge is joined by the lashings to the other barges in System 1.

Input data for these idealized impact models are the approach angle, the mass of the system, the steel-to-steel kinetic coefficient of friction and the lashing properties. The most difficult data to locate are the kinetic coefficient of friction for steel to steel. As the result of a literature review conducted, the steel-to-steel coefficient of friction was found to vary between 0.20 and 0.50. The lashing configuration was also studied. It is important to note that the lashing

arrangement and properties are important because the resultant forces in the lashing depend on the relative motion (or rotation) that occurs between barges which, in turn, defines the limiting maximum impact force computed normal to the wall (see Figure 1-5). It is important to obtain a limiting maximum force normal to the wall because in the Arroyo, Ebeling, and Barker (2003) empirical correlation (see Figure 1-3), this limit state was not represented (see Figure 1-5). The maximum impact force normal to the wall is limited by two possible failures. One is the crushing of the corner barge and the second is the yielding of the lashings during impact. This report covers the failure of the barge train based on the lashings yielding.

The ETL 1110-2-338 engineering procedure had been used to compute values of maximum impact force normal to the wall, $(F_w)_{max}$. A key aspect of this engineering formulation is computation of collision energy dissipated in nonrecoverable, plastic hull deformation of (i.e., damage to) the corner of the barge where impact with the wall occurs. Note that no damage was observed to the barge corner during any of these low-velocity, controlled-impact experiments at Robert C. Byrd Lock. After a careful evaluation of the ETL 1110-2-338 formulation and review of results given in Chapters 5 and 6, the authors of this report recommend that this engineering procedure not be used when damage to the barge *will not occur* during impact. The failure due to lashing yielding could dominate over the crushing of the corner barge.

Based on the three idealized lashing limit-state formulations described in this report, for shallow approach angles, the corner failure mechanism predicts lower forces normal to the wall. This condition could be explained if one observes that the corner failure mechanism has more degrees of freedom. That is, this failure mechanism provides for a primary degree of freedom, "rotation of System 1," and a secondary degree of freedom, "rotation of the corner barge" within System 1. For that reason, for shallow angles (< 30 degrees), the corner failure mechanism is recommended.

To demonstrate the effectiveness of the methodology presented, several examples based on the data of the 1998 full-scale experiment (Patev et al. 2003) are presented. Table 7-1 presents the relevant information for the eight most credible field experiments, the computed normal force at the wall based on ETL 1110-2-338, the field test results, and the force normal to the wall computed based on the transverse and corner failure mechanisms discussed in this report.

Table 7-1 shows that in all eight impact cases the results provided by the corner failure mechanism are lower than the transverse failure mechanism, indicating that the corner failure mechanism is more probable to occur than the transverse failure mechanism. In most of the experiments, the value of the force normal to the wall obtained using the corner failure mechanism (for barge System 2) plus the empirical correlation (for barge System 1) was greater than the value obtained from the field test data (column 8). Only Experiment 42 produced a field value greater than the numerical model developed in this report. The reason for this is likely due to the very low value for the kinetic coefficient of friction between wall armor-to-steel barge (0.09) as determined by Arroyo, Ebeling, and Barker (2003) during their data reduction of the field test. As found in the technical literature, this value is typically between 0.2 and 0.5.

Table 7-1
Comparison of Results Based on Data of 1998 Full-Scale Experiment

(1) Experiment Number	(2) Approach Velocity, fps	(3) Approach Angle, deg	(4) Velocity Normal to the Wall, fps	(5) Coefficient of Friction[1]	(6) Linear Momentum Normal to the Wall, kip*sec	(7) Computed $(F_W)_{max}$ by ETL 1110-2-338[2], kip	(8) Field Test[1] $(F_W)_{max}$, kip	(9) $(F_W)_{max}$, Transverse Failure Mechanism, kip	(10) $(F_W)_{max}$, Transverse Failure Mechanism + Emp. Correlation, kip	(11) $(F_W)_{max}$, Corner Failure Mechanism, kip	(12) $(F_W)_{max}$, Corner Mechanism + Emp. Correlation, kip
29	2.21	12.63	0.48	0.60	895.48	410	287	838	916	438	516
30	2.35	12.19	0.50	0.48	932.80	421	370	789	870	413	494
31	1.62	10.60	0.30	0.43	559.68	264	236	754	803	394	443
37	1.96	10.29	0.35	0.52	652.96	317	327	776	833	406	463
38	1.84	11.94	0.38	0.57	708.92	328	230	816	878	427	489
39	1.62	14.12	0.39	0.51	727.58	317	272	828	891	433	496
41	2.87	8.76	0.44	0.51	820.86	424	419	754	825	394	465
42	1.84	17.48	0.55	0.09	1,026.07	387	577	716	805	374	463

Note: Mass without hydrodynamic added mass = 1,865.59 kips-sec^2/ft. Coefficient of barge-to-barge friction = 0.2.
[1] Table 5.3 in Arroyo, Ebeling, and Barker (2003)
[2] Table 5.4 in Arroyo, Ebeling, and Barker (2003)

Results in Column 8 reflect the impact force from the eight full-scale, low-velocity, controlled-impact barge experiments in which no lashing failure occurred. Results of Columns 10 and 12 must be larger than Column 8 because they were calculated assuming failure of the lashing. Results from Column 12 are lower than the results from Column 10, indicating that the corner failure mechanism will dominate if the lashings break. The results from Column 12 provide greater $(F_W)_{max}$ values than Column 8 as expected, because no breaking of the lashings occurred during the full-scale, low-velocity, controlled-impact barge experiments.

The Limit_LASHING calculations were repeated but using a kinetic coefficient of friction between the armored wall and the barge train equal to 0.5 and a kinetic coefficient of friction between barge System 1 and barge System 2 equal to 0.25. The results for this case are presented in Table 7-2. In all eight cases the computed force normal to the wall was greater than the field test results. In these cases, the field test values *must* be lower than the computed values because *no lashing failure occurred* during the experiments.

To summarize, Table 7-1 demonstrates the range of applicability of the lashing limit-state numerical models developed in this report. For example, the corner failure mechanism will dominate over the other two mechanisms if the approach angle is below 30 degrees. This trend is observed for the green curve in Figure 7-1. This curve is below the other curves (purple and blue). These results were obtained using a kinetic coefficient of friction between steel to steel of 0.5. The lashings properties and configurations were the ones presented in Appendix A. The longitudinal failure mechanism is appropriate when the approach angle is greater than 70 degrees because it produces positive values of F_W. The other mechanism predicts negative values of F_W, which is impossible because the barge train pushes, not pulls the wall.

Table 7-2
Comparison of Results

Experiment Number	Assumed Coefficient of Friction	Field Test[1] $(F_w)_{max}$, kip	$(F_w)_{max}$ Corner Mechanism + Emp. Correlation, kip
29	0.50	287	647
30	0.50	370	644
31	0.50	236	596
37	0.50	327	601
38	0.50	230	623
39	0.50	272	650
41	0.50	419	601
42	0.50	577	721

Note: Mass without hydrodynamic added mass = 1,865.59 kips-sec^2/ft
[1] Table 5.3 in Arroyo, Ebeling, and Barker (2003)
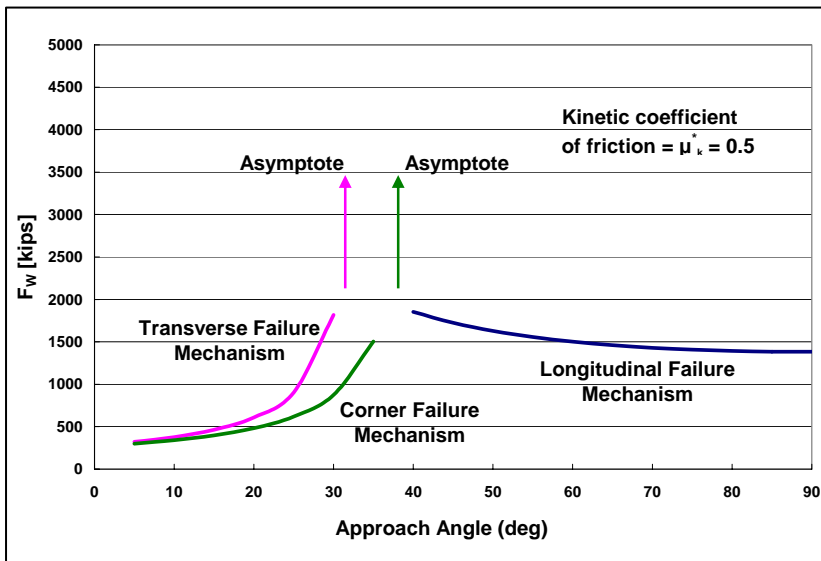
Figure 7-1. Range of applicability of the failure mechanisms

References

Arroyo, J. R., Ebeling, R., and Barker, B. (2003). "Analysis of full-scale low-velocity, controlled barge impact experiments, December 1998," ERDC/ITL TR-03-3, U.S. Army Engineer Research and Development Center, Vicksburg, MS.

Bailey, J. M., and Douglas, G. (1954). "Coefficient of friction and damage to contact area during the early stage of fretting," Technical Note 3144, National Advisory Committee for Aeronautics, Washington, DC.

Bhushan, B., and Gupta, B. K. (1991). *Handbook of tribology.* McGraw-Hill, New York, 2.11.

Bisson, E. E., Johnson, R. L., Swikert, M. A., and Godfrey, D. (1955). "Friction, wear, and surface damage of metal as affected by solid surface films," Report 1254, National Advisory Committee for Aeronautics, Washington, DC.

Blau, P. J. (1992). "Appendix: Static and kinetic friction coefficient for selected material." ASM Handbook: *Friction, Lubrication, and Wear Technology,* ASM International, Materials Park, OH. Vol. 18.

General Magnaplate Corporation, Linden, NJ. *http://www.magnaplate.com.*

Headquarters, U.S. Army Corps of Engineers. (1993). "Barge impact analysis," Engineer Technical Letter 1110-2-338, Washington, DC.

Minorsky, V. U. (1959). "An analysis of ship collisions with reference to protection of nuclear power plants," *Journal of Ship Research* 3(2), 1-4.

Patev, R. C., Barker, B. C., and Koestler, L. V. (2003). "Full-scale barge impact experiments, Robert C. Byrd Lock and Dam, Gallipolis Ferry, West Virginia," Technical Report ERDC/ITL TR-03-7, U.S. Army Engineer Research and Development Center, Vicksburg, MS.

Pantermuehl, P. J., and Smalley, A. J. (1997). "Friction tests typical chock materials and cast iron," Technical Report TR 97-3, Mechanical and Fluid Engineering Division, Southwest Research Institute, San Antonio, TX.

Peterson, M. B., and Johnson, R. L. (1952). "Friction and surface damage of several corrosion-resistant materials," NACA Research Memorandum E51L20, National Advisory Committee for Aeronautics, Washington, DC.

Appendix A
Lashing Configurations

All simplified failure mechanisms developed during the course of this research were based on the assumption that the lashings joining the barges provide the strength to the barge train such that barge System 2 decelerates when barge System 1 impacts the wall. This assumption combined with the equations of equilibrium for the two-barge system allows for the calculation of the normal and shear force between the barge train and the *rigid* wall during the impact process. The configurations of the lashings between barges are allowed to differ. However, in the examples shown in this report, the configuration of lashings used in the full-scale experiments performed in 1998 and reported in Patev et al. (2003)[1] were used. The four configurations observed in the three- by five-barge train used in the full-scale experiment are presented in Figures A-1 through A-4. The computer program Limit_LASHING has the capacity to analyze a barge train with lashing configurations that are typical of what is used on inland waterways.
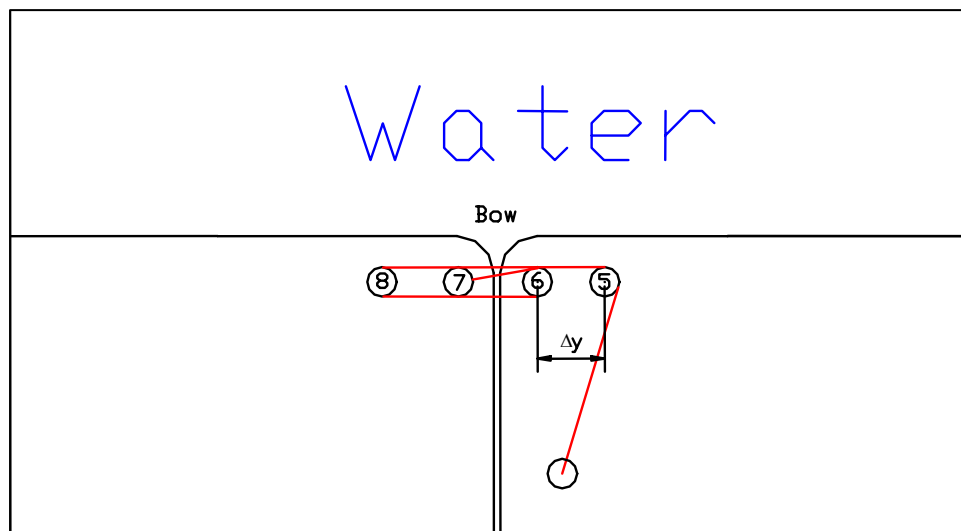
Figure A-1. Configuration 1 located at bow, port, aft, and starboard sides: generic sequence – 7,6,8,5

---

[1] References cited in this appendix are included in the References section following the main text.
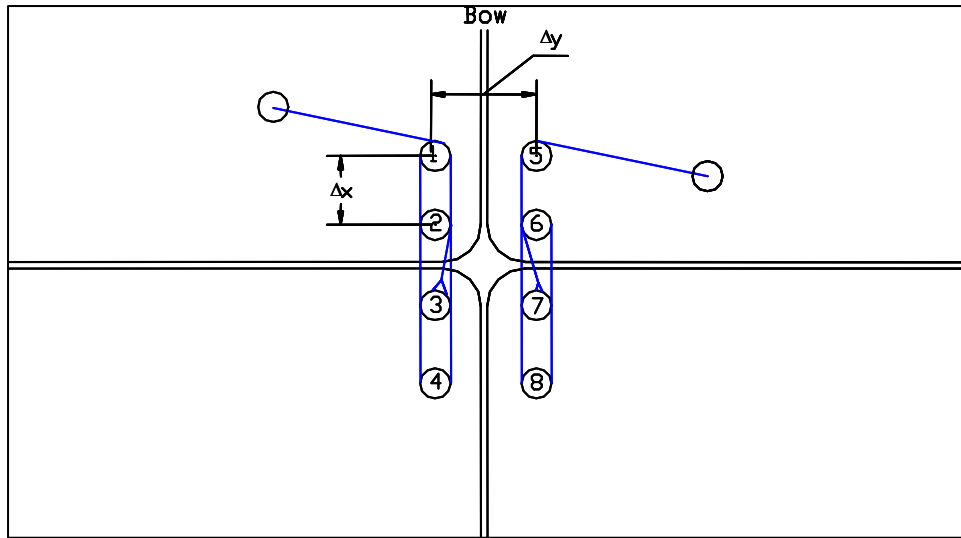
Figure A-2. Configuration 2 located at the bottom layer in the inside connection:
generic sequence – 7, 6, 8, 5 and 3, 2, 4, 1
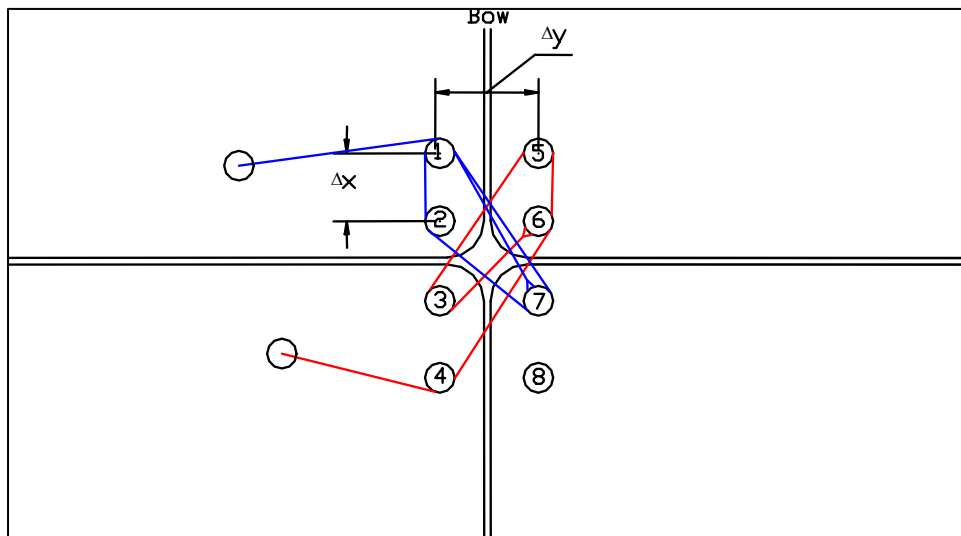
Figure A-3. Configuration 3 located at the middle layer in the inside connection:
generic sequence – 6, 3, 5, 6, 4 and 7, 1, 2, 7, 1

Configuration 1, as presented in Figure A-1, was the arrangement used in the 1998 full-scale experiments to join a pair of barges along the outside edge of the barge train. It is also the configuration used on the bow, port, aft, and starboard sides. It consists of three turns of the bits along the edge of the two joined barges. The generic sequence of the bits connected is also shown in Figure A-1. The name generic sequence means that the assigned numbers can change in each model configuration. However, the lashing configuration must be the same according to the sequence shown in Figure A-1.
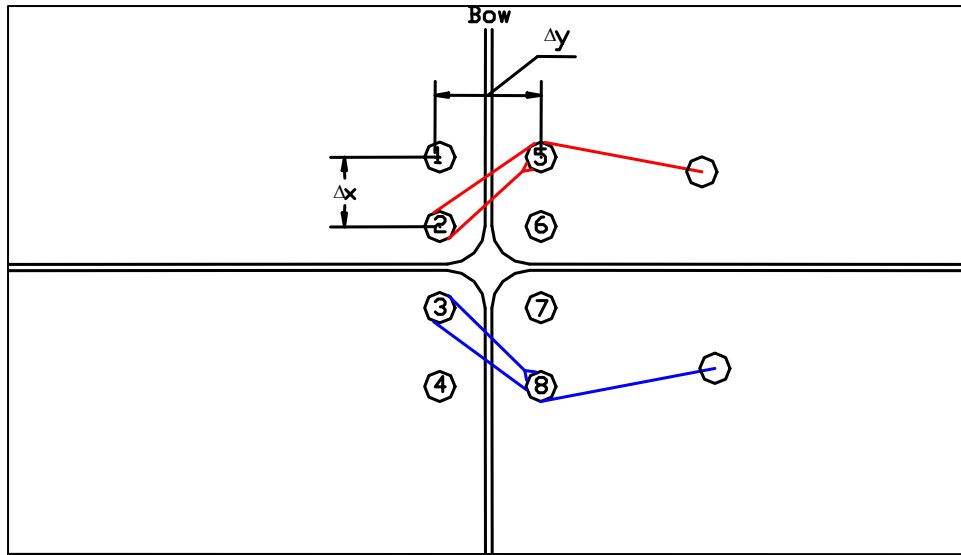
Figure A-4. Configuration 4 located at the top layer in the inside connection: generic sequence – 5, 2, 5 and 8, 3, 8

At the center joints where four barges come together, three configuration levels were available. The 1998 experiments had eight of these connections because 15 barges were joined together. The top, middle, and bottom configurations are shown in Figures A-2 through A-4. The bottom layer, designated Configuration 2, is similar to Configuration 1. This configuration is considered as a separate configuration because it is associated with the center connections between barges. The middle configuration at the inner connections, designated Configuration 3, is like a scissor passing each lashing over the edge of the joined barges three times. Finally, Configuration 4, or the top layer in the inner connection, has two turns for each lashing over the edge of the joined barges. Note that the configurations shown in these figures are not the only configurations available for use in Limit_LASHING. In Limit_LASHING, the user can include more turns in each of these configurations, eliminate configurations, and use different lashings, etc. For that reason, the variable of lashing configuration and lashing properties is one of the primary variables in this program.

To determine the angle that each force within the lashing makes with the local axis of the system, the coordinates of each bit on the barges are specified by the user. In this way, the necessary angles to determine the components of the internal force for the lashings are calculated in the local axis by Limit_LASHING. It is important to note that these arrangements are prepared for a forward or backward motion of the lashings.

The lashings are made of steel, and in this research an elastoplastic relationship that breaks when an ultimate (tensile) strain value is achieved within the lashing was used to describe their mechanical behavior. As shown in Figure A-5, this behavior allows the lashing to carry load from zero up to the ultimate stress of the lashing. At this instant, the lashing remains with the ultimate stress until the ultimate strain is reached. The load that produces the ultimate stress is the ultimate load divided by the cross-sectional area of the

lashing. The initial slope of the stress-strain line is the Young's modulus of elasticity *E,* typically assigned a value of 29,000 ksi. Figure A-5 shows the elastoplastic behavior adopted to model the constitutive relationship for the lashings. The typical lashings properties are presented in Table A-1. The lashing diameters used in the full-scale experiments were either 1 or 1.25 in. with an ultimate load of 90 or 120 kips, respectively. Using this information combined with an ultimate load of 90 kips for a 1-in.-diameter lashing results in an ultimate stress of 114.6 ksi = 16,501.2 ksf.
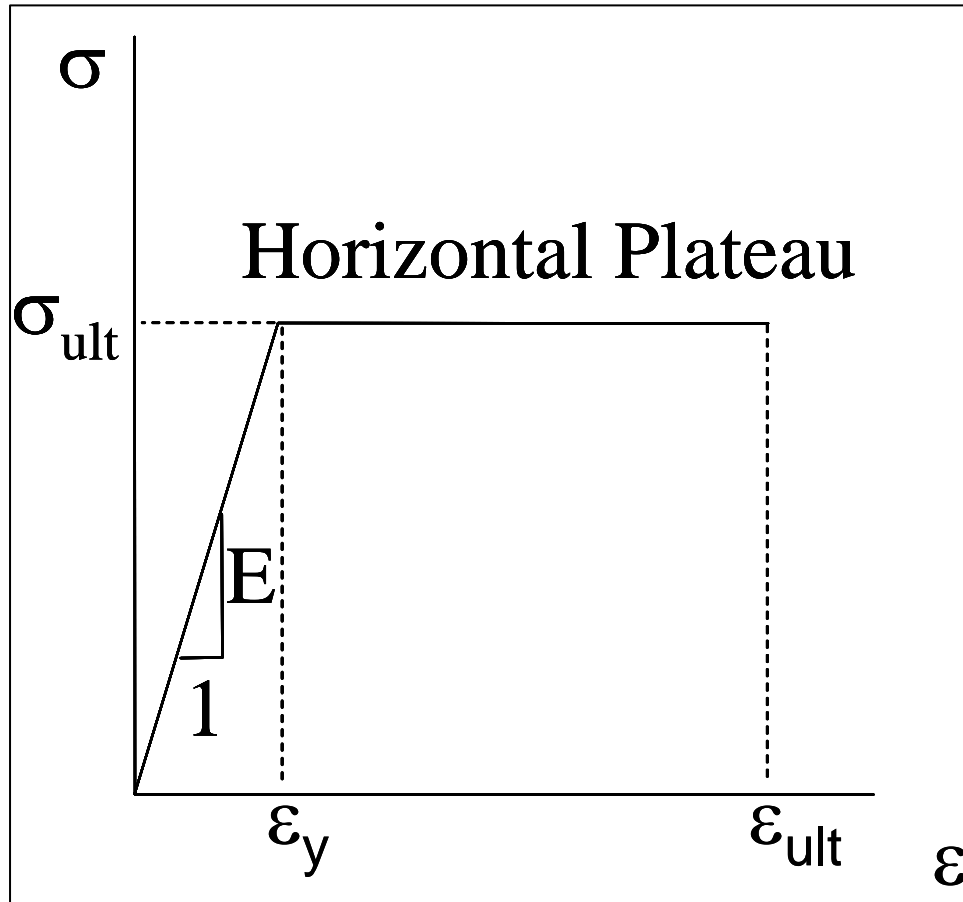
Figure A-5. Constitutive relationship of the lashings

Table A-1 Typical Lashing Properties				
Lashing Type	Diameter, in.	Modulus of elasticity, ksi	Cross-Sectional Area, in.^{2}	Ultimate Load, kips
1	1	29,000	0.7854	90
2	1.25	29,000	1.2272	120

Appendix B
FORTRAN Source Programs
and Maple™ Worksheets

B.1 Program to Calculate the Force Normal to the Wall Based On the Lashing Ultimate Load

```
        PROGRAM LIMIT_LASHING
        INTEGER *2 NOP
CCCCCCCCCCCCCCCCCCCCCCCCCCCCCCCCCCCCCCCCCCCCCCCCCCCCCCCCCCCCCCCCCCCCCC
C                                                                    C
C                                                                    C
C                    PROGRAM   LIMIT_LASHING                         C
C                                                                    C
C     This computer program calculates the force normal to the wall C
C     and the shear in the wall due to the impact of a barge train. C
C     The linear accelerations in the global X- and Y-axes are also C
C     calculated based on the hydrodynamic added mass effect.        C
C     Three different failure mechanisms are used:                   C
C                                                                    C
C              1) Longitudinal failure mechanism                     C
C              2) Transverse failure mechanism                       C
C              3) Corner failure mechanism                           C
C                                                                    C
C           LAST REVISION:  December 22, 2003                        C
C                                                                    C
CCCCCCCCCCCCCCCCCCCCCCCCCCCCCCCCCCCCCCCCCCCCCCCCCCCCCCCCCCCCCCCCCCCCCC
        WRITE(*,*)
C
C     OPEN INPUT AND OUTPUT FILES
C
        OPEN(UNIT=1,FILE='DATA.DAT')
        OPEN(UNIT=2,FILE='DATA.OUT')
        READ(1,*) NOP
C
C     SELECT THE FAILURE MECHANISM (TRANSVERSE, LONGITUDINAL,CORNER)
C
        IF (NOP .EQ. 1) THEN
           CALL TRAN
        ELSE
        ENDIF
        IF (NOP .EQ. 2) THEN
           CALL LONG
        ELSE
```

```
          ENDIF
          IF (NOP .EQ. 3) THEN
             CALL CORNER
          ELSE
          ENDIF
          IF (NOP .EQ. 4) THEN
             CALL LONG
          ELSE
          ENDIF
          IF (NOP .EQ. 5) THEN
             CALL LONG
          ELSE
          ENDIF

C
C     OPEN A FILE TO INDICATE VISUAL BASIC LiMIT_LASHING END
C
          OPEN(UNIT=3,FILE='END.OUT')
          STOP
          END



          SUBROUTINE LONG
CCCCCCCCCCCCCCCCCCCCCCCCCCCCCCCCCCCCCCCCCCCCCCCCCCCCCCCCCCCCCCCCCCCCCCC
C                                                                     C
C                                                                     C
C Subroutine to calculate the maximum force normal to the wall, the   C
C shear force in the wall, the acceleration normal and tangent to the C
C wall.  These values are calculated using Newton's second law for a  C
C longitudinal failure mechanism.                                     C
C                                                                     C
C                                                                     C
CCCCCCCCCCCCCCCCCCCCCCCCCCCCCCCCCCCCCCCCCCCCCCCCCCCCCCCCCCCCCCCCCCCCCCC
          INTEGER *2 I,NBITS,NODE(2000),NLASH,NBS(500,100),NBE(500,100),J,
     1            NC(500)
         REAL *8 COORD(2000,2),AREA(2000),EE(2000),PI(2000),PULT(2000),
     1      DSTEP,DC(2000),L(2000),LF(2000),MASST,EPS(2000),SIGMA(2000),
     2      CO(2000),PY(2000),PX(2000),DIAM(2000),DMAX,FWEC,FWT(2000),
     3      RX(2000),RY(2000),LO(2000),P(2000),PP(2000),
     4      LT,PPT,MASS1,MASS2,THETA,MUK,FW(2000),CORX,CORY,CORI,
     5      SW(2000),THET,MUKK,AX(2000),AY(2000),DEL(2000),
     6      MPAR1,MPAR2,MNORM1,MNORM2,EPULT(2000),VX,VY
C
C      OPEN FILES AND INPUT DATA
C
C
         READ(1,*) NBITS
         DO I = 1 , NBITS
            READ(1,*) NODE(I),COORD(NODE(I),1),COORD(NODE(I),2)
         ENDDO
         READ(1,*) NLASH
         DO I = 1, NLASH
            L(I) = 0.0
         ENDDO
         DO I = 1, NLASH
            READ(1,*) NC(I),(NBS(I,J),NBE(I,J),J=1,NC(I)),DIAM(I),
     1            EE(I),PI(I),PULT(I),EPULT(I)
            AREA(I) = 3.14159*0.25*DIAM(I)*DIAM(I)
            DO II = 1, NC(I)
               LT =SQRT((ABS(COORD(NBS(I,II),1)-COORD(NBE(I,II),1)))**2+
```

```
      1             (ABS(COORD(NBS(I,II),2)-COORD(NBE(I,II),2)))**2)
              L(I) = L(I) + LT
           ENDDO
           LO(I) = AREA(I)*EE(I)*L(I)/(PI(I)+AREA(I)*EE(I))
        ENDDO
        READ(1,*) THET,MASST,MASS1,MUKK,MUK,VX,VY
        READ(1,*) CORX,CORY,CORI
C
C  CALCULATE THE HYDRODYNAMIC ADDED MASS PARALLEL AND NORMAL TO THE WALL
C     FOR SYSTEM ONE AND TWO
C
        CORX = 1.0 + CORX
        CORY = 1.0 + CORY
        CORI = 1.0 + CORI
        MASS2=MASST-MASS1
        THETA = THET * 3.14159/180.0
        MPAR1 = ((CORX*MASS1*CORY*MASS1) /
      1        (CORX*MASS1*DSIN(THETA)**2+CORY*MASS1*DCOS(THETA)**2))
        MPAR2 =  ((CORX*MASS2*CORY*MASS2) /
      1        (CORX*MASS2*DSIN(THETA)**2+CORY*MASS2*DCOS(THETA)**2))
        MNORM1 = ((CORX*MASS1*CORY*MASS1) /
      1        (CORY*MASS1*DSIN(THETA)**2+CORX*MASS1*DCOS(THETA)**2))
        MNORM2 = ((CORX*MASS2*CORY*MASS2) /
      1        (CORY*MASS2*DSIN(THETA)**2+CORX*MASS2*DCOS(THETA)**2))
C
C INITIALIZE THE VARIABLES TO ZERO BEFORE THE INCREMENTAL ANALYSIS
STARTS
C
        DO I = 1, 1500
           PX(I) = 0.0
           PY(I) = 0.0
           RX(I) = 0.0
           RY(I) = 0.0
           P(I) =  0.0
           PP(I) = 0.0
           PY(I) = 0.0
        ENDDO
        PPT = 0.0
        DMAX = 0.0
        DSTEP = 0.001
        DC(1) = 0.0
C
C     GENERATE A VECTOR WITH THE 1,500-STEP RELATIVE DISPLACEMENTS
C
        DO I =2, 1500
           DC(I) = DC(I-1) + DSTEP
        ENDDO
C
C     CALCULATION OF EACH LASHING FORCES AND RESULTANT LASHING FORCES
C
C
        DO I = 1, NLASH
           WRITE(2,*)
           WRITE(2,105) I
           WRITE(2,*)
           WRITE(2,103)
           WRITE(2,104)
           TT = 0.0
C
C  CALCULATION OF THE LASHING LENGTH FOR EACH INCREMENT OF DISPLACEMENT
C
```

```
          DO J = 1,1500
             LF(I) = 0.0
             DO II = 1, NC(I)
                IF(COORD(NBS(I,II),1) .LE. COORD(NBE(I,II),1)+DC(J)) THEN
                   LT =SQRT((ABS(COORD(NBS(I,II),1)-COORD(NBE(I,II),1))
     1                +DC(J))**2+(COORD(NBS(I,II),2)-
     2                COORD(NBE(I,II),2))**2)
                   LF(I) = LF(I) + LT
                   CO(II) = DACOS(ABS(COORD(NBS(I,II),2)-
     1                   COORD(NBE(I,II),2)) / LT)
                ELSE
                   IF (COORD(NBS(I,II),1) .GT.
     1               COORD(NBE(I,II),1)+DC(J)) THEN
                      LT =SQRT((ABS(COORD(NBS(I,II),1)-
     1                  COORD(NBE(I,II),1))
     2                 -DC(J))**2+(ABS(COORD(NBS(I,II),2)-
     3                 COORD(NBE(I,II),2)))**2)
                      LF(I) = LF(I) + LT
                      CO(II) = DACOS(ABS(COORD(NBS(I,II),2)-
     1                     COORD(NBE(I,II),2)) / LT)
                   ELSE
                   ENDIF
                ENDIF
             ENDDO
C
C CALCULATION OF THE INTERNAL FORCE IN THE LASHING AND CHECK IF THE
C LASHING REACHES ULTIMATE STRAIN
C
             P(J) = AREA(I)*EE(I)/LO(I)*(LF(I)-LO(I))
             PP(J) = AREA(I)*EE(I)/LO(I)*DC(J)
               EPS(J) = (LF(I)-LO(I)) / LO(I)
             IF(P(J) .GT. PULT(I)) THEN
                IF( EPS(J) .GT. EPULT(I)) THEN
                   P(J) = 0.0
                   PP(J) = 0.0
                ELSE
                   P(J) = PULT(I)
                   PP(J) = PULT(I)
                ENDIF
             ELSE
             ENDIF
             IF (P(J) .LT. 0.0) THEN
                P(J) = 0.0
             ELSE
             ENDIF
             SIGMA(J) = P(J) / AREA(I)
             IF(EPS(J) .LT. 0.0) THEN
                EPS(J) = 0.0
             ELSE
             ENDIF
               PPT = 0.0
             PY(J) = 0.0
             PX(J) = 0.0
C
C     CALCULATION OF THE GLOBAL COMPONENT OF THE LASHING FORCES
C
             DO II = 1, NC(I)
                PPT = P(J) * DCOS(CO(II))
                PY(J) = PY(J) + PPT
                IF (COORD(NBS(I,II),1) .GT. COORD(NBE(I,II),1)+DC(J))THEN
                   PX(J) = - P(J) * DSIN(CO(II)) + PX(J)
```

```
                   ELSE
                      PX(J) = P(J) * DSIN(CO(II)) + PX(J)
                   ENDIF
                ENDDO
                RX(J) = RX(J) + PX(J)
                RY(J) = RY(J) + PY(J)
                DEL(J) = (LF(I)-LO(I))
                IF(DEL(J) .LT. 0.0) THEN
                   DEL(J) = 0.0
                  ELSE
                ENDIF
                   WRITE(2,101) J,EPS(J), SIGMA(J),DEL(J),P(J),PX(J),PY(J)
             ENDDO
          ENDDO
   C
   C      CALCULATION OF Fw, Sw, aX, aY
   C
   C
       IF (THET .EQ. 90.0) THEN
          FW(1) = MUK*RY(1)+RX(1)
        ELSE
          FW(1)=(MPAR1*DCOS(THETA)*(RX(1)*DCOS(THETA)+RY(1)*DSIN(THETA))
   1          +MPAR2*DCOS(THETA)*(RX(1)*DCOS(THETA)+RY(1)*DSIN(THETA))
   2     +MUK*MPAR1*DSIN(THETA)*(RX(1)*DCOS(THETA)+RY(1)*DSIN(THETA))
   3     +MUK*MPAR2*DSIN(THETA)*(RX(1)*DCOS(THETA)+RY(1)*DSIN(THETA))
   4          +MUK*MPAR1*DCOS(THETA)*(RY(1)*DCOS(THETA)
   5          -RX(1)*DSIN(THETA))
   6     +MUK*MPAR2*DCOS(THETA)*(RY(1)*DCOS(THETA)-RX(1)*DSIN(THETA))
   7     +MPAR1*DSIN(THETA)*(-RY(1)*DCOS(THETA)+RX(1)*DSIN(THETA))
   8     +MPAR2*DSIN(THETA)*(-RY(1)*DCOS(THETA)+RX(1)*DSIN(THETA))) /
   9     (MPAR1*DSIN(THETA)+MPAR2*DSIN(THETA)-MUK*MPAR1*DCOS(THETA)
   1     -MUK*MPAR2*DCOS(THETA)+MUKK*MPAR2*DCOS(THETA)
   2     +MUKK*MUK*MPAR2*DSIN(THETA))
        ENDIF
        IF (FW(1) .LE. 0.0) THEN
           DO I =1,1500
              FW(I) =0.0
              SW(I) = 0.0
              AY(I) = 0.0
              AX(I) = 0.0
           ENDDO
        ELSE
           DO I = 1, 1500
              IF (THET .EQ. 90.0) THEN
                 FW(I) = MUK*RY(I)+RX(I)
                 IF (FW(I) .LE. 0.0) THEN
                    FW(I) = 0.0
                 ELSE
                 ENDIF
                    AX(I) = 0.0
                 SW(I) = 0.0
                  AY(I) = FW(I) / ((CORX*MASS2*CORY*MASS2) /
   1                (CORX*MASS2*DCOS(THETA)**2+CORY*MASS2*DSIN(THETA)**2))
              ELSE
                 FW(I)=(MPAR1*DCOS(THETA)*(RX(I)*DCOS(THETA)
   1                 +RY(I)*DSIN(THETA))+MPAR2*DCOS(THETA)
   2                 *(RX(I)*DCOS(THETA)+RY(I)*DSIN(THETA))
   3                 +MUK*MPAR1*DSIN(THETA)*(RX(I)*DCOS(THETA)
   4                 +RY(I)*DSIN(THETA))+MUK*MPAR2*DSIN(THETA)
   5                 *(RX(I)*DCOS(THETA)+RY(I)*DSIN(THETA))+MUK*MPAR1
   6                 *DCOS(THETA)*(RY(I)*DCOS(THETA)-RX(I)*DSIN(THETA))
```

```
      7                    +MUK*MPAR2*DCOS(THETA)*(RY(I)*DCOS(THETA)-RX(I)
      8                    *DSIN(THETA))+MPAR1*DSIN(THETA)*(-RY(I)
      9                    *DCOS(THETA)+RX(I)*DSIN(THETA))+MPAR2*DSIN(THETA)
      1                    *(-RY(I)*DCOS(THETA)+RX(I)*DSIN(THETA))) /
      2                    (MPAR1*DSIN(THETA)+MPAR2*DSIN(THETA)-MUK
      2                    *MPAR1*DCOS(THETA)-MUK*MPAR2*DCOS(THETA)
      3                    +MUKK*MPAR2*DCOS(THETA)+MUKK*MUK*MPAR2*DSIN(THETA))
               IF (FW(I) .LE. 0.0) THEN
                  FW(I) = 0.0
               ELSE
               ENDIF
                  SW(I) = MUKK * FW(I)
               AX(I) = SW(I) / ((CORX*MASST*CORY*MASST) /
      1          (CORX*MASST*DSIN(THETA)**2+CORY*MASST*DCOS(THETA)**2))
               AY(I) = FW(I) / ((CORX*MASS2*CORY*MASS2) /
      1          (CORX*MASS2*DCOS(THETA)**2+CORY*MASS2*DSIN(THETA)**2))
            ENDIF
         ENDDO
      ENDIF
C
C  CALCULATION OF Fw DUE TO SYSTEM ONE CONTRIBUTION USING THE EMPIRICAL
C  CORRELATION
C
      FWEC = 0.435*MASS1*(VX*DSIN(THETA)+VY*DCOS(THETA))
      DO I = 1, 1500
         IF (FW(I) .LE. 0.0) THEN
            FWT(I) = 0.0
         ELSE
            FWT(I) = FW(I) + FWEC
         ENDIF
      ENDDO
C
C     PRINT OF RESULTS
C
      WRITE(2,*)
      WRITE(2,*)
      WRITE(2,106)
      WRITE(2,100)
      WRITE(2,*)
      DO I = 1,1500
         WRITE(2,102) I,DC(I),RX(I),RY(I),FW(I),SW(I),AX(I),AY(I),FWEC,
     1FWT(I)
      ENDDO
 100  FORMAT(19X,'TOTAL RESULTANT FORCE',/,10X,'DISP.',5X,'LOCAL X',5X,
     1'LOCAL Y',7X,'Fw',11X,'Sw',12X,'aX',10X,'aY',7X,'Fw',7X,'TOTAL Fw'
     2,/,71X,'Systems',5X,'System',3X,'Empirical',
     3/,71X,'1 and 2',7X,'2',5X,'Correlation')
 101  FORMAT(I4,E12.4,F12.4,E12.4,3F12.4)
 102  FORMAT(I4,E12.4,8F12.4)
 103  FORMAT(9X,'NORMAL',6X,'NORMAL',18X,'INTERNAL',6X,
     1'RESULTANT FORCE')
 104  FORMAT(9X,'STRAIN      STRESS       ELONG.         FORCE',7X,
     1'LOCAL X     LOCAL Y',//)
 105  FORMAT(29X,'LASHING NUMBER',I4)
 106  FORMAT(//,90('='),//,29X,'FINAL RESULTS',//,90('='),//)
      RETURN
      END
```

```
      SUBROUTINE TRAN
CCCCCCCCCCCCCCCCCCCCCCCCCCCCCCCCCCCCCCCCCCCCCCCCCCCCCCCCCCCCCCCCCCC
C                                                                 C
C                                                                 C
C Subroutine to calculate the maximum force normal to the wall, the   C
C shear force in the wall, the acceleration normal and tangent to the C
C wall.  These values are calculated using Newton's second law for a  C
C transverse failure mechanism.                                   C
C                                                                 C
C                                                                 C
CCCCCCCCCCCCCCCCCCCCCCCCCCCCCCCCCCCCCCCCCCCCCCCCCCCCCCCCCCCCCCCCCCC
      INTEGER *2 I,NBITS,NODE(2000),NLASH,NBS(500,100),NBE(500,100),J,
     1           NC(500)
      REAL *8 COORD(2000,2),AREA(2000),EE(2000),PI(2000),PULT(2000),
     1        DSTEP,DC(2000),L(2000),LF(2000),MASST,FWEC,FWT(2000),
     2        CO(2000),PY(2000),PX(2000),DIAM(2000),DMAX,
     3        RX(2000),RY(2000),LO(2000),P(2000),PP(2000),BLMAX,
     4        LT,PPT,MASS1,MASS2,THETA,MUK,FW(2000),EPULT(2000),
     5        SW(2000),THET,MUKK,AX(2000),AY(2000),BL(2000),
     6        EPS(2000),SIGMA(2000),DEC(2000),DEL(2000),
     7        CORX,CORY,CORI,MNORM1,MNORM2,MPAR1,MPAR2,VX,VY
C
C     OPEN FILES AND INPUT DATA
C
C
      READ(1,*) NBITS
      DO I = 1 , NBITS
         READ(1,*) NODE(I),COORD(NODE(I),1),COORD(NODE(I),2)
      ENDDO
      READ(1,*) NLASH
      DO I = 1, NLASH
         L(I) = 0.0
      ENDDO
      BLMAX = 0.0
      DO I = 1, NLASH
         BL(I) = 0.0
         READ(1,*) NC(I),(NBS(I,J),NBE(I,J),J=1,NC(I)),DIAM(I),
     1        EE(I),PI(I),PULT(I),EPULT(I)
         DO J = 1, NC(I)
            BL(I) = BL(I) + COORD(NBS(I,J),2)
         ENDDO
         BL(I) = BL(I) / NC(I)
         IF (BL(I) .GT. BLMAX) THEN
            BLMAX = BL(I)
         ELSE
            BLMAX = BLMAX
         ENDIF
         AREA(I) = 3.14159*0.25*DIAM(I)*DIAM(I)
         DO II = 1, NC(I)
            LT =SQRT((ABS(COORD(NBS(I,II),1)-COORD(NBE(I,II),1)))**2+
     1          (ABS(COORD(NBS(I,II),2)-COORD(NBE(I,II),2)))**2)
            L(I) = L(I) + LT
         ENDDO
         LO(I) = AREA(I)*EE(I)*L(I)/(PI(I)+AREA(I)*EE(I))
      ENDDO
      READ(1,*) THET,MASST,MASS1,MUKK,MUK,VX,VY
      READ(1,*) CORX,CORY,CORI
C
C  CALCULATE THE HYDRODYNAMIC ADDED MASS PARALLEL AND NORMAL TO THE WALL
```

```
C  FOR SYSTEM ONE AND TWO
C
      CORX = 1.0 + CORX
      CORY = 1.0 + CORY
      CORI = 1.0 + CORI
      MASS2=MASST-MASS1
      THETA = THET * 3.14159/180.0
      MPAR1 = ((CORX*MASS1*CORY*MASS1) /
     1      (CORX*MASS1*DSIN(THETA)**2+CORY*MASS1*DCOS(THETA)**2))
      MPAR2 =  ((CORX*MASS2*CORY*MASS2) /
     1      (CORX*MASS2*DSIN(THETA)**2+CORY*MASS2*DCOS(THETA)**2))
      MNORM1 = ((CORX*MASS1*CORY*MASS1) /
     1      (CORY*MASS1*DSIN(THETA)**2+CORX*MASS1*DCOS(THETA)**2))
      MNORM2 = ((CORX*MASS2*CORY*MASS2) /
     1      (CORY*MASS2*DSIN(THETA)**2+CORX*MASS2*DCOS(THETA)**2))
C
C INITIALIZE THE VARIABLES TO ZERO BEFORE THE INCREMENTAL ANALYSIS START
C
      DO I = 1, 1500
         PX(I) = 0.0
         PY(I) = 0.0
         RX(I) = 0.0
         RY(I) = 0.0
         P(I) =  0.0
         PP(I) = 0.0
         PY(I) = 0.0
      ENDDO
      PPT = 0.0
      DMAX = 0.0
      DSTEP = 0.001 / BLMAX
      DC(1) = 0.0
      DEC(1) = 0.0
C
C     GENERATE A VECTOR WITH THE 1,500 STEP ROTATION
C
      DO I =2, 1500
         DC(I) = DC(I-1) + DSTEP
         DEC(I) = DEC(I-1)+ 0.001
      ENDDO
C
C      CALCULATION OF EACH LASHING FORCE AND RESULTANT LASHING FORCES
C
C
      DO I = 1, NLASH
         WRITE(2,*)
         WRITE(2,105) I
         WRITE(2,*)
         WRITE(2,103)
         WRITE(2,104)
         TT = 0.0
C
C     CALCULATION OF THE LASHING LENGTH FOR EACH INCREMENT OF ROTATION

C
         DO J = 1,1500
            LF(I) = 0.0
            DO II = 1, NC(I)
               LT =SQRT((ABS(COORD(NBS(I,II),1)-COORD(NBE(I,II),1))
     1             +DC(J)*COORD(NBS(I,II),2))**2+(COORD(NBS(I,II),2)-
     2             COORD(NBE(I,II),2))**2)
               LF(I) = LF(I) + LT
```

```
                CO(II) = DACOS(ABS(COORD(NBS(I,II),2)-
     1                      COORD(NBE(I,II),2)) / LT)
            ENDDO
C
C CALCULATION OF THE INTERNAL FORCE IN THE LASHING AND CHECK IF THE
C LASHING REACHES ULTIMATE STRAIN
C
            P(J) = AREA(I)*EE(I)/LO(I)*(LF(I)-LO(I))
            PP(J) = AREA(I)*EE(I)/LO(I)*DC(J)*1000.0
            EPS(J) = (LF(I)-LO(I)) / LO(I)
            IF(P(J) .GT. PULT(I)) THEN
             IF( EPS(J) .GT. EPULT(I)) THEN
                P(J) = 0.0
                PP(J) = 0.0
              ELSE
                 P(J) = PULT(I)
                 PP(J) = PULT(I)
              ENDIF
            ELSE
            ENDIF
            IF (P(J) .LT. 0.0) THEN
               P(J) = 0.0
            ELSE
            ENDIF
            SIGMA(J) = P(J) / AREA(I)
            IF(EPS(J) .LT. 0.0) THEN
               EPS(J) = 0.0
            ELSE
            ENDIF
              PPT = 0.0
            PY(J) = 0.0
            PX(J) = 0.0
C
C     CALCULATION OF THE GLOBAL COMPONENT OF THE LASHING FORCES
C
            DO II = 1, NC(I)
               PPT = P(J) * DSIN(CO(II))
               PX(J) = PX(J) + PPT
               IF (COORD(NBS(I,II),2) .GE. COORD(NBE(I,II),2)) THEN
                  PY(J) = P(J) * DCOS(CO(II)) + PY(J)
                ELSE
                  PY(J) = - P(J) * DCOS(CO(II)) + PY(J)
                ENDIF
            ENDDO
              RX(J) = RX(J) + PX(J)
            RY(J) = RY(J) + PY(J)
            DEL(J) = (LF(I)-LO(I))
            IF(DEL(J) .LT. 0.0) THEN
               DEL(J) = 0.0
              ELSE
            ENDIF
              WRITE(2,101) J,EPS(J),SIGMA(J),DEL(J),P(J), PX(J),PY(J)
          ENDDO
        ENDDO
C
C      CALCULATION OF Fw, Sw, aX, aY
C
C
      FW(1) = (MPAR1*DSIN(THETA)*(RX(1)*DCOS(THETA)-RY(1)*DSIN(THETA))
     1+MPAR2*DSIN(THETA)*(RX(1)*DCOS(THETA)-RY(1)*DSIN(THETA))
     2+MUK*MPAR1*DCOS(THETA)*(RX(1)*DCOS(THETA)-RY(1)*DSIN(THETA))
```

```
      3+MUK*MPAR2*DCOS(THETA)*(RX(1)*DCOS(THETA)-RY(1)*DSIN(THETA))
      4+MUK*MPAR1*DSIN(THETA)*(RX(1)*DSIN(THETA)+RY(1)*DCOS(THETA))
       5-MPAR1*DCOS(THETA)*(RX(1)*DSIN(THETA)+RY(1)*DCOS(THETA))
      6+MUK*MPAR2*DSIN(THETA)*(RX(1)*DSIN(THETA)+RY(1)*DCOS(THETA))
      7-MPAR2*DCOS(THETA)*(RX(1)*DSIN(THETA)+RY(1)*DCOS(THETA))) /
       8(-MUK*MPAR1*DSIN(THETA)+MPAR1*COS(THETA)-MUK*MPAR2*DSIN(THETA)
       9+MPAR2*DCOS(THETA)-MUKK*MPAR2*DSIN(THETA)
      1-MUK*MUKK*MPAR2*DCOS(THETA))
       IF( FW(1) .LE. 0.0) THEN
          FW(1) = 0.0
       ELSE
       ENDIF
       SW(1) = MUKK * FW(1)
       AX(1) = SW(1) / ((CORX*MASST*CORY*MASST) /
      1          (CORX*MASST*DSIN(THETA)**2+CORY*MASST*DCOS(THETA)**2))
       AY(1) = FW(1) / ((CORX*MASS2*CORY*MASS2) /
      1          (CORX*MASS2*DCOS(THETA)**2+CORY*MASS2*DSIN(THETA)**2))
       DO I = 2, 1500
          IF (FW(I-1) .LE. 0.0) THEN
             FW(I) =  0.0
             SW(I) =  0.0
             AX(I) =  0.0
             AY(I) =  0.0
          ELSE
             FW(I)=(MPAR1*DSIN(THETA)*(RX(I)*DCOS(THETA)
      1-RY(I)*DSIN(THETA))+MPAR2*DSIN(THETA)*(RX(I)*DCOS(THETA)
      2-RY(I)*DSIN(THETA))+MUK*MPAR1*DCOS(THETA)*(RX(I)*DCOS(THETA)
      3-RY(I)*DSIN(THETA))+MUK*MPAR2*DCOS(THETA)*(RX(I)*DCOS(THETA)
      4-RY(I)*DSIN(THETA))+MUK*MPAR1*DSIN(THETA)*(RX(I)*DSIN(THETA)
      5+RY(I)*DCOS(THETA))-MPAR1*DCOS(THETA)*(RX(I)*DSIN(THETA)+RY(I)
      6*DCOS(THETA))+MUK*MPAR2*DSIN(THETA)*(RX(I)*DSIN(THETA)
      7+RY(I)*DCOS(THETA))-MPAR2*DCOS(THETA)*(RX(I)*DSIN(THETA)
      8+RY(I)*DCOS(THETA))) / (-MUK*MPAR1*DSIN(THETA)+MPAR1*COS(THETA)
      9-MUK*MPAR2*DSIN(THETA)+MPAR2*DCOS(THETA)-MUKK*MPAR2*DSIN(THETA)
      1-MUK*MUKK*MPAR2*DCOS(THETA))
             IF (FW(I) .LE. 0.0) THEN
               FW(I) = 0.0
             ELSE
             ENDIF
             SW(I) = MUKK * FW(I)
             AX(I) = SW(I) / ((CORX*MASST*CORY*MASST) /
      1          (CORX*MASST*DSIN(THETA)**2+CORY*MASST*DCOS(THETA)**2))
             AY(I) = FW(I) / ((CORX*MASS2*CORY*MASS2) /
      1          (CORX*MASS2*DCOS(THETA)**2+CORY*MASS2*DSIN(THETA)**2))
          ENDIF
       ENDDO
C
C     CALCULATION OF Fw DUE TO SYSTEM ONE CONTRIBUTION USING THE
C     EMPIRICAL CORRELATION
C
       FWEC = 0.435*MASS1*(VX*DSIN(THETA)+VY*DCOS(THETA))
       DO I = 1, 1500
          IF (FW(I) .LE. 0.0) THEN
             FWT(I) = 0.0
          ELSE
             FWT(I) = FW(I) + FWEC
          ENDIF
       ENDDO
C
C     PRINT OF RESULTS
C
```

```
      WRITE(2,*)
      WRITE(2,*)
      WRITE(2,106)
      WRITE(2,100)
      WRITE(2,*)
      DO I = 1,1500
          WRITE(2,102) I,DC(I),RX(I),RY(I),FW(I),SW(I),AX(I),AY(I),FWEC,
     1FWT(I)
      ENDDO

 100  FORMAT(19X,'TOTAL RESULTANT FORCE',/,11X,'ROT.',5X,'LOCAL X',5X,
     1'LOCAL Y',7X,'Fw',11X,'Sw',12X,'aX',10X,'aY',7X,'Fw',7X,'TOTAL Fw'
     2,/,71X,'Systems',5X,'System',3X,'Empirical',
     3/,71X,'1 and 2',7X,'2',5X,'Correlation')

 101  FORMAT(I4,E12.4,F12.4,E12.4,3F12.4)
 102  FORMAT(I4,E12.4,8F12.4)
 103  FORMAT(9X,'NORMAL',6X,'NORMAL',18X,'INTERNAL',6X,
     1'RESULTANT FORCE')
 104  FORMAT(9X,'STRAIN      STRESS      ELONG.       FORCE',7X,
     1'LOCAL X    LOCAL Y',//)
 105  FORMAT(29X,'LASHING NUMBER',I4)
 106  FORMAT(//,90('='),//,29X,'FINAL RESULTS',//,90('='),//)
      RETURN
      END




      SUBROUTINE CORNER
CCCCCCCCCCCCCCCCCCCCCCCCCCCCCCCCCCCCCCCCCCCCCCCCCCCCCCCCCCCCCCCCCCCCCCC
C                                                                     C
C                                                                     C
C Subroutine to calculate the maximum force normal to the wall, the   C
C shear force in the wall, the acceleration normal and tangent to the C
C wall.  These values are calculated using Newton's second law for a  C
C corner failure mechanism.                                           C
C                                                                     C
C                                                                     C
CCCCCCCCCCCCCCCCCCCCCCCCCCCCCCCCCCCCCCCCCCCCCCCCCCCCCCCCCCCCCCCCCCCCCCC
      INTEGER *2 I,NBITS,NODE(2000),NLASH,NBS(500,100),NBE(500,100),J,
     1           NC(500),JMAX(2000),JM(2000),JMM,NLASH1,IJJ,NFLAG(2000)
      REAL *8 COORD(2000,2),AREA(2000),EE(2000),PI(2000),PULT(2000),
     1        DSTEP,DC(2000),L(2000),LF(2000),MASST,FWEC,FWT(2000),
     2        CO(2000),PY(2000),PX(2000),DIAM(2000),DMAX,
     3        RX(2000),RY(2000),LO(2000),P(2000),PP(2000),BLMAX,
     4        LT,MASS1,MASS2,THETA,MUK,FW(2000),EPULT(2000),
     5        SW(2000),THET,MUKK,AX(2000),AY(2000),BL(2000),
     6        EPS(2000),SIGMA(2000),DEC(2000),DEL(2000),
     7        CORX,CORY,CORI,MPAR1,MPAR2,MNORM1,MNORM2,VX,VY
C
C     OPEN FILES AND INPUT DATA
C
C
      READ(1,*) NBITS
      DO I = 1 , NBITS
          READ(1,*) NODE(I),COORD(NODE(I),1),COORD(NODE(I),2)
      ENDDO
      READ(1,*) NLASH,NLASH1
```

```
          DO I = 1, NLASH
             L(I) = 0.0
          ENDDO
          BLMAX = 0.0
          DO I = 1, NLASH
             BL(I) = 0.0
             READ(1,*) NC(I),(NBS(I,J),NBE(I,J),J=1,NC(I)),DIAM(I),
         1          EE(I),PI(I),PULT(I),EPULT(I),NFLAG(I)
             DO J = 1, NC(I)
                BL(I) = BL(I) + COORD(NBS(I,J),2)
             ENDDO
             BL(I) = BL(I) / NC(I)
             IF (BL(I) .GT. BLMAX) THEN
                BLMAX = BL(I)
             ELSE
                BLMAX = BLMAX
             ENDIF
             AREA(I) = 3.14159*0.25*DIAM(I)*DIAM(I)
             DO II = 1, NC(I)
                LT =SQRT((ABS(COORD(NBS(I,II),1)-COORD(NBE(I,II),1)))**2+
         1          (ABS(COORD(NBS(I,II),2)-COORD(NBE(I,II),2)))**2)
                L(I) = L(I) + LT
             ENDDO
             LO(I) = AREA(I)*EE(I)*L(I)/(PI(I)+AREA(I)*EE(I))
          ENDDO
          READ(1,*) THET,MASST,MASS1,MUKK,MUK,VX,VY
          READ(1,*) CORX,CORY,CORI
    C
    C     CALCULATE THE HYDRODYNAMIC ADDED MASS PARALLEL AND NORMAL TO THE
    C     WALL FOR SYSTEM ONE AND TWO
    C
          CORX = 1.0 + CORX
          CORY = 1.0 + CORY
          CORI = 1.0 + CORI
          MASS2=MASST-MASS1
          THETA = THET * 3.14159/180.0
          MPAR1 = ((CORX*MASS1*CORY*MASS1) /
         1       (CORX*MASS1*DSIN(THETA)**2+CORY*MASS1*DCOS(THETA)**2))
          MPAR2 =  ((CORX*MASS2*CORY*MASS2) /
         1       (CORX*MASS2*DSIN(THETA)**2+CORY*MASS2*DCOS(THETA)**2))
          MNORM1 = ((CORX*MASS1*CORY*MASS1) /
         1       (CORY*MASS1*DSIN(THETA)**2+CORX*MASS1*DCOS(THETA)**2))
          MNORM2 = ((CORX*MASS2*CORY*MASS2) /
         1       (CORY*MASS2*DSIN(THETA)**2+CORX*MASS2*DCOS(THETA)**2))
    C
    C     INITIALIZE THE VARIABLES TO ZERO BEFORE THE INCREMENTAL ANALYSIS
    C     STARTS
    C
          DO I = 1, 1500
             PX(I) = 0.0
             PY(I) = 0.0
             RX(I) = 0.0
             RY(I) = 0.0
             P(I) =  0.0
             PP(I) = 0.0
             PY(I) = 0.0
          ENDDO
          PPT = 0.0
          DMAX = 0.0
          DSTEP = 0.001 / BLMAX
          DC(1) = 0.0
```

```
      DEC(1) = 0.0
C
C     GENERATE A VECTOR WITH THE 1,500 STEP ROTATION
C
      DO I =2, 1500
         DC(I) = DC(I-1) + DSTEP
         DEC(I) = DEC(I-1)+ 0.001
      ENDDO
C
C      CALCULATION OF EACH LASHING FORCE AND RESULTANT LASHING FORCES
C
C
      DO I = 1, NLASH
         WRITE(2,*)
         WRITE(2,105) I
         WRITE(2,*)
         WRITE(2,103)
         WRITE(2,104)
         TT = 0.0
C
C     CALCULATION OF THE LASHING LENGTH FOR EACH INCREMENT OF ROTATION

C
         JMM = 0
         JM(I) = 0
         DO J = 1,1500
            LF(I) = 0.0
            DO II = 1, NC(I)
               IF(NFLAG(I) .EQ. 1) THEN
                  LT =SQRT((ABS(COORD(NBS(I,II),1)-COORD(NBE(I,II),1))
     1            +DC(J)*COORD(NBS(I,II),2))**2+(COORD(NBS(I,II),2)-
     2            COORD(NBE(I,II),2))**2)
                  LF(I) = LF(I) + LT
                  CO(II) = DACOS(ABS(COORD(NBS(I,II),2)-
     1                  COORD(NBE(I,II),2)) / LT)
               ELSE
                  IF(COORD(NBS(I,II),1) .GE. COORD(NBE(I,II),1)) THEN
                     LT=SQRT((ABS(COORD(NBS(I,II),1)-COORD(NBE(I,II),1))
     1            -DC(J)*COORD(NBS(I,II),2))**2+(COORD(NBS(I,II),2)-
     2            COORD(NBE(I,II),2))**2)
                     LF(I) = LF(I) + LT
                     CO(II) = DACOS(ABS(COORD(NBS(I,II),2)-
     1                  COORD(NBE(I,II),2)) / LT)
                  ELSE
                     LT=SQRT((ABS(COORD(NBE(I,II),1)-COORD(NBS(I,II),1))
     1            +DC(J)*COORD(NBS(I,II),2))**2+(COORD(NBS(I,II),2)-
     2            COORD(NBE(I,II),2))**2)
                     LF(I) = LF(I) + LT
                     CO(II) = DACOS(ABS(COORD(NBS(I,II),2)-
     1                  COORD(NBE(I,II),2)) / LT)
                  ENDIF
               ENDIF
            ENDDO
C
C     CALCULATION OF THE INTERNAL FORCE IN THE LASHING AND CHECK IF THE
C     LASHING REACHES ULTIMATE STRAIN
C
            P(J) = AREA(I)*EE(I)/LO(I)*(LF(I)-LO(I))
              PP(J) = AREA(I)*EE(I)/LO(I)*DC(J)*1000.0
               EPS(J) = (LF(I)-LO(I)) / LO(I)
```

```fortran
                    IF(P(J) .GT. PULT(I)) THEN
                     IF( EPS(J) .GT. EPULT(I)) THEN
                        P(J) = 0.0
                        PP(J) = 0.0
                        JM(I) = J
                        JMM = 1 + JMM
                         ELSE
                        P(J) = PULT(I)
                        PP(J) = PULT(I)
                     ENDIF
                  ELSE
                  ENDIF
                  IF(JMM .EQ. 1) THEN
                     JMAX(I) = JM(I)
                  ELSE
                    ENDIF
                  DO IJJ =2,NLASH1
                     IF(JMAX(IJJ) .GT. JMAX(IJJ-1))THEN
                        JMAX1 = JMAX(IJJ)
                     ELSE
                           JMAX1 = JMAX(IJJ-1)
                     ENDIF
                    ENDDO
                  IF (P(J) .LT. 0.0) THEN
                     P(J) = 0.0
                  ELSE
                  ENDIF
                  SIGMA(J) = P(J) / AREA(I)
                  IF(EPS(J) .LT. 0.0) THEN
                     EPS(J) = 0.0
                  ELSE
                  ENDIF
                  PY(J) = 0.0
                  PX(J) = 0.0
C
C     CALCULATION OF THE GLOBAL COMPONENT OF THE LASHING FORCES
C
                  DO II = 1, NC(I)
                     IF (COORD(NBS(I,II),1)+DC(J)*COORD(NBS(I,II),2)
     1          .GE. COORD(NBE(I,II),1)) THEN
                        PX(J) = P(J) * DSIN(CO(II)) + PX(J)
                     ELSE
                        PX(J) = - P(J) * DSIN(CO(II)) + PX(J)
                     ENDIF
                     IF (COORD(NBS(I,II),2) .GE. COORD(NBE(I,II),2)) THEN
                        PY(J) = P(J) * DCOS(CO(II)) + PY(J)
                      ELSE
                        PY(J) = - P(J) * DCOS(CO(II)) + PY(J)
                     ENDIF
                  ENDDO
                  IF (J .GE. JMAX1) THEN
                     RX(J) = 0.0
                     RY(J) = 0.0
                  ELSE
                     RX(J) = RX(J) + PX(J)
                     RY(J) = RY(J) + PY(J)
                  ENDIF
                  DEL(J) = (LF(I)-LO(I))
                  IF(DEL(J) .LT. 0.0) THEN
                     DEL(J) = 0.0
```

```fortran
             ELSE
           ENDIF
             WRITE(2,101) J,EPS(J),SIGMA(J),DEL(J),P(J), PX(J),PY(J)
         ENDDO
       ENDDO
       MASS2 = MASST - MASS1
       THETA = THET * 3.14159/180.0
C
C     CALCULATION OF Fw, Sw, aX, aY
C
C
       FW(1) = (MPAR1*DSIN(THETA)*(RX(1)*DCOS(THETA)-RY(1)*DSIN(THETA))
      1+MPAR2*DSIN(THETA)*(RX(1)*DCOS(THETA)-RY(1)*DSIN(THETA))
      2+MUK*MPAR1*DCOS(THETA)*(RX(1)*DCOS(THETA)-RY(1)*DSIN(THETA))
      3+MUK*MPAR2*DCOS(THETA)*(RX(1)*DCOS(THETA)-RY(1)*DSIN(THETA))
      4+MUK*MPAR1*DSIN(THETA)*(RX(1)*DSIN(THETA)+RY(1)*DCOS(THETA))
      5-MPAR1*DCOS(THETA)*(RX(1)*DSIN(THETA)+RY(1)*DCOS(THETA))
      6+MUK*MPAR2*DSIN(THETA)*(RX(1)*DSIN(THETA)+RY(1)*DCOS(THETA))
      7-MPAR2*DCOS(THETA)*(RX(1)*DSIN(THETA)+RY(1)*DCOS(THETA))) /
      8(-MUK*MPAR1*DSIN(THETA)+MPAR1*COS(THETA)-MUK*MPAR2*DSIN(THETA)
      9+MPAR2*DCOS(THETA)-MUKK*MPAR2*DSIN(THETA)
      1-MUK*MUKK*MPAR2*DCOS(THETA))
       IF( FW(1) .LE. 0.0) THEN
          FW(1) = 0.0
       ELSE
       ENDIF
       SW(1) = MUKK * FW(1)
       AX(1) = SW(1) / ((CORX*MASST*CORY*MASST) /
      1        (CORX*MASST*DSIN(THETA)**2+CORY*MASST*DCOS(THETA)**2))
       AY(1) = FW(1) / ((CORX*MASS2*CORY*MASS2) /
      1        (CORX*MASS2*DCOS(THETA)**2+CORY*MASS2*DSIN(THETA)**2))
       DO I = 2, 1500
          IF (FW(I-1) .LE. 0.0) THEN
             FW(I) =  0.0
             SW(I) =  0.0
             AX(I) =  0.0
             AY(I) =  0.0
          ELSE
             FW(I)=(MPAR1*DSIN(THETA)*(RX(I)*DCOS(THETA)
      1-RY(I)*DSIN(THETA))+MPAR2*DSIN(THETA)*(RX(I)*DCOS(THETA)
      2-RY(I)*DSIN(THETA))+MUK*MPAR1*DCOS(THETA)*(RX(I)*DCOS(THETA)
      3-RY(I)*DSIN(THETA))+MUK*MPAR2*DCOS(THETA)*(RX(I)*DCOS(THETA)
      4-RY(I)*DSIN(THETA))+MUK*MPAR1*DSIN(THETA)*(RX(I)*DSIN(THETA)
      5+RY(I)*DCOS(THETA))-MPAR1*DCOS(THETA)*(RX(I)*DSIN(THETA)+RY(I)
      6*DCOS(THETA))+MUK*MPAR2*DSIN(THETA)*(RX(I)*DSIN(THETA)
      7+RY(I)*DCOS(THETA))-MPAR2*DCOS(THETA)*(RX(I)*DSIN(THETA)
      8+RY(I)*DCOS(THETA))) / (-MUK*MPAR1*DSIN(THETA)+MPAR1*COS(THETA)
      9-MUK*MPAR2*DSIN(THETA)+MPAR2*DCOS(THETA)-MUKK*MPAR2*DSIN(THETA)
      1-MUK*MUKK*MPAR2*DCOS(THETA))
          IF (FW(I) .LE. 0.0) THEN
             FW(I) = 0.0
          ELSE
          ENDIF
          SW(I) = MUKK * FW(I)
          AX(I) = SW(I) / ((CORX*MASST*CORY*MASST) /
      1        (CORX*MASST*DSIN(THETA)**2+CORY*MASST*DCOS(THETA)**2))
          AY(I) = FW(I) / ((CORX*MASS2*CORY*MASS2) /
      1        (CORX*MASS2*DCOS(THETA)**2+CORY*MASS2*DSIN(THETA)**2))
          ENDIF
       ENDDO
C
```

```
C     CALCULATION OF Fw DUE TO SYSTEM ONE CONTRIBUTION USING THE
C     EMPIRICAL CORRELATION
C
      FWEC = 0.435*MASS1*(VX*DSIN(THETA)+VY*DCOS(THETA))
      DO I = 1, 1500
         IF (FW(I) .LE. 0.0) THEN
            FWT(I) = 0.0
         ELSE
            FWT(I) = FW(I) + FWEC
         ENDIF
      ENDDO
C
C     PRINT OF RESULTS
C
      WRITE(2,*)
      WRITE(2,*)
      WRITE(2,106)
      WRITE(2,100)
      WRITE(2,*)
      DO I = 1,1500
         WRITE(2,102) I,DC(I),RX(I),RY(I),FW(I),SW(I),AX(I),AY(I),FWEC,
     1FWT(I)
      ENDDO
100   FORMAT(19X,'TOTAL RESULTANT FORCE',/,11X,'ROT.',5X,'LOCAL X',5X,
     1'LOCAL Y',7X,'Fw',11X,'Sw',12X,'aX',10X,'aY',7X,'Fw',7X,'TOTAL Fw'
     2,/,71X,'Systems',5X,'System',3X,'Empirical',
     3/,71X,'1 and 2',7X,'2',5X,'Correlation')
 101  FORMAT(I4,E12.4,F12.4,E12.4,3F12.4)

 102  FORMAT(I4,E12.4,8F12.4)
 103  FORMAT(9X,'NORMAL',6X,'NORMAL',18X,'INTERNAL',6X,
     1'RESULTANT FORCE')
 104  FORMAT(9X,'STRAIN      STRESS      ELONG.        FORCE',7X,
     1'LOCAL X     LOCAL Y',//)
 105  FORMAT(29X,'LASHING NUMBER',I4)
 106  FORMAT(//,90('='),//,29X,'FINAL RESULTS',//,90('='),//)
      RETURN
      END
```

B.2 Worksheet to Calculate the F_w Expression for the Longitudinal Failure Mechanism

This Maple™ sheet develops the formulation of longitudinal failure mechanism for a barge train in variable form.
Developed by Dr. Jose Ramon Arroyo (University of Puerto Rico, Mayaguez Campus)
Research into a Numerical Method for Computing Barge Impact Based on Limit State for the Lashings Between Barges
Principal Investigator: Dr. Robert Ebeling (U.S. Army Engineer Research and Development Center)

This model considers the following:

a. High approach angle < 90 degrees. If the approach angle is 90 degrees, then the coefficient of friction for steel-steel at the point of impact (*mukk*) must be zero. The model considers the eccentricity between the line of action of F_w and the longitudinal axis over the mass center.

b. The input data are the approach angle and the resultant force in the local x-axis *Rs* and the resultant force in the local y-axis *Rn*.

c. The acceleration of the impacted barge system is zero at the instant of collision.

d. The coefficient of friction between barge systems (steel-steel) is the kinetic coefficient of friction.

e. It considers one failure plane.

f. This worksheet can calculate only one combination of forces in the lashing. The whole event will be calculated using the FORTRAN and Visual Basic Program.

```
># Program
> restart:
> with(linalg):
```
Warning, the protected names norm and trace have been redefined and unprotected.

Establish the equation of motion in the global X-direction of the system of barges that impact the wall.

```
>EQN1:=muk*FNC*cos(theta)+RsX+RnX-FNC*sin(theta)-
SW+m1X*aX;
```
$EQN1 := muk\ FNC\ \cos(\theta) + RsX + RnX - FNC\ \sin(\theta) - SW + m1X\ aX$

Establish the equation of motion in the global Y-direction of the system of barges that impact the wall

```
> EQN2:=FNC*cos(theta)+muk*FNC*sin(theta)-FW+RsY-
RnY;
```
$EQN2 := FNC\ \cos(\theta) + muk\ FNC\ \sin(\theta) - FW + RsY - RnY$

Establish the sum of moments of the system of barges that impact the wall

```
> EQN3:=FNC*(x1-xG1)+M-
(FW*sin(theta)+SW*cos(theta))*(y1-y2)-MRfn-
It1*alpha+m1X*aX*cos(theta)*(yG1-y2)-
m1X*aX*sin(theta)*(x1-xG1);
```
$EQN3 := FNC\ (x1 - xG1) + M - (FW\ \sin(\theta) + SW\ \cos(\theta))\ (y1 - y2) - MRfn - It1\ \alpha + m1X\ aX\ \cos(\theta)\ (yG1 - y2)$
$\quad - m1X\ aX\ \sin(\theta)\ (x1 - xG1)$

Establish the equation of motion in the global X-direction of the system of barges that do not impact the wall

```
> EQN4:=-muk*FNC*cos(theta)-RsX-
RnX+FNC*sin(theta)+m2X*aX;
```
$EQN4 := -muk\ FNC\ \cos(\theta) - RsX - RnX + FNC\ \sin(\theta) + m2X\ aX$

Establish the equation of motion in the global Y-direction of the system of barges that do not impact the wall

```
> EQN5:=-FNC*cos(theta)-muk*FNC*sin(theta)-
RsY+RnY+m2Y*aY;
```
$EQN5 := -FNC\ \cos(\theta) - muk\ FNC\ \sin(\theta) - RsY + RnY + m2Y\ aY$

Establish the sum of moments of the system of barges that do not impact the wall

```
> EQN6:=-FNC*(xG2-x2)-M+MRfn-It2*alpha-
(m2X*aX*cos(theta)+m2Y*aY*sin(theta))*(y2-
yG2)+(m2Y*aY*cos(theta)-m2X*aX*sin(theta))*(x2-
xG2);
```
$EQN6 := -FNC\ (xG2 - x2) - M + MRfn - It2\ \alpha - (m2X\ aX\ \cos(\theta) + m2Y\ aY\ \sin(\theta))\ (y2 - yG2)$
$\qquad + (m2Y\ aY\ \cos(\theta) - m2X\ aX\ \sin(\theta))\ (x2 - xG2)$

Establish an additional equation of coefficient of friction definition

```
> EQN7:=SW-mukk*FW;
```
$EQN7 := SW - mukk\ FW$

Now the program solves for the seven unknowns using these seven equations.

```
> SOL:=solve({EQN1,EQN2,EQN3,EQN4,EQN5,EQN6,EQN7},
{FW,SW,FNC,M,alpha,aX,aY}):assign(SOL):
```

Now the program presents using variables the resultant expression for Fw = force normal to the wall, Sw = shear force at the wall, aX = acceleration in global X direction, aY = acceleration in Y global direction in the most simplified form.

```
> FW:=simplify(FW); SW:=simplify(SW);
aX:=simplify(aX); aY:=simplify(aY); FNC:=FNC;
```
$FW := -\ (\cos(\theta)\ m1X\ RsX + \cos(\theta)\ m1X\ RnX + \cos(\theta)\ RsX\ m2X + \cos(\theta)\ RnX\ m2X + muk\ \sin(\theta)\ m1X\ RsX + muk\ \sin(\theta)\ m1X\ RnX$
$\qquad + muk\ \sin(\theta)\ RsX\ m2X + muk\ \sin(\theta)\ RnX\ m2X - RsY\ m1X\ muk\ \cos(\theta) + RsY\ m1X\ \sin(\theta) - RsY\ muk\ \cos(\theta)\ m2X$
$\qquad + RsY\ \sin(\theta)\ m2X + RnY\ m1X\ muk\ \cos(\theta) - RnY\ m1X\ \sin(\theta) + RnY\ muk\ \cos(\theta)\ m2X - RnY\ \sin(\theta)\ m2X\ )/($
$\qquad m1X\ muk\ \cos(\theta) - m1X\ \sin(\theta) + muk\ \cos(\theta)\ m2X - \sin(\theta)\ m2X - mukk\ \cos(\theta)\ m2X - mukk\ muk\ \sin(\theta)\ m2X\ )$

$SW := -\ mukk\ (\cos(\theta)\ m1X\ RsX + \cos(\theta)\ m1X\ RnX + \cos(\theta)\ RsX\ m2X + \cos(\theta)\ RnX\ m2X + muk\ \sin(\theta)\ m1X\ RsX$
$\qquad + muk\ \sin(\theta)\ m1X\ RnX + muk\ \sin(\theta)\ RsX\ m2X + muk\ \sin(\theta)\ RnX\ m2X - RsY\ m1X\ muk\ \cos(\theta) + RsY\ m1X\ \sin(\theta)$
$\qquad - RsY\ muk\ \cos(\theta)\ m2X + RsY\ \sin(\theta)\ m2X + RnY\ m1X\ muk\ \cos(\theta) - RnY\ m1X\ \sin(\theta) + RnY\ muk\ \cos(\theta)\ m2X - RnY\ \sin(\theta)\ m2X$
$\qquad)/(m1X\ muk\ \cos(\theta) - m1X\ \sin(\theta) + muk\ \cos(\theta)\ m2X - \sin(\theta)\ m2X - mukk\ \cos(\theta)\ m2X - mukk\ muk\ \sin(\theta)\ m2X\ )$

$aX := -\, mukk\ ($

$\quad -muk\ \cos(\theta)\ RsY + muk\ \cos(\theta)\ RnY + RsX\ \cos(\theta) + RsX\ muk\ \sin(\theta) + RnX\ \cos(\theta) + RnX\ muk\ \sin(\theta) + \sin(\theta)\ RsY - \sin(\theta)\ RnY)$

$\quad /(m1X\ muk\ \cos(\theta) - m1X\ \sin(\theta) + muk\ \cos(\theta)\ m2X - \sin(\theta)\ m2X - mukk\ \cos(\theta)\ m2X - mukk\ muk\ \sin(\theta)\ m2X\,)$

$aY := -\,(\cos(\theta)\ m1X\ RsX + \cos(\theta)\ m1X\ RnX + \cos(\theta)\ RsX\ m2X + \cos(\theta)\ RnX\ m2X + muk\ \sin(\theta)\ m1X\ RsX + muk\ \sin(\theta)\ m1X\ RnX$

$\quad + muk\ \sin(\theta)\ RsX\ m2X + muk\ \sin(\theta)\ RnX\ m2X - RsY\ m1X\ muk\ \cos(\theta) + RsY\ m1X\ \sin(\theta) - RsY\ muk\ \cos(\theta)\ m2X$

$\quad + RsY\ \sin(\theta)\ m2X + RnY\ m1X\ muk\ \cos(\theta) - RnY\ m1X\ \sin(\theta) + RnY\ muk\ \cos(\theta)\ m2X - RnY\ \sin(\theta)\ m2X\,)/($

$\quad (m1X\ muk\ \cos(\theta) - m1X\ \sin(\theta) + muk\ \cos(\theta)\ m2X - \sin(\theta)\ m2X - mukk\ \cos(\theta)\ m2X - mukk\ muk\ \sin(\theta)\ m2X\,)\ m2Y)$

$$FNC := -\,\frac{m1X\ RsX + m1X\ RnX + RsX\ m2X + RnX\ m2X - mukk\ RsY\ m2X + mukk\ RnY\ m2X}{m1X\ muk\ \cos(\theta) - m1X\ \sin(\theta) + muk\ \cos(\theta)\ m2X - \sin(\theta)\ m2X - mukk\ \cos(\theta)\ m2X - mukk\ muk\ \sin(\theta)\ m2X}$$

Data that use the program to calculate the forces.

PARAMETERS: Consistent units (units used in the example: kips, ft/sec^2, kip*sec^2 / ft)

$\quad\quad theta$ = approach angle in degrees

$\quad\quad muk$ = kinetic coefficient of friction between barges

$\quad\quad mukk$ = dynamic coefficient of friction of steel and steel between the barge that impacts the wall and the wall

$\quad\quad m1X$ = mass of barge system one (system that impact the wall) including the hydrodynamic added mass (Mpar1)

$\quad\quad m2X$ = mass of barge system two (system that does not impact the wall) including the hydrodynamic added mass (Mpar2)

$\quad\quad m1Y$ = mass of barge system one (system that impacts the wall) including the hydrodynamic added mass (Mnorm1)

$\quad\quad m2Y$ = mass of barge system two (system that does not impact the wall) including the hydrodynamic added mass (Mnorm2)

$\quad\quad Rs$ = Resultant force along failure plane (local x-axis)

$\quad\quad Rn$ = Resultant force perpendicular to the failure plane (local y-axis)

```
> theta:= 85.0;
```
$\theta := 85.0$

```
> muk:= 0.4;
```
$muk := .4$

```
> m1X:=907;
```
$m1X := 907$

```
> m1Y:=683.27;
```
$m1Y := 683.27$

```
> m2X:=907;
```
$m2X := 907$

```
> m2Y:=683.27;
```
$m2Y := 683.27$

```
> Rs:=1146;
```
$Rs := 1146$

```
> Rn:=1335;
```
$Rn := 1335$

Initial calculation for data transformation

```
> theta:=theta*(3.14159/180);RsY:=Rs*sin(theta);
RnY:=Rn*cos(theta);RsX:=Rs*cos(theta);RnX:=Rn*sin
(theta);
```
$\theta := 1.483528611$

$RsY := 1141.638999$

$RnY := 116.3545832$

$RsX := 99.88191188$

$RnX := 1329.919776$

Result of program in term of muk = Kinetic coefficient of friction between steel and steel.

```
> FW:=FW;SW:=SW;aX:=aX;aY:=aY;
```

$$FW := -.3047520002 \ 10^7 \ \frac{1}{-1743.855871 - 440.4707879 \ mukk}$$

$$SW := -.3047520002 \ 10^7 \ \frac{mukk}{-1743.855871 - 440.4707879 \ mukk}$$

$$aX := -1680.000000 \ \frac{mukk}{-1743.855871 - 440.4707879 \ mukk}$$

$$aY := -4460.198753 \ \frac{1}{-1743.855871 - 440.4707879 \ mukk}$$

Plot of *Fw* and *Sw* vs kinetic coefficient of friction.

```
> plot([FW,SW],mukk=0..1,legend=["FW","SW"]);
```

```
> mukk:=0.2;FW:=FW;
```
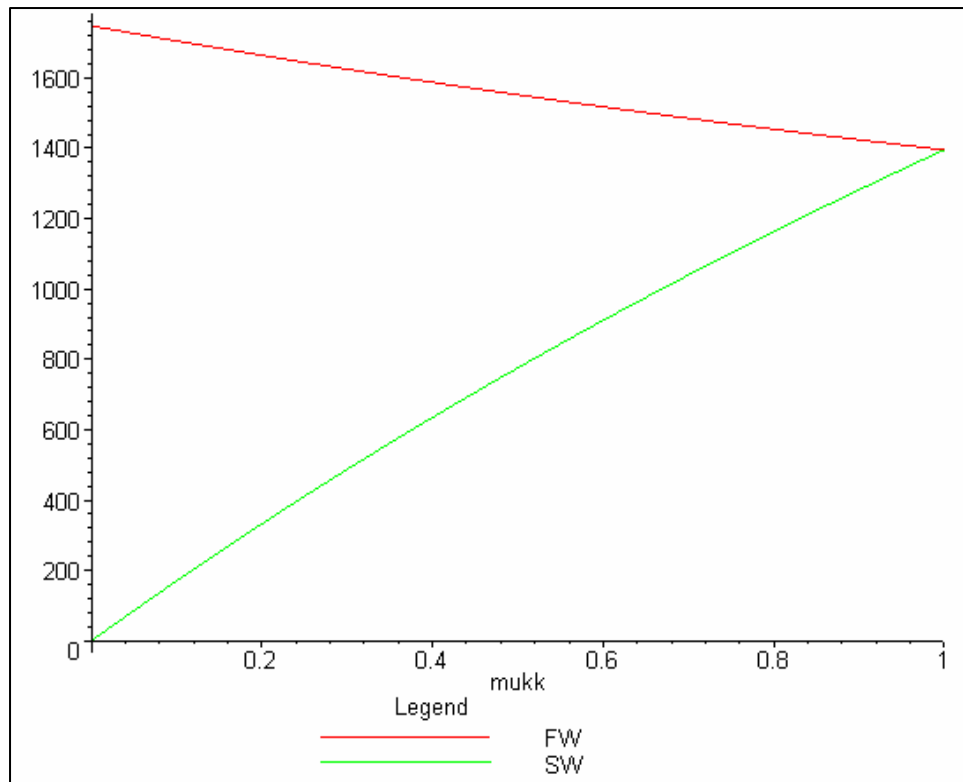
mukk := .2

FW := 1663.538827

```
>
```

B.3 Worksheet to Calculate the F_w Expression for the Longitudinal Failure Mechanism (Direct Impact with Eccentricity)

This Maple™ sheet develops the formulation of longitudinal failure mechanism for a barge train in variable form.
This is a special case with eccentricity.
Developed by Dr. Jose Ramon Arroyo (University of Puerto Rico, Mayaguez Campus)
Research into a Numerical Method for Computing Barge Impact Based on Limit State for the Lashings Between Barges
Principal Investigator: Dr. Robert Ebeling (U.S. Army Engineer Research and Development Center)

This model considers the following:

a. This model is for a special case of the longitudinal failure mechanism model, for barge impact at approach angle of 90 degrees.

b. The input data are the approach angle and the resultant force in the local x-axis *Rs* and the resultant y-axis *Rn*.

c. The acceleration of the impacted barges is zero at the instant of collision.

d. The coefficient of friction between barge systems (steel-steel) is the kinetic coefficient of friction.

e. It considers one failure plane.

f. This worksheet can calculate only one combination of forces in the lashing. The whole event will be calculated using the FORTRAN and Visual Basic Program.

```
> #Program
> restart:
> with(linalg):
```

Warning, the protected names norm and trace have been redefined and unprotected

Establish the equation of motion in the global X-direction of the system of barges that impact the wall

```
> EQN1:=-FNC+Rn;
```

$EQN1 := -FNC + Rn$

Establish the equation of motion in the global Y-direction of the system of barges that impact the wall

```
> EQN2:=muk*FNC-FW+Rs;
```

$EQN2 := muk\ FNC - FW + Rs$

Establish the sum of moments of the system of barges that impact the wall

```
> EQN3:=-FW*(y1-yG1)-Rs*(yG1-y2)+MRfn+M-It1*alpha;
```

$EQN3 := -FW\ (y1 - yG1) - Rs\ (yG1 - y2) + MRfn + M - It1\ \alpha$

Establish the equation of motion in the global Y-direction of the system of barges that do not impact the wall

```
> EQN4:=-muk*FNC-Rs+m2Y*aY;
```

$EQN4 := -muk\ FNC - Rs + m2Y\ aY$

Establish the sum of moments of the system of barges that do not impact the wall

```
> EQN5:=-Rs*(y2-yG2)-MRfn-M-It2*alpha;
```

$EQN5 := -Rs\,(y2 - yG2) - MRfn - M - It2\,\alpha$

Now the program solves for the five unknowns using these five equations.

```
> SOL:=solve({EQN1,EQN2,EQN3,EQN4,EQN5},
{FW,FNC,M,alpha,aY}):assign(SOL):
```

Now the program presents in variable form the result of *Fw* = force normal to the wall and *aY* = acceleration in *Y* global direction in the most simplified form.

```
> FW:=simplify(FW);aY:=simplify(aY);
```

$FW := muk\,Rn + Rs$

$aY := \dfrac{muk\,Rn + Rs}{m2Y}$

Data used by the program to calculate the forces.
PARAMETERS: Consistent units (units used in the example: kips, ft/sec^2, kip*sec^2 / ft)

- *theta* = approach angle in degrees (in this special case this value will be always 90 degrees (head-on collision))
- *muk* = Kinetic coefficient of friction between barges
- *m2Y* = mass of barge system two (system that does not impact the wall) (Mnorm2)
- *Rs* = Resultant force along failure plane (local x-axis)
- *Rn* = Resultant force perpendicular to the failure plane (local y-axis)

```
> theta:= 90.0;
```

$\theta := 90.0$

```
> muk:=0.4;
```

$muk := .4$

```
> m2Y:=909.3;
```

$m2Y := 909.3$

```
> Rs:=1146;
```

$Rs := 1146$

```
> Rn:=1335;
```

$Rn := 1335$

Numerical result of *Fw* and *aY* for the example of impact with eccentricity.

```
> FW:=FW;aY:=aY;
```

FW := 1680.0

aY := 1.847575058

B.4 Worksheet to Calculate the *F_w* Expression for the Longitudinal Failure Mechanism (Direct Impact without Eccentricity)

This Maple™ sheet develops the formulation of longitudinal failure mechanism for a barge train in variable form.
This is a special case without eccentricity.
Developed by Dr. Jose Ramon Arroyo (University of Puerto Rico, Mayaguez Campus)
Research into a Numerical Method for Computing Barge Impact Based on Limit State for the Lashings Between Barges
Principal Investigator: Dr. Robert Ebeling (U.S. Army Engineer Research and Development Center)

This model considers the following:

a. This model is for a special case of the longitudinal failure mechanism model, for barge impact at approach angle of 90 degrees. Then, the coefficient of friction for steel-steel at the point of impact (*mukk*) must be zero. The model considers the special case with no eccentricity between the lines of action of the *Fw* and the longitudinal axis over the mass center.

b. The input data are the approach angle and the resultant force in the local x-axis *Rs* and the resultant y-axis *Rn*. Each of these forces is divided in two, in left and right forces in respect to the barge system where *Rsl* = resultant force in local x-axis of left side of barge train; *Rsr* = resultant force in local x-axis of right side of barge train; *Rnl* = resultant force in local y-axis of left side of barge train; *Rnr* = resultant force in local y-axis of right side of barge train.

c. The acceleration of the impacted barges is zero at the instant of collision.

d. The coefficient of friction between barge systems (steel-steel) is the kinetic coefficient of friction.

e. It considers two failure planes.

f. This worksheet can calculate only one combination of forces in the lashings. The whole event will be calculated using the FORTRAN and Visual Basic Program.

```
> #Program
> restart:
> with(linalg):
```

Warning, the protected names norm and trace have been redefined and unprotected

Data that use the program to calculate the forces.
PARAMETERS: Consistent units (Units used in the example: kips, ft/sec^2, kip*sec^2 / ft)

theta = approch angle in degrees
muk = kinetic coefficient of friction between steel and steel in the barges
Rnr = resultant normal force of the lashing in the right plane of failure
Rsr = resultant parallel force of the lashing in the right plane of failure
Rnl = resultant normal force of the lashing in the left plane of failure
Rnl = resultant parallel force of the lashing in the left plane of failure

```
> theta:=90;
```
$\theta := 90$

```
> muk:=0.4;
```
$muk := .4$

```
> Rnr:=1335;
```
$Rnr := 1335$

```
> Rnl:=1335;
```
$Rnl := 1335$

```
> Rsr:=1146;
```
$Rsr := 1146$

```
> Rsl:=1146;
```
$Rsl := 1146$

```
> theta:=90*3.14159/180;
```
$\theta := 1.570795000$

Result of *Fw* and *Sw* in terms of *muk* = kinetic coefficient of friction between steel and steel

```
> FW:=Rsr+Rsl+muk*Rnr+muk*Rnl;
```
$FW := 3360.0$

B.5 Worksheet to Calculate the F_w Expression for the Transverse Failure Mechanism

This Maple™ sheet develops the formulation of transverse failure mechanism of a barge train in variable form.
Developed by Dr. Jose Ramon Arroyo (University of Puerto Rico, Mayaguez Campus)
Research into a Numerical Method for Computing Barge Impact Based on Limit State for the Lashings Between Barges
Principal Investigator: Dr. Robert Ebeling (U.S. Army Engineer Research and Development Center)

This model considers the following:

a. The failure that occurs is in the transverse direction.

b. The input data are the approach angle and the resultant force in the local x-axis *Rn* and the resultant y-axis *Rs*.

c. The acceleration of the impacted barges is zero at the instant of collision.

d. The coefficient of friction between barge systems (steel-steel) is the kinetic coefficient of friction.

e. It considers one failure plane.

f. This worksheet can calculate only one combination of forces in the lashing. The whole event will be calculated using FORTRAN and Visual Basic.

```
> #Program
> restart:
> with(linalg):
```
Warning, the protected names norm and trace have been redefined and unprotected

Establish the equation of motion in the global X-direction of the system of barges that impact the wall

```
> EQN1:=-muk*FNC*sin(theta)+RsX-
RnX+FNC*cos(theta)-SW+m1X*aX;
```
$EQN1 := -muk\ FNC\ \sin(\theta) + RsX - RnX + FNC\ \cos(\theta) - SW + m1X\ aX$

Establish the equation of motion in the global Y-direction of the system of barges that impact the wall

```
> EQN2:=FNC*sin(theta)+muk*FNC*cos(theta)-FW-RsY-
RnY;
```
$EQN2 := FNC\ \sin(\theta) + muk\ FNC\ \cos(\theta) - FW - RsY - RnY$

Establish the sum of moments of the system of barges that impact the wall

```
> EQN3:=-FNC*(y1-yG1)+M+muk*FNC*a+MRfn-MRfs-
It1*alpha+(m1X*aX*cos(theta))*(y1-
yG1)+(m1X*aX*sin(theta))*a/2;
```

$EQN3 := -FNC\,(y1 - yG1) + M + muk\,FNC\,a + MRfn - MRfs - It1\,\alpha + m1X\,aX\,\cos(\theta)\,(y1 - yG1) + \frac{1}{2}\,m1X\,aX\,\sin(\theta)\,a$

Establish the equation of motion in the global X-direction of the system of barges that do not impact the wall

```
> EQN4:=muk*FNC*sin(theta)-RsX+RnX-
FNC*cos(theta)+m2X*aX;
```

$EQN4 := muk\,FNC\,\sin(\theta) - RsX + RnX - FNC\,\cos(\theta) + m2X\,aX$

Establish the equation of motion in the global Y-direction of the system of barges that do not impact the wall

```
> EQN5:=-FNC*sin(theta)-
muk*FNC*cos(theta)+RsY+RnY+m2Y*aY;
```

$EQN5 := -FNC\,\sin(\theta) - muk\,FNC\,\cos(\theta) + RsY + RnY + m2Y\,aY$

Establish the sum of moments of the system of barges that do not impact the wall

```
> EQN6:=muk*FNC*(c-xG2)-M+MRfn-MRfs-It2*alpha;
```

$EQN6 := muk\,FNC\,(c - xG2) - M + MRfn - MRfs - It2\,\alpha$

Establish an additional equation of coefficient of friction definition

```
> EQN7:=SW-mukk*FW;
```

$EQN7 := SW - mukk\,FW$

Now the program solves for the seven unknowns using these seven equations:

```
> SOL:=solve({EQN1,EQN2,EQN3,EQN4,EQN5,EQN6,EQN7},
{FW,SW,FNC,M,alpha,aX,aY}):assign(SOL):
```

Now the program presents in variable form the result of *Fw* = force normal to the wall, *Sw* = shear force at the wall, *aX* = acceleration in global X-direction in the most simplified form.

```
> FW:=simplify(FW);SW:=SW;aX:=aX;aY:=aY;
```

$FW := -(-\sin(\theta)\,m1X\,RsX + \sin(\theta)\,m1X\,RnX - \sin(\theta)\,RsX\,m2X + \sin(\theta)\,RnX\,m2X - muk\,\cos(\theta)\,m1X\,RsX + muk\,\cos(\theta)\,m1X\,RnX$
$- muk\,\cos(\theta)\,RsX\,m2X + muk\,\cos(\theta)\,RnX\,m2X + RsY\,m1X\,muk\,\sin(\theta) - RsY\,m1X\,\cos(\theta) + RsY\,muk\,\sin(\theta)\,m2X$
$- RsY\,\cos(\theta)\,m2X + RnY\,m1X\,muk\,\sin(\theta) - RnY\,m1X\,\cos(\theta) + RnY\,muk\,\sin(\theta)\,m2X - RnY\,\cos(\theta)\,m2X)/($
$m1X\,muk\,\sin(\theta) - m1X\,\cos(\theta) + muk\,\sin(\theta)\,m2X - \cos(\theta)\,m2X + mukk\,\sin(\theta)\,m2X + mukk\,muk\,\cos(\theta)\,m2X)$

$$SW := -\,mukk\,(-\sin(\theta)\,m1X\,RsX + \sin(\theta)\,m1X\,RnX - \sin(\theta)\,RsX\,m2X + \sin(\theta)\,RnX\,m2X - muk\,\cos(\theta)\,m1X\,RsX$$
$$+ \,muk\,\cos(\theta)\,m1X\,RnX - muk\,\cos(\theta)\,RsX\,m2X + muk\,\cos(\theta)\,RnX\,m2X + RsY\,m1X\,muk\,\sin(\theta) - RsY\,m1X\,\cos(\theta)$$
$$+ \,RsY\,muk\,\sin(\theta)\,m2X - RsY\cos(\theta)\,m2X + RnY\,m1X\,muk\,\sin(\theta) - RnY\,m1X\,\cos(\theta) + RnY\,muk\,\sin(\theta)\,m2X - RnY\cos(\theta)\,m2X$$
$$)/(m1X\,muk\,\sin(\theta) - m1X\,\cos(\theta) + muk\,\sin(\theta)\,m2X - \cos(\theta)\,m2X + mukk\,\sin(\theta)\,m2X + mukk\,muk\,\cos(\theta)\,m2X)$$

$$aX := -\,mukk\,($$
$$-RsX\,\sin(\theta) + RnX\,\sin(\theta) - RsX\,muk\,\cos(\theta) + RnX\,muk\,\cos(\theta) + muk\,\sin(\theta)\,RsY - \cos(\theta)\,RsY + muk\,\sin(\theta)\,RnY - \cos(\theta)\,RnY$$
$$/(m1X\,muk\,\sin(\theta) - m1X\,\cos(\theta) + muk\,\sin(\theta)\,m2X - \cos(\theta)\,m2X + mukk\,\sin(\theta)\,m2X + mukk\,muk\,\cos(\theta)\,m2X)$$

$$aY := -\,(-\sin(\theta)\,m1X\,RsX + \sin(\theta)\,m1X\,RnX - \sin(\theta)\,RsX\,m2X + \sin(\theta)\,RnX\,m2X - muk\,\cos(\theta)\,m1X\,RsX + muk\,\cos(\theta)\,m1X\,RnX$$
$$-\,muk\,\cos(\theta)\,RsX\,m2X + muk\,\cos(\theta)\,RnX\,m2X + RsY\,m1X\,muk\,\sin(\theta) - RsY\,m1X\,\cos(\theta) + RsY\,muk\,\sin(\theta)\,m2X$$
$$-\,RsY\cos(\theta)\,m2X + RnY\,m1X\,muk\,\sin(\theta) - RnY\,m1X\,\cos(\theta) + RnY\,muk\,\sin(\theta)\,m2X - RnY\cos(\theta)\,m2X)/($$
$$(m1X\,muk\,\sin(\theta) - m1X\,\cos(\theta) + muk\,\sin(\theta)\,m2X - \cos(\theta)\,m2X + mukk\,\sin(\theta)\,m2X + mukk\,muk\,\cos(\theta)\,m2X)\,m2Y)$$

Data used by the program to calculate the forces:
PARAMETERS: Consistent units (units used in the example: kips, ft/sec^2, kip*sec^2 / ft)

theta = approach angle in degrees
muk = steel-steel kinetic coefficient of friction between barges
mukk = steel-steel kinetic coefficient of friction between the corner barge and the wall
m1X = mass of barge system one (system that impacts the wall) including the hydrodynamic added mass (Mpar1)
m2X = mass of barge system two (system that does not impact the wall) including the hydrodynamic added mass (Mpar2)
m1Y = mass of barge system one (system that impacts the wall) including the hydrodynamic added mass (Mnorm1)
m2Y = mass of barge system two (system that does not impact the wall) including the hydrodynamic added mass (Mnorm2)
Rs = Resultant force along failure plane (local y-axis)
Rn = Resultant force perpendicular to the failure plane (local x-axis)

```
> theta:=20;
```
$\theta := 20$

```
> muk:=0.4;
```
$muk := .4$

```
> m1X:=351.25;
```
$m1X := 351.25$

```
> m1Y:=437.58;
```
$m1Y := 437.58$

```
> m2X:=1053.77;
```
$m2X := 1053.77$

```
> m2Y:=1312.76;
```

$m2Y := 1312.76$

```
> Rs:=100;
```

$Rs := 100$

```
> Rn:=1500;
```

$Rn := 1500$

Initial calculation for data transformation

```
> theta:=theta*3.14159/180;RsY:=Rs*cos(theta);
RnY:=Rn*sin(theta);RsX:=Rs*sin(theta);
RnX:=Rn*cos(theta);
```

$\theta := .3490655556$

$RsY := 93.96927216$

$RnY := 513.0297994$

$RsX := 34.20198663$

$RnX := 1409.539082$

Result of program in terms of *mukk* = Kinetic coefficient of friction between steel and steel of the barge and the wall.

```
> FW:=FW;SW:=SW;aX:=aX;aY:=aY;
```

$$FW := -702509.9984 \, \frac{1}{-1128.069167 + 756.4982742 \, mukk}$$

$$SW := -702509.9984 \, \frac{mukk}{-1128.069167 + 756.4982742 \, mukk}$$

$$aX := -499.9999997 \, \frac{mukk}{-1128.069167 + 756.4982742 \, mukk}$$

$$aY := -535.1397044 \, \frac{1}{-1128.069167 + 756.4982742 \, mukk}$$

Plot of Fw and Sw vs kinetic coefficient of friction.

```
> plot([FW,SW],mukk=0..1.0, legend=["Fw","Sw"]);
```

```
> mukk:=0.2;FW:=FW;
```

mukk := .2
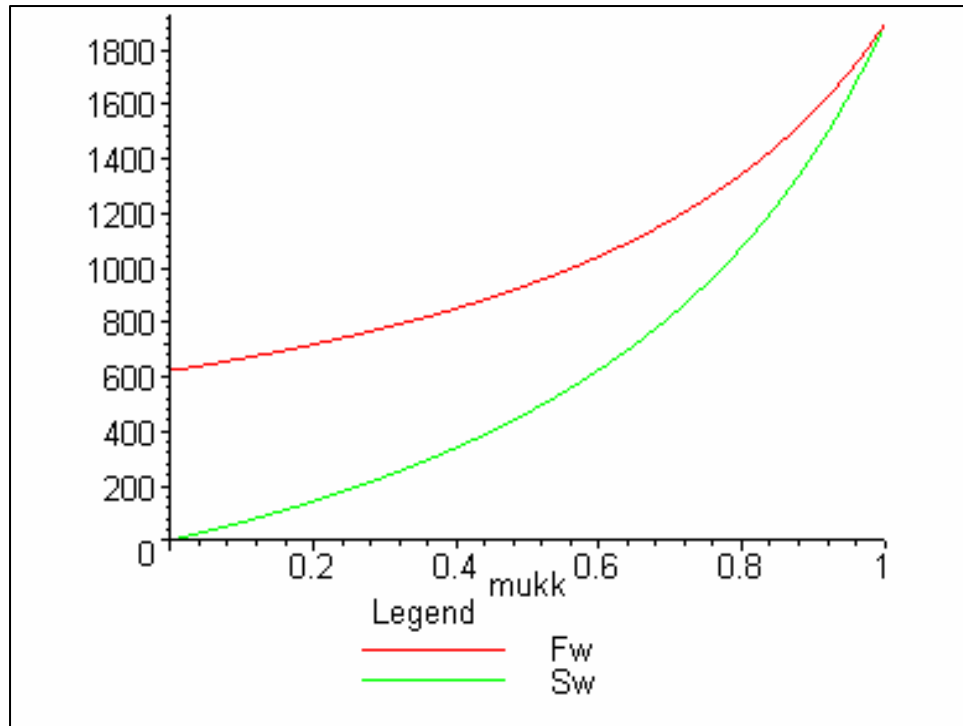
FW := 719.2177782

B.6 Worksheet to Calculate the F_w Expression for the Corner Failure Mechanism

This Maple™ sheet develops the formulation of corner failure mechanism of a barge train in variable form.
Developed by Dr. Jose Ramon Arroyo (University of Puerto Rico, Mayaguez Campus)
Research into a Numerical Method for Computing Barge Impact Based on Limit State for the Lashings Between Barges
Principal Investigator: Dr. Robert Ebeling (U.S. Army Engineer Research and Development Center)

This model considers the following:

a. The failure that occurs is in the transverse direction and the relative motion between barges of the system in contact with the wall is allowed.

b. The input data are the approach angle and the resultant force in the local x-axis *Rn* and the resultant y-axis *Rs*.

c. The acceleration of the impacted barges is zero at the instant of collision.

> d. The coefficient of friction between barge systems (steel-steel) is the kinetic coefficient of friction.

> e. One failure plane in an L shape is considered.

> f. This worksheet can calculate only one combination of forces in the lashing. The whole event will be calculated using FORTRAN and Visual Basic.

```
> #Program
> restart:
> with(linalg):
```
Warning, the protected names norm and trace have been redefined and unprotected

Establish the equation of motion in the global X-direction of the system of barges that impact the wall

```
> EQN1:=-muk*FNC*sin(theta)+RsX-
RnX+FNC*cos(theta)-SW+m1X*aX;
```
$EQN1 := -muk\ FNC\ \sin(\theta) + RsX - RnX + FNC\ \cos(\theta) - SW + m1X\ aX$

Establish the equation of motion in the global Y-direction of the system of barges that impact the wall

```
> EQN2:=FNC*sin(theta)+muk*FNC*cos(theta)-FW-RsY-
RnY;
```
$EQN2 := FNC\ \sin(\theta) + muk\ FNC\ \cos(\theta) - FW - RsY - RnY$

Establish the sum of moments of the system of barges that impact the wall

```
> EQN3:=-FNC*(y1-yG1)+M+muk*FNC*a+MRfn-MRfs-
It1*alpha+(m1X*aX*cos(theta))*(y1-
yG1)+(m1X*aX*sin(theta))*a/2;
```
$EQN3 := -FNC\ (y1 - yG1) + M + muk\ FNC\ a + MRfn - MRfs - It1\ \alpha + m1X\ aX\ \cos(\theta)\ (y1 - yG1) + \frac{1}{2}\ m1X\ aX\ \sin(\theta)\ a$

Establish the equation of motion in the global X-direction of the system of barges that do not impact the wall

```
> EQN4:=muk*FNC*sin(theta)-RsX+RnX-
FNC*cos(theta)+m2X*aX;
```
$EQN4 := muk\ FNC\ \sin(\theta) - RsX + RnX - FNC\ \cos(\theta) + m2X\ aX$

Establish the equation of motion in the global Y-direction of the system of barges that do not impact the wall

```
> EQN5:=-FNC*sin(theta)-
muk*FNC*cos(theta)+RsY+RnY+m2Y*aY;
```
$EQN5 := -FNC\ \sin(\theta) - muk\ FNC\ \cos(\theta) + RsY + RnY + m2Y\ aY$

Establish the sum of moments of the system of barges that do not impact the wall

```
> EQN6:=muk*FNC*(c-xG2)-M+MRfn-MRfs-It2*alpha;
```

$EQN6 := muk\, FNC\, (c - xG2) - M + MRfn - MRfs - It2\, \alpha$

Establish an additional equation of coefficient of friction definition

```
> EQN7:=SW-mukk*FW;
```

$EQN7 := SW - mukk\, FW$

Now the program solves for the seven unknowns using these seven equations.

```
> SOL:=solve({EQN1,EQN2,EQN3,EQN4,EQN5,EQN6,EQN7},
{FW,SW,FNC,M,alpha,aX,aY}):assign(SOL):
```

Now the program presents in variable form the result of *Fw* = force normal to the wall, *Sw* = shear force at the wall, *aX* = acceleration in global X-direction in the most simplified form.

```
> FW:=simplify(FW);SW:=SW;aX:=aX;aY:=aY;
```

$$FW := -\,(-\sin(\theta)\, m1X\, RsX + \sin(\theta)\, m1X\, RnX - \sin(\theta)\, RsX\, m2X + \sin(\theta)\, RnX\, m2X - muk\, \cos(\theta)\, m1X\, RsX + muk\, \cos(\theta)\, m1X\, RnX$$
$$-\, muk\, \cos(\theta)\, RsX\, m2X + muk\, \cos(\theta)\, RnX\, m2X + RsY\, m1X\, muk\, \sin(\theta) - RsY\, m1X\, \cos(\theta) + RsY\, muk\, \sin(\theta)\, m2X$$
$$-\, RsY\cos(\theta)\, m2X + RnY\, m1X\, muk\, \sin(\theta) - RnY\, m1X\, \cos(\theta) + RnY\, muk\, \sin(\theta)\, m2X - RnY\cos(\theta)\, m2X)/($$
$$m1X\, muk\, \sin(\theta) - m1X\, \cos(\theta) + muk\, \sin(\theta)\, m2X - \cos(\theta)\, m2X + mukk\, \sin(\theta)\, m2X + mukk\, muk\, \cos(\theta)\, m2X)$$

$$SW := -\, mukk\, (-\sin(\theta)\, m1X\, RsX + \sin(\theta)\, m1X\, RnX - \sin(\theta)\, RsX\, m2X + \sin(\theta)\, RnX\, m2X - muk\, \cos(\theta)\, m1X\, RsX$$
$$+\, muk\, \cos(\theta)\, m1X\, RnX - muk\, \cos(\theta)\, RsX\, m2X + muk\, \cos(\theta)\, RnX\, m2X + RsY\, m1X\, muk\, \sin(\theta) - RsY\, m1X\, \cos(\theta)$$
$$+\, RsY\, muk\, \sin(\theta)\, m2X - RsY\cos(\theta)\, m2X + RnY\, m1X\, muk\, \sin(\theta) - RnY\, m1X\, \cos(\theta) + RnY\, muk\, \sin(\theta)\, m2X - RnY\cos(\theta)\, m2X$$
$$)/(m1X\, muk\, \sin(\theta) - m1X\, \cos(\theta) + muk\, \sin(\theta)\, m2X - \cos(\theta)\, m2X + mukk\, \sin(\theta)\, m2X + mukk\, muk\, \cos(\theta)\, m2X)$$

$$aX := -\,\frac{mukk\, (muk\, \sin(\theta)\, RsY + muk\, \sin(\theta)\, RnY - RsX\, \sin(\theta) - RsX\, muk\, \cos(\theta) + RnX\, \sin(\theta) + RnX\, muk\, \cos(\theta) - \cos(\theta)\, RsY - \cos(\theta)}{m1X\, muk\, \sin(\theta) - m1X\, \cos(\theta) + muk\, \sin(\theta)\, m2X - \cos(\theta)\, m2X + mukk\, \sin(\theta)\, m2X + mukk\, muk\, \cos(\theta)\, m2X}$$

$$aY := -\,(-\sin(\theta)\, m1X\, RsX + \sin(\theta)\, m1X\, RnX - \sin(\theta)\, RsX\, m2X + \sin(\theta)\, RnX\, m2X - muk\, \cos(\theta)\, m1X\, RsX + muk\, \cos(\theta)\, m1X\, RnX$$
$$-\, muk\, \cos(\theta)\, RsX\, m2X + muk\, \cos(\theta)\, RnX\, m2X + RsY\, m1X\, muk\, \sin(\theta) - RsY\, m1X\, \cos(\theta) + RsY\, muk\, \sin(\theta)\, m2X$$
$$-\, RsY\cos(\theta)\, m2X + RnY\, m1X\, muk\, \sin(\theta) - RnY\, m1X\, \cos(\theta) + RnY\, muk\, \sin(\theta)\, m2X - RnY\cos(\theta)\, m2X)/($$
$$(m1X\, muk\, \sin(\theta) - m1X\, \cos(\theta) + muk\, \sin(\theta)\, m2X - \cos(\theta)\, m2X + mukk\, \sin(\theta)\, m2X + mukk\, muk\, \cos(\theta)\, m2X)\, m2Y)$$

Data the program uses to calculate the forces:
PARAMETERS: Consistent units (Units used in the example: kips, ft/sec^2, kip*sec^2 / ft)

> *theta* = approach angle in degrees
> *muk* = steel-steel kinetic coefficient of friction between barges
> *mukk* = steel-steel kinetic coefficient of friction between the corner barge and the wall
> *m1X* = mass of barge system one (system that impacts the wall) including the hydrodynamic added mass (Mpar1)

$m2X$ = mass of barge system two (system that does not impact the wall) including the hydrodynamic added mass (Mpar2)

$m1Y$ = mass of barge system one (system that impacts the wall) including the hydrodynamic added mass (Mnorm1)

$m2Y$ = mass of barge system two (system that does not impact the wall) including the hydrodynamic added mass (Mnorm2)

Rs = Resultant force along failure plane (local y-axis)

Rn = Resultant force perpendicular to the failure plane (local x-axis)

```
> theta:=20;
```
$\theta := 20$

```
> muk:=0.2;
```
$muk := .2$

```
> m1X:=351.25;
```
$m1X := 351.25$

```
> m1Y:=437.58;
```
$m1Y := 437.58$

```
> m2X:=1053.77;
```
$m2X := 1053.77$

```
> m2Y:=1312.76;
```
$m2Y := 1312.76$

```
> Rs:=-136.72;
```
$Rs := -136.72$

```
> Rn:=669.06;
```
$Rn := 669.06$

Initial calculation for data transformation

```
> theta:=theta*3.14159/180;RsY:=Rs*cos(theta);
RnY:=Rn*sin(theta);RsX:=Rs*sin(theta);
RnX:=Rn*cos(theta);
```
$\theta := .3490655556$

$RsY := -128.4747889$

$RnY := 228.8318117$

$RsX := -46.76095612$

$RnX := 628.7108123$

Result of program in term of *mukk* = Kinetic coefficient of friction between steel and steel of the barge and the wall.

```
> FW:=FW;SW:=SW;aX:=aX;aY:=aY;
```

$$FW := -380102.8705 \; \frac{1}{-1224.178117 + 558.4542743 \; mukk}$$

$$SW := -380102.8705 \; \frac{mukk}{-1224.178117 + 558.4542743 \; mukk}$$

$$aX := -270.5320001 \; \frac{mukk}{-1224.178117 + 558.4542743 \; mukk}$$

$$aY := -289.5448296 \; \frac{1}{-1224.178117 + 558.4542743 \; mukk}$$

Plot of Fw and Sw vs kinetic coefficient of friction.

```
> plot([FW,SW],mukk=0..1.0, legend=["Fw","Sw"]);
```
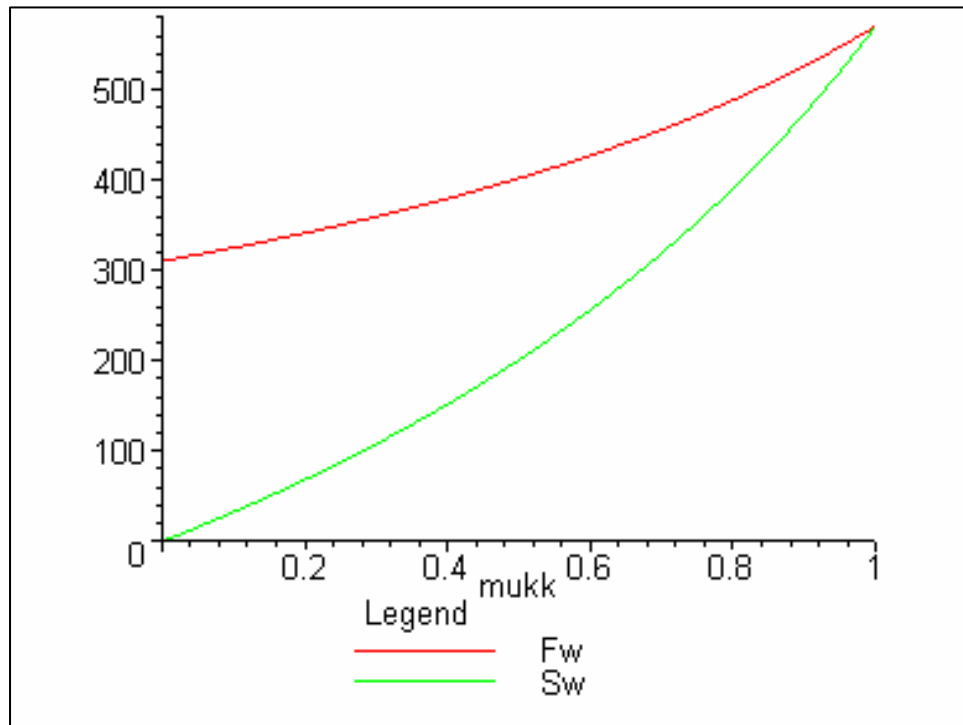


```
> mukk:=0.2;FW:=FW;
```

$mukk := .2$

$FW := 341.6694136$

```
>
```

Appendix C
Bits Location on a Barge from Documentary Pictures and Plans

One of the factors that affect the results in the analysis of the barge train impact based on the lashing yielding is the location of the bits that the lashing joins. The bit coordinates define the start and end of the lashing as well as their length. The normal strain in the lashing is calculated using the length of the lashing at each step of the relative motion for each failure mechanism.

The approach used to calculate the location of the bits in typical barges used the documentary photographs taken during the full-scale experiments of 1998 (Patev et al. 2003).[1] The dimensions of the barge used in the experiments are presented in Figure C-1. The model of the barge was an open hopper barge 35 by 105 ft. From these photographs the distance between bits were obtained based on other known dimensions.

To make a reasonable verification of the relative position of the bits on a barge, the figures presented in Arroyo, Ebeling, and Barker 2003 were used. The following procedure was used to calculate this position:

a. Using Figure 3.3 of Arroyo, Ebeling, and Barker (2003), the scale in CAD Computer Program of known distances was determined.

b. The known dimension used was the chord of the steel arc bumper. The magnitude of this distance is 35.5 in. In the CAD Program this dimension was calculated as 2.4024 units drawing.

c. The factor to convert the real dimension to the CAD dimension can be obtained by calculating the ratio as 35.5/2.4024 = 14.78 in./unit. This factor helps to find the real length of a distance if the CAD Program distance is specified. This process is demonstrated using Figure C-2.

---

[1] References cited in this appendix are included in the References section at the end of the main text.
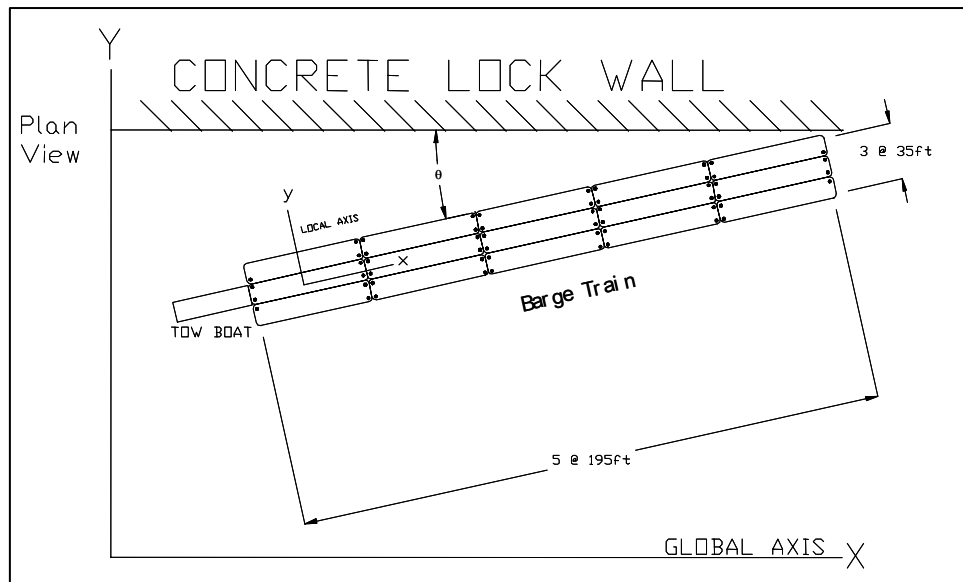
Figure C-1. Barge train-wall system
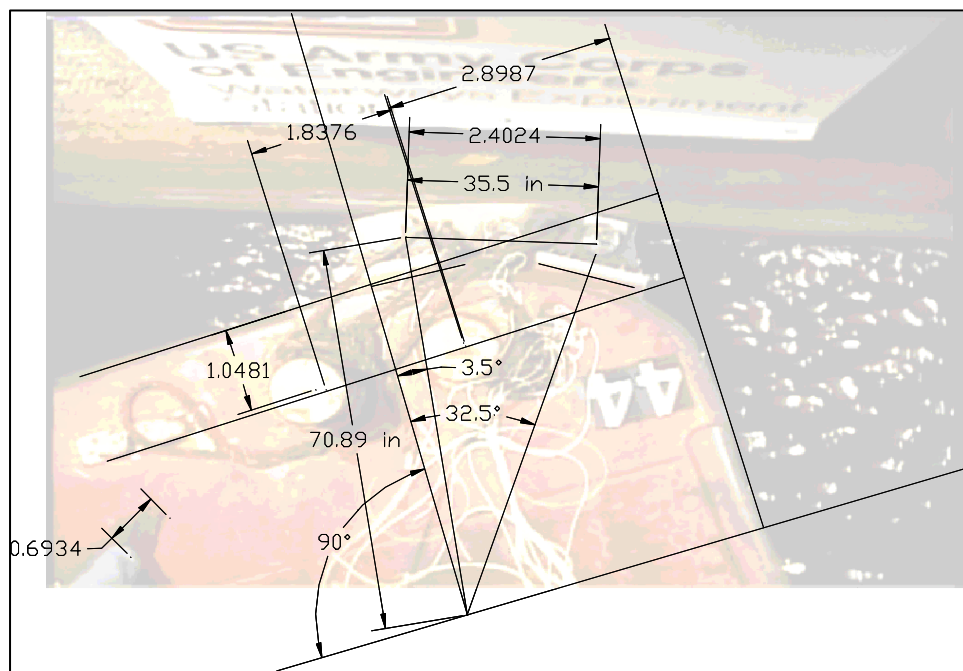
Figure C-2. Top view and bits location of the corner barge

d. Then, a line between bits was drawn and the distance in CAD dimensions was obtained. The resulting value was 1.8373 units drawing, equivalent to 2.26 ft. This value is close to the value obtained from detailed plans.

e. A line from the center of the bits to the port side of the barge was also drawn. In the CAD scale this dimension was 1.0481 units drawing, which is equivalent to 1.29 ft.

f. Finally, a line was drawn from the front bit to the bow of the barge. This dimension was obtained as 2.8987 units drawing, which is equivalent to 3.5 ft, using the factor previously calculated.

The plans prepared for the full-scale experiments in 1998 (Patev et al. 2003) provide dimensions very similar to those shown in Figures C-3 and C-4. Another check made using the documentary photos was to estimate the size of the foot of a man that appears in the picture. This foot provides a dimension in the CAD Program of 0.6934 unit drawing resulting in 10.24 in., as calculated with the ratio previously discussed. The resulting size of the man's foot is reasonable, and confirms the bits distance computations.

Finally, the results provided by the plans and the documentary photographs are very similar as presented in Table C-1. With this typical distance two models were developed. A barge train of 8 barges as shown in Figure C-5 and one barge train of 15 barges were prepared and presented in Chapter 6.

Table C-1 Comparison of Bits Locations, inches			
Procedure	From Bow	From Port	Between Bits
Plans	36	18	24
Documentary Photos	42	15.5	27
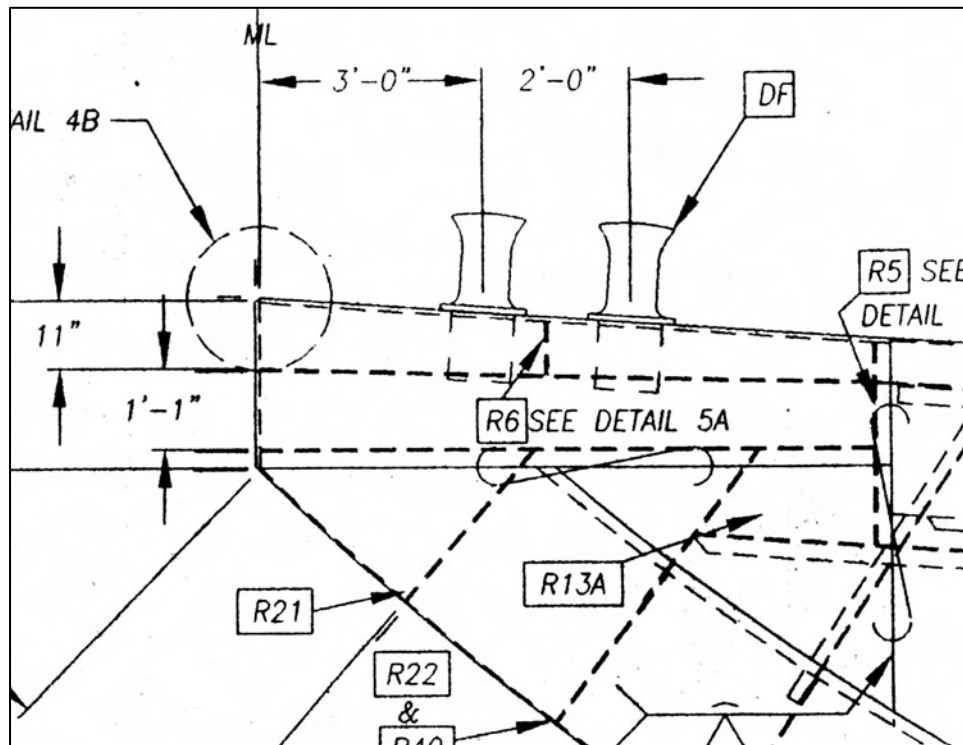
Figure C-3. Side view of the bits as plans of the full-scale experiments, 1998 (Patev et al. 2003)
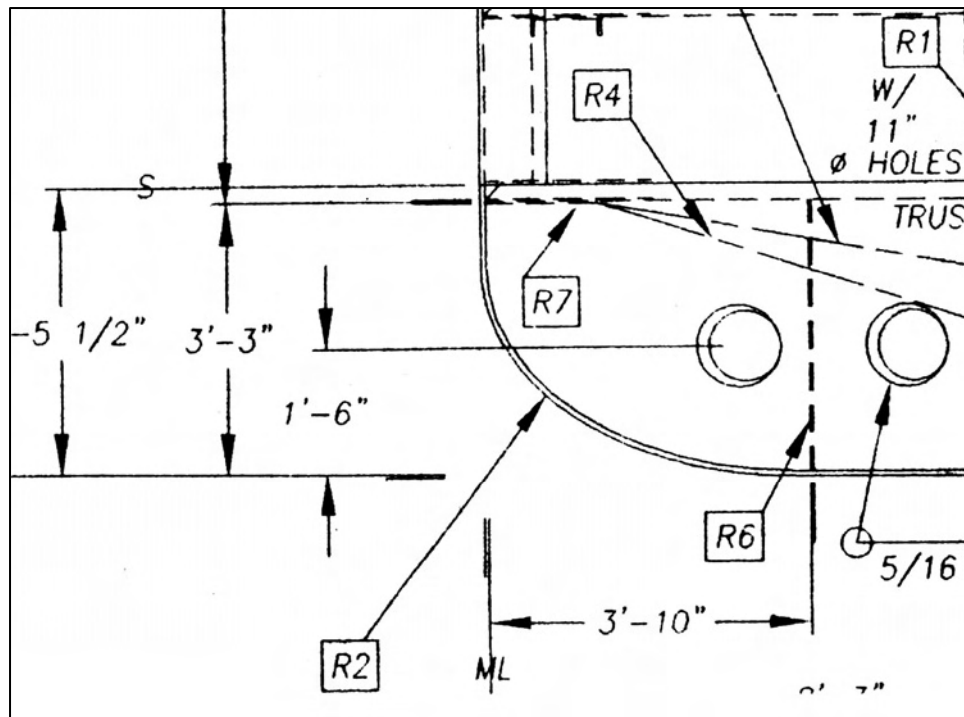
Figure C-4. Top view of the bits as plans of the full-scale experiments, 1998 (Patev et al. 2003)
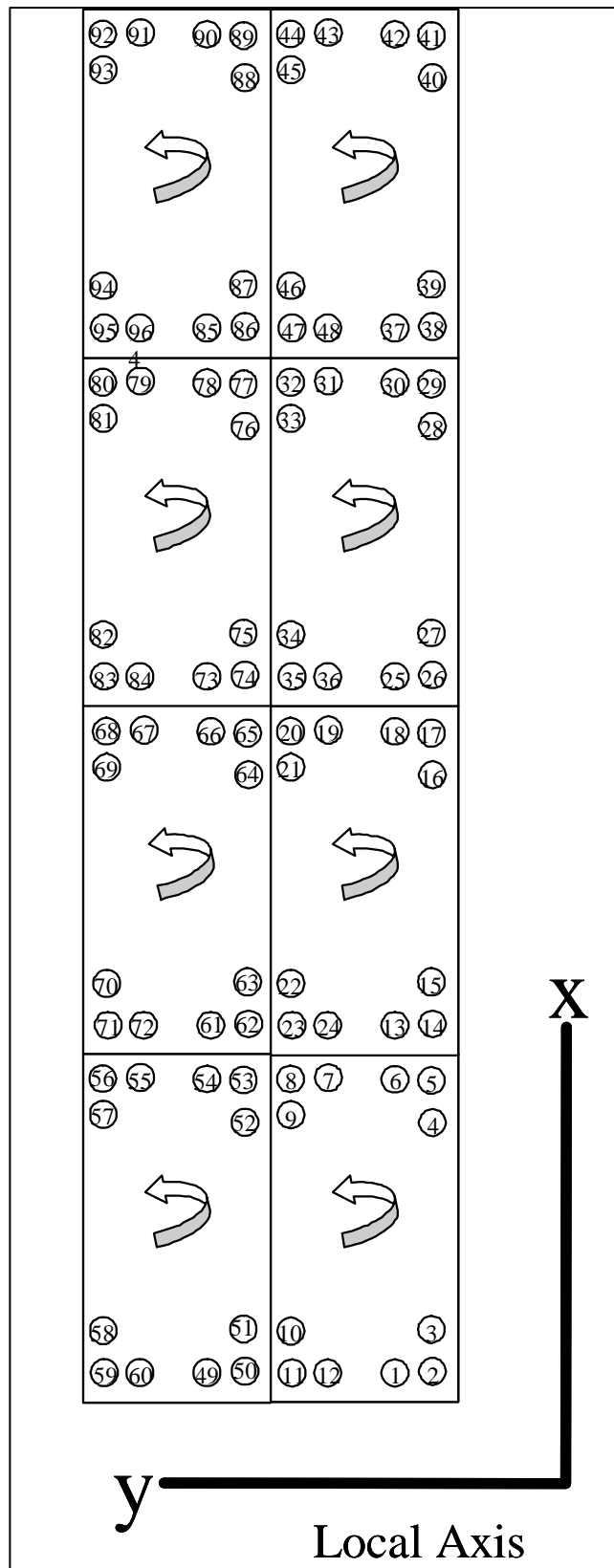
Figure C-5. Final 8-barge train system used in the research

Appendix D
Derivation of the F_W Equations

D.1 Longitudinal Failure Mechanism

The expression to calculate the force normal to the wall for the longitudinal failure mechanism is presented in Equation 2-14. This equation was obtained from the equilibrium equations and the definition of the kinetic coefficient of friction. First, express Equation 2-2 as

$$F_W = -Rn_Y + Rs_Y + F_{NC}\,cos\,\theta + \mu_k F_{NC}\,sin\,\theta \tag{D-1}$$

and substituting Equation D-1 into Equation 2-1 results in

$$\mu_K F_{NC}\,cos\,\theta - F_{NC}\,sin\,\theta = -M_{par1}a_X + \mu_K^*(-Rn_Y + Rs_Y + F_{NC}\,cos\,\theta + \mu_K F_{NC}\,sin\,\theta) - Rs_X - Rn_X \tag{D-2}$$

Now from Equation 2-10

$$a_X = \frac{Rs_X + Rn_X - F_{NC}\,sin\,\theta + \mu_K F_{NC}\,cos\,\theta}{M_{par2}} \tag{D-3}$$

and substituting Equation D-3 into Equation D-2 obtains

$$\mu_K F_{NC}\,cos\,\theta - F_{NC}\,sin\,\theta = -\frac{M_{par1}}{M_{par2}}Rs_X - \frac{M_{par1}}{M_{par2}}Rn_X + \frac{M_{par1}}{M_{par2}}F_{NC}\,sin\,\theta \tag{D-4}$$

$$-\frac{\mu_K M_{par1}}{M_{par2}}F_{NC}\,cos\,\theta - \mu_K^* Rn_Y + \mu_K^* Rs_Y + \mu_K^* F_{NC}\,cos\,\theta + \mu_K \mu_K^* F_{NC}\,sin\,\theta - Rs_X - Rn_X$$

Rearranging terms gives F_{NC} in terms of the resultant lashing forces in the global X- and Y-directions that is

$$F_{NC} = \frac{-\dfrac{M_{par1}}{M_{par2}} Rs_X - \dfrac{M_{par1}}{M_{par2}} Rn_x - \mu_K^* Rn_Y + \mu_K^* Rs_Y - Rs_X - Rn_X}{\mu_K \cos\theta - \sin\theta - \dfrac{M_{par1}}{M_{par2}} \sin\theta + \mu_K \dfrac{M_{par1}}{M_{par2}} \cos\theta - \mu_K^* \cos\theta - \mu_K^* \mu_K \sin\theta}$$ (D-5)

Equation D-5 can be expressed as

$$F_{NC} = \frac{-M_{par1} Rs_X - M_{par1} Rn_X - M_{par2} \mu_K^* Rn_Y + M_{par2} \mu_K^* Rs_Y - M_{par2} Rs_X - M_{par2} Rn_X}{M_{par2} \mu_K \cos\theta - M_{par2} \sin\theta - M_{par1} \sin\theta + \mu_K M_{par1} \cos\theta - M_{par2} \mu_K^* \cos\theta - M_{par2} \mu_K^* \mu_K \sin\theta}$$ (D-6)

The expression of the force normal to the wall is obtained by substituting Equation D-6 into Equation D-1 as

$$F_W = \frac{M_{par}\left(-\mu_K Rn_Y \cos\theta + Rn_Y \sin\theta + \mu_K Rs_Y \cos\theta - Rs_Y \sin\theta - Rs_X \cos\theta - Rn_X \cos\theta - \mu_K Rs_X \sin\theta - \mu_K Rn_X \sin\theta\right)}{\mu_K M_{par2} \cos\theta - M_{par2} \sin\theta - M_{par1} \sin\theta + \mu_K M_{par1} \cos\theta - \mu_K^* M_{par2} \cos\theta - M_{par2} \mu_K^* \mu_K \sin\theta}$$ (D-7)

and can be expressed as

$$F_W = \frac{M_{par}\left[(Rs_X + Rn_X)(\cos\theta + \mu_K \sin\theta) + \mu_k(Rn_Y - Rs_Y)\cos\theta + (Rs_Y - Rn_Y)\sin\theta\right]}{M_{par1} \sin\theta + M_{par2} \sin\theta - \mu_K M_{par1} \cos\theta - \mu_K M_{par2} \cos\theta + \mu_K \mu_K^* M_{par2} \sin\theta + \mu_K^* M_{par2} \cos\theta}$$ (D-8)

Equation D-8 is the expression provided by Maple as shown in Equation 2-14.

D.2 Transverse Failure Mechanism

The expression to calculate the force normal to the wall for the transverse failure mechanism is presented in Equation 3-14. This equation was obtained from the equilibrium equations and the definition of the kinetic coefficient of friction. First, express Equation 3-2 as

$$F_W = -Rn_Y - Rs_Y + F_{NC} \sin\theta + \mu_K F_{NC} \cos\theta$$ (D-9)

and substituting Equation D-9 into Equation 3-1 results in

$$F_{NC} \cos\theta - \mu_K F_{NC} \sin\theta = -M_{par1} a_X + \mu_K^*(-Rs_Y - Rn_Y + F_{NC} \sin\theta + \mu_K F_{NC} \sin\theta) + Rs_X + Rn_X$$ (D-10)

Now from Equation 3-10

$$a_X = \frac{Rs_X - Rn_X + F_{NC} \cos\theta - \mu_K F_{NC} \sin\theta}{M_{par2}}$$ (D-11)

Now, substituting Equation D-11 into Equation D-10 gives

$$F_{NC} \cos\theta - \mu_K F_{NC} \sin\theta = -\frac{M_{par1}}{M_{par2}} Rs_X + \frac{M_{par1}}{M_{par2}} Rn_X - \frac{M_{par1}}{M_{par2}} F_{NC} \cos\theta \tag{D-12}$$

$$+ \frac{\mu_K M_{par1}}{M_{par2}} F_{NC} \sin\theta - \mu_K^* Rs_Y - \mu_K^* Rn_Y + \mu_K^* F_{NC} \sin\theta + \mu_K \mu_K^* F_{NC} \cos\theta - Rs_X + Rn_X$$

Rearranging terms produces F_{NC} in terms of the resultant lashing forces in the global X- and Y-directions, that is

$$-\mu_K F_{NC} \sin\theta + F_{NC} \cos\theta + \frac{M_{par1}}{M_{par2}} F_{NC} \cos\theta - \frac{\mu_K M_{parx1}}{M_{par2}} F_{NC} \sin\theta - \mu_K^* F_{NC} \sin\theta - \mu_K \mu_K^* F_{NC} \cos\theta = \tag{D-13}$$

$$-\frac{M_{par1}}{M_{par2}} Rs_X + \frac{M_{par1}}{M_{parx2}} Rn_X - \mu_K^* Rn_Y - \mu_K^* Rs_Y - Rs_X + Rn_X$$

Equation D-13 can be expressed as

$$F_{NC} = \frac{-M_{par1} Rs_X + M_{par1} Rn_X - M_{par2} \mu_K^* Rn_Y - M_{par2} \mu_K^* Rs_Y - M_{par2} Rs_X + M_{par2} Rn_X}{-M_{par2} \mu_K \sin\theta + M_{par2} \cos\theta + M_{par1} \cos\theta - \mu_K M_{par1} \sin\theta - M_{par2} \mu_K^* \sin\theta - M_{par2} \mu_K^* \mu_K \cos\theta} \tag{D-14}$$

The expression of the force normal to the wall is obtained by substituting Equation D-14 into Equation D-9 resulting in the following expression:

$$F_W = \frac{\begin{array}{l}(-M_{par2} Rs_Y \cos\theta + \mu_K M_{par2} Rs_Y \sin\theta + \mu_K^* M_{par2} Rs_Y \sin\theta + \mu_K \mu_K^* M_{par2} Rs_Y \cos\theta - M_{par1} Rs_Y \cos\theta \\ + \mu_K M_{par1} Rs_Y \sin\theta - M_{par2} Rn_Y \cos\theta + \mu_K M_{par2} Rn_Y \sin\theta + \mu_K^* M_{par2} Rn_Y \sin\theta + \mu_K \mu_K^* M_{par2} Rn_Y \cos\theta \\ - M_{par1} Rn_Y \cos\theta + \mu_K M_{par1} Rn_Y \sin\theta + M_{par2} Rn_X \sin\theta - M_{par2} Rs_X \sin\theta - \mu_K^* M_{par2} Rn_Y \sin\theta - \mu_K^* M_{par2} Rs_Y \sin\theta \\ + M_{par1} Rn_X \sin\theta - M_{par1} Rs_X \sin\theta + \mu_K M_{par2} Rn_Y \cos\theta - \mu_K M_{par2} Rs_X \cos\theta - \mu_K \mu_K^* M_{par2} Rn_Y \cos\theta \\ - \mu_K \mu_K^* M_{par2} Rs_Y \cos\theta + \mu_K M_{par1} Rn_X \cos\theta - \mu_K M_{par1} Rs_X \cos\theta)\end{array}}{-\mu_K M_{par2} \sin\theta + M_{par2} \cos\theta + M_{par1} \cos\theta - \mu_K M_{par1} \sin\theta - \mu_K^* M_{par2} \sin\theta - M_{par2} \mu_K^* \mu_K \cos\theta} \tag{D-15}$$

and can be expressed as

$$F_W = \frac{M_{par}(-Rs_Y \cos\theta + \mu_K Rs_Y \sin\theta - Rn_Y \cos\theta + \mu_K Rn_Y \sin\theta + Rn_X \sin\theta - Rs_X \sin\theta + \mu_K Rn_X \cos\theta - \mu_K Rs_X \cos\theta)}{-\mu_K M_{par2} \sin\theta + M_{par2} \cos\theta + M_{par1} \cos\theta - \mu_K M_{par1} \sin\theta - \mu_K^* M_{par2} \sin\theta - M_{par2} \mu_K^* \mu_K \cos\theta} \tag{D-16}$$

Equation D-16 is the expression provided by Maple as shown in Equation 3-14.

Appendix E
Limit_LASHING User's Manual

E.1 Limit_LASHING User's Manual

This Appendix presents the user's manual for the computer program Limit_LASHING. Limit_LASHING is a user-friendly program developed to simplify the use of the engineering methodology developed during this research. It was prepared to be used in several computer environments, for example WINDOWS XP Operating System.

E.2 Disclaimer

Considerable time, effort, and expense have gone into the development and documentation of Limit_LASHING. The program has been thoroughly tested and used. In using the program, however, the user accepts and understands that no warranty is expressed or implied by the developers or the distributors on the accuracy or the reliability of the program.

The user must explicitly understand the assumptions of the program and must independently verify the results. He/she must have some knowledge of barge train impact events to understand the concepts used by the program. The user and only the user is responsible for the improper use of the program.

E.3 Introduction to Limit_LASHING

Limit_LASHING is a user-friendly program developed to analyze the barge train impact on the lock walls, approach walls, guide walls, and guard walls. This program uses the methodology developed in this research and many other theories such as kinetic energy and linear momentum impulse, as discussed in Arroyo, Ebeling, and Barker (2003).[1] The program was written using FORTRAN code and uses a preprocessor and postprocessor written in Visual Basic providing a Windows environment. The program can analyze the combination of the effects of mass of the barges and the effect of lashings at the moment it reaches the

---

[1] References cited in this appendix are included in the References section at the end of the main text.

ultimate deformation for three different failure mechanisms: the transverse failure mechanism, longitudinal failure mechanism, and the corner failure mechanism. The program conducts the analysis with user-provided data for the approach angle, number of barges, lashing configuration, etc. It presents all the results of the analysis for the possible failure mechanism in graphical form and reports the maximum normal force in the wall.

The user's manual explains the Limit_LASHING program and shows three examples for the different failure mechanisms, including special cases. It then explains the ASCI file that is generated by the FORTRAN code to run the cases.

E.4 Installation of Limit_LASHING

The procedure used to install Limit_LASHING is simple. The software has an approximate size of 3 MB. It can be installed on any computer using a CD-ROM device. The program runs in Windows 9x, Windows 2000, or Windows XP operating systems.

To install Limit_LASHING from a CD:

- Insert the Limit_LASHING CD into the CD-ROM drive and follow the on-screen instructions. If the installation setup does not start automatically, then continue with the following steps.

- Open the files from the CD.

- Then double-click the **Setup** icon.

- Follow the on-screen instructions.

It is recommended to restart the computer after installing the program.
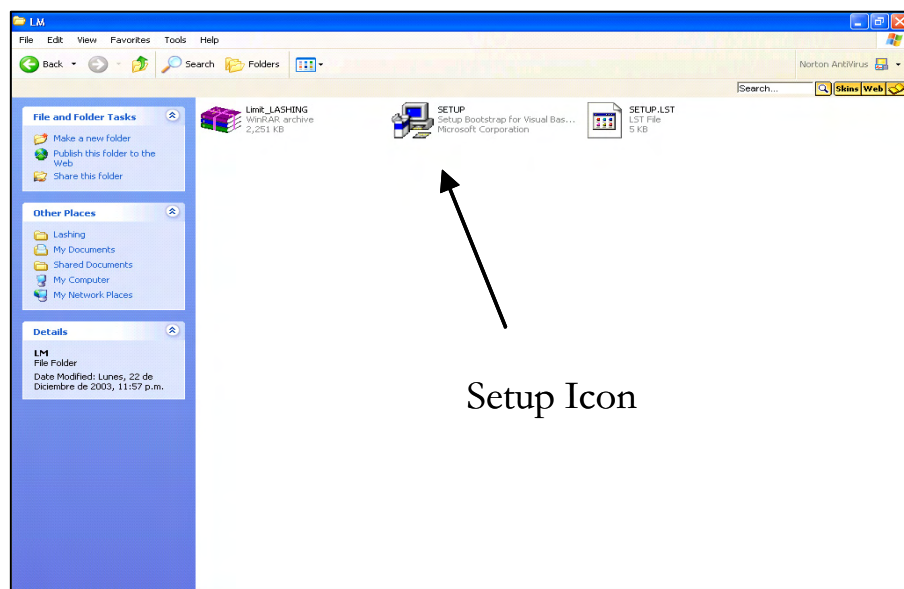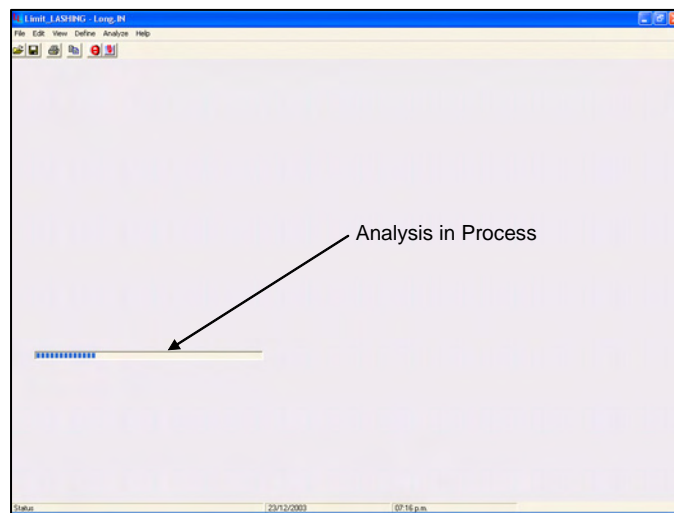
E.5 File Menu

The options provided in the **File** pull-down menu are described in this section. Each option is defined and illustrated graphically using icons and windows.

E.5.1 Open

To open an existing file click the **Open** icon , press **Ctrl + O**, or go to file menu and select **Open**.
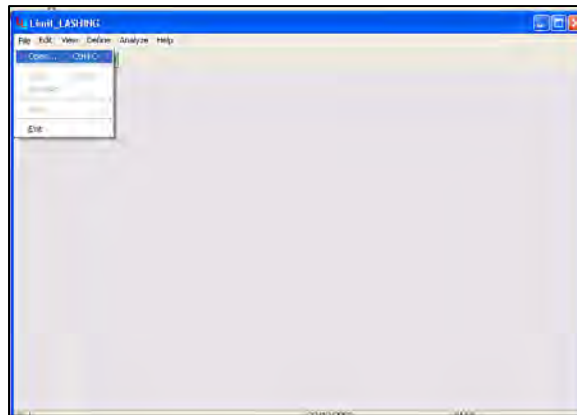
Then select from a folder the file to be opened.
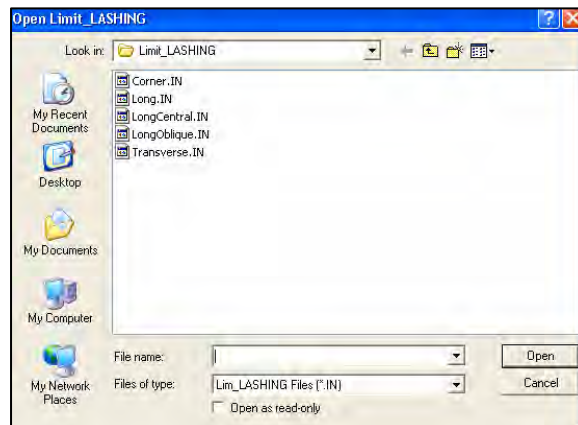
E.5.2 Save

To save a file, click the **Save** icon , press **Ctrl + S**, or go to the file menu and select **Save.**
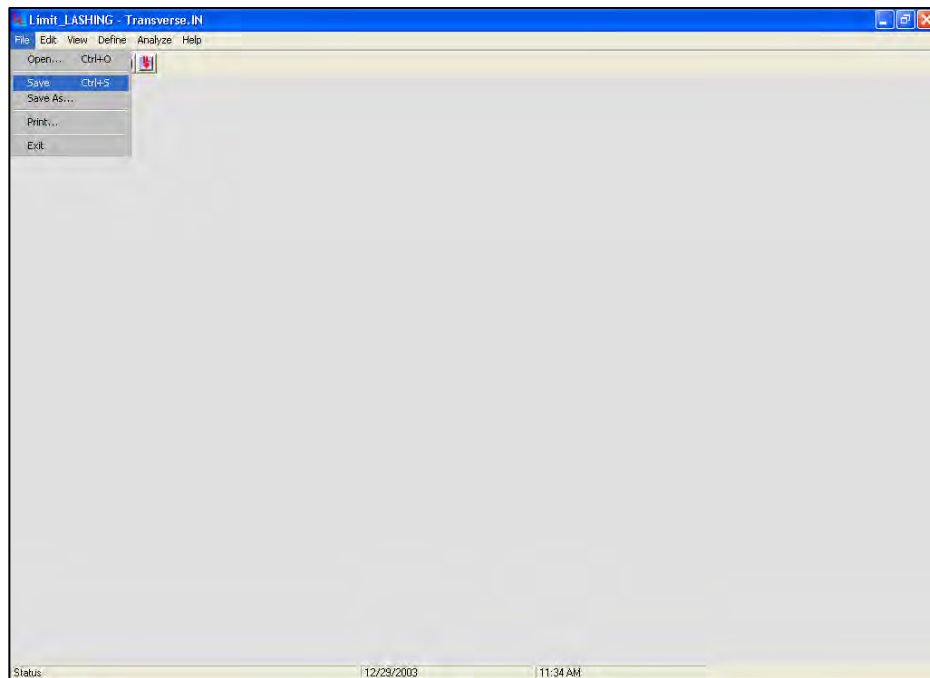
E.5.3 Save As

To save the file with a new name, select from the file menu **Save As.**
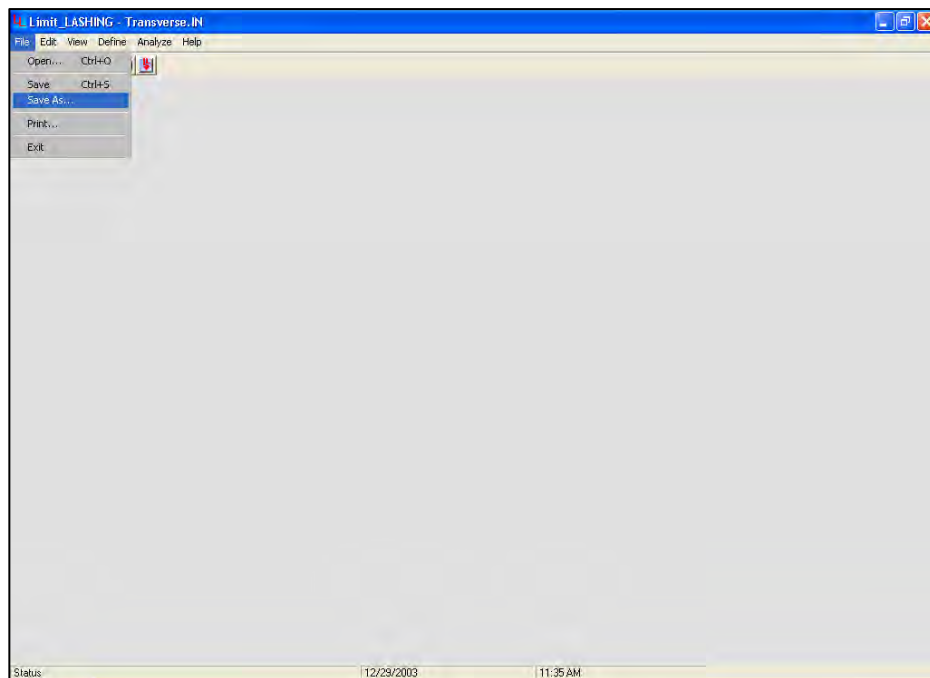
Then select from a folder where the file needs to be saved or type a new name.
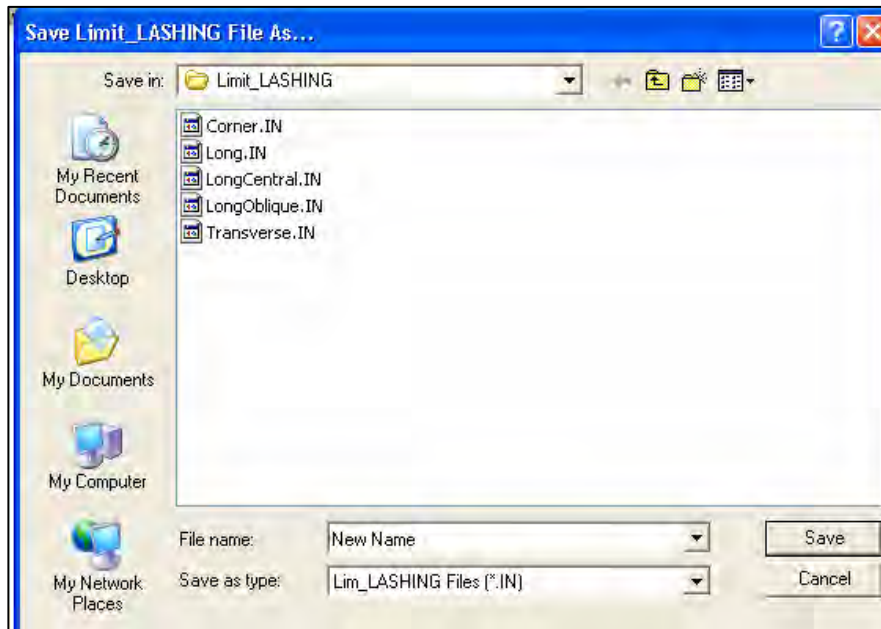
E.5.4 Print Plot

To print a plot, go to the file menu and select **Print.**
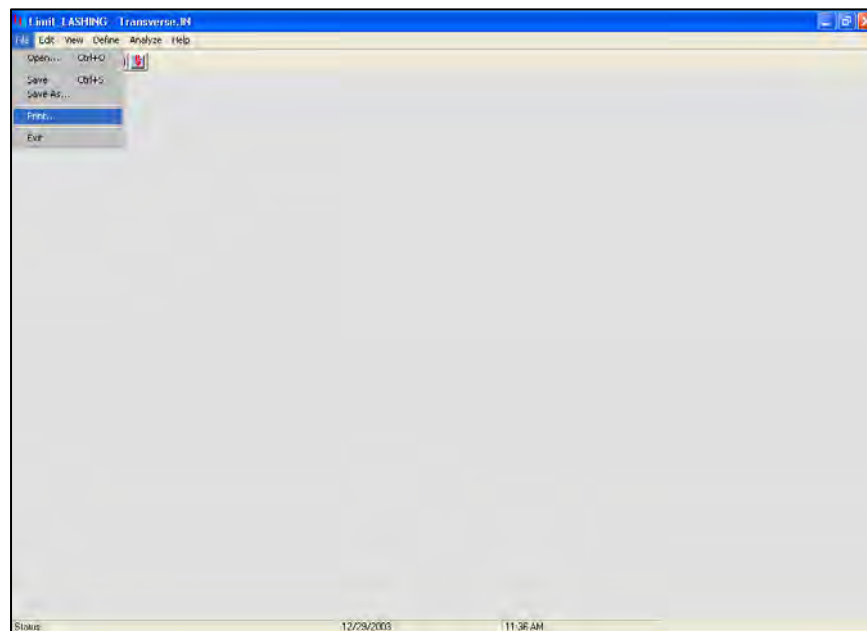
E.5.5 Exit

To exit and finish the program, go to the file menu and select **Exit**, or press the **Exit** icon ⊠.
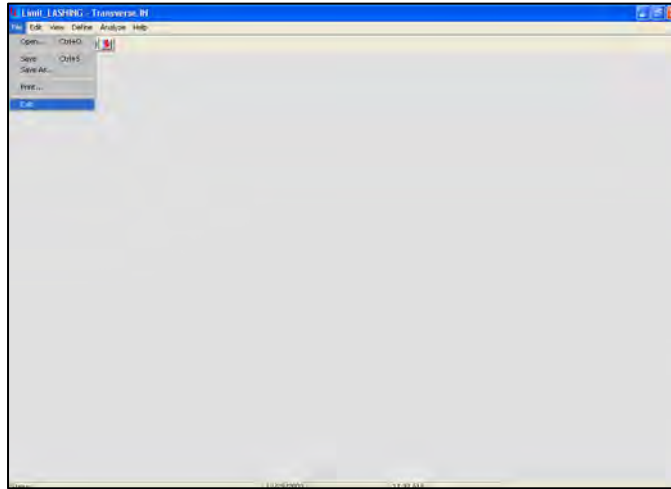
E.6 Edit Menu

The options provided in the **Edit** pull-down menu are described in the following sections. Each option is defined and explained graphically using icons and windows.

E.6.1 Copy Plot to Clipboard

To copy a plot to save in the clipboard of Windows, go to the **Edit** menu and select the **Copy Plot to Clipboard** option or press **Ctrl + C**.
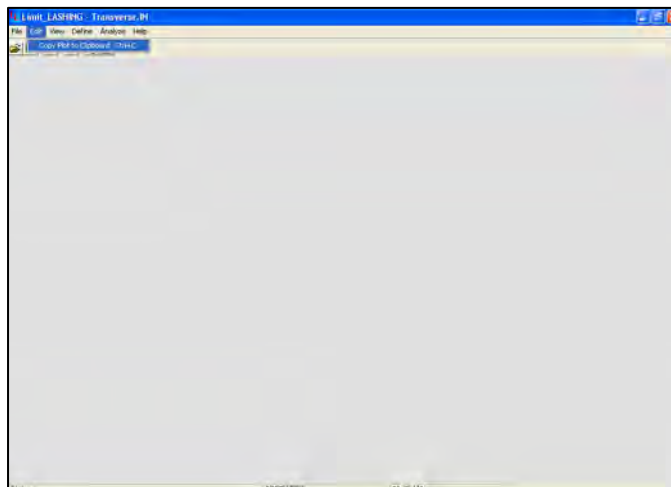
E.7 View Menu

The options provided in the **View** pull-down menu are described in this section. Each option is defined and illustrated graphically using icons and windows.

E.7.1 Toolbar

To turn the toolbar on or off, go to the **View** menu and select **Toolbar**.
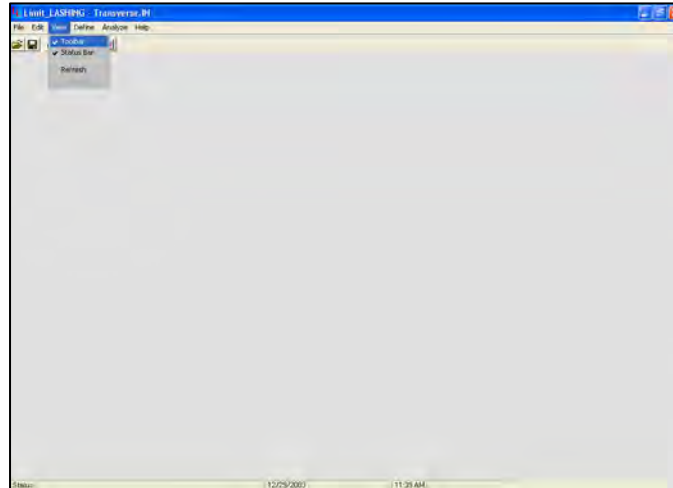
E.7.2 Status bar

To turn the status bar on or off, go to the **View** menu and select **Status bar.**
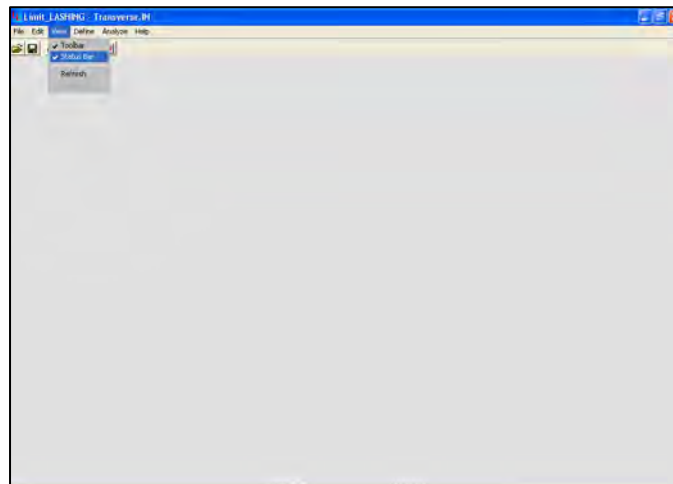
E.7.3 Refresh

To refresh the screen and actualize the information and plots, go to the **View** menu and select **Refresh**.
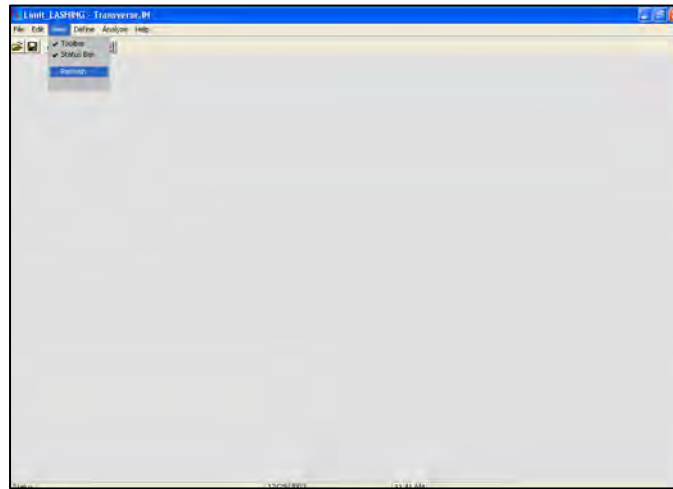
E.8 Define Menu

The options provided in the **Define** pull-down menu are described in this section. Each option is defined and illustrated graphically using icons and windows.

E.8.1 Barge Properties & Dimension

To define the properties and dimension of a barge use the **Barge Properties & Dimension** in the pull-down menu.
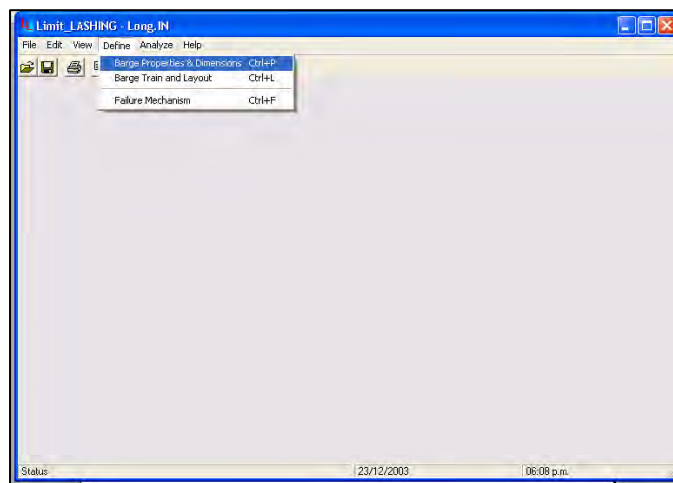
E.8.2 Individual Barge Data

Use this option to define such geometric properties of the individual barge as width, length, edge distance of the bits, and separation of the bits; the coefficient of friction between the barges; and the coefficient of friction between barge and impacted wall. The program assumes that all the barges are the same. After the required data are entered, click the **OK** button.

E.8.3 Barge Train Layout

Use this option to define the layout of the barge train. Provide the number of barges in the local x- and y-axes. Then, click the **Display Barge** button, and the program will display the layout in the local coordinate system. Also provide the **Hydrodynamics Added Mass Coefficients** (Refer to Engineer Technical Letter (ETL) 1110-2-338). Finally define the mass of each barge in the table at the lower left corner of the screen. Click the **OK** button after entering all data.
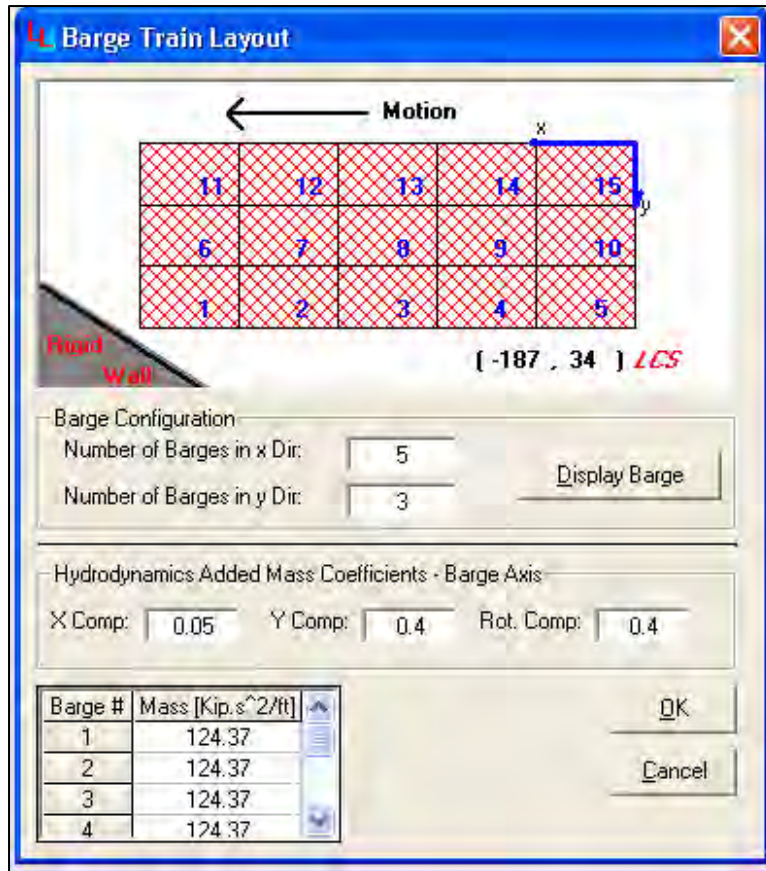
If a system with one row or one column of barges is specified, the lashing failure plane may not exist for some failure mechanisms. The program shows this message if only one row or column is defined.

For example, if a barge train system consisting of a row of five barges in the local x-direction is defined, then the longitudinal failure mechanism will not exist because System 2 in this failure mechanism does not exist.
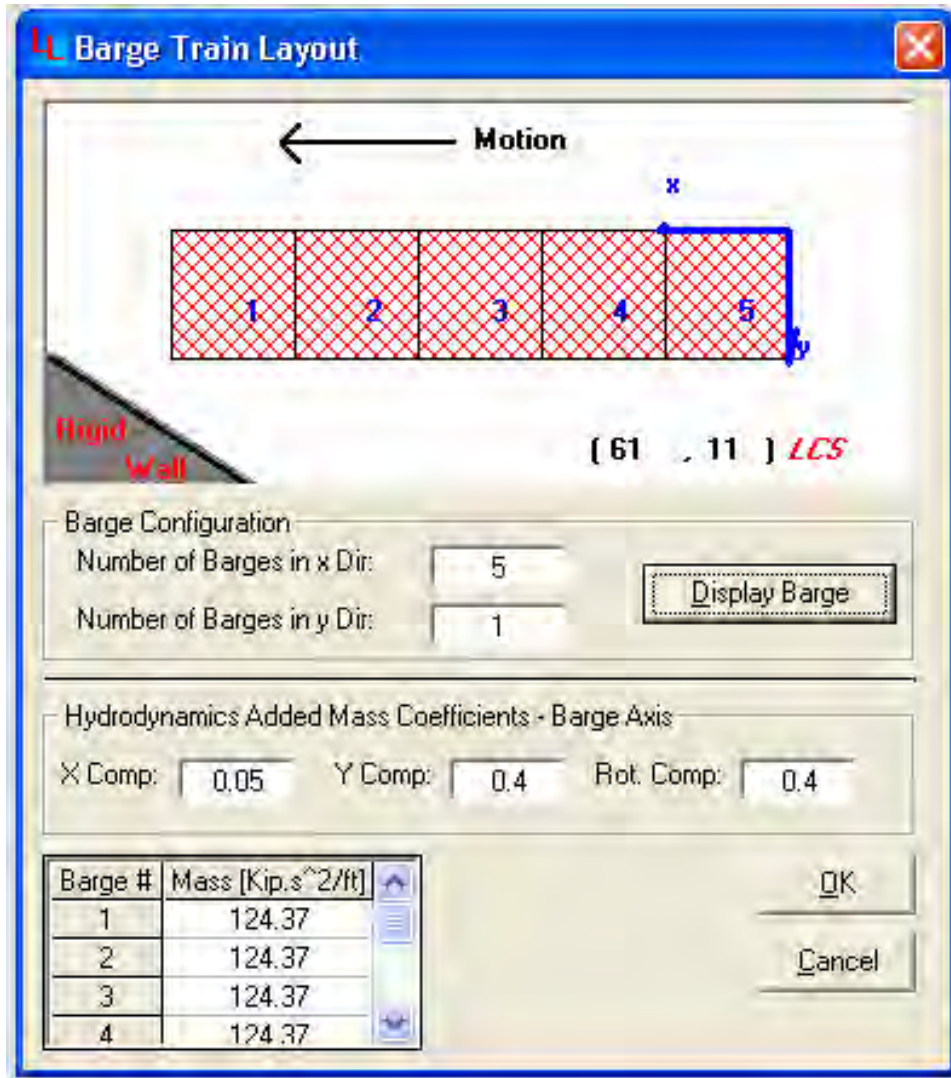
E.8.4 Approach Angle

Define the approach angle of the barge train system using the icon located on the toolbar. The angle will be between 0 and 90 degrees (head-on impacts are 90 degrees). Then, a new screen where the user can define the velocity in the local x- and y-direction is presented. This screen also presents the orientation of the global coordinate system. Then click **OK** button.
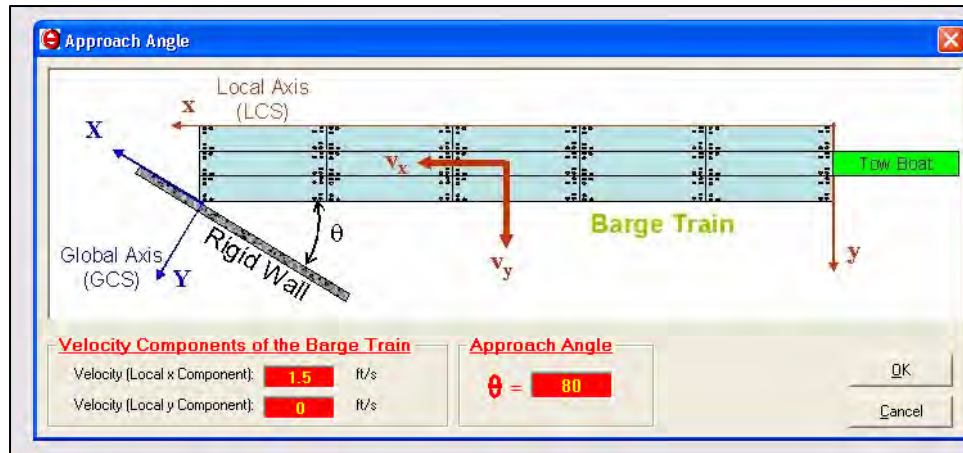
E.8.5 Failure Mechanism

Define the failure mechanism by using the pull-down menu and selecting **Failure Mechanism** or Ctrl-F.
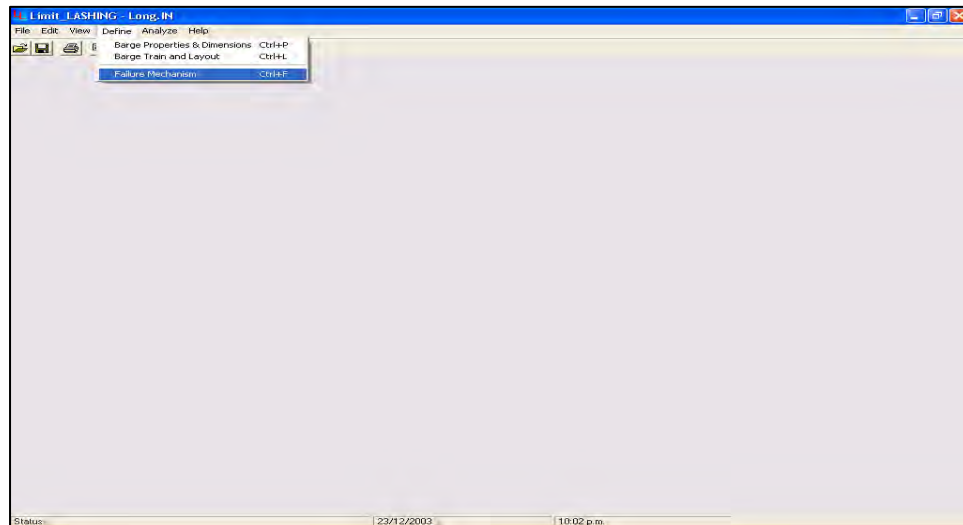
Then a new screen will appear where the mechanism to be analyzed can be defined.
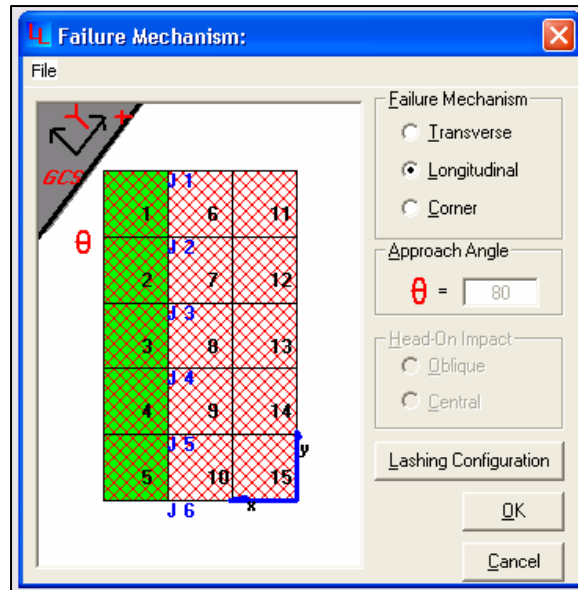
After the failure mechanism is selected, it is necessary to establish the configuration of lashing using the **Lashing Configuration** button. That screen presents the failure planes of the system. The failure plane is produced between the barges in green (barge System 1) and the barges in red (barge System 2) defined by the joints (J1, J2, J3,…). This screen presents the local (blue) barge and global (GCS) coordinate system.

Lashing Configuration Button
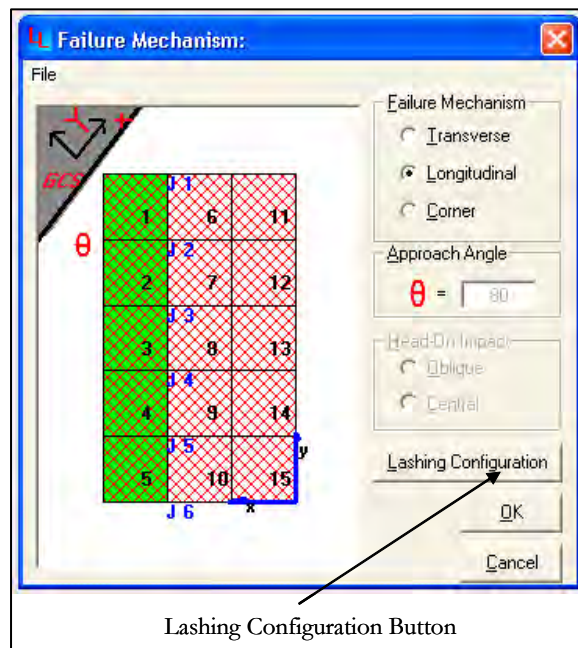
After the failure mechanism is selected and the **Lashing Configuration** button is pressed, two screens will appear. In the left screen appears the barge

train system indicating the failure plane and the joints defining this plane. The right screen presents bits associated with each joint and the table of connectivity based on the lashing configuration desired. The three idealized failure mechanisms that the program can analyze are explained in this report as follows: Chapter 2, longitudinal failure mechanism, Chapter 3, transverse failure mechanism, and Chapter 4, corner failure mechanism.
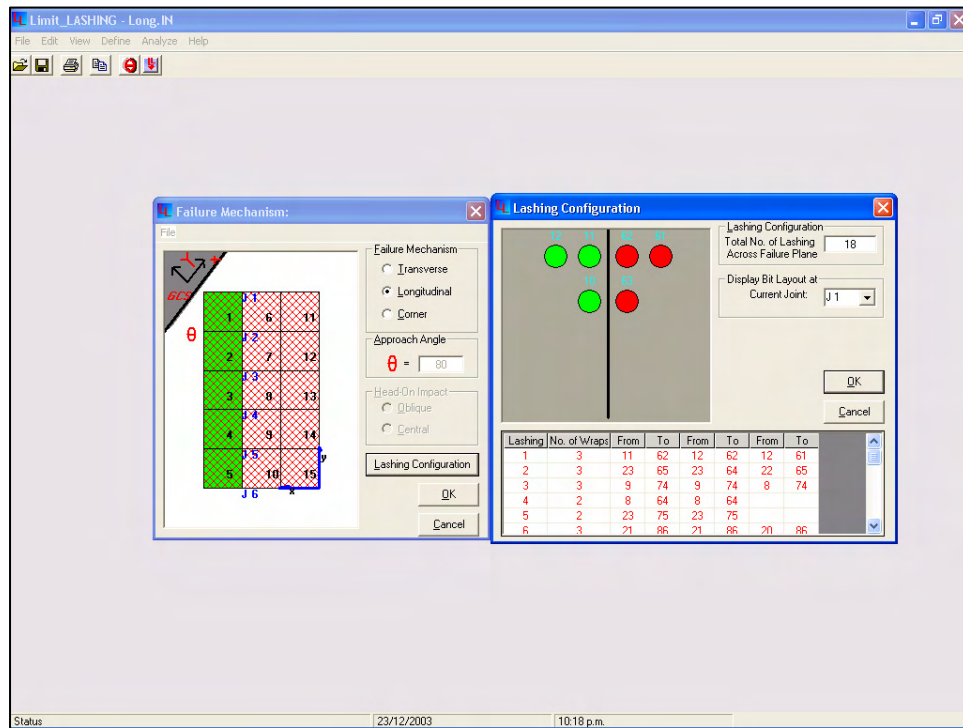
E.8.6 Lashing Configuration

To define the lashing configuration it is necessary to use the right screen of the previous step (i.e., **Failure Mechanism**). After the **Lashing Configuration** button is selected, it is necessary to define the number of lashings that act across the failure plane. Then, the user can zoom in on the bits arrangement of every joint along the failure plane by using the pull-down menu **Display Bit Layout at Current Joint**. The bits are presented in two colors, green and red. The green color bits are associated with barge System 1, and the red color bits are associated with barge System 2. In the bottom of the screen appears a table with the number of rows equal to the number of lashings. It is necessary to enter the number of wraps of each lashing in this table. One lashing can have n wraps. The wraps are defined in the columns that indicate **From** and **To**. Always define the wraps from barge System 1 (green) to barge System 2 (red).

Appendix E   Limit_LASHING User's Manual

Clicking on the lashing number causes a new screen to appear to define the mechanical properties of this lashing. Next, it is necessary to define the diameter of the lashing, modulus of elasticity, the initial tension (i.e., lashing prestress), ultimate load capacity, and the ultimate rupture strain of the lashing. Also presented on this screen is a diagram of the elastoplastic stress-strain behavior of lashing. More information about typical lashing configurations can be found in Appendix A.

E.9 Analyze Menu

The options provided by the **Analyze** pull-down menu are described in this section. Each option is defined and illustrated graphically using icons and windows.

E.9.1 Run Barge Train System

To analyze the system click the **Analyze** icon [icon], press **F5**, or go to **Analyze** menu and select **Barge Train System**.
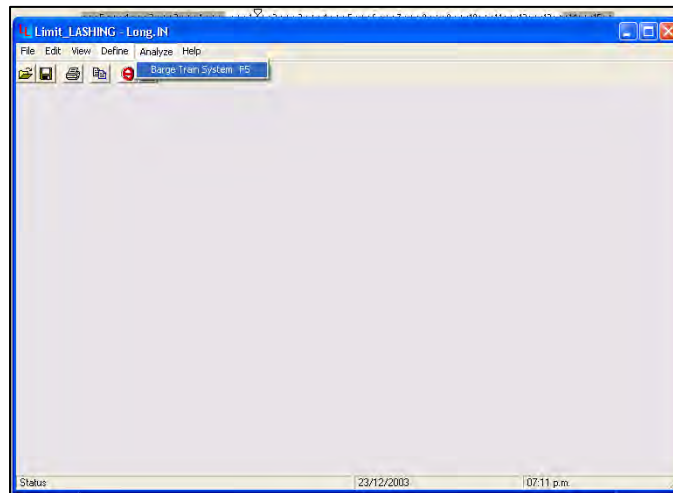
Then a small window will appear indicating that the analysis is in process.

When the analysis is concluded, the results will appear.

E.10 Help Menu

The options provided in the **Help** pull-down menu are described in this section. Each option is defined and illustrated graphically using icons and windows.

E.10.1 Contents

The information needed to understand the use of this computer program is presented in this user's manual.
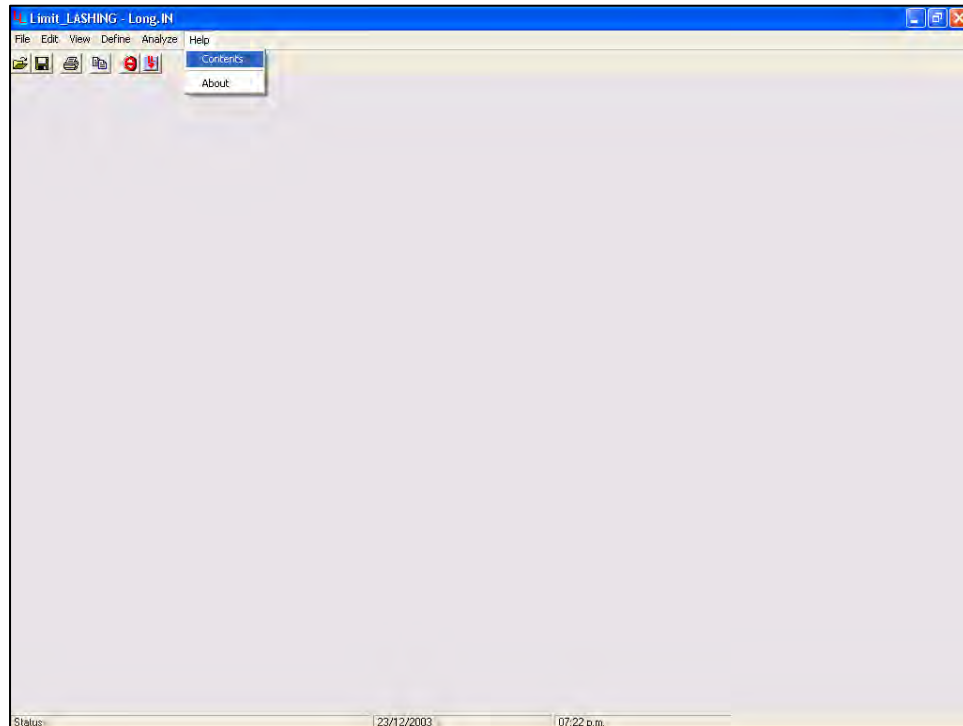
Selecting **Contents** brings up a small window indicating that the help associated with this project is on the user manual.
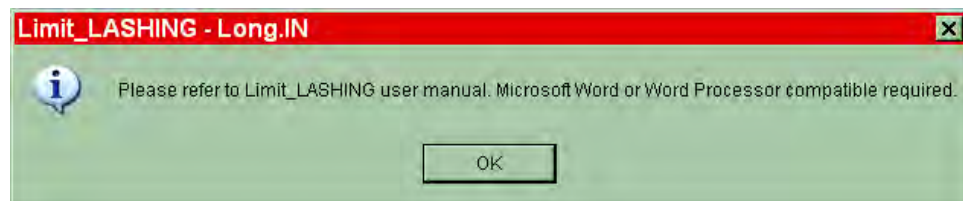
E.10.2 About

To know such details of the program as purpose and authors, go to the **Help** menu and select **About.**
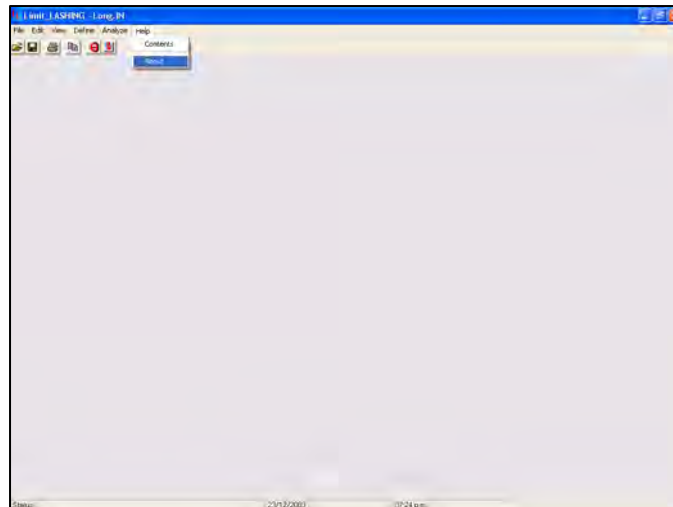
The following window will appear.

E.11 Step-by-Step Example for the Transverse Failure Mechanism

An example of a 15-barge train is presented for the transverse failure mechanism. Each of these barges has a width of 35 ft, a length of 195 ft, and a mass of 124.37 kips-sec^2/ft. The bits have an edge distance of 1.25 ft and 3 ft of separation. The approach angle is 10 degrees with a velocity of 1.5 ft/sec in the local x barge direction and zero in the local y barge direction. The barge-to-barge kinetic coefficients of friction are 0.2 and 0.2 for barge to wall.

E.11.1 Step 1

Open the Limit_LASHING program and wait until the main window is displayed.
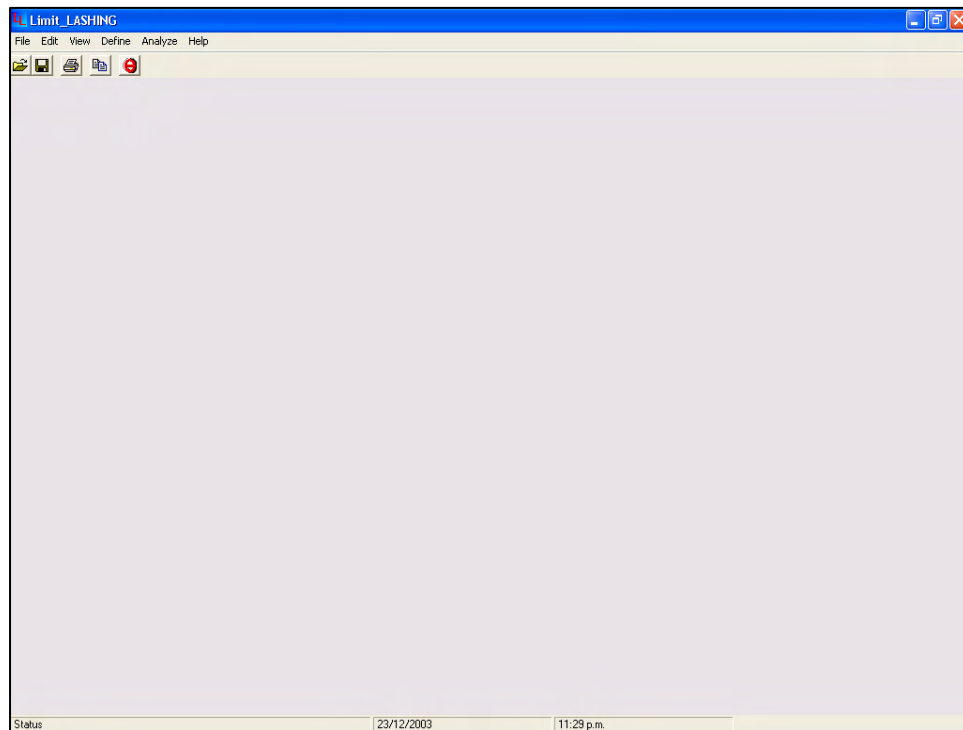
E.11.2 Step 2

Select the **Approach Angle** button and define the approach angle and the approach velocity. Then click **OK** button.
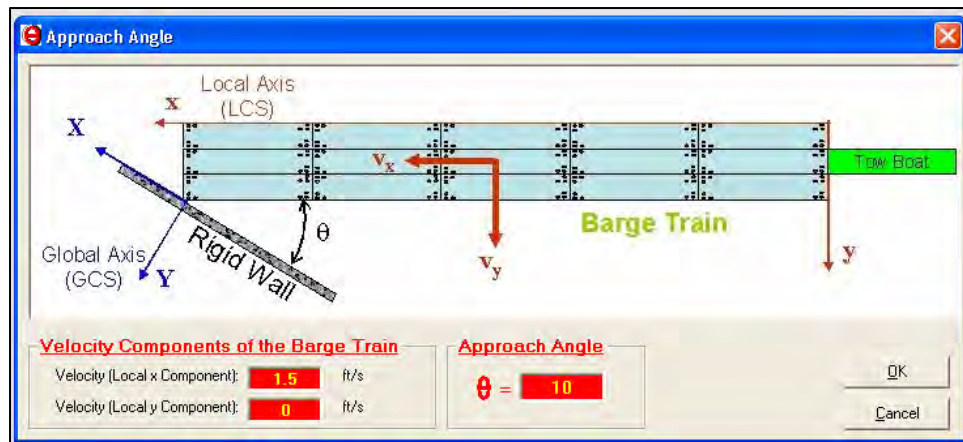
E.11.3 Step 3

Define the properties of the barge and the coefficient of friction.
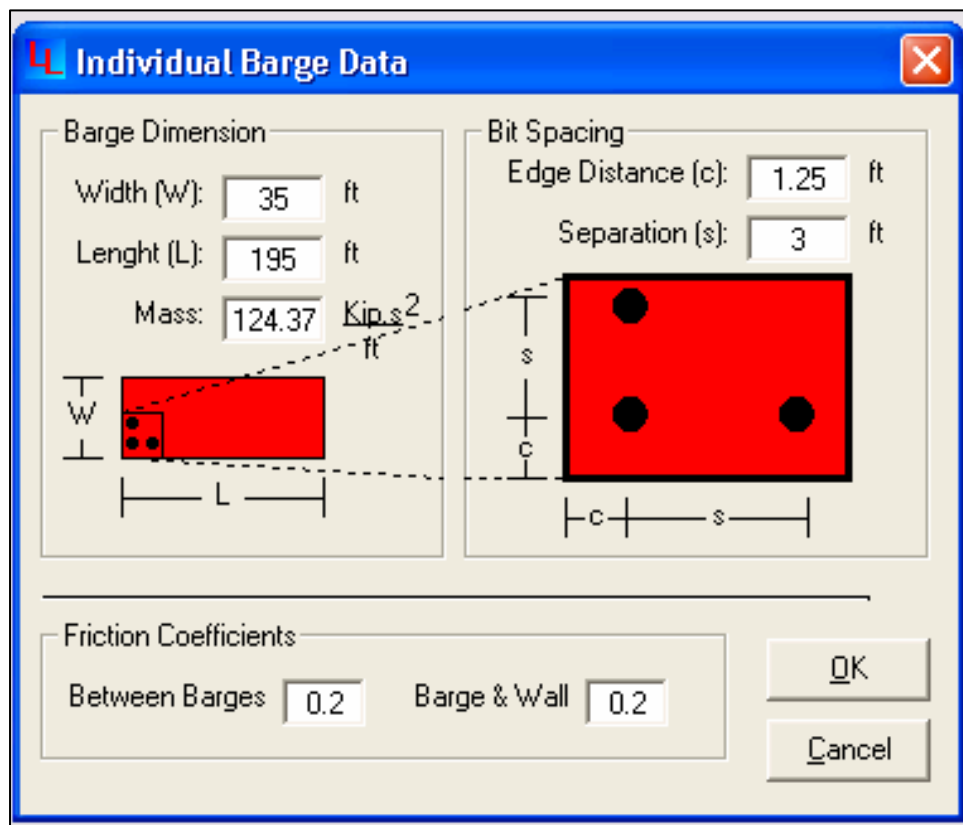
E.11.4 Step 4

Define the barge train layout. For this example, there are five barges in the local x-direction and three barges in the local y-direction. Input values for the

Hydrodynamics Added Mass Coefficient. If the mass of any barge needs to be changed, change it in the table in the lower left corner of the screen. Then click **OK**.

E.11.5 Step 5

Define the failure mechanism. This example uses the transverse mechanism. The approach angle was fixed in Step 2. Now it is necessary to establish the lashing configuration. At this moment, Limit_LASHING will determine the position of the pivot point as explained in Chapter 3, Section 3.2, of this report. That point is a blinking dot in the diagram. Please wait until the dot stops blinking and stays red to continue entering the data. The following screen shows System 1 in green and System 2 in red. The joints that form the failure plane are also shown.

Joints at failure plane

Selected Failure Mechanism
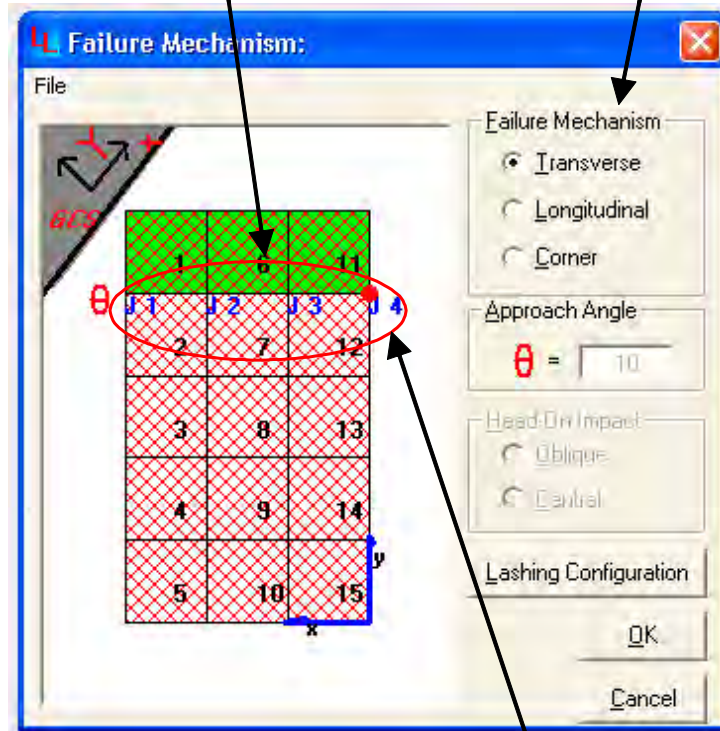
Pivot Point (Red dot)

E.11.6 Step 6

Now to establish the lashing configuration, click on the button **Lashing Configuration** in the screen of the previous step. For this example, taken from the Appendix A typical configuration, there are nine lashings. Then the table at the bottom of the screen prepares nine rows for the information for the lashings. Remember that the lashings at joint 4 are not considered in the analysis because it is the pivot point.

Click to assign mechanical properties
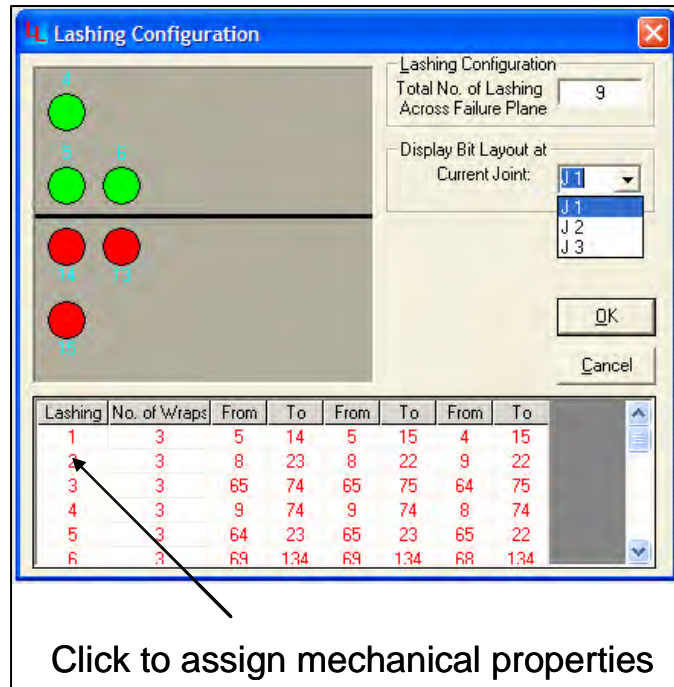
Clicking on the lashing number enables the definition of the mechanical properties of the selected lashing. After the properties of the lashing are defined, then define the number of wraps of the lashing. Remember that the configuration is always defined from System 1 to System 2.
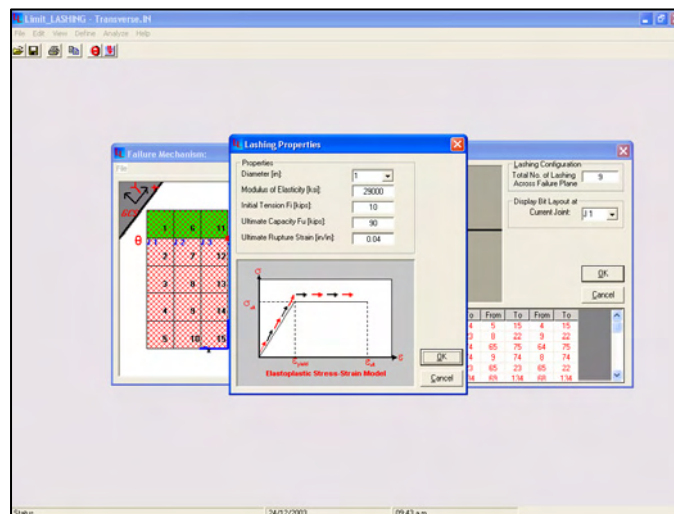
E.11.7 Step 7

Then analyze the system by pressing the **Run** button and obtain the results. This screen gives the results and graphs of **Stress vs. Strain** and **Internal Load vs. Elongation** for each lashing.
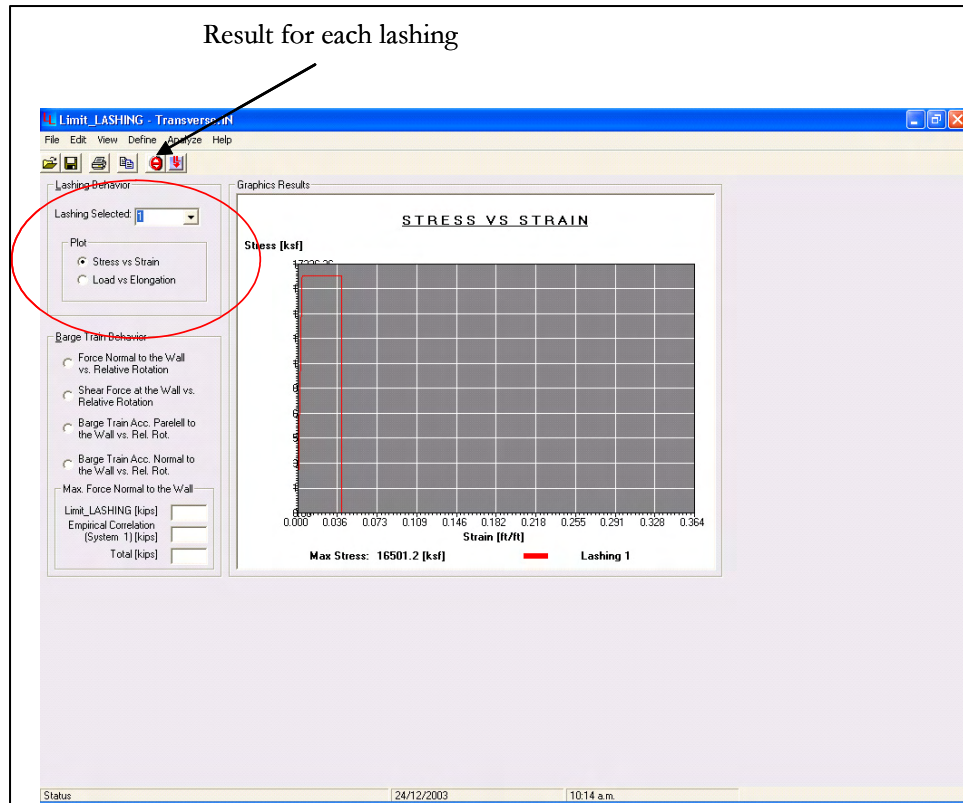
This same screen gives the results of the system.

The results for the transverse failure mechanism are as follows:

1. Force Normal to the Wall vs. Relative Rotation.

2. Shear Force at the Wall vs. Relative Rotation.

3. Barge Train Acceleration Parallel to the Wall vs. Relative Rotation. (System one + System two)

4. Barge Train Acceleration Normal to the Wall vs. Relative Rotation. (System two)

In the lower left corner appears the maximum force normal to the wall calculated by the empirical correlation for barge System 1 and presented in Arroyo, Ebeling, and Barker (2003), the lashing contribution as discussed in this report, and the total normal force on the wall.

Maximum Normal Forces
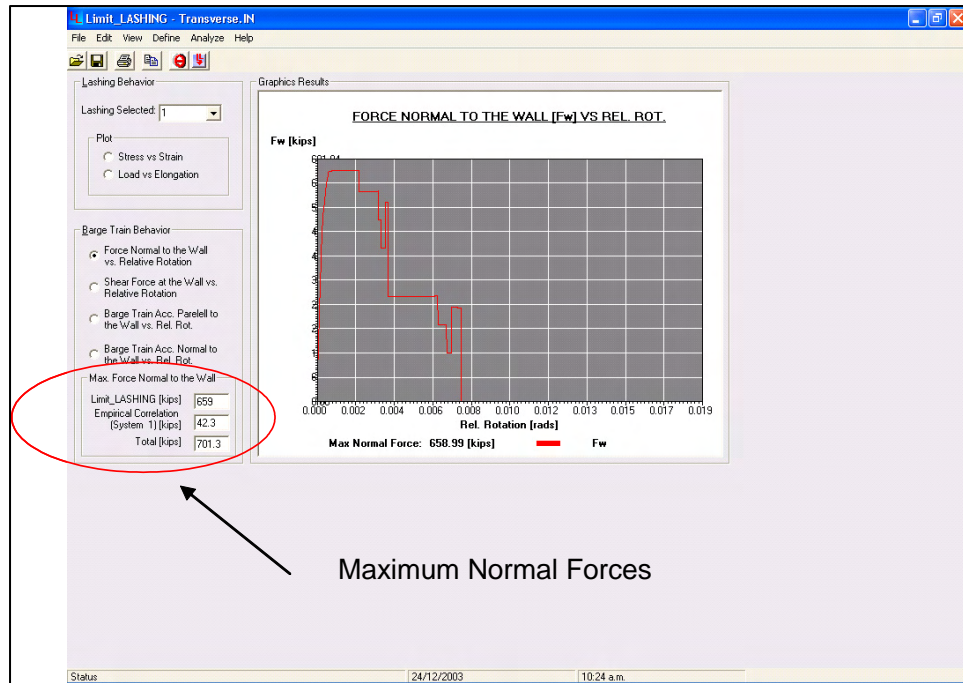
E.12 Step-by-Step Example for the Longitudinal Failure Mechanism

An example of a 15-barge train is presented for the longitudinal failure mechanism. Each of these barges has a width of 35 ft, a length of 195 ft, and a mass of 124.37 kips-sec^2/ft. The bits have an edge distance of 1.25 ft and 3 ft of separation. The approach angle is 80 degrees with a velocity of 1.5 ft/sec in the local x barge direction and zero in the local y barge direction. The barge-to-barge kinetic coefficients of friction are 0.2 and 0.2 for barge to wall.

E.12.1 Step 1

Open the Limit_LASHING program and wait until the main window is displayed.
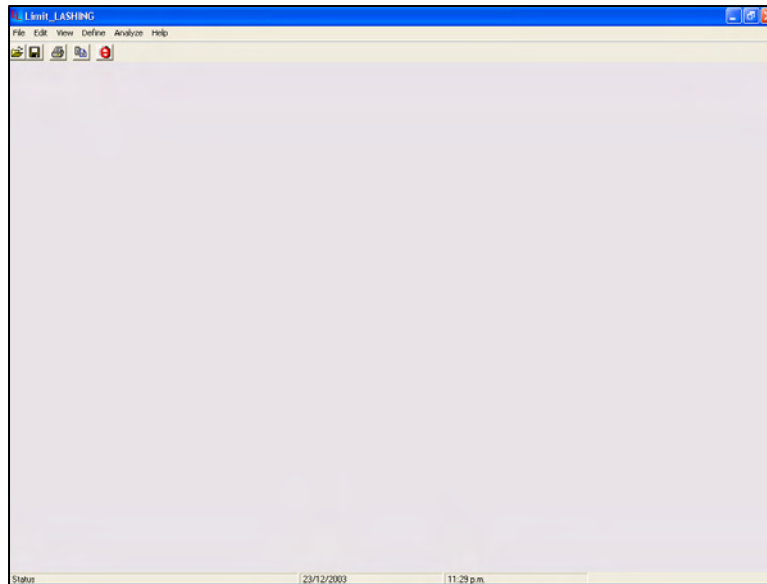
E.12.2 Step 2

Select the **Approach Angle** button and define the approach angle and the approach velocity. Then, click the **OK** button.
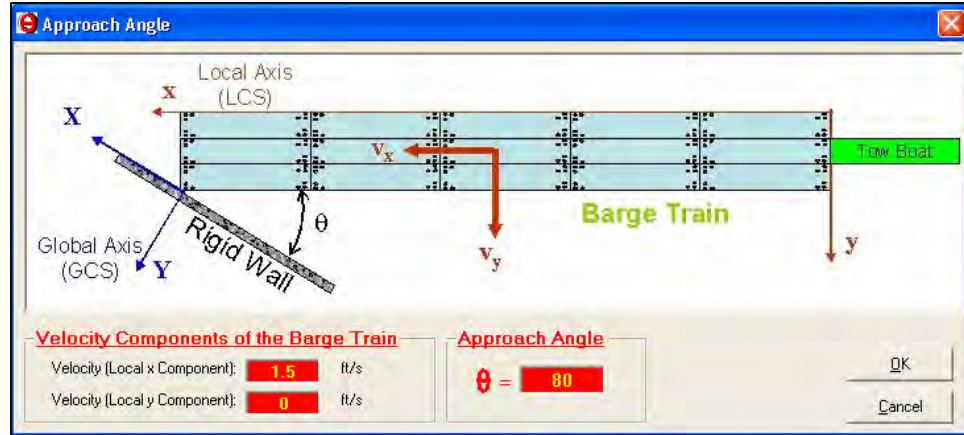
E.12.3 Step 3

Define the properties of the barge and the coefficient of friction.
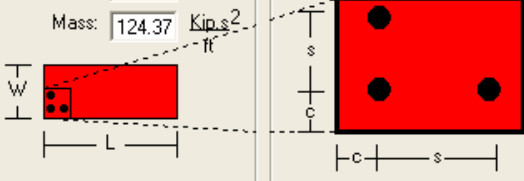
E.12.4 Step 4

Define the barge train layout. This example has five barges in the local x-direction and three in the local y-direction. Input values for the **Hydrodynamics Added Mass Coefficient**. If the mass of any barge needs to be changed, it can be changed in the table that is presented in the lower left corner of the screen. Then click **OK**.
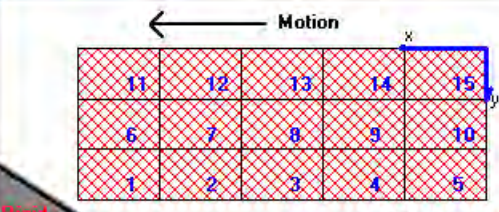
E.12.5 Step 5

Define the failure mechanism. This example uses the longitudinal failure mechanism. The approach angle was fixed in Step 2. Now it is necessary to establish the lashing configuration. The following screen shows System 1 in green and System 2 in red. The joints that form the failure plane are also shown.

Selected Failure Mechanism

Joints at failure plane
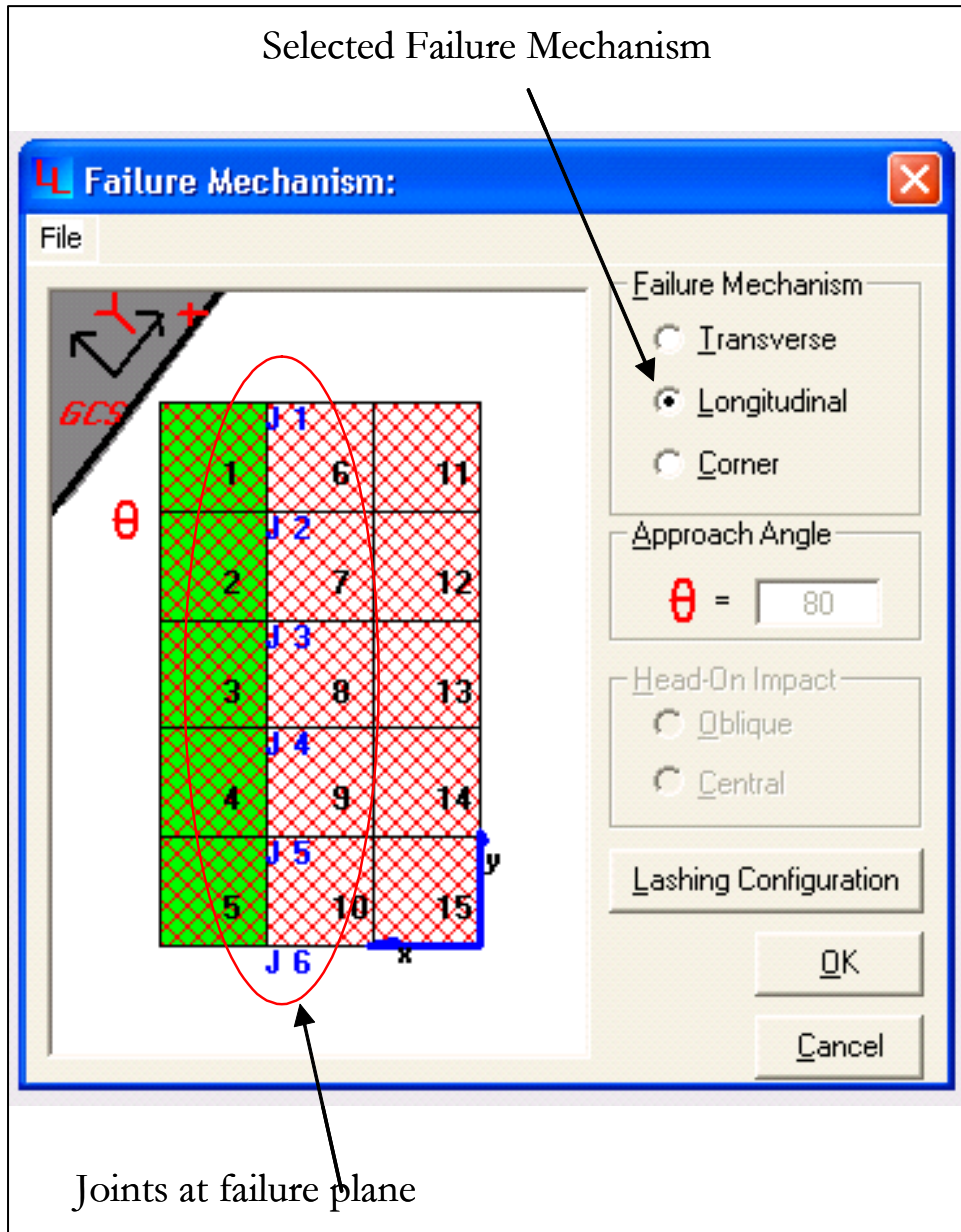
E.12.6 Step 6

Now to establish the lashing configuration, click on the button **Lashing Configuration** in the screen of the previous step. For this example, taken from

the typical configuration in Appendix A, there are 18 lashings. Then the table at the bottom of the screen prepares 18 rows for the lashing information.
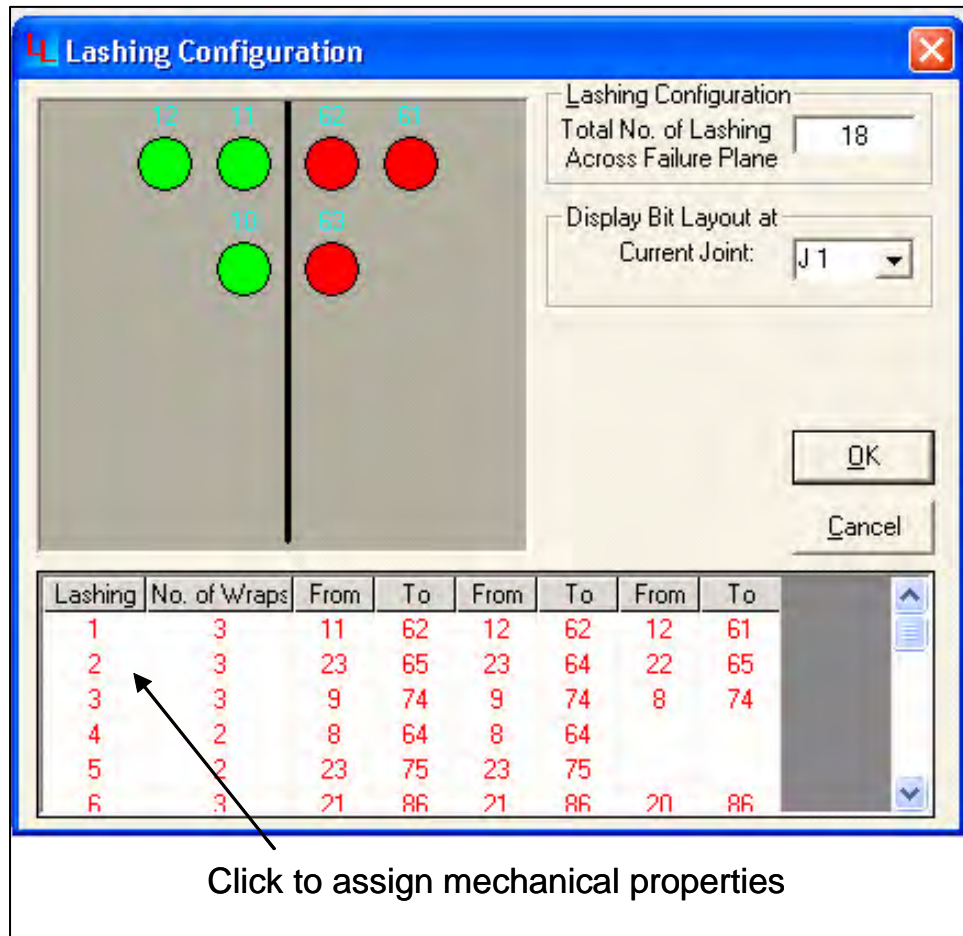
Click to assign mechanical properties

Clicking on the lashing number enables the definition of the mechanical properties of the selected lashing. After defining the mechanical properties of the lashing, define the number of wraps for the lashing. Remember that the configuration is always defined from System 1 to System 2.
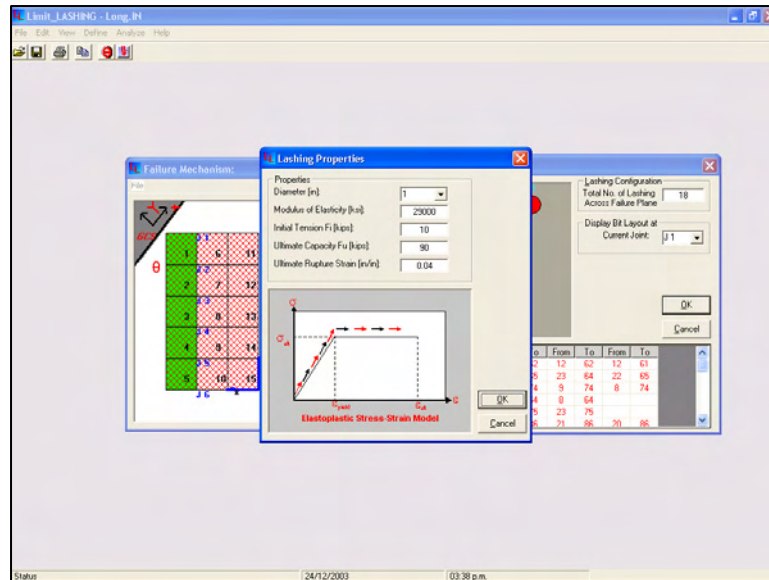
E.12.7 Step 7

Then analyze the system by pressing the **Run** button and obtain the results. This screen gives the results and graphs of **Stress vs. Strain** and **Internal Load vs. Elongation** for each lashing.

Result for each lashing
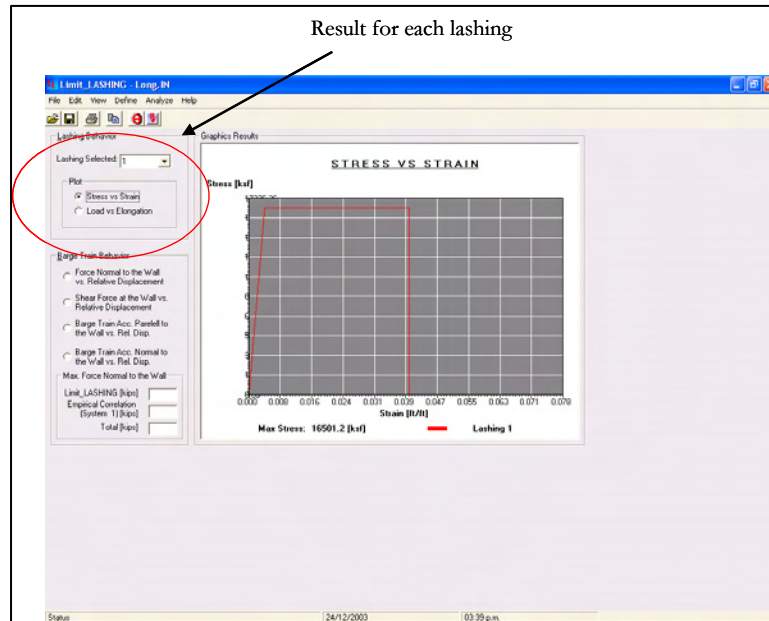
This same screen gives the results of the system.

The results for the longitudinal failure mechanism are as follows:

1. Force Normal to the Wall vs. Relative Displacement (Displacement of System two relative to System one).

2. Shear Force at the Wall vs. Relative Displacement.

3. Barge Train Acceleration Parallel to the Wall vs. Relative Displacement. (System one + System two)

4. Barge Train Acceleration Normal to the Wall vs. Relative Displacement. (System two)

In the lower left corner appears the maximum force normal to the wall calculated by the empirical correlation for barge System 1 and presented in Arroyo, Ebeling, and Barker (2003), the lashing contribution as discussed in this report, and the total normal force on the wall.
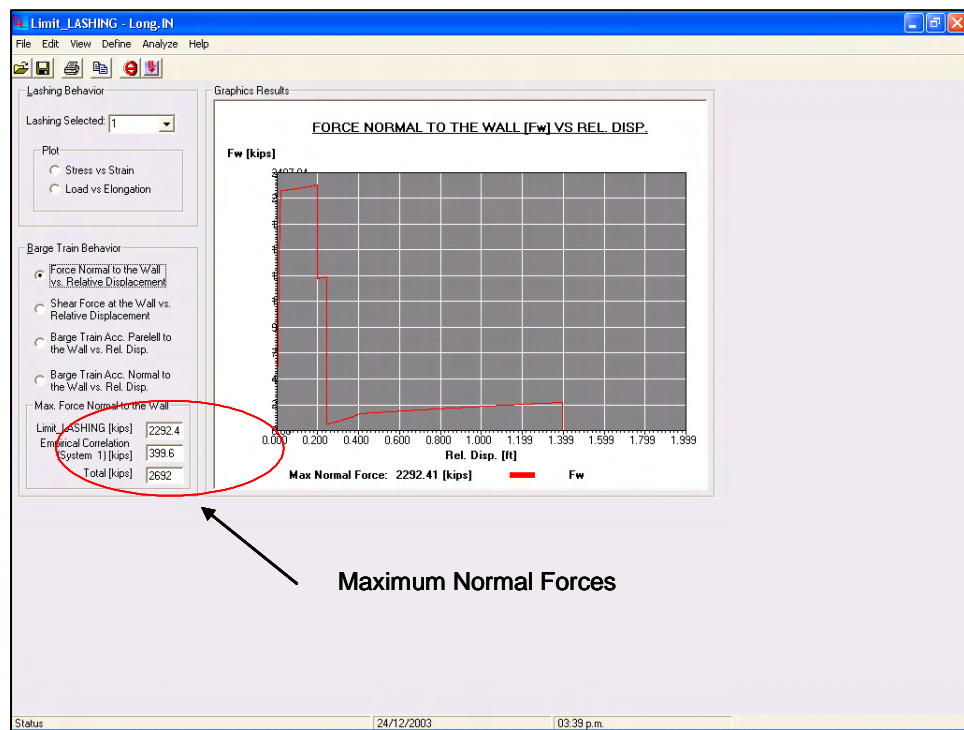

E.12.8 Special Cases in Longitudinal Failure Mechanism

In the longitudinal failure mechanism there exist two special cases. These cases are produced if the approach angle is 90 degrees. These cases are the oblique collision and the central collision. In the oblique impact, the line of action of the normal force at the wall does not pass through the center of mass of the barge train, thus producing one failure plane. In the central impact the line of action of the normal force at the wall passes through the center of mass of the barge train, thus producing two failure planes. In general, these two cases can happen when a barge train impacts a cell or nose pier structure. It is important to explain that if the system has only two columns of barges, the central mechanism is not possible. Also, when the lashing configuration is defined, only the lashing

of one plane of failure should be defined. The program assumes the same lashing configuration for the second failure plane (when present).

The Transverse and Corner failure mechanism button will be disabled if the approach angle is 90 degrees. It is physically impossible to produce these two failure mechanisms during a direct impact to the wall.

One Failure Plane   Oblique Impact Case

Joints at Failure Plane

Two Failure Planes

Central Impact Case

Joints at Failure Plane: Assume the Same configuration for both failure planes.
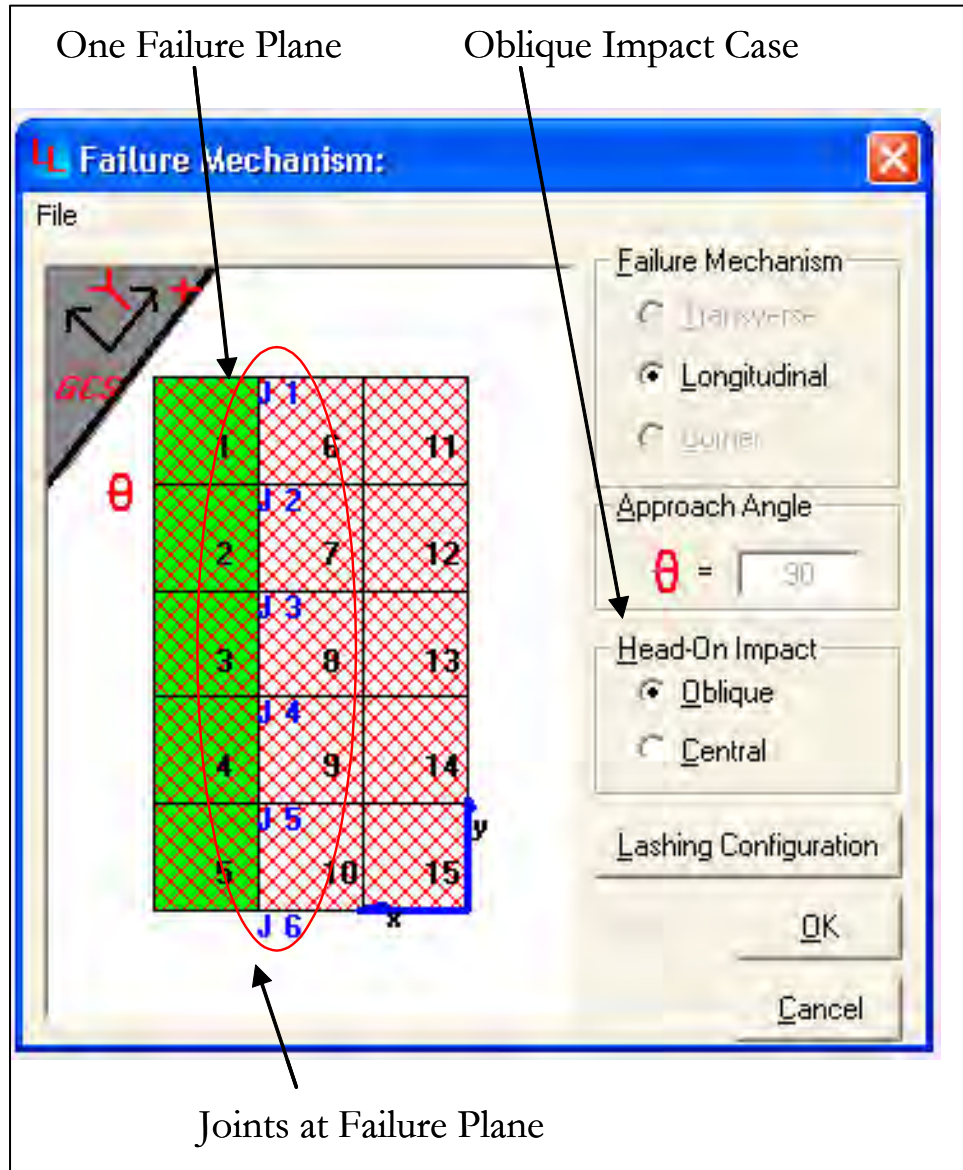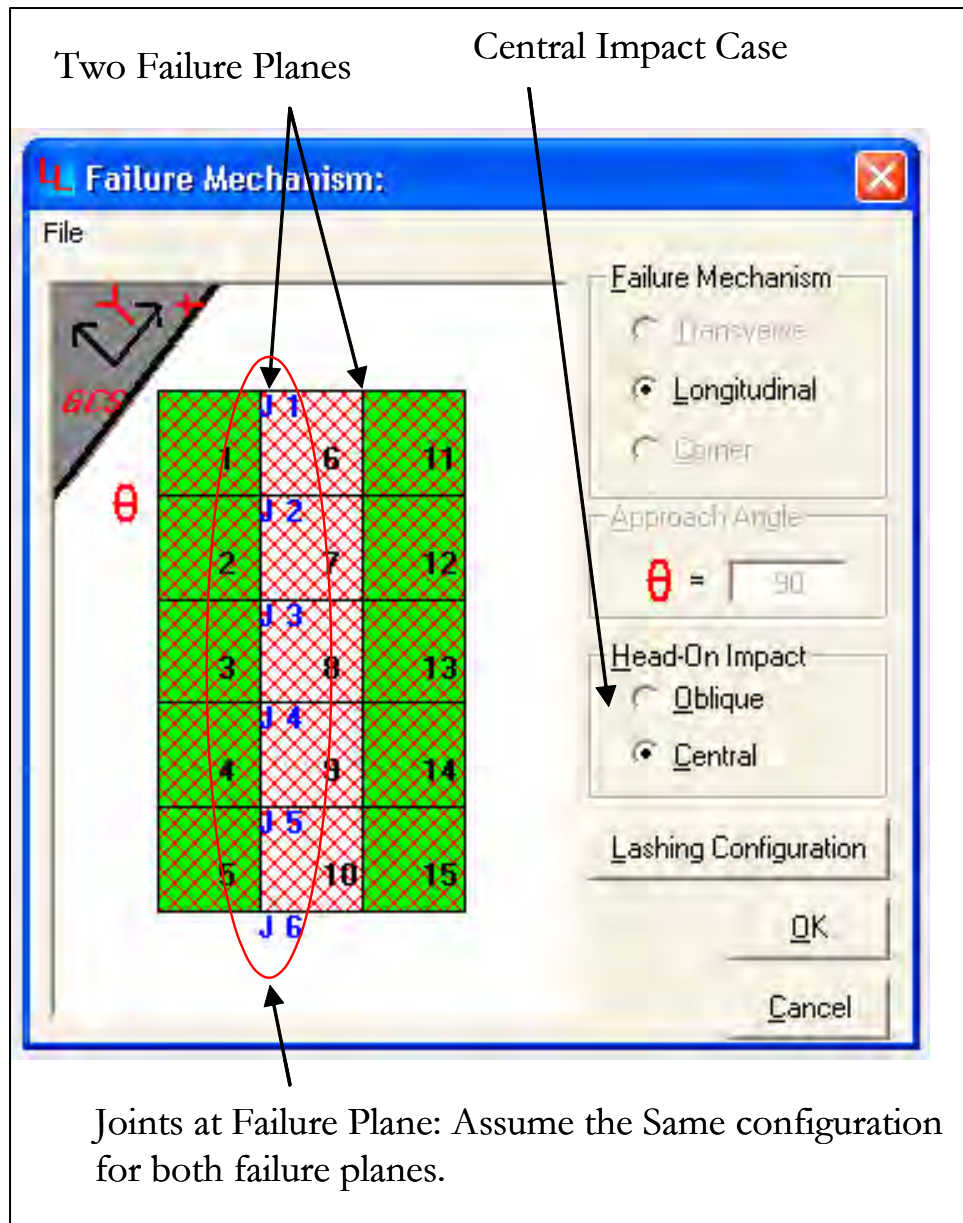
The results of these cases are the same as those of the previous example but without shear force at the wall and the acceleration parallel to the wall vs. relative displacement because these cases are associated with a direct impact process and no impact responses are assumed to occur parallel to the wall.

The following results are presented:

1. Force Normal to the Wall vs. Relative Displacement (Displacement of System two relative to System one).

2. Barge Train Acceleration Normal to the Wall vs. Relative Displacement.

In the left corner appear the maximum impact force normal to the wall calculated by the empirical correlation presented in Arroyo, Ebeling, and Barker (2003), the lashing contribution as shown in this report, and the total force normal to the wall.

Disable Result for Longitudinal Special Cases
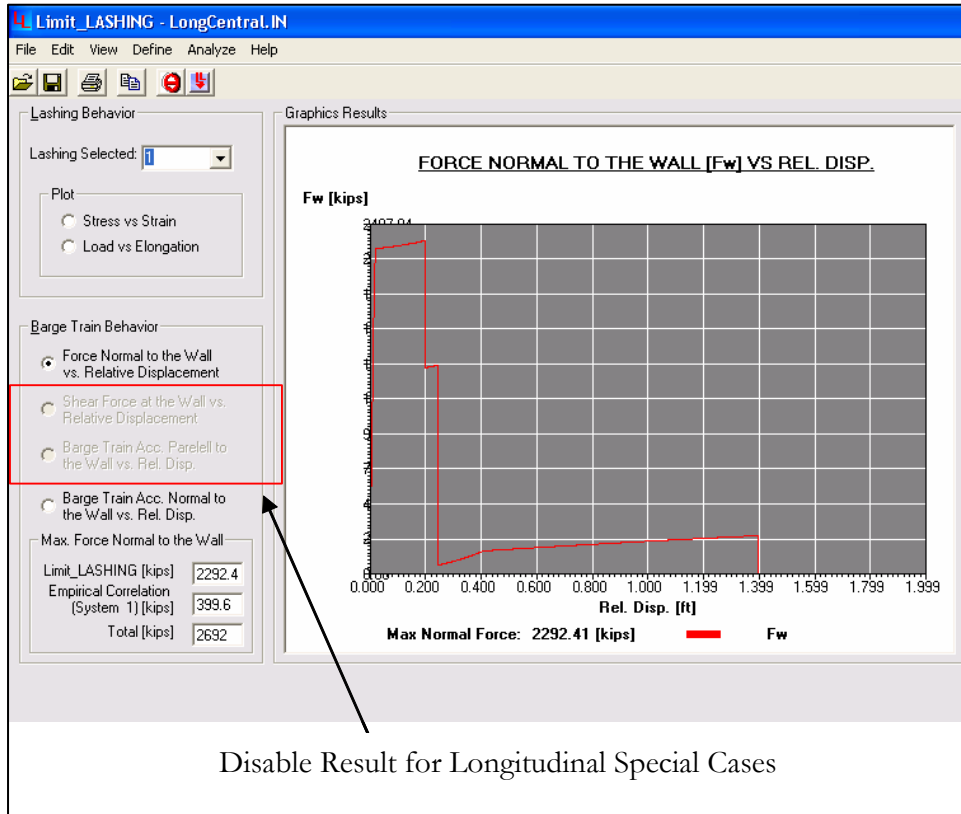
E.13 Step-by-Step Example for the Corner Failure Mechanism

An example of a 15-barge train is presented for the corner failure mechanism. Each of these barges has a width of 35 ft, a length of 195 ft, and a mass of 124.37 kips-sec^2/ft. The bits have an edge distance of 1.25 ft and 3 ft of separation. The approach angle is 10 degrees with a velocity of 1.5 ft/sec in the local x barge direction and zero in the local y barge direction. The barge-to-barge kinetic coefficients of friction are 0.2 and 0.2 for barge to wall.

E.13.1 Step 1

Open the Limit_LASHING program and wait until the main window is displayed.
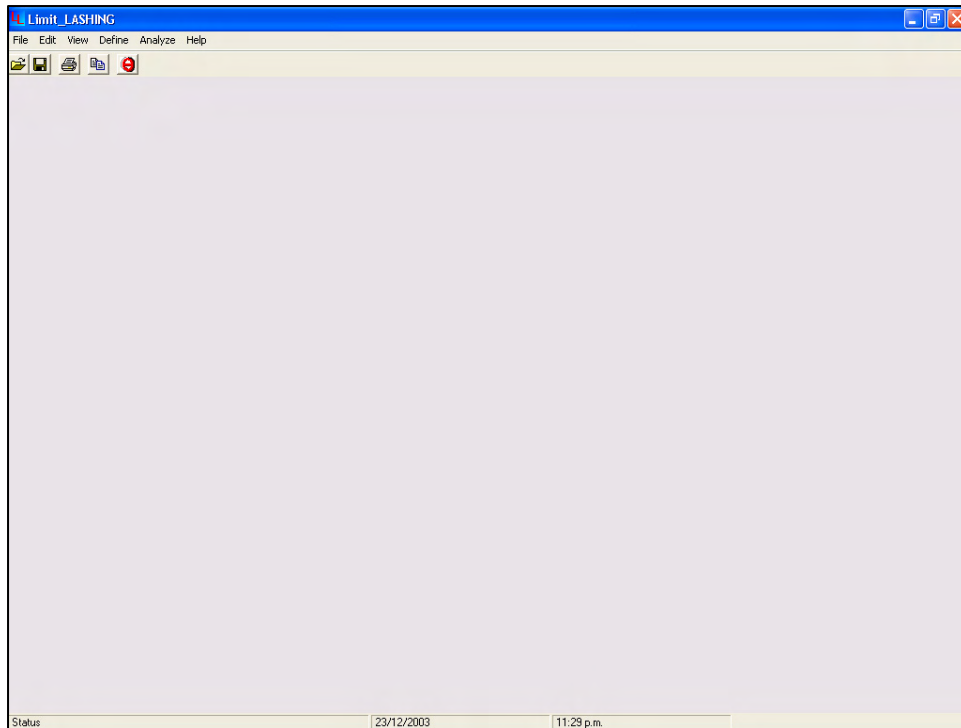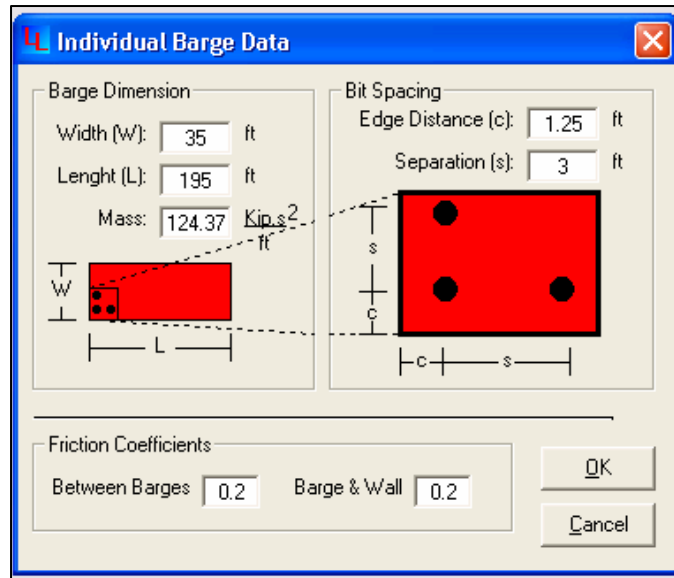
E.13.2 Step 2

Select the **Approach Angle** button and define the approach angle and the approach velocity. Then, click the **OK** button.
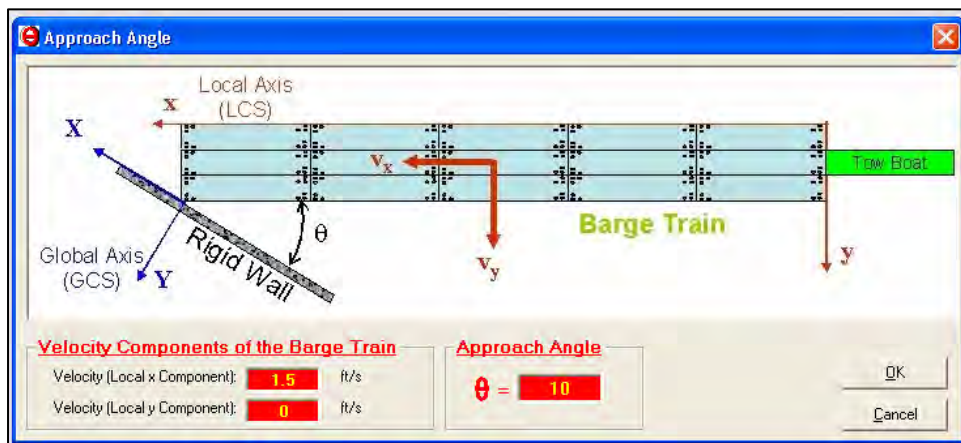
E.13.3 Step 3

Define the properties of the barge and the coefficient of friction.
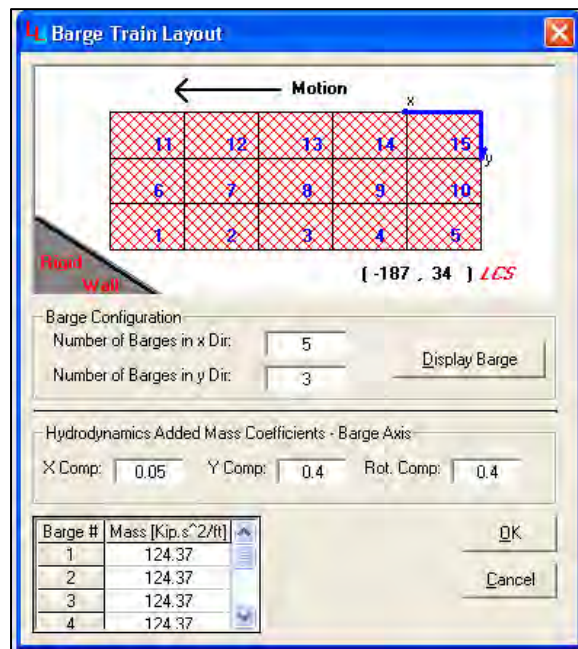
E.13.4 Step 4

Define the barge train layout. This example has five barges in the local x-direction and three barges in the local y-direction. Input values for the **Hydrodynamics Added Mass Coefficient**. If the mass of any barge needs to be changed, change it in the table that is presented in the lower left corner of the screen. Then click **OK**.

E.13.5 Step 5

Define the failure mechanism. In this example select the corner mechanism. The angle of approach was fixed in Step 2. Now it is necessary to establish the lashing configuration. The following screen shows System 1 in green and System 2 in red. The joints that form the failure plane are also shown.
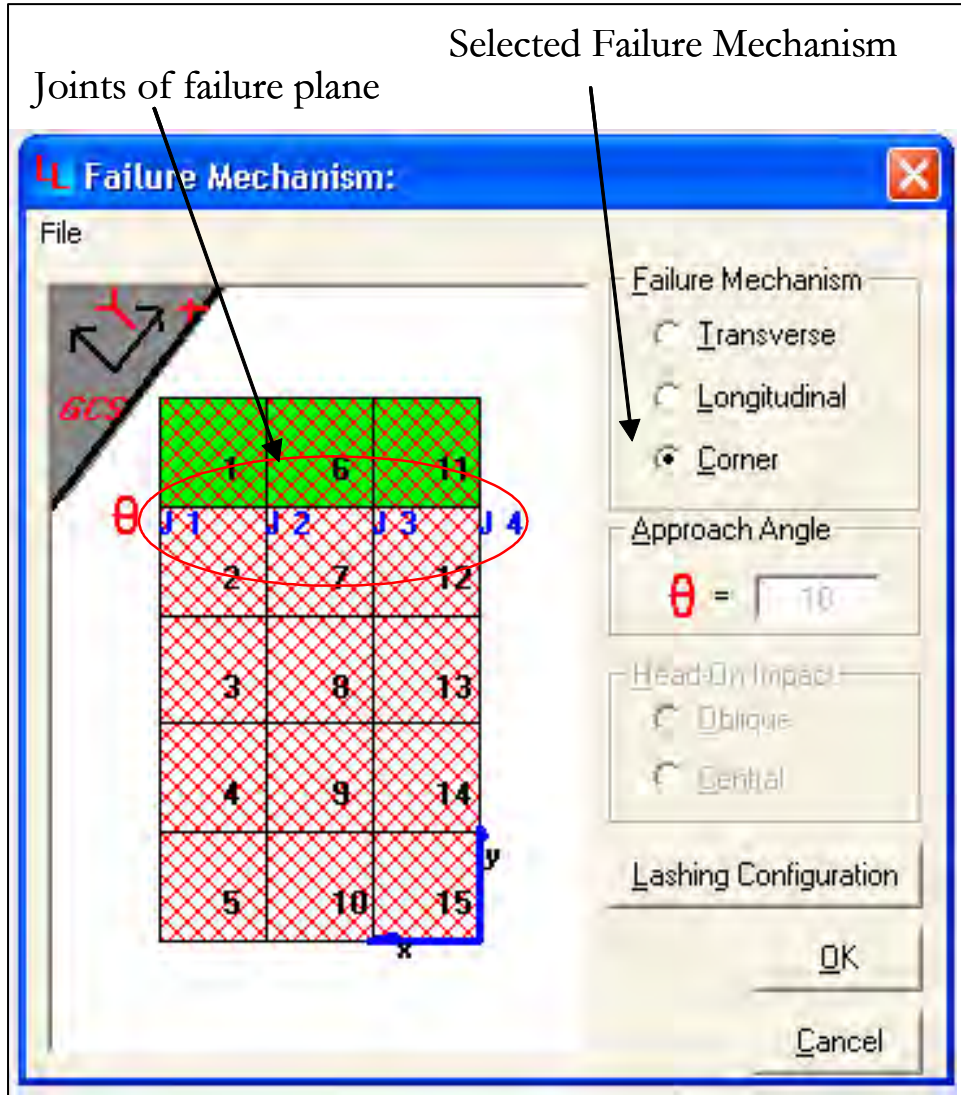
E.13.6 Step 6

Now to establish the lashing configuration, click the button **Lashing Configuration** in the screen of the previous step. This example, taken from the typical configuration shown in Appendix A, uses 10 lashings. The table in the bottom of the screen prepares 10 rows for the lashing information. This failure mechanism is believed to be a more realistic model than the transverse failure mechanism alone. In the transverse failure mechanism presented in Chapter 3, barge System 1 in contact with the wall was considered as a single rigid body; no

local rotation was allowed to occur. In this potential failure mechanism, designated the corner failure mechanism, local rotation of the corner barge within System 1 is allowed. Remember that the lashings at joint 4 are not considered in the analysis because it is the pivot point.

This failure mechanism is defined by the *L* shape of the two sides that join the corner barge to the remaining barge train. In the box labeled **Corner Lashings**, specify the number of lashings that connect the corner barge to the rest of the system. This example uses four lashings to connect the corner barge to the rest of the barge train. For this reason the first four lashings in the table of input data are for these four lashings. The first *n* lashings in the data input table are the *n* lashings that connect the corner barge to the rest of the barge train. For all lashings the mode in which they act needs to be indicated. Mode was defined as a number that associates each lashing to a specific failure plane. If Mode equals one, these lashings are assigned to act across the transverse failure plane. If Mode equals two, this lashing is assigned to act across the plane between the corner barge and the remaining barges of System 1. In general, a reduced number of lashings are used between the corner barge and the rest of the barges in System 1. For this reason, Mode = 2 appears only in a few cells at the end column of this table.

Clicking on the lashing number box enables the definition of the mechanical properties of the selected lashing. After defining the mechanical properties of the lashing, define the number of wraps for the lashing. Remember that the configuration is always defined from System 1 to System 2. However, the lashings that act between the corner barge and the rest of the barges in System one (MODE = 2) have to be defined starting from the corner barge and ending at the remaining barges of System 1. In this case, the user has to define the lashing from a green bit (8) to another green bit (64), because all the bits in System 1 are green, as shown in the next screen.
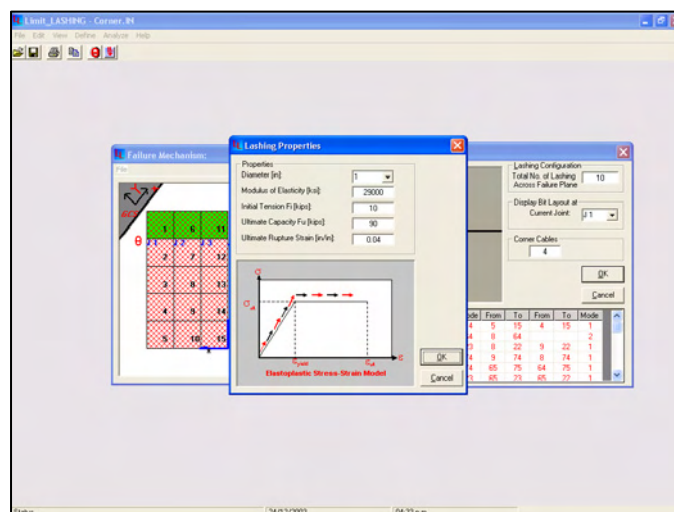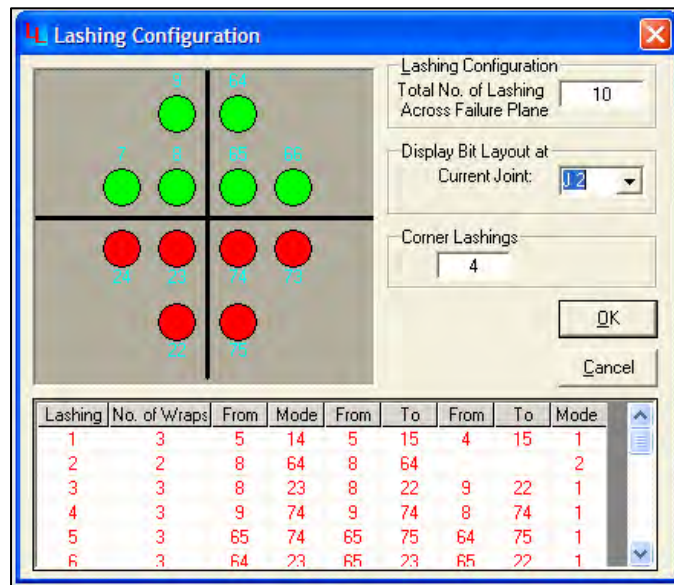
E.13.7 Step 7

Analyze the system using the **Run** button and obtain the results. In this screen the results and graphs of **Stress vs. Strain**, and **Internal Load vs. Elongation** for each lashing can be obtained.
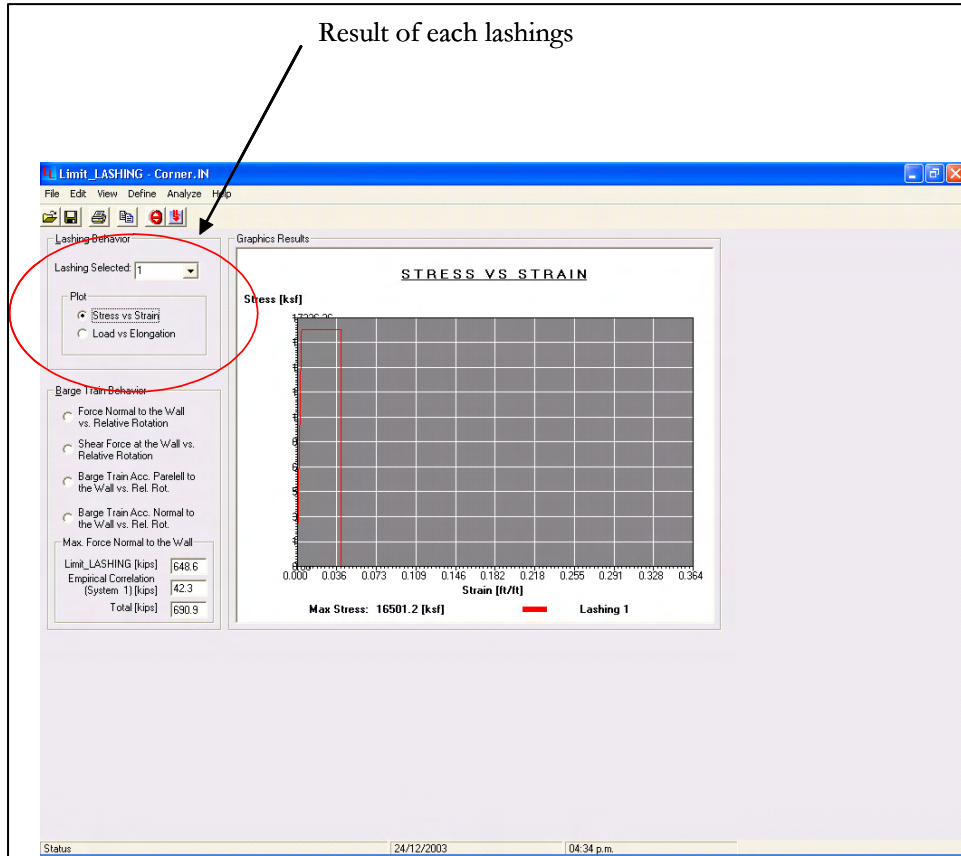

This same screen gives the results of the system.

The following results for the corner failure mechanism are given:

1. Force Normal to the Wall vs. Relative Rotation.

2. Shear Force at the Wall vs. Relative Rotation.

3. Barge Train Acceleration Parallel to the Wall vs. Relative Rotation. (System one + System two)

4. Barge Train Acceleration Normal to the Wall vs. Relative Rotation. (System two)

In the lower left corner appears the maximum force normal to the wall calculated by the empirical correlation for barge System 1 and presented in Arroyo, Ebeling, and Barker (2003), the lashing contribution as discussed in this report, and the total normal force on the wall.

Maximum Forces
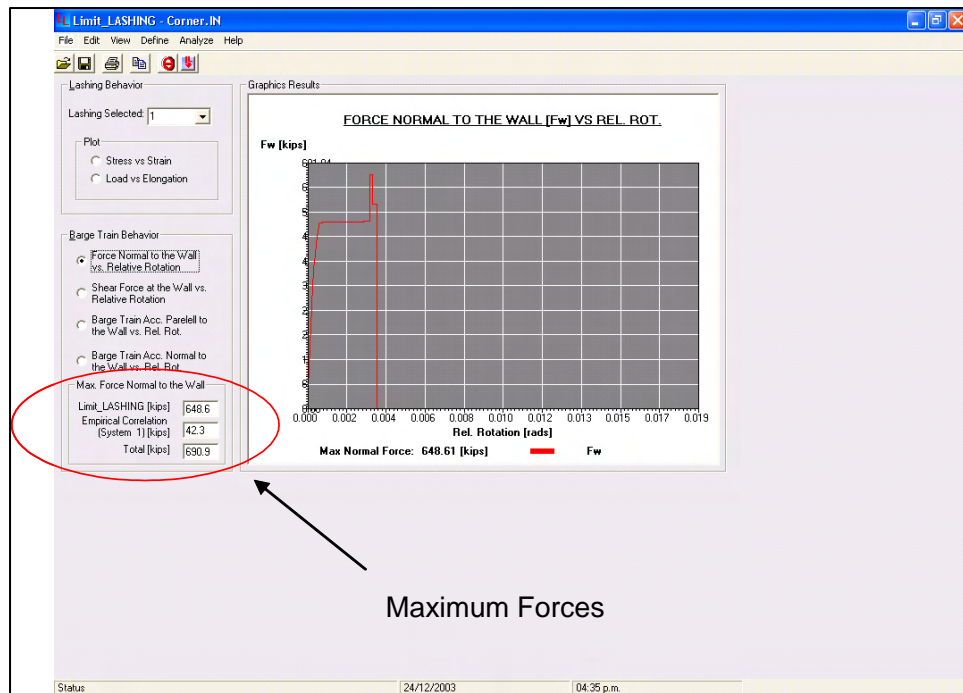
E.14 ASCI Files Descriptions

Some examples of the ASCI file submitted to the FORTRAN code of the Limit_LASHING computer program are presented in this section. The Windows preprocessor of Limit_Lashing generates additional data not described in this section. This additional information does not affect the use of the FORTRAN executable program. This additional information is the following: number of barges in the local x- and y-directions, barge dimensions in the local x- and y-directions, mass of one barge, bits edge distance and separation, and mass of each barge. Remember, these data do not affect the FORTRAN program.

E.14.1 Description of input user's guide for the transverse failure mechanism

The input file that uses the program to calculate F_w in the wall is written in ASCI file. This is an example of the components that are in the input file.

    a. Line 1: Number of cases that will be analyzed. For the transverse failure mechanism this number is equal to 1.

    b. Line 2: Number of bits that contain the barge system.

    c. Line 3: From this line recollect the geometrical information for the bits. To run the program, it is necessary to complete (number of bits) lines beginning from line 3. This case has 180 bits; therefore there is information from line 3 to line 183.

        (1) *Columns #1:* Bit number.
        (2) *Columns #2:* Local x-coordinates of bit.
        (3) *Columns #3:* Local y-coordinates of bit.
   d. Line 184: Number of lashing that acts across the idealized failure plane.

   e. Line 185: This line contains the properties description of the lashing. Now the input file has *n* lines, to describe each lashing. This example uses nine lashings; for this reason there are nine lines used to describe the lashings. From line 185 to 193 is presented the lashing information as specified in Line 184. The description is in the following format:
        (1) *Columns #1:* Number of times that the lashing crosses the failure plane.
        (2) *Next 2n wraps columns:* This gives the form that the lashing was connected as specified in Appendix A. These lashings are specified from the barge system that impacts the wall to the barge system that does not impact the wall. For this example, the first lashing has three wraps, and then six numbers. The order is the following: starting bit from System 1 to end bit at System 2. The user has to repeat this scheme two more times to account for the amount of wraps.This is the reason six numbers are specified for the connectivity.
        (3) *Columns # 8:* Diameter of the lashing in feet.
        (4) *Columns # 9:* Modulus of elasticity of the lashing in ksi.
        (5) *Columns #10:* Initial force in the lashing in kip.
        (6) *Columns #11:* Maximum force that the lashing can reach in kip.
        (7) *Columns #12:* Maximum strain in the lashing.

   f. Line 194: This line contains the description of the system.
        (1) *Columns #1:* Approach angle of barge train in degrees.
        (2) *Columns #2:* M1 = Total mass of barge system (without hydrodynamic added mass).
        (3) *Columns #3:* M2 = Mass of barge System 1 that impacts the wall (without hydrodynamic added mass).
        (4) *Columns #4:* Coefficient of friction between the wall and barge train.
        (5) *Columns #5:* Coefficient of friction between barges.
        (6) *Columns #6:* Velocity of barge train in local x-direction.
        (7) *Columns #7:* Velocity of barge train in local y-direction.

   g. Line 195: This line contains the hydrodynamic added mass coefficients to consider the effect of water during impact.
        (1) Columns #1: Hydrodynamic added mass coefficient in local x-direction.
        (2) Columns #2: Hydrodynamic added mass coefficient in local y-direction.
        (3) Columns #3: Hydrodynamic added mass coefficient due to rotational effects.

E.14.2 Example of input user's guide to transverse case

1
180
1 3   3.25

```
2 3        1.25
3 5        1.25
4 190      1.25
5 192      1.25
6 192      3.25
7 192      31.25
8 192      33.75
9 190      33.75
10 5       33.75
11 3       33.75
12 3       31.25
13 198     3.25
14 198     1.25
15 200     1.25
16 385     1.25
17 387     1.25
18 387     3.25
19 387     31.25
20 387     33.75
21 385     33.75
22 200     33.75
23 198     33.75
24 198     31.25
25 393     3.25
26 393     1.25
27 395     1.25
28 580     1.25
29 582     1.25
30 582     3.25
31 582     31.25
32 582     33.75
33 580     33.75
34 395     33.75
35 393     33.75
36 393     31.25
37 588     3.25
38 588     1.25
39 590     1.25
40 775     1.25
41 777     1.25
42 777     3.25
43 777     31.25
44 777     33.75
45 775     33.75
46 590     33.75
47 588     33.75
48 588     31.25
49 783     3.25
50 783     1.25
51 785     1.25
```

52	970	1.25
53	972	1.25
54	972	3.25
55	972	31.25
56	972	33.75
57	970	33.75
58	785	33.75
59	783	33.75
60	783	31.25
61	3	38.25
62	3	36.25
63	5	36.25
64	190	36.25
65	192	36.25
66	192	38.25
67	192	66.25
68	192	68.75
69	190	68.75
70	5	68.75
71	3	68.75
72	3	66.25
73	198	38.25
74	198	36.25
75	200	36.25
76	385	36.25
77	387	36.25
78	387	38.25
79	387	66.25
80	387	68.75
81	385	68.75
82	200	68.75
83	198	68.75
84	198	66.25
85	393	38.25
86	393	36.25
87	395	36.25
88	580	36.25
89	582	36.25
90	582	38.25
91	582	66.25
92	582	68.75
93	580	68.75
94	395	68.75
95	393	68.75
96	393	66.25
97	588	38.25
98	588	36.25
99	590	36.25
100	775	36.25
101	777	36.25

```
102 777      38.25
103 777      66.25
104 777      68.75
105 775      68.75
106 590      68.75
107 588      68.75
108 588      66.25
109 783      38.25
110 783      36.25
111 785      36.25
112 970      36.25
113 972      36.25
114 972      38.25
115 972      66.25
116 972      68.75
117 970      68.75
118 785      68.75
119 783      68.75
120 783      66.25
121 3        73.25
122 3        71.25
123 5        71.25
124 190      71.25
125 192      71.25
126 192      73.25
127 192      101.25
128 192      103.75
129 190      103.75
130 5        103.75
131 3        103.75
132 3        101.25
133 198      73.25
134 198      71.25
135 200      71.25
136 385      71.25
137 387      71.25
138 387      73.25
139 387      101.25
140 387      103.75
141 385      103.75
142 200      103.75
143 198      103.75
144 198      101.25
145 393      73.25
146 393      71.25
147 395      71.25
148 580      71.25
149 582      71.25
150 582      73.25
151 582      101.25
```

```
152 582        103.75
153 580        103.75
154 395        103.75
155 393        103.75
156 393        101.25
157 588        73.25
158 588        71.25
159 590        71.25
160 775        71.25
161 777        71.25
162 777        73.25
163 777        101.25
164 777        103.75
165 775        103.75
166 590        103.75
167 588        103.75
168 588        101.25
169 783        73.25
170 783        71.25
171 785        71.25
172 970        71.25
173 972        71.25
174 972        73.25
175 972        101.25
176 972        103.75
177 970        103.75
178 785        103.75
179 783        103.75
180 783        101.25
9
3 179 164 179 165 178 165 0.08333 4176000.0 20.0 90.0 0.05
3 170 161 170 160 171 160 0.1041666 4176000.0 20.0 120.0 0.05
3 171 104 170 104 171 104 0.1041666 4176000.0 20.0 120.0 0.05
3 119 104 119 105 118 105 0.1041666 4176000.0 20.0 120.0 0.05
3 118 161 119 161 118 161 0.1041666 4176000.0 20.0 120.0 0.05
3 110 101 110 100 111 100 0.1041666 4176000.0 20.0 120.0 0.05
3 59 44 59 45 58 45 0.1041666 4176000.0 20.0 120.0 0.05
3 111 44 110 44 111 44 0.1041666 4176000.0 20.0 120.0 0.05
3 58 101 58 101 59 101 0.1041666 4176000.0 20.0 120.0 0.05
10.0 1865.59 373.118 0.2 0.2 1.4 0.0
0.05 0.4 0.4
```

E.14.3 Description of input user's guide for the longitudinal failure mechanism

The input file that uses the program to calculate F_w in the wall is written in ASCI file. This is an example of the components that are in the input file.

    a. Line 1: Number of case that will be analyzed. For the longitudinal failure mechanism this is equal to 2. For special cases, use 4 for oblique case and use 5 for central case.

b. Line 2: Number of bits that contain the barge system.

c. Line 3: From this line recollect the geometrical information for the bits. To run the program, it is necessary to complete (number of bits) lines beginning from line 3. This case has 180 bits; for this reason there is information from line 3 to line 183.
   (1) *Columns #1:* Bit number.
   (2) *Columns #2:* Local x-coordinates of bit.
   (3) *Columns #3:* Local y-coordinates of bit.

d. Line 184: Number of lashings acting across the idealized failure plane. If there is the central impact, a special case (line 1 = 5) is necessary to include the lashings for the two failure planes.

e. Line 185: This line contains the properties description of the lashing. Now the input file has *n* lines, to describe each lashing. This example has 18 lashings; for this reason 18 lines are used to describe the lashings. Lines 185 to 202 present the lashing information as specified in Line 184. If the central impact case is analyzed, then the value equal to 18 becomes 36; two failure planes. The description is in the following format:
   (1) *Columns #1:* Number of times that the lashing crosses the failure plane.
   (2) *Next (2n wraps) columns:* Now find the form in which the lashing was connected as specified in Appendix A. These lashings are specified from the barge system that impacts the wall to the barge system that does not impact the wall. For this example, the first lashing has three wraps and six numbers. The order is the following: starting bit from System 1 to end bit at System 2. The user has to repeat this scheme two more times to account for the amount of wraps. This is the reason six numbers are specified for the connectivity.
   (3) *Columns # 8:* Diameter of the lashing in feet.
   (4) *Columns # 9:* Modulus of elasticity of the lashing in ksi.
   (5) *Columns #10:* Initial force in the lashing in kip.
   (6) *Columns #11:* Maximum force that the lashing can reach in kip.
   (7) *Columns #12:* Maximum strain in the lashing.

f. Line 203: This line contains the description of the system.
   (1) *Columns #1:* Approach angle of barge train in degrees.
   (2) *Columns #2:* M1 = Total mass of barge system (without hydrodynamic added mass).
   (3) *Columns #3:* M2 = Mass of barge System 1 that impacts the wall (without hydrodynamic added mass).
   (4) *Columns #4:* Coefficient of friction between the wall and barge train.
   (5) *Columns #5:* Coefficient of friction between barges.
   (6) *Columns #6:* Velocity of barge train in local x-direction.
   (7) *Columns #7:* Velocity of barge train in local y-direction.

g. Line 204: This line contains the hydrodynamic added mass coefficients to consider the effect of water during impact.

(1) *Columns #1*: Hydrodynamic added mass coefficient in local x-direction.
(2) *Columns #2*: Hydrodynamic added mass coefficient in local y-direction.
(3) *Columns #3*: Hydrodynamic added mass coefficient due to rotational effects.

E.14.4 Example of input user's guide to longitudinal case

```
2
180
1 3           3.25
2 3           1.25
3 5           1.25
4 190         1.25
5 192         1.25
6 192         3.25
7 192         31.25
8 192         33.75
9 190         33.75
10 5          33.75
11 3          33.75
12 3          31.25
13 198        3.25
14 198        1.25
15 200        1.25
16 385        1.25
17 387        1.25
18 387        3.25
19 387        31.25
20 387        33.75
21 385        33.75
22 200        33.75
23 198        33.75
24 198        31.25
25 393        3.25
26 393        1.25
27 395        1.25
28 580        1.25
29 582        1.25
30 582        3.25
31 582        31.25
32 582        33.75
33 580        33.75
34 395        33.75
35 393        33.75
36 393        31.25
37 588        3.25
38 588        1.25
39 590        1.25
```

40	775	1.25
41	777	1.25
42	777	3.25
43	777	31.25
44	777	33.75
45	775	33.75
46	590	33.75
47	588	33.75
48	588	31.25
49	783	3.25
50	783	1.25
51	785	1.25
52	970	1.25
53	972	1.25
54	972	3.25
55	972	31.25
56	972	33.75
57	970	33.75
58	785	33.75
59	783	33.75
60	783	31.25
61	3	38.25
62	3	36.25
63	5	36.25
64	190	36.25
65	192	36.25
66	192	38.25
67	192	66.25
68	192	68.75
69	190	68.75
70	5	68.75
71	3	68.75
72	3	66.25
73	198	38.25
74	198	36.25
75	200	36.25
76	385	36.25
77	387	36.25
78	387	38.25
79	387	66.25
80	387	68.75
81	385	68.75
82	200	68.75
83	198	68.75
84	198	66.25
85	393	38.25
86	393	36.25
87	395	36.25
88	580	36.25
89	582	36.25

```
90 582      38.25
91 582      66.25
92 582      68.75
93 580      68.75
94 395      68.75
95 393      68.75
96 393      66.25
97 588      38.25
98 588      36.25
99 590      36.25
100 775     36.25
101 777     36.25
102 777     38.25
103 777     66.25
104 777     68.75
105 775     68.75
106 590     68.75
107 588     68.75
108 588     66.25
109 783     38.25
110 783     36.25
111 785     36.25
112 970     36.25
113 972     36.25
114 972     38.25
115 972     66.25
116 972     68.75
117 970     68.75
118 785     68.75
119 783     68.75
120 783     66.25
121 3       73.25
122 3       71.25
123 5       71.25
124 190     71.25
125 192     71.25
126 192     73.25
127 192     101.25
128 192     103.75
129 190     103.75
130 5       103.75
131 3       103.75
132 3       101.25
133 198     73.25
134 198     71.25
135 200     71.25
136 385     71.25
137 387     71.25
138 387     73.25
139 387     101.25
```

```
140 387       103.75
141 385       103.75
142 200       103.75
143 198       103.75
144 198       101.25
145 393       73.25
146 393       71.25
147 395       71.25
148 580       71.25
149 582       71.25
150 582       73.25
151 582       101.25
152 582       103.75
153 580       103.75
154 395       103.75
155 393       103.75
156 393       101.25
157 588       73.25
158 588       71.25
159 590       71.25
160 775       71.25
161 777       71.25
162 777       73.25
163 777       101.25
164 777       103.75
165 775       103.75
166 590       103.75
167 588       103.75
168 588       101.25
169 783       73.25
170 783       71.25
171 785       71.25
172 970       71.25
173 972       71.25
174 972       73.25
175 972       101.25
176 972       103.75
177 970       103.75
178 785       103.75
179 783       103.75
180 783       101.25
18
3 122 71 122 71 122 72 0.08333 4176000.0 20.0 90.0 0.05
3 173 116 173 116 173 115 0.08333 4176000.0 20.0 90.0 0.05
2 124 68 124 68 0.104166 4176000.0 20.0 120.0 0.05
2 135 83 135 83 0.104166 4176000.0 20.0 120.0 0.05
3 134 69 135 68 134 68 0.104166 4176000.0 20.0 120.0 0.05
3 125 82 125 83 125 82 0.104166 4176000.0 20.0 120.0 0.05
2 136 80 136 80 0.104166 4176000.0 20.0 120.0 0.05
2 147 95 147 95 0.104166 4176000.0 20.0 120.0 0.05
```

3 146 81 147 80 146 80 0.104166 4176000.0 20.0 120.0 0.05
3 137 94 137 95 137 94 0.104166 4176000.0 20.0 120.0 0.05
2 148 92 148 92 0.104166 4176000.0 20.0 120.0 0.05
2 159 107 159 107 0.104166 4176000.0 20.0 120.0 0.05
3 158 93 159 92 158 92 0.104166 4176000.0 20.0 120.0 0.05
3 149 106 149 107 149 106 0.104166 4176000.0 20.0 120.0 0.05
2 160 104 160 104 0.104166 4176000.0 20.0 120.0 0.05
2 171 119 171 119 0.104166 4176000.0 20.0 120.0 0.05
3 170 105 171 104 170 104 0.104166 4176000.0 20.0 120.0 0.05
3 161 118 161 119 161 118 0.104166 4176000.0 20.0 120.0 0.05
80.0 1865.59 621.86 0.2 0.2 1.4 0.0
0.05 0.4 0.4

E.14.5 Description of input user's guide for the corner failure mechanism

The input file that uses the program to calculate the F_w in the wall is written in ASCI file. This is an example of the components that are in the input file.

- *a.* Line 1: Number of case that will be analyzed. For the corner failure mechanism is equal to 1.

- *b.* Line 2: Number of bits that contain the barge system.

- *c.* Line 3: From this line recollect the geometrical information for the bits. To run the program, it is necessary to complete (number of bits) lines beginning from line 3. This case has 180 bits; for this reason there is information from line 3 to line 183.
  (1) *Columns #1:* Bit number.
  (2) *Columns #2:* Local x-coordinates of bit.
  (3) *Columns #3:* Local y-coordinates of bit.

- *d.* Line 184: Number of lashings that act across the idealized failure plane.

- *e.* Line 185: Number of lashings that connect the corner barge with the rest of barges of System 1.

- *f.* Line 186: This line contains the properties description of the lashing. Now the input file has *n* lines, to describe each lashing. This example has 10 lashings; for this reason 10 lines are used to describe the lashings. Lines 186 to 194 present the lashing information as specified in Line 184. The description is in the following format:
  (1) *Columns #1:* Number of times that the lashing crosses the failure plane.
  (2) *Next 2n wraps columns:* Now the form in which the lashing was connected as specified in Appendix A can be found. These lashings are specified from the barge system that impacts the wall to the barge system that does not impact the wall. For this example, the first lashing has three wraps, and then six numbers. The order is the following: starting bit from System 1 to end bit at System 2. The user has to repeat this scheme two more times to account for the amount

of wraps. This is the reason six numbers are specified for the connectivity.

    (3) *Columns # 8:* Diameter of the lashing in feet.
    (4) *Columns # 9:* Modulus of elasticity of the lashing in ksi.
    (5) *Columns #10:* Initial force in the lashing in kip.
    (6) *Columns #11:* Maximum force that the lashing can reach in kip.
    (7) *Columns #12:* Maximum strain in the lashing.
    (8) *Columns #13:* Mode of action for the lashing.

    g. Line 194: This line contains the description of the system.
        (1) *Columns #1:* Approach angle of barge train in degrees.
        (2) *Columns #2:* M1 = Total mass of barge system (without hydrodynamic added mass).
        (3) *Columns #3:* M2 = Mass of barge System 1 that impacts the wall (without hydrodynamic added mass).
        (4) *Columns #4:* Coefficient of friction between the wall and barge train.
        (5) *Columns #5:* Coefficient of friction between barges.
        (6) *Columns #6:* Velocity of barge train in local x-direction.
        (7) *Columns #7:* Velocity of barge train in local y-direction.

    h. Line 196: This line contains the hydrodynamic added mass coefficients to consider the effect of water during impact.
        (1) *Columns #1*: Hydrodynamic added mass coefficient in local x-direction.
        (2) *Columns #2*: Hydrodynamic added mass coefficient in local y-direction.
        (3) *Columns #3*: Hydrodynamic added mass coefficient due to rotational effects.

E.14.6 Example of input user's guide to corner case

```
3
180
1 3          3.25
2 3          1.25
3 5          1.25
4 190        1.25
5 192        1.25
6 192        3.25
7 192        31.25
8 192        33.75
9 190        33.75
10 5         33.75
11 3         33.75
12 3         31.25
13 198       3.25
14 198       1.25
15 200       1.25
16 385       1.25
17 387       1.25
18 387       3.25
```

19	387	31.25
20	387	33.75
21	385	33.75
22	200	33.75
23	198	33.75
24	198	31.25
25	393	3.25
26	393	1.25
27	395	1.25
28	580	1.25
29	582	1.25
30	582	3.25
31	582	31.25
32	582	33.75
33	580	33.75
34	395	33.75
35	393	33.75
36	393	31.25
37	588	3.25
38	588	1.25
39	590	1.25
40	775	1.25
41	777	1.25
42	777	3.25
43	777	31.25
44	777	33.75
45	775	33.75
46	590	33.75
47	588	33.75
48	588	31.25
49	783	3.25
50	783	1.25
51	785	1.25
52	970	1.25
53	972	1.25
54	972	3.25
55	972	31.25
56	972	33.75
57	970	33.75
58	785	33.75
59	783	33.75
60	783	31.25
61	3	38.25
62	3	36.25
63	5	36.25
64	190	36.25
65	192	36.25
66	192	38.25
67	192	66.25
68	192	68.75

69 190	68.75
70 5	68.75
71 3	68.75
72 3	66.25
73 198	38.25
74 198	36.25
75 200	36.25
76 385	36.25
77 387	36.25
78 387	38.25
79 387	66.25
80 387	68.75
81 385	68.75
82 200	68.75
83 198	68.75
84 198	66.25
85 393	38.25
86 393	36.25
87 395	36.25
88 580	36.25
89 582	36.25
90 582	38.25
91 582	66.25
92 582	68.75
93 580	68.75
94 395	68.75
95 393	68.75
96 393	66.25
97 588	38.25
98 588	36.25
99 590	36.25
100 775	36.25
101 777	36.25
102 777	38.25
103 777	66.25
104 777	68.75
105 775	68.75
106 590	68.75
107 588	68.75
108 588	66.25
109 783	38.25
110 783	36.25
111 785	36.25
112 970	36.25
113 972	36.25
114 972	38.25
115 972	66.25
116 972	68.75
117 970	68.75
118 785	68.75

```
119 783    68.75
120 783    66.25
121 3      73.25
122 3      71.25
123 5      71.25
124 190    71.25
125 192    71.25
126 192    73.25
127 192    101.25
128 192    103.75
129 190    103.75
130 5      103.75
131 3      103.75
132 3      101.25
133 198    73.25
134 198    71.25
135 200    71.25
136 385    71.25
137 387    71.25
138 387    73.25
139 387    101.25
140 387    103.75
141 385    103.75
142 200    103.75
143 198    103.75
144 198    101.25
145 393    73.25
146 393    71.25
147 395    71.25
148 580    71.25
149 582    71.25
150 582    73.25
151 582    101.25
152 582    103.75
153 580    103.75
154 395    103.75
155 393    103.75
156 393    101.25
157 588    73.25
158 588    71.25
159 590    71.25
160 775    71.25
161 777    71.25
162 777    73.25
163 777    101.25
164 777    103.75
165 775    103.75
166 590    103.75
167 588    103.75
168 588    101.25
```

```
169 783        73.25
170 783        71.25
171 785        71.25
172 970        71.25
173 972        71.25
174 972        73.25
175 972        101.25
176 972        103.75
177 970        103.75
178 785        103.75
179 783        103.75
180 783        101.25
11
4
3 179 164 179 165 178 165 0.08333 4176000.0 20.0 90.0 0.05 1
3 170 161 170 160 171 160 0.1041666 4176000.0 20.0 120.0 0.05 1
2 170 118 170 118 0.1041666 4176000.0 20.0 120.0 0.05 2
3 171 104 170 104 171 104 0.1041666 4176000.0 20.0 120.0 0.05 1
3 119 104 119 105 118 105 0.1041666 4176000.0 20.0 120.0 0.05 1
3 119 160 118 161 119 161 0.1041666 4176000.0 20.0 120.0 0.05 1
3 110 101 110 100 111 100 0.1041666 4176000.0 20.0 120.0 0.05 1
3 59 44 59 45 58 45 0.1041666 4176000.0 20.0 120.0 0.05 1
2 110 58 110 58 0.1041666 4176000.0 20.0 120.0 0.05 2
3 111 44 110 44 111 44 0.1041666 4176000.0 20.0 120.0 0.05 1
3 58 101 59 100 59 101 0.1041666 4176000.0 20.0 120.0 0.05 1
10.0 1865.59 373.118 0.2 0.2 1.4 0.0
0.05 0.4 0.4
```

E.14.7 Description of output user's guide to longitudinal, transverse, and corner failure mechanism cases

The output file produced by the program is in ASCI file and is described next.

The program has the same output information for all failure mechanisms.

The output file presents the information about the lashings in groups. If there are 11 lashings, there will be the same information for each lashing. It is identified by starting with the lashing number. The information is organized in the following form.

   a. *Column #1*: Number of iterations.
   b. *Column #2*: Normal strain in the lashing.
   c. *Column #3*: Normal stress.
   d. *Column #4*: Elongation of the lashing.
   e. *Column #5*: Internal force in the lashing in kip.
   f. *Column #6*: Force in local x-direction.
   g. *Column #7*: Force in local y-direction.

When the output lashings information is concluded, the program will initiate the final results of the system in the following format:

   a. Column #1: Number of iteration.

b. Column #2: Displacement between System 1 and System 2. For corner and transverse mechanisms the rotation is expressed in radians. For the longitudinal failure mechanisms the displacement is expressed in feet.
c. Column #3: Resultant local x force produced by the lashing in kip.
d. Column #4: Resultant local y force produced by the lashing in kip.
e. Column #5: Maximum normal force at the wall in kip.
f. Column #6: Maximum shear force at the wall in kip.
g. Column #7: Deceleration in the global X-direction of Systems 1 and 2 in ft/sec^2. It is the same for System 1 and System 2.
h. Column #8: Deceleration in the global Y-direction of System 2 in ft/sec^2. The deceleration of System 1 in the global Y-direction was assumed to be zero.
i. Column #9: Maximum force normal to the wall using the empirical correlation in kip.
j. Column #10: Total maximum force normal to the wall in kip.

Appendix F
Notation

a Acceleration in Newton's second law

a,b Width of barge train (left and right of the center row of barges, respectively)

a_{X1} Global X-axis linear acceleration of System 1

a_{Y1} Global Y-axis linear acceleration of System 1 equal to zero

A Cross-sectional area of the lashing

B_1 Width of barge System 1

c Location of the failure plane along the local x-axis measured from the aft

E Young's modulus of elasticity

f_{Ni}, f_{Si} Internal force in each lashing as motion takes place

F Net force in Newton's second law

F_k Kinetic frictional force

F_L Internal force at each segment (from bit to bit) of each lashing

F_{NC} Resultant normal force at the failure plane due to contact of barges (normal pressure between barge sides at the failure plane)

F_{NCL} Left-side resultant normal force at the failure plane due to contact of barges (normal pressure between barge sides at the failure plane)

F_{NCR} Right-side resultant normal force at the failure plane due to contact of barges (normal pressure between barge sides at the failure plane)

F_s Static frictional force

F_W Force normal to the wall at point of impact

$(F_W)_{max}$ Maximum normal force

I_{G1} Second mass moment of inertia for barge System 1

$I_{\theta1}, I_{\theta2}$ Mass moment of inertia of Systems 1 and 2, respectively (including hydrodynamic added mass)

L_1 Length of barge System 1

L_0 Initial length of the lashing before initial load is applied

L_f Elongated length of lashing

m Mass in Newton's second law

m_1, m_2 Mass of System 1 or System 2, respectively (excluding hydrodynamic added mass)

mV_{norm} Linear momentum normal to the wall

M Internal moment at failure plane (it is due to eccentricity of the resultant normal force related to the center of mass)

M_{1L} Internal moment at left failure plane (it is due to eccentricity of the resultant normal force related to the center of mass)

M_{2R} Internal moment at right failure plane (it is due to eccentricity of the resultant normal force related to the center of mass)

M_{norm1}, M_{norm2} Mass of Systems 1 and 2, respectively, normal to the wall (including hydrodynamic added mass)

M_{par} Total mass of barge train ($M_{par1} + M_{par2}$), including hydrodynamic added mass

M_{par1}, M_{par2} Mass of Systems 1 and 2, respectively, parallel to the wall (including hydrodynamic added mass)

M_R Resultant moment produced by the internal forces in the lashings with respect to the mass center of gravity

M_{Rfn} Resultant moment due to the lashing forces normal to the failure plane

M_{Rfs} Resultant moment about the mass center of gravity due to the f_{Si} forces

m_T	Total mass of the barge train without hydrodynamic added mass
M_{x1}	Mass plus hydrodynamic added mass of barge System 1 in the barge longitudinal direction
M_{y1}	Mass plus hydrodynamic added mass of barge System 1 in the barge transverse direction
N	Normal force
R_{fs}	Resultant of the tangential component of the lashing force at the failure plane
R_n, R_s	Resultant normal and longitudinal forces, respectively, in the lashing at the failure plane
R_{nL}	Left-side resultant of the normal component of the lashing force at the failure plane
R_{nR}	Right-side resultant of the normal component of the lashing force at the failure plane
Rn_X , Rn_Y	Global X- and Y-axis components, respectively, of the resultant force perpendicular to the failure plane obtained from the lashing forces
R_{sL}	Left-side resultant of the tangential component of the lashing force at the failure plane
R_{sR}	Right-side resultant of the tangential component of the lashing force at the failure plane
Rs_X, Rs_Y	Global X- and Y-axis components, respectively, of the resultant force parallel to the failure plane obtained from the lashing forces
S_{NC}	Resultant shear force at the failure plane due to contact of barges (normal pressure between barge sides at the failure plane)
S_W	Shear force between corner barge and the wall
V	Speed of an object, ft/sec
V_{par}, V_{norm}	Velocity parallel (global X-axis) and normal (global Y-axis) to the wall, respectively
V_x, V_y	Velocity of the x- and y-axes
x_e, y_e	Local coordinates of the end bits that connect each segment of each lashing

x_{G1}, y_{G1} Local axis coordinates of the mass center of gravity measured from the corner between the aft and the starboard sides

x_{G2} Location of the center of mass of barge system 2 along the local x-axis measured from the aft

x_s, y_s Local coordinates of the start bits that connect each segment of each lashing

x_1 Length of barge train

y_1 Distance measured along the local y-axis that locates the port side from the corner between the aft and the starboard sides

y_2 Distance measured along the local y-axis that locates the failure plane from the corner between the aft and the starboard sides

α_1, α_2 Angular acceleration of Systems 1 and 2, respectively

β Angle between the resultant forces at the wall with respect to the global X-axis

γ Angle that defines the line from the point of contact to the center of mass from the rigid wall

δ Angle that makes each segment (from bit to bit) of each lashing measured from the local positive x-axis

Δ Elongation of the lashing

ε Normal strain

ε_{ult} Ultimate normal strain

θ Approach angle

θ_{CR} Critical value of the approach angle

μ_K Steel-to-steel kinetic coefficient of friction

μ_K^* Steel (barge)-to-steel (armor) kinetic coefficient of friction between barge train and wall

μ_s Static coefficient of friction

σ Normal stress

σ_{ult} Ultimate normal stress

1. REPORT DATE (DD-MM-YYYY) August 2004	2. REPORT TYPE Final report	3. DATES COVERED (From - To)

4. TITLE AND SUBTITLE

A Numerical Method for Computing Barge Impact Forces Based on Ultimate Strength of the Lashings Between Barges

5a. CONTRACT NUMBER

5b. GRANT NUMBER

5c. PROGRAM ELEMENT NUMBER

6. AUTHOR(S)

José Ramón Arroyo, Robert M. Ebeling

5d. PROJECT NUMBER

5e. TASK NUMBER

5f. WORK UNIT NUMBER
33143

7. PERFORMING ORGANIZATION NAME(S) AND ADDRESS(ES)

General Engineering Department, University of Puerto Rico, P.O. Box 9044, Mayagüez, PR 00681;
U.S. Army Engineer Research and Development Center, Information Technology Laboratory, 3909 Halls Ferry Road, Vicksburg, MS 39180-6199

8. PERFORMING ORGANIZATION REPORT NUMBER

ERDC/ITL TR-04-2

9. SPONSORING / MONITORING AGENCY NAME(S) AND ADDRESS(ES)

U.S. Army Corps of Engineers
Washington, DC 20314-1000

10. SPONSOR/MONITOR'S ACRONYM(S)

11. SPONSOR/MONITOR'S REPORT NUMBER(S)

12. DISTRIBUTION / AVAILABILITY STATEMENT

Approved for public release; distribution is unlimited.

13. SUPPLEMENTARY NOTES

14. ABSTRACT

In 1993 Headquarters, U.S. Army Corps of Engineers, issued the first formal Corps-wide analysis procedure providing guidance for analyzing the effects of barge impact loading on navigation structures. According to the ETL 1110-2-338 engineering procedure, the magnitude of the impact forces generated by a particular collision event is dependent on the mass including hydrodynamic added mass of the barge train, the approach velocity, the approach angle, the barge train moment of inertia, *damage sustained by the barge structure*, and friction between the barge and the wall. Two significant concerns have been raised since the release of the ETL 1110-2-338 procedure: (1) A key aspect of the ETL 1110-2-338 engineering formulation is computation of collision energy dissipated in nonrecoverable, plastic hull deformation of (i.e., damage to) the corner of the barge where impact with the wall occurs. However, the majority of the impacts made by barge trains transiting Corps locks do not result in damage to the barge structure nor damage to the walls. (2) In addition, several engineers who have used the ETL 1110-2-338 engineering procedure have questioned the accuracy of the computed results.

(Continued)

15. SUBJECT TERMS

Barge train	Impact	Lashing limit state
Failure mechanism of barge train	Kinetic coefficient of friction	Rigid wall

16. SECURITY CLASSIFICATION OF:			17. LIMITATION OF ABSTRACT	18. NUMBER OF PAGES	19a. NAME OF RESPONSIBLE PERSON
a. REPORT UNCLASSIFIED	**b. ABSTRACT** UNCLASSIFIED	**c. THIS PAGE** UNCLASSIFIED		226	19b. TELEPHONE NUMBER (include area code)

14. ABSTRACT (concluded)

In 2003, the U.S. Army Engineer Research and Development Center issued the report ERDC/ITL TR-03-3, "Analysis of Impact Loads from Full-Scale, Low-Velocity, Controlled Barge Impact Experiments, December 1998," by Arroyo, Ebeling, and Barker. This report addresses the interpretation of 8 of the 44 December 1998 full-scale, low-velocity, controlled-impact, barge train impact experiments conducted at the decommissioned Gallipolis Lock at Robert C. Byrd Lock and Dam, Gallipolis Ferry, WV. According to ERDC/ITL TR-03-3, an easy-to-use empirical correlation is derived that reports the maximum impact force (normal to the wall) as a function of the linear momentum normal to the wall (immediately prior to impact), using the results from the impact forces measured during these full-scale impact experiments. This new empirical correlation will be used for impacts that do not involve damage during impact to either the corner barge of a barge train or to the wall. An alternate empirical correlation is given for the maximum impact force (normal to the wall) as a function of the kinetic energy normal to the wall (immediately prior to impact).

However, ERDC/ITL TR-03-3 did not present the limit value of the force normal to the wall based on the empirical correlations. The present report presents the analysis of a barge train impacting a rigid wall. The limit value of the force normal to the wall is based on the yield of the lashing. That is, predefined failure planes are analyzed and based on the yield of the lashing, a maximum force normal to the wall is calculated. The three failure mechanisms studied are longitudinal, transverse, and corner. Finally, the maximum force normal to the struck wall is calculated from the equations of motion and the yielding of the lashing.